

University of Southern Queensland
Faculty of Engineering and Surveying

Shear Strength Properties of Clean and Clay Infilled Rock Joints: An analysis of the impact of moisture content under CNL conditions

A dissertation submitted by
Elizabeth Downing

In fulfilment of the requirements of
Bachelor of Engineering (Honours) (Civil)

November 2022

ABSTRACT

The aim of this project is to quantitatively analyse the effects of clay infill moisture content and infill layer thickness on the shear strength characteristics of clean and infilled rock joints being subjected to Constant Normal Loading (CNL) boundary conditions. Understanding the failure mechanisms and conditions of slope stability is key to both safety and economic considerations in geotechnical engineering. Rock joints are common geological features with the potential to decrease the shear capacity of the rock material and affect the stability of slopes on small and large scales. While significant research has been performed previously with consideration to critical conditions (full saturation of infill), there has been relatively little consideration to infill material with a moisture content below full saturation. In areas of high risk, such as Asia and South America, a high factor of safety needs to be implemented. However, in areas of lower risk the factor of safety might be able to be decreased (potentially minimizing construction and maintenance costs).

This project consists of six main phases: extensive literature review, procurement of materials and organization of laboratory facilities, modelling (and printing) of three-dimensional moulds and concrete casting, testing of samples, data analysis and modelling, and final dissertation report as outlined in Table 2.

Rock-like samples will be constructed using three-dimensional printed moulds and concrete. The scope of this project is limited to one clay soil type with various moisture contents and applied normal stress (100 to 700 kPa) subject to CNL boundary conditions, with the potential for further research using a wider variety of conditions. The expected outcomes for this project were decreased shear strength as infill thickness and moisture content increase, the shear strength of the clean rock joint to be greater than that of an infilled rock joint, and sufficient and conclusive data that can contribute to the development of a new slope stability model in relation to rock joints. Testing was conducted in accordance with *AS1289* to ensure the validity of the results and minimize human factor errors, and graphical data analysis was conducted using Microsoft Excel. The testing and data analysis in this project, and future research, has the potential to establish a new slope stability model for use in industry.

Actual outcomes (as outlined in Chapter 5) include: higher shear strength of clean rock joints in comparison to clay infilled joints, when the infill thickness was less than the asperity height the asperity profile of the artificial rock joint controlled the behaviour of the sample, at higher thicknesses (infill thickness equal to or greater than asperity height) the infill material predominantly controlled the behaviour of the joint, and that as the moisture content increased the magnitude of the converging trend remained largely unaffected. The key finding of this project is that as the moisture content increased,

the rate of convergence of the shear stress, normal stress and normal displacement trends increased at lower applied normal loading conditions. However, due to the limiting loading of 2200 N of the direct shear apparatus used the data at higher applied normal loadings is generally inconclusive. Due to limited data set at higher applied normal stresses, further research should investigate the impact of variable moisture conditions on the shear strength properties of clay infilled rock joints by narrowing the scope to include more moisture content conditions tested at relatively low applied normal stresses (up to 300 kPa). In addition, testing under CNS conditions should be investigated to determine the behaviour on deeper rock joints.

University of Southern Queensland
Faculty of Health, Engineering and Sciences
ENG4111/ENG4112 Research Project

Limitations of Use

The Council of the University of Southern Queensland, its Faculty of Health, Engineering & Sciences, and the staff of the University of Southern Queensland, do not accept any responsibility for the truth, accuracy or completeness of material contained within or associated with this dissertation.

Persons using all or any part of this material do so at their own risk, and not at the risk of the Council of the University of Southern Queensland, its Faculty of Health, Engineering & Sciences or the staff of the University of Southern Queensland.

This dissertation reports an educational exercise and has no purpose or validity beyond this exercise. The sole purpose of the course pair entitled “Research Project” is to contribute to the overall education within the student’s chosen degree program. This document, the associated hardware, software, drawings, and other material set out in the associated appendices should not be used for any other purpose: if they are so used, it is entirely at the risk of the user.

University of Southern Queensland
Faculty of Health, Engineering and Sciences
ENG4111/ENG4112 Research Project

Certification of Dissertation

I certify that the ideas, designs and experimental work, results, analyses, and conclusions set out in this dissertation are entirely my own effort, except where otherwise indicated and acknowledged.

I further certify that the work is original and has not been previously submitted for assessment in any other course or institution, except where specifically stated.

E.Downing

██████████

ACKNOWLEDGEMENTS

This research was carried out under the principal supervision of Dr Ali Mirzaghobanali. I thank my supervisor Dr Ali Mirzaghobanali for his guidance, passion, and support throughout this project. Secondly, I thank the engineering technical staff at the University of Southern Queensland, in particular Chintan Chandebhamar, for their dedication, time and expertise. Thirdly, I thank the staff at the University of Southern Queensland for their support in the financial and professional aspects that have facilitated this research project. Finally, I thank my family and friends for their support throughout this project and my studies.

TABLE OF CONTENTS

ABSTRACT	i
ACKNOWLEDGEMENTS	v
TABLE OF CONTENTS	vi
LIST OF FIGURES	xii
LIST OF TABLES	xvi
CHAPTER 1: INTRODUCTION	1
1.1 Outline of the study	1
1.2 Introduction	1
1.3 The Problem	3
1.4 Research Objectives	4
1.5 Summary	6
CHAPTER 2: LITERATURE REVIEW	7
2.1 Introduction	7
2.1.1 Asperity Profile and Specimen Design	7
2.1.2 Infill Thickness	10
2.1.3 Infill Material	12
2.1.4 Effect of Moisture Content	13
2.1.5 Effects of Normal Loading	14
2.2 Testing Techniques	18
2.3 Joint Failure	19
2.4 Dangers of Idealization	21
2.5 Knowledge Gap	21
2.6 Conclusion	22
CHAPTER 3: PROJECT DEVELOPMENT	23
3.1 Aims and Objectives	23
3.2 Limitations	23
3.3 Scope	23
3.4 Expected Outcomes	24
3.5 Methodology	24
3.6 Collection of Data	27
3.7 Modelling Procedure	28
3.8 Project Feasibility and Study Justification	28
CHAPTER 4: EXPERIMENTAL DESIGN & PROCEDURE	29
4.1 Mould Design and Formation	29

4.1.1 Asperity Profile and 3D Modelling	29
4.1.2 Mould Formation and Preparation	30
4.1.3 Casting	31
4.2 Compression Testing	35
4.3 Infill Properties	35
4.3.1 Infill Particle Size Distribution (d)	36
4.3.2 Infill Soil Particle Density (ρ_s)	39
4.3.3 Moisture Content (w)	43
4.3.4 Liquid Limit (w_{CL})	46
4.3.5 Plastic Limit (w_p)	49
4.3.6 Shrinkage Limit (SL)	52
4.3.7 Compression Index (C_c) and Swell Index (C_s)	53
4.3.8 Friction Angle (ϕ') and Cohesion (c')	59
4.4 Direct Shear Testing of Rock Joints	67
4.4.1 Direct Shear Testing Data Collation	75
4.4.2 Graphing and Analysis	76
CHAPTER 5: RESULTS & DISCUSSION	78
5.1 Compressive Strength Testing	78
5.2 Infill Properties	79
5.2.1 Particle Size Distribution (d)	79
5.2.2 Infill Soil Particle Density (ρ_s)	80
5.2.3 Moisture Content (w)	81
5.2.4 Cone Liquid Limit (w_{CL})	81
5.2.5 Plastic Limit (w_p)	83
5.2.6 Shrinkage Limit (SL)	84
5.2.7 Compression Index (C_c) and Swell Index (C_s)	85
5.2.8 Friction Angle (ϕ') and Cohesion (c')	88
5.2.9 Summary of Soil Properties	90
5.3 Direct Shear Testing of Rock Joints (Shear Displacement vs Shear Stress)	90
5.3.1 Clean Joints at normal stresses of 100 kPa, 300 kPa, 500 kPa, and 700 kPa	90
5.3.2 Infilled Joints with normal stress of 100 kPa	91
5.3.3 Infilled Joints with normal stress of 300 kPa	93
5.3.4 Infilled Joints with normal stress of 500 kPa	95
5.3.5 Infilled Joints with normal stress of 700 kPa	96
5.3.6 Summary	98
5.4 Direct Shear Testing of Rock Joints (Shear Displacement vs Normal Stress)	98

5.4.1 Clean Joints at normal stresses of 100 kPa, 300 kPa, 500 kPa, and 700 kPa	99
5.4.2 Infilled Joints with normal stress of 100 kPa	100
5.4.3 Infilled Joints with normal stress of 300 kPa	102
5.4.4 Infilled Joints with normal stress of 500 kPa	103
5.4.5 Infilled Joints with normal stress of 700 kPa	105
5.4.6 Summary	106
5.5 Direct Shear Testing of Rock Joints (Shear Displacement vs Normal Displacement).....	107
5.5.1 Clean Joints at normal stresses of 100 kPa, 300 kPa, 500 kPa, and 700 kPa	107
5.5.2 Infilled Joints with normal stress of 100 kPa	109
5.5.3 Infilled Joints with normal stress of 300 kPa	111
5.5.4 Infilled Joints with normal stress of 500 kPa	113
5.5.5 Infilled Joints with normal stress of 700 kPa	115
5.5.6 Summary	117
5.6 UDEC and International Coal Operators' Conference.....	117
CHAPTER 6: CONCLUSION	118
LIST OF REFERENCES	119
Appendix A – Project Specification	124
Appendix B – Risk Assessment	125
Appendix C – Uniaxial Compression Testing Summary	126
C.1 7 Day Compression Testing	126
Before Testing (All Samples):	126
Sample 1:	126
Sample 2:	127
Sample 3:	128
Post Testing (All Samples):	128
C.2 14 Day Compression Testing	129
Before Testing (All Samples):	129
Sample 1:	129
Sample 2:	130
Sample 3:	131
Post Testing (All Samples):	132
C.3 21 Day Compression Testing	132
Before Testing (All Samples):	132
Sample 1:	133
Sample 2:	133
Sample 3:	134

Sample 4:	135
Post Testing (All Samples):	136
C.4 28 Day Compression Testing	136
Before Testing (All Samples):	136
Sample 1:	136
Sample 2:	137
Sample 3:	138
Sample 4:	138
Sample 5:	139
Post Testing (All Samples):	140
Appendix D – Moisture Content Results	141
Appendix E – Cone Liquid Limit Results	142
Appendix F – Plastic Limit Results	143
Appendix G – Collated Direct Shear Testing Results (Soil Only)	144
G.1 Moisture Content 1 (16%).....	144
Applied Normal Stress of 100 kPa	144
Applied Normal Stress of 300 kPa	146
Applied Normal Stress of 500 kPa	149
Applied Normal Stress of 700 kPa	150
G.2 Moisture Content 2 (0%).....	150
Applied Normal Stress of 100 kPa	150
Applied Normal Stress of 300 kPa	153
Applied Normal Stress of 500 kPa	155
Applied Normal Stress of 700 kPa	156
G.3 Moisture Content 3 (10%).....	156
Applied Normal Stress of 100 kPa	156
Applied Normal Stress of 300 kPa	159
Applied Normal Stress of 500 kPa	161
Applied Normal Stress of 700 kPa	162
Appendix H – Collated Rock Joint Direct Shear Testing Results	163
H.1 Clean Rock Joints	163
Clean Joint CL1 at 100 kPa:	163
Clean Joint CL2 at 300 kPa:	165
Clean Joint CL3 at 500 kPa:	166
Clean Joint CL4 at 700 kPa:	166
H.2 Rock Joints with Moisture Condition 1 (16%)	167

Infilled Joint 111 (100 kPa, $t/a=0.5$, MC1):.....	167
Infilled Joint 211 (300 kPa, $t/a=0.5$, MC1):.....	169
Infilled Joint 311 (500 kPa, $t/a=0.5$, MC1):.....	170
Infilled Joint 411 (700 kPa, $t/a=0.5$, MC1):.....	170
Infilled Joint 121 (100 kPa, $t/a=1.0$, MC1):.....	171
Infilled Joint 221 (300 kPa, $t/a=1.0$, MC1):.....	174
Infilled Joint 321 (500 kPa, $t/a=1.0$, MC1):.....	177
Infilled Joint 421 (700 kPa, $t/a=1.0$, MC1):.....	177
Infilled Joint 131 (100 kPa, $t/a=1.5$, MC1):.....	177
Infilled Joint 231 (300 kPa, $t/a=1.5$, MC1):.....	180
Infilled Joint 331 (500 kPa, $t/a=1.5$, MC1):.....	183
Infilled Joint 431 (700 kPa, $t/a=1.5$, MC1):.....	184
H.3 Rock Joints with Moisture Condition 2 (0%)	185
Infilled Joint 112 (100 kPa, $t/a=0.5$, MC2):.....	185
Infilled Joint 212 (300 kPa, $t/a=0.5$, MC2):.....	188
Infilled Joint 312 (500 kPa, $t/a=0.5$, MC2):.....	188
Infilled Joint 412 (700 kPa, $t/a=0.5$, MC2):.....	189
Infilled Joint 122 (100 kPa, $t/a=1.0$, MC2):.....	189
Infilled Joint 222 (300 kPa, $t/a=1.0$, MC2):.....	192
Infilled Joint 322 (500 kPa, $t/a=1.0$, MC2):.....	192
Infilled Joint 422 (700 kPa, $t/a=1.0$, MC2):.....	193
Infilled Joint 132 (100 kPa, $t/a=1.5$, MC2):.....	193
Infilled Joint 232 (300 kPa, $t/a=1.5$, MC2):.....	196
Infilled Joint 332 (500 kPa, $t/a=1.5$, MC2):.....	199
Infilled Joint 432 (700 kPa, $t/a=1.5$, MC2):.....	199
H.4 Rock Joints with Moisture Condition 3 (10%)	200
Infilled Joint 113 (100 kPa, $t/a=0.5$, MC3):.....	200
Infilled Joint 213 (300 kPa, $t/a=0.5$, MC3):.....	203
Infilled Joint 313 (500 kPa, $t/a=0.5$, MC3):.....	203
Infilled Joint 413 (700 kPa, $t/a=0.5$, MC3):.....	204
Infilled Joint 123 (100 kPa, $t/a=1.0$, MC3):.....	204
Infilled Joint 223 (300 kPa, $t/a=1.0$, MC3):.....	207
Infilled Joint 323 (500 kPa, $t/a=1.0$, MC3):.....	210
Infilled Joint 423 (700 kPa, $t/a=1.0$, MC3):.....	210
Infilled Joint 133 (100 kPa, $t/a=1.5$, MC3):.....	211
Infilled Joint 233 (300 kPa, $t/a=1.5$, MC3):.....	214

Infilled Joint 333 (500 kPa, $t/a=1.5$, MC3):.....	217
Infilled Joint 433 (700 kPa, $t/a=1.5$, MC3):.....	217

LIST OF FIGURES

Figure 1: World Annual Precipitation Map (El Dorado Weather 2019)	2
Figure 2: World Elevation Map (Brodnig & Prasad 2010)	2
Figure 3: Fracture Modes (Philipp, Afsar & Gudmundsson 2013)	3
Figure 4: Normal and Shear Stresses (Ray 2016, p. 26)	3
Figure 5: World Population by Country (World Population Review 2022)	4
Figure 6: Combination Dip-Sawtooth Profile Mould (Indraratna, Jayanathan & Brown 2008)	8
Figure 7: Sawtooth and Sinusoidal Joint Profiles (Zohaib, Mirzaghobanali, Helwig, Azzia, Gregor, Rastegarmanesh & McDougall 2020)	9
Figure 8: Joint Roughness Coefficient (JRC) (Barton & Choubey 1977)	9
Figure 9: Generalized Testing Model (Wang, Wang & Zhang 2018)	10
Figure 10: Interlocking Behaviour of Sawtooth Joints (Zohaib, Mirzaghobanali, Helwig, Azzia, Gregor, Rastegarmanesh & McDougall 2020)	11
Figure 11: Loading conditions for shear tests a) CNL b) CNS c) CND (Liu, Zhu & Li 2020)	15
Figure 12: Impact of normal load magnitude on shear strength a) Set A b) Set B c) Set C (Tang and Wong 2015)	17
Figure 13: ShearTrac2 Shear Apparatus	18
Figure 14: Failure Patterns (Wang, Wang & Zhang 2018)	19
Figure 15: Sliding Failure: a) sawtooth profile b) sliding failure concept c) degraded specimen (Cao, Deng, Chen & Fu 2018)	20
Figure 16: Shear Failure: a) sawtooth profile b) shear failure concept c) degraded specimen (Cao, Deng, Chen & Fu 2018)	20
Figure 17: Tensile Failure: a) sawtooth profile b) tensile failure concept c) degraded specimen (Cao, Deng, Chen & Fu 2018)	21
Figure 18: 3D model of interlocking sawtooth mould	29
Figure 19: 3D printed asperity profile and Resin Curing Process	30
Figure 20: 19mm DN65 DWV PVC pipe lengths	30
Figure 21: Taped Moulds	31
Figure 22: Greased Moulds	31
Figure 23: UCS Sample Moulds	31
Figure 24: Demoulding of Initial Cement Grout Mix	32
Figure 25: Cement Grout Mixing	33
Figure 26: Freshly Poured Moulds	33
Figure 27: Set Artificial Rock Joints	34
Figure 28: Demoulded Sample top (left) bottom (right)	34
Figure 29: Demoulded Samples in curing room	34
Figure 30: Compression testing set up	35
Figure 31: Mechanical Sieving	38
Figure 32: Soil particles on sieve	38
Figure 33: Water added to two-thirds full (before 24 hours)	41
Figure 34: Water and soil mixture (after 24 hours)	41
Figure 35: Applying partial vacuum to remove entrapped air	42
Figure 36: Soil samples (natural state) ready for oven drying	44
Figure 37: Weighing of dried soil sample	45
Figure 38: Rigid cup measurements a) diameter b) height	47
Figure 39: Cone Penetrometer ready for release	48

Figure 40: Cone Penetrometer after release with penetration reading.....	48
Figure 41: Liquid Limit samples after oven drying to find moisture content	49
Figure 42: Plastic Limit samples before oven drying to find moisture content.....	51
Figure 43: Plastic Limit samples after oven drying to find moisture content.....	51
Figure 44: Casagrande's Soil Plasticity Chart (TransCalc 2022).....	52
Figure 45: Consolidation ring measurements diameter (left) and height (right)	54
Figure 46: Consolidation Cell (The Constructor 2021).....	55
Figure 47: First load applied to sample.....	56
Figure 48: Dial gauge reading at 24 hours for 1 kg weight	56
Figure 49: Sample removed from reservoir after unloading	57
Figure 50: Extruded and cut sample (post consolidation)	57
Figure 51: Typical log-time versus compression graph (Standards Australia 2020a)	58
Figure 52: Typical log-effective pressure versus void ratio graph (CIV2403 2015, p. 129)	59
Figure 53: Internal diameter of split box top (left) and bottom (right)	60
Figure 54: Height of split box top (left) and bottom (right).....	60
Figure 55: Diameter (left) and thickness (right) of porous plate	61
Figure 56: height of bottom split box with base plate installed	61
Figure 57: height of bottom split box with base plate and one (1) porous plate installed	62
Figure 58: Total height of split box with base plate and one (1) porous stone installed	62
Figure 59: Dimensions of load pad height (left) and diameter (right).....	62
Figure 60: Height of load pad base	63
Figure 61: Soil material in shear box.....	65
Figure 62: Artificial rock joints with test codes.....	69
Figure 63: Joint Preparation.....	71
Figure 64: Alignment of bottom joint in shear box.....	71
Figure 65: Preparation of sample with 1 mm infill thickness	73
Figure 66: Raw Data (example).....	75
Figure 67: Collated Corrected Data (example)	76
Figure 68: Particle Size Distribution Chart	79
Figure 69: Liquid Limit as per Cone Penetration Test.....	82
Figure 70: Plasticity Chart Results.....	84
Figure 71: Consolidation (log-time versus displacement)	86
Figure 72: Consolidation (log-effective pressure versus void ratio)	87
Figure 73: Normal vs shear stress for determination of friction angle and cohesion	89
Figure 74: Clean Joint Results ($t/a=0$) (Shear Displacement vs Shear Stress).....	91
Figure 75: Shear Testing Results for 100 kPa (Shear Displacement vs Shear Stress)	93
Figure 76: Shear Testing Results for 300 kPa (Shear Displacement vs Shear Stress)	94
Figure 77: Shear Testing Results for 500 kPa (Shear Displacement vs Shear Stress)	96
Figure 78: Shear Testing Results for 700 kPa (Shear Displacement vs Shear Stress)	97
Figure 79: Clean Joint Results ($t/a=0$) (Shear Displacement vs Normal Stress).....	99
Figure 80: Shear Testing Results for 100 kPa (Shear Displacement vs Normal Stress)	101
Figure 81: Shear Testing Results for 300 kPa (Shear Displacement vs Normal Stress)	103
Figure 82: Shear Testing Results for 500 kPa (Shear Displacement vs Normal Stress)	104
Figure 83: Shear Testing Results for 700 kPa (Shear Displacement vs Normal Stress)	106
Figure 84: Clean Joint Results ($t/a=0$) (Shear Displacement vs Normal Displacement)	108
Figure 85: Joint Failure on Sample CL1	108
Figure 86: Joint Failure of Sample CL2	108
Figure 87: Joint CL3 (after testing).....	109

Figure 88: Joint CL4 (after testing).....	109
Figure 89: Shear Testing Results for 100 kPa (Shear Displacement vs Normal Displacement)	111
Figure 90: Shear Testing Results for 300 kPa (Shear Displacement vs Normal Displacement)	113
Figure 91: Shear Testing Results for 500 kPa (Shear Displacement vs Normal Displacement)	115
Figure 92: Shear Testing Results for 700 kPa (Shear Displacement vs Normal Displacement)	116
Figure 93: 7 Day Compression Testing Samples (Before Testing).....	126
Figure 94: 7 Day Compression Testing Sample 1 (Before Testing)	126
Figure 95: 7 Day Compression Testing Sample 1 (After Testing).....	126
Figure 96: 7 Day Compression Testing Sample 1 (Results)	127
Figure 97: 7 Day Compression Testing Sample 2 (Before Testing)	127
Figure 98: 7 Day Compression Testing Sample 2 (After Testing).....	127
Figure 99: 7 Day Compression Testing Sample 2 (Results)	127
Figure 100: 7 Day Compression Testing Sample 3 (Before Testing)	128
Figure 101: 7 Day Compression Testing Sample 3 (After Testing).....	128
Figure 102: 7 Day Compression Testing Sample 3 (Results)	128
Figure 103: 7 Day Compression Testing Samples (After Testing)	128
Figure 104: 14 Day Compression Testing Samples (Before Testing).....	129
Figure 105: 14 Day Compression Testing Sample 1 (Before Testing)	129
Figure 106: 14 Day Compression Testing Sample 1 (After Testing)	129
Figure 107: 14 Day Compression Testing Sample 1 (Results)	130
Figure 108: 14 Day Compression Testing Sample 2 (Before Testing)	130
Figure 109: 14 Day Compression Testing Sample 2 (After Testing).....	130
Figure 110: 14 Day Compression Testing Sample 2 (Results)	131
Figure 111: 14 Day Compression Testing Sample 3 (Before Testing)	131
Figure 112: 14 Day Compression Testing Sample 3 (After Testing).....	131
Figure 113: 14 Day Compression Testing Sample 3 (Results)	132
Figure 114: 14 Day Compression Testing Samples (After Testing)	132
Figure 115: 21 Day Compression Testing Samples (Before Testing).....	132
Figure 116: 21 Day Compression Testing Sample 1 (Before Testing)	133
Figure 117: 21 Day Compression Testing Sample 1 (After Testing).....	133
Figure 118: 21 Day Compression Testing Sample 1 (Results)	133
Figure 119: 21 Day Compression Testing Sample 2 (Before Testing)	133
Figure 120: 21 Day Compression Testing Sample 2 (After Testing).....	134
Figure 121: 21 Day Compression Testing Sample 2 (Results)	134
Figure 122: 21 Day Compression Testing Sample 3 (Before Testing)	134
Figure 123: 21 Day Compression Testing Sample 3 (After Testing).....	134
Figure 124: 21 Day Compression Testing Sample 3 (Results)	135
Figure 125: 21 Day Compression Testing Sample 4 (Before Testing)	135
Figure 126: 21 Day Compression Testing Sample 4 (After Testing).....	135
Figure 127: 21 Day Compression Testing Sample 4 (Results)	135
Figure 128: 21 Day Compression Testing Samples (After Testing)	136
Figure 129: 28 Day Compression Testing Samples (Before Testing).....	136
Figure 130: 28 Day Compression Testing Sample 1 (Before Testing)	136
Figure 131: 28 Day Compression Testing Sample 1 (After Testing).....	136
Figure 132: 28 Day Compression Testing Sample 1 (Results)	137
Figure 133: 28 Day Compression Testing Sample 2 (Before Testing)	137
Figure 134: 28 Day Compression Testing Sample 2 (After Testing).....	137
Figure 135: 28 Day Compression Testing Sample 2 (Results)	137

Figure 136: 28 Day Compression Testing Sample 3 (Before Testing)	138
Figure 137: 28 Day Compression Testing Sample 3 (After Testing)	138
Figure 138: 28 Day Compression Testing Sample 3 (Results)	138
Figure 139: 28 Day Compression Testing Sample 4 (Before Testing)	138
Figure 140: 28 Day Compression Testing Sample 4 (After Testing)	139
Figure 141: 28 Day Compression Testing Sample 4 (Results)	139
Figure 142: 28 Day Compression Testing Sample 5 (Before Testing)	139
Figure 143: 28 Day Compression Testing Sample 5 (After Testing)	139
Figure 144: 28 Day Compression Testing Sample 5 (Results)	140
Figure 145: 28 Day Compression Testing Samples (After Testing)	140

LIST OF TABLES

Table 1: Deadliest Landslides in History (The Engineering Community 2018)	1
Table 2: Outline of required steps	26
Table 3: Asperity Profile Characteristics	29
Table 4: Custom Cement Grout Mix	32
Table 5: Testing Conditions.....	67
Table 6: Compressive Strength Results Summary	78
Table 7: Sieve Analysis Results.....	79
Table 8: Particle Density Results	80
Table 9: Initial Moisture Content Results	81
Table 10: Liquid Limit Cone Penetrometer Results.....	82
Table 11: Plastic Limit Results	83
Table 12: Consolidation Results	85
Table 13: Void Ratio Calculations.....	87
Table 14: Moisture Content Test Results from Consolidation Test	88
Table 15: Summary of normal and shear stress results for determination of friction angle and cohesion.....	89
Table 16: Infill Material Properties Results Summary	90
Table 17: Peaks, troughs, and amplitudes of Figure 76a	92
Table 18: Peak normal displacement under 100 kPa normal pressure at $t/a=0.5$	110

CHAPTER 1: INTRODUCTION

1.1 Outline of the study

This study investigates the impact of moisture content on the shear strength properties of clean and clay infilled rock joints. These conditions will be modelled using cast concrete rock joints and a plaster infill to reflect the general properties of clay infill. These joints will be subject to normal loading and the resulting data recorded and analysed to determine the impact of the moisture content.

1.2 Introduction

Understanding the effects of structural geological features on foundation stability is key to the development of best practice in engineering. Current models and industry standards have been developed to provide set procedures to improve the safety and sustainability of a range of projects. This project focuses on the effect of infill on the shear strength of rock joints. Shear characteristics control the stability of geological material and slope stability is a vital area of research due to the hazards it causes when failure occurs.

Rockslides and other slope instabilities occur around the world and can have devastating effects. Table 1 shows a summary of the deadliest landslide events in recorded history. These slope failures occurred in Asia and South America. These regions are both high in elevation, providing the rock material, and high in precipitation (as shown in Figure 1 and Figure 2). The combination of these factors results in unstable slope conditions that often lead to slope failure.

Table 1: Deadliest Landslides in History (The Engineering Community 2018)

Fatalities	Event	Location	Date
100,000+	Haiyuan Flows	Ningxia, China	December 1920
30,000	Vargas Tragedy	Vargas, Venezuela	December 1999
23,000	Armero Tragedy	Tolima, Colombia	November 1985
22,000	70 Nevado Huascaran Debris Fall	Yungay, Peru	May 1970
5,700	North India Flood mudslides	Kedarnath, India	June 2013
5,000+	Kelud Lahars	East Java, Indonesia	May 1919
5,000	Huaraz Debris Flows	Ancash, Peru	December 1941
4,500	62 Nevado Huascaran Debris Fall	Ranrahirca, Peru	January 1962
4,000	Khait Landslide	Tajikstan, Japan	July 1949
3,000+	Diexi Slides	Sichuan, China	August 1933

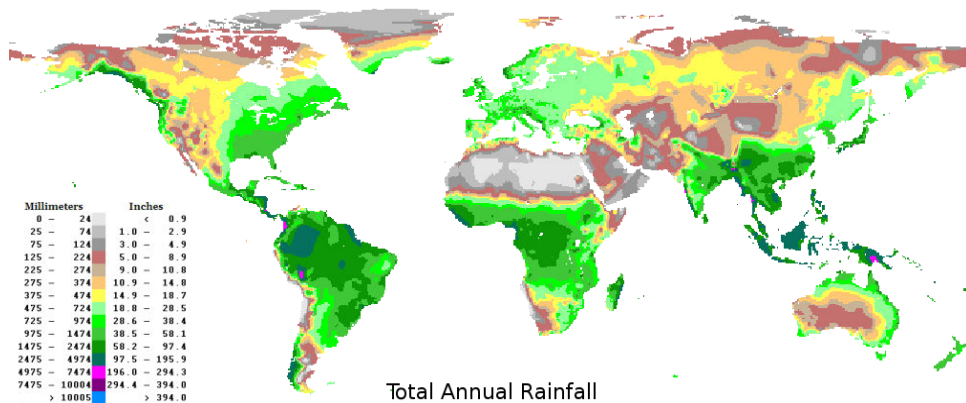


Figure 1: World Annual Precipitation Map (El Dorado Weather 2019)

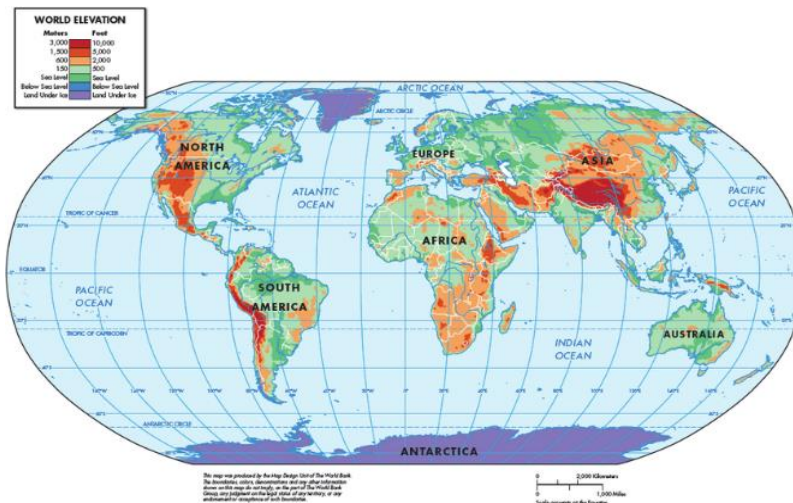


Figure 2: World Elevation Map (Brodnig & Prasad 2010)

There are three modes of rock fracture (Figure 3), which are classified based on the forces controlling the break (Philipp, Afsar & Gudmundsson 2013). Extension fractures or tension gashes (Mode 1) are caused by forces acting perpendicular to the fractured walls, where the opening of the break is parallel to the face of least resistance (Ray 2016, p.17). Shear fractures have displacement that is parallel to the fracture plane (Ray 2016, p.18). Mode 2 shear fractures are caused by sliding forces acting perpendicular to the fracture edge. Mode 3 shear fractures are caused by sliding force acting parallel to the fracture edge. A combination of these failure modes is called an oblique extension or mixed mode fracture. A joint is a type of fracture or discontinuity that has little or no movement parallel to the plane of fracture. These are common structural phenomena in geology around the world and range from small

scale to tectonic fault lines. The first part of this project focuses on the effect of clean rock joints on the shear strength of the joint at various normal loads.

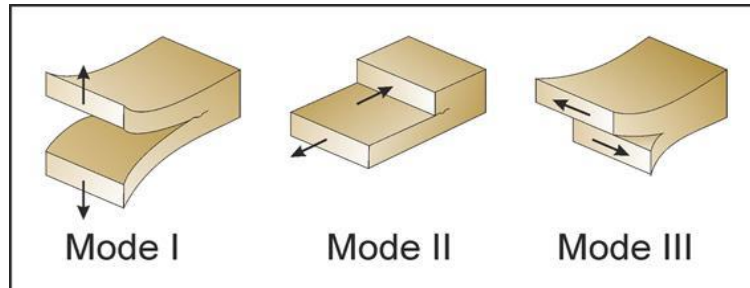


Figure 3: Fracture Modes (Philipp, Afsar & Gudmundsson 2013)

Rock joints leave an opportunity for infill to occur. Infill can occur in the form of soil, water or mineral precipitates. The second part of this project focuses on the effects of soil infill (with various moisture contents and normal stresses) of rock joints. The presence of infill changes various properties of the overall rock structure. The project focuses on the effect on the shear strength of the joint. Figure 4 shows the relationship between normal and shear stresses on a fracture plane. As shear strength is a controlling factor for slope stability it is important to continue research into this area in order to maximize safety and minimize costs.

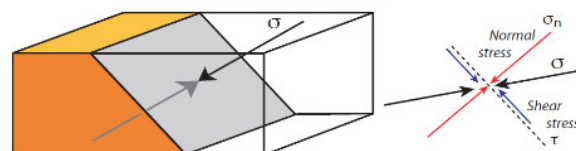


Figure 4: Normal and Shear Stresses (Ray 2016, p. 26)

1.3 The Problem

The areas outlined above as having high elevation (rock building processes) and high precipitation coincide with many of the highest population centres in the world (Figure 5) including China, India, and Pakistan (World Population Review 2022). As such, it is important to understand the catalysts for slope failure to develop effective design standards. While there are many variables related to slope stability and rock mechanics, this project investigates the effect of moisture content on the shear strength of rock joints. This topic is important in efforts to decrease construction and maintenance costs, without compromising safety.

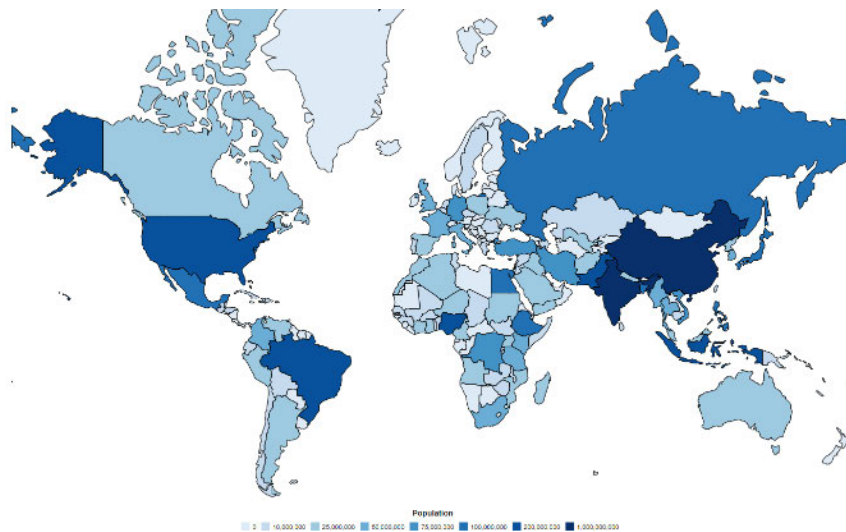


Figure 5: World Population by Country (World Population Review 2022)

1.4 Research Objectives

This project has six key objectives, which are outlined and investigated in each chapter. Chapter 1 outlines the real-world context for the project and structure of this project. Chapter 2 investigates and reviews current literature to determine the level and type of past and current research on clean and infilled rock joints. This focuses on the following aspects of rock joint experimental analysis and parameters:

- asperity profile,
- specimen design,
- infill thickness,
- infill material type,
- effect of moisture content,
- effect of normal loading,
- joint failure criteria,
- the dangers of idealization, and
- identification of the gap in current research and knowledge.

Chapter 3 outlines the project development and methodology, including:

- aims and objectives of the experimental investigation,
- limitations of the project,
- scope of the project,
- expected outcomes,
- data collection,
- data modelling procedure, and
- project feasibility and justification.

Chapter 4 outlines the experimental design and procedures to be undertaken during experimental testing to be performed in accordance with the appropriate Australian Standards (where applicable), including:

- Artificial rock joint creation includes the following steps:
 - three-dimensional modelling of the asperity profile for the mould,
 - mould formation and preparation,
 - casting of the cement ground mix for both the artificial joints and compression testing samples, and
 - 28 day cure of the artificial joints with compression testing at 7, 14, 21 and 28 days.
- Testing of the infill material includes the following:
 - particle size distribution,
 - infill particle density,
 - moisture content,
 - liquid limit,
 - plastic limit,
 - shrinkage limit,
 - compression index,
 - swell index,

- internal friction angle, and
- cohesion.
- Direct shear testing using the ShearTrac2 apparatus to determine the impact of the following independent variables on the dependent variable of shear strength:
 - moisture content,
 - normal loading, and
 - infill thickness.

Chapter 5 reveals the results of the experimental testing data from the procedures outlined in Chapter 4. This data is then analysed using graphical evaluation, and the influence on slope stability is investigated using UDEC software if time permits. This chapter also includes an in-depth discussion about these results before the outcomes of the project are summarised in the project conclusion in Chapter 6.

1.5 Summary

Continual development and expansion of the understanding of the factors that influence engineering decision-making processes is central to improving safety and engineering project outcomes. It is important to consider and investigate the various factors such as geological influences on the geotechnical aspects of projects for a holistic view. As such, this study investigates the impact of moisture content of rock joint infill material and the impact it has on the shear strength of the joint in comparison to the impact of normal loading and infill thickness.

CHAPTER 2: LITERATURE REVIEW

2.1 Introduction

There has been extensive previous research into the effects of various joint and infill combinations on the overall shear strength. The use of rock-like specimens has allowed for more control testing parameters. Key parameters for such testing have included: the asperity profile or shape, asperity height or angle, rock joint profile (horizontal or dip-based), initial infill material properties, infill thickness, infill moisture content, and loading. For this project the asperity profile, asperity height, rock joint profile (horizontal) and initial infill material properties will be held constant, with independent variables of infill thickness, infill moisture content, and normal loading. The establishment of these independent control variables is key to guiding and driving project outcomes.

2.1.1 Asperity Profile and Specimen Design

Prior studies have used a range of asperity profiles, mould design shapes and infill thicknesses. Cao, Deng, Chen & Fu (2018) cast rectangular rock-like specimens (150 mm by 150 mm by 150 mm) with an interlocking sawtooth surface with six teeth across a 150 mm surface. The specimen profile included a sawtooth width of 25 mm and asperity angles of 25°, 40° and 55°. The specimen was cast using 42.5 Portland Cement with fine sand (maximum particle size of 2 mm) and water weight ratio of 2:2:1, which was allowed to set in the mould for 24 hours before curing for 28 days in a controlled curing box to increase stability and better represent the properties of rock mass.

Jahanian & Sadaghiani (2015) also used rectangular sawtooth specimens (150 mm by 150 mm by 180 mm total high); however, asperity angles of 30° and 45° were used with an asperity base length of 20 mm. These specimens were cast using gypsum plaster mixed with water at a 1:1 ratio (by weight) to reflect the properties of soft rock joints such as limestone, shale and mudstone. Once cast these specimens were cured for one day in a 90°C oven before undergoing a seven-day cure at a consistent 25°C and humidity of 60%. During testing it was found that the shear strength of Type 1 (30° asperity angle) joints was impacted less by the effect of interlocking asperity profiles than Type 2 (45° asperity angle) joints. As such, the shear strength of joints with lower asperity angles are more likely to be impacted by the infill material properties, especially as higher infill thicknesses.

Alternative testing methods used a circular dip-based sawtooth surface rather than a horizontal surface as shown in Figure 6 (Indraratna, Jayanathan & Brown 2008). This study used a 60° dip angle and 2 mm

asperity height to minimise damage to the specimen. The specimens were cast using a 5:3 gypsum plaster to water (by weight) to represent sedimentary rocks with a low porosity. They were then vibrated to release entrapped air and allowed to set for a minimum of one hour before being removed from the mould and cured in a 45°C oven for two weeks.

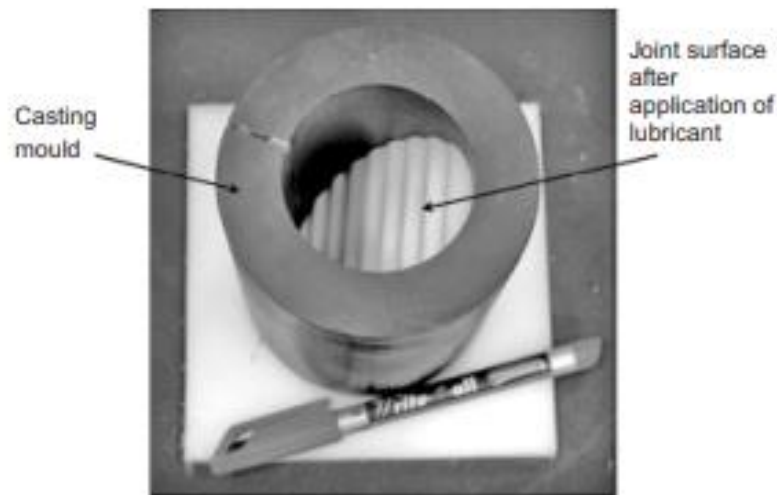


Figure 6: Combination Dip-Sawtooth Profile Mould (Indraratna, Jayanathan & Brown 2008)

Both of these previous investigations used a sawtooth profile; however, the asperity shape has been found to impact the failure mode of the surface structure. The shear strength properties of artificial rock joints have been investigated in relation to the joint surface profile and the impact of infill on failure when subjected to normal stress using the ShearTrac2 direct shear testing machine (Zohaib, Mirzaghobanali, Helwig, Azzia, Gregor, Rastegarmanesh & McDougall 2020). This study compared the effects of triangular asperity profiles with plain and sinusoidal asperity profiles (Figure 7). This investigation found that the plain profile provided the least resistance to shear due to having no interlocking profile, and the sinusoidal profile resulted in a more consistent shear strength than the triangular profile. The specimens used in this investigation had a diameter of 63.5 mm and were cast using a grout mixture consisting of Portland Cement (0.1 kg) to sand (0.334 kg) to water (0.072 kg) per sample. Once cast the specimens were left for a minimum of 24 hours before the mould forms were removed and specimens placed in a curing room for a minimum of 28 days for strength development.



Figure 7: Sawtooth and Sinusoidal Joint Profiles (Zohaib, Mirzagherbanali, Helwig, Azzia, Gregor, Rastegarmanesh & McDougall 2020)

The joint roughness coefficient (JRC) has been found to be another influencing factor on the design and testing of various asperity profiles. The JRC was developed by Barton & Choubey (1977) as a numerical representation of the profile of rock joints as shown in Figure 8.

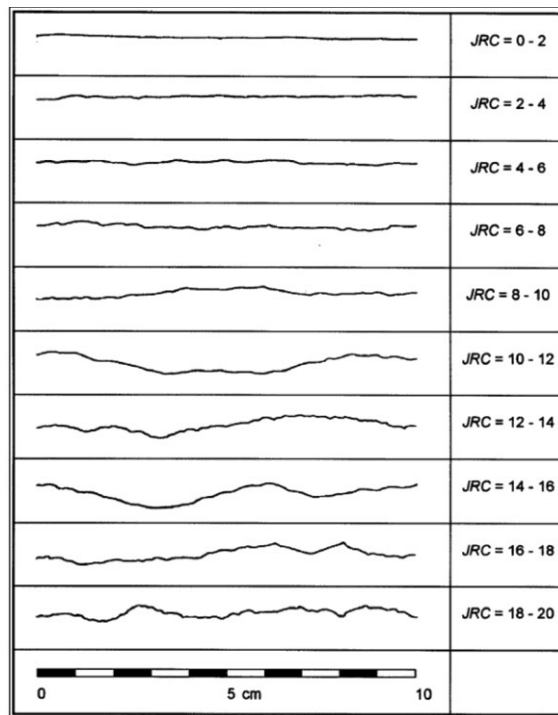


Figure 8: Joint Roughness Coefficient (JRC) (Barton & Choubey 1977)

As the key objectives of this project are focused on the impact of moisture content, normal loading and infill thickness, a single uniform triangular (sawtooth) asperity profile was used and remain constant through testing. While JRC has been a focus of some investigations into the shear strength of rock joints,

it is not considered a contributing factor in this project as a single joint profile was used throughout the shear testing. However, future project expansion could include the impact of JRC on the shear strength of rock joints, in combination with the influence of infill moisture content.

2.1.2 Infill Thickness

The infill thickness to asperity height (t/a) ratio is a common factor of consideration. This relationship is shown in Figure 9.

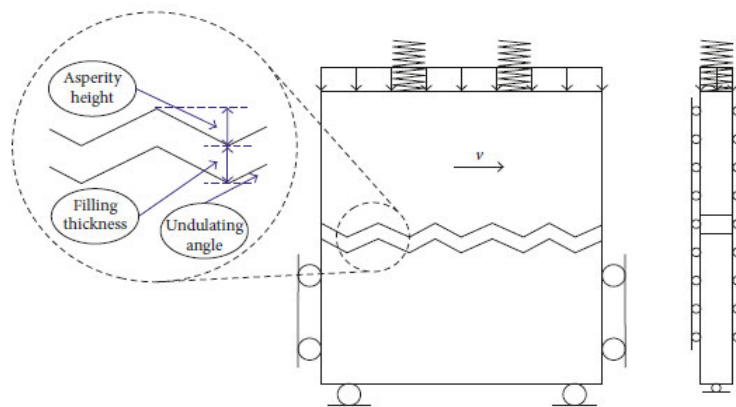


Figure 9: Generalized Testing Model (Wang, Wang & Zhang 2018)

In a 2005 study the t/a ratio was varied to determine its effect on the shear strength properties of the joint (Indraratna, Welideniya & Brown 2005). It was found that asperity interference influenced the shearing properties at all ratios. However, at higher infill thicknesses ($t/a > 1$) the impact of the asperity profile on the shear strength of the joint was reduced. The outcomes of Zohaib, Mirzaghobanali, Helwig, Azzia, Gregor, Rastegarmanesh & McDougall (2020) supports the above conclusion that the thickness of the infill influences the controlling factors that impact shear strength of the joint, over the asperity profile and height, when the infill thickness is greater than the asperity height due to no significant friction between the joint surfaces. However, for sawtooth (triangular) joint surfaces where the thickness of infill was less than the asperity height (i.e. $t/a < 1$) both the joint strength and infill influenced the final shear strength. For plain and sinusoidal joint profiles, the presence of infill has minimal impact on the shear strength as there is minimal friction to begin with. This is further supported by Shrivastava & Rao (2017) where they found that an increase in the t/a ratio resulted in a decrease of the shear strength of the rock joint, regardless of the boundary conditions investigated.

Other key outcomes in relation to infill thickness and asperity height included (Zohaib, Mirzaghobanali, Helwig, Azzia, Gregor, Rastegarmanesh & McDougall 2020):

- Maximum shear stress occurring at the maximum contact of the joint surfaces (Figure 10a) when $t/a=0$ (clean joint).
- As the surface contact area decreased the shear stress decreased (Figure 10b) until minimum shear stress occurred where the joint was no longer interlocked (i.e. the tips of the joints surfaces were contacting) as shown in Figure 10c.
- Increased asperity height resulted in an increased shear stress when maximum contact occurred.
- Where the thickness of infill was equal to the asperity height (i.e. $t/a=1$), the infill material predominately controlled the shear strength.
- As the infill thickness increased the damage to the triangular joint profile decreased due to decreasing contact.

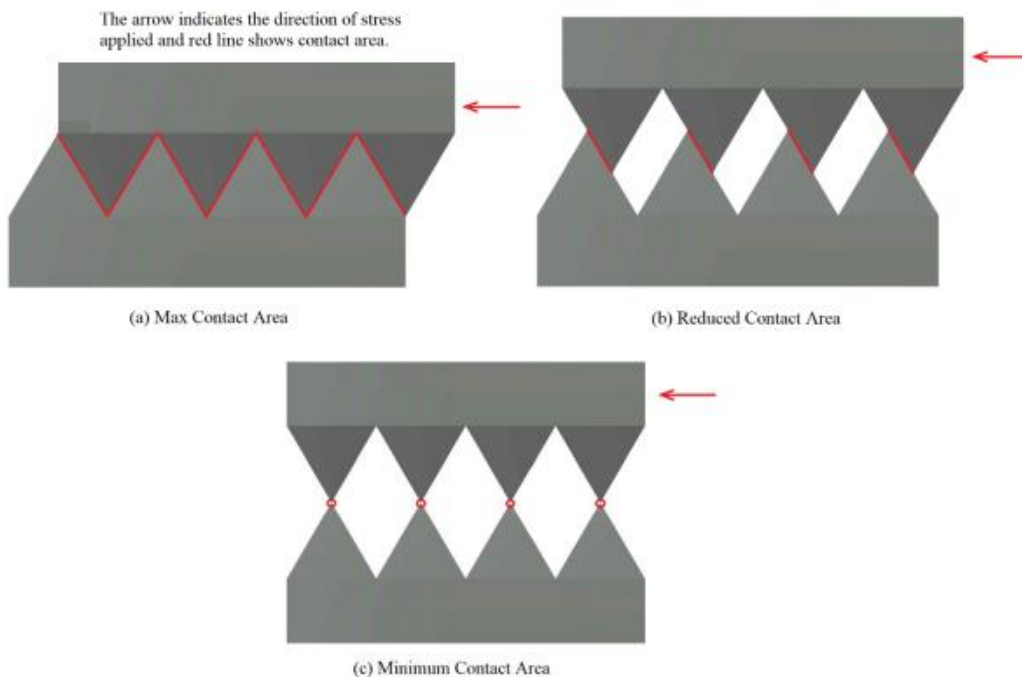


Figure 10: Interlocking Behaviour of Sawtooth Joints (Zohaib, Mirzaghobanali, Helwig, Azzia, Gregor, Rastegarmanesh & McDougall 2020)

2.1.3 Infill Material

Infill material is a common variable to experimental testing, and soils are commonly used for testing to represent real work conditions more accurately. However, natural soil material can be problematic for conceptual investigation as it is highly variable. The introduction of an infill material allows for the surfaces to slide at a lower shear stress due to decreasing the friction between joint surfaces (Zohaib, Mirzaghobanali, Helwig, Azzia, Gregor, Rastegarmanesh & McDougall 2020); thus, decreasing the shear strength of the rock joint in comparison to clean rock joints of the same surface properties.

Infill material used in testing have included: silty-clay (Indraratna, Jayanathan & Brown 2008), sandy-clay (Jahanian & Sadaghiani 2015), bentonite (Indrarathna, Welideniya & Brown 2005), and plaster (Cao, Deng, Chen & Fu 2018). Considerations such as over-consolidation (Indraratna, Jayanathan & Brown 2008) and full saturation have also been investigated. Regardless of the infill material used, it is important to classify the infill and determine the related characteristics such as liquid limit, plastic limit, cohesion, and stress friction angle (Indraratna, Premadasa & Brown 2015). In addition, the JRC was determined in many studies as an influencing factor. Key soil characteristics of Dafalla's (2012) research included the liquid limit, plastic limit, plasticity index, maximum dry density, and optimum moisture content.

The shear strength of soils is defined as the maximum resistance of soil to shear stress (i.e. the resistance to sliding forces within the soil mass) (Craig 2004, p. 91). If the shear stress exceeds the shear strength of the soil mass then failure occurs. The shear strength of the soil is comprised of three key components: structural resistance of interlocking particles, frictional resistance (represented by the effective angle of internal friction (ϕ)) and effective cohesion (c).

The interlocking nature of soil mass particles is highly variable and cannot be known, and as such is ignored as a key numerical factor when determining the shear strength. The remaining two components, friction and cohesion, determine the soil type (frictional, cohesive, or frictional-cohesive) and impact on the shear strength of the soil material. As only the solid structure of soil can resist shear stress (i.e. water cannot resist shear forces), shear strength is a function of the effective strength parameters shown in Equation 1 (Craig 2004, p. 91) and is used to determine the failure envelope:

$$\tau_f = c' + \sigma_f' \tan(\phi') \quad (1)$$

$$\tau_f = \text{Shear strength (kPa)}$$

$$c' = \text{cohesion}$$

$$\sigma'_f = \text{effective normal stress (kPa)}$$

$$\varphi' = \text{effective friction angle (}^\circ\text{)}$$

The three core soil types are:

- Frictional Soils - where the cohesion is zero, $c=0$ (e.g. sand and gravel)
- Cohesive Soils - frictionless, $\varphi=0$ (e.g. saturated silt and clay in undrained conditions)
- Frictional-cohesive ($c-\varphi$) Soils – where c and φ are both non-zero values (e.g. silt and clay sand)

For this project a bentonite clay infill will be used to best represent the behaviour of clay while having the added benefit of being a commercially produced uniform product. The use of a uniform product minimizes the impact of irregularities during the testing procedure, thus promoting the validity of the findings in relation to the main variable of moisture content. In addition, the use of a uniform product helps to promote a more even saturation effect through the infill material. If a natural clay product were used instead, the results may be impacted by inconsistencies in the soil material and non-moisture related variations between each tests infill.

2.1.4 Effect of Moisture Content

Current research on the impact of moisture content on the shear strength of infilled rock joints has been primarily focused on the critical condition of fully saturated soil. General research on the impact of moisture content on the shear strength properties of soil has generally shown that as the moisture content increased the shear strength decreased.

Dafalla (2012) investigated the effect of moisture content on the shear strength characteristics of stabilized soils (in general rather than as part of the impact on rock joint stability). The key characteristics of the soil material (liquid limit, plastic limit, plasticity index, maximum dry density, and optimum moisture content) were key to determining the relationship and impact of moisture content on the shear strength properties. As the moisture content was increased the shear strength decreased. This is due to the impact of the moisture content on the cohesion (c) and angle of internal friction (φ), which directly influences the shear strength properties of the soil.

Zyrdoń, Wojciechowska-Dymańska, Gruchot & Tomasz (2017) investigated the influence of moisture content on the shear strength properties of cohesive soils. This investigation concluded that higher shear strength values occurred when the moisture content of the soil was less than or equal to the optimum moisture content. This was due to the increasing moisture content decreasing the angle of internal friction. In addition, the highest values of cohesion were at the optimum moisture content. Beyond the optimum moisture content, the cohesion would be expected to decrease due to the increasing water content causing a decrease in the negative pressure of the water filling soil material voids (Craig 2004, p. 4).

This, in combination with the findings of the beforementioned study on the effects of infill thickness and asperity profile (Zohaib, Mirzaghobanali, Helwig, Azzia, Gregor, Rastegarmanesh & McDougall 2020), suggests that as the moisture content increases the angle of internal friction (ϕ) will decrease, and once the optimum moisture content is exceeded the shear strength of the infill material will decrease due to the impact on the cohesion (c) regardless of the infill thickness to asperity height ratio as all investigated ratios are impacted by the infill material. However, it is expected to have a more pronounced effect on ratios of t/a greater than or equal to 1 as the infill characteristics are the primary factors that influence the joints shear strength.

Bentonite clay infill material will be used on this project as clay-rich soils are problematic due to their expansive swelling behaviour. Swelling causes changes in the volume of the material in response to the presence of water. Craig (2004, p. 75) defines swelling as a result of the adsorbed water facilitating the clay minerals to undergo “recoverable compression due to increases in interparticle forces” and when the normal stress acting on the soil decreases the solid soil skeleton can expand. This causes a decrease in the pore water pressure, which then increases to a static state as flow within the soil structure occurs, resulting in a decrease in effective normal stress and an increase in volume (Craig 2004, p. 75). In areas of varying precipitation and climate conditions (e.g. extreme wet and dry seasons) this could lead to instabilities in the rock mass and further degradation of existing rock joints in a similar manner to the damage caused by freeze-thaw processes as investigated by Lei, Lin & Wang (2022).

2.1.5 Effects of Normal Loading

Two key testing conditions for the direct shear testing of artificial rock joints are Constant Normal Loading (CNL) and Constant Normal Stiffness (CNS). Liu, Zhu & Li (2020) investigated the differences in artificial rock joints in relation to joint size and shear testing conditions. The conditions used were CNL, CNS, and Constant Normal Displacement (CND). CND is considered a specific case on CNS conditions. Figure 11 shows a depiction of these three conditions.

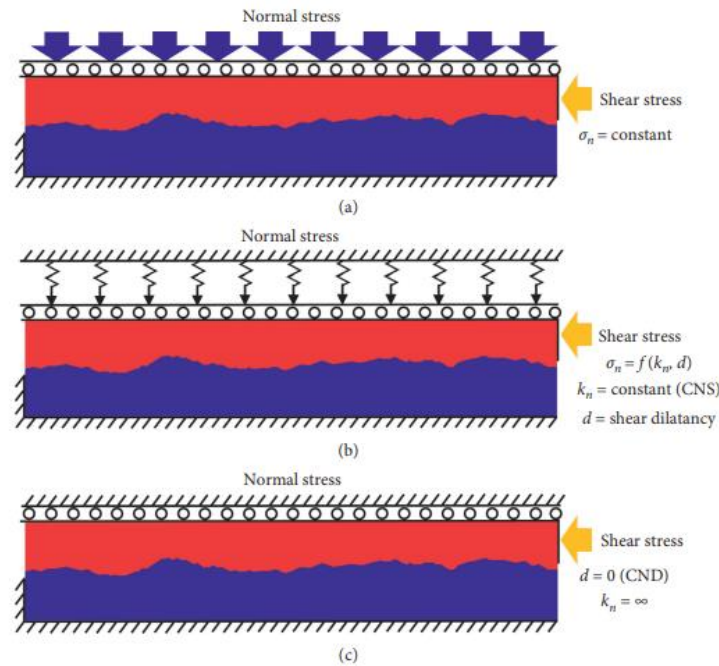


Figure 11: Loading conditions for shear tests a) CNL b) CNS c) CND (Liu, Zhu & Li 2020)

When the CNL condition is applied, the normal stress (σ_n) is held constant and the normal displacement of the shear boxes is servo-controlled (Figure 11a) (Liu, Zhu & Li 2020). CNL testing conditions are common in artificial rock joint research. However, previous research in the area has determined that CNL conditions are likely only applicable for shallow rock joints as deeper rock joints are constrained by the surrounding rock material (Liu, Zhu & Li 2020). This is further supported by Han, Jing, Jiang, Liu & Wu (2019) in relation to underground rock joint conditions. Shrivastava & Rao (2015) also support this classification of CNL boundary conditions in real-world applications.

“This particular mode of shear is suitable for situation where the surrounding rock freely allows the joint to shear without restricting the dilation or there is no dilation during the shearing process, thereby keeping normal stress constant during shear process. Shear testing under a constant normal load (CNL) boundary condition is only beneficial for cases such as non-reinforced rock slopes or planar rock joints, but natural rock joints are seldom planar...For analysis and design of tunnels, foundations and rock slopes, shear tests results under CNL condition are not appropriate. A more representative behaviour of joints would be achieved if the shear tests were carried out under boundary conditions of constant normal stiffness (CNS).” (Shrivastava & Rao 2015, p. 961-962)

CNS conditions better represent deeper rock joints where the shear dilatancy is constrained (Liu, Zhu & Li 2020). As the normal stress increases, the normal displacement is linearly deformed. Controlling factors of CNS conditions are (Liu, Zhu & Li 2020) as shown in Figure 11b and 11c:

- Applied normal stress (σ_n)
- Normal displacement of the upper pressing plate (Δd), where the lower plate is fixed, during period (Δt). CNS conditions are a special case within CNS conditions, where the normal displacement (d) is held at zero.
- Normal stiffness of the upper plate (k_n)

Liu, Zhu & Li (2020) concluded that the peak shear strength of the joint showed the same general characteristics for both CNL and CNS boundary conditions.

“When the normal stress is sufficiently high and shear dilatancy displacement is very small, the shear behaviour of rock joints under CNL and CNS conditions seems to be constant. However, for shear tests under low initial normal stress, the peak shear strength achieved under the CNS condition is much higher than that under the CNL condition.”
(Liu, Zhu & Li 2020, p. 1)

This is supported by Shrivastava & Rao (2015) who investigated the impact of CNL and CNS conditions on infilled artificial rock joints and concluded that, in general and provided all other variables remained constant, lower normal loading CNS conditions resulted in a higher shear strength than CNL conditions. However, this relationship did not hold true when the rock joints were subjected to high normal stresses, where CNS and CNL conditions resulted in the same shear strength of the joint (Shrivastava & Rao 2015). This shows that in addition to the impact of boundary conditions, the impact of the magnitude of the applied normal loading needs to be considered as it has been found to be a key contributor to the shear strength outcomes.

Tang and Wong (2015) investigated the impact of the magnitude of normal loading (0.1 MPa, 0.5 MPa and 1 MPa) on rock joints. This investigation concluded that, as the normal stress increased, the shear strength of the joint increased as shown in Figure 12. Zohaib, Mirzaghobanali, Helwig, Azzia, Gregor, Rastegarmanesh & McDougall (2020) concluded that the increase in normal loading resulted in an increased maximum shearing stress by inducing higher friction between the two rock joint surfaces.

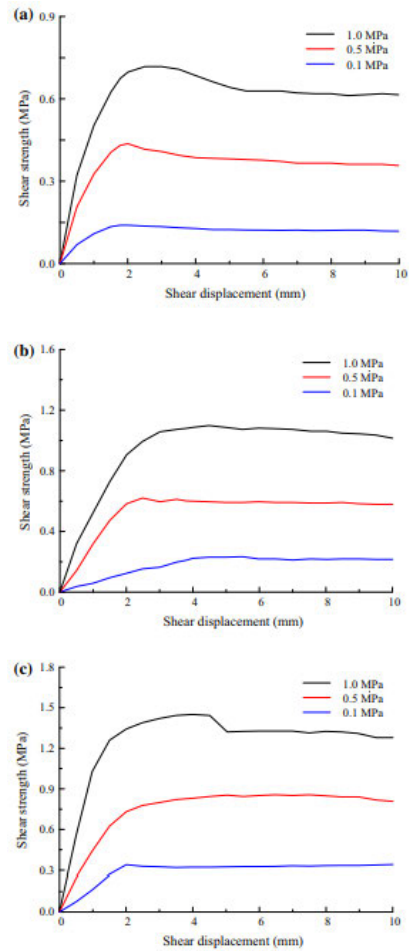


Figure 12: Impact of normal load magnitude on shear strength a) Set A b) Set B c) Set C (Tang and Wong 2015)

As CNL and CNS conditions are representative of different real-world applications it is critical to understand the scope and context of each investigation. This project will be conducted under the CNL boundary condition as it predominately focuses on the impact of moisture content on the shear strength of rock joints under unsaturated conditions. These conditions are more likely to occur in shallow rock formations due to infill and moisture fluctuations caused by water infiltration and precipitation. However, if this project were to investigate the impact of moisture content from a water table or aquifer, that would likely result in fully saturated infill material, the CNS boundary condition would be more appropriate due to increased constraint provided by the surrounding rock material at lower depths. As such, it is important to reflect on project outcomes in the intended context, as using knowledge in an inappropriate setting increases the risk of hazardous incidents, which can compromise safety and impact the economical outcome of an engineering project.

A range of normal loading magnitudes will be applied as previous research has shown that shear strength can vary under the combination of two variables rather than a single variable in isolation (e.g. the impact of CNS and CNL condition in combination with low and high normal stresses).

2.2 Testing Techniques

Previous investigations have used a range of testing methods directly related to the aim and objectives of the research topic. These testing techniques include:

- high-pressure two phase triaxial testing (Indraratna, Premadasa & Brown 2015)
- drained direct shear apparatus (to determine c' and ϕ') (Indraratna, Premadasa & Brown 2015)
- suction probe in joint to measure negative pore pressure (Indraratna, Premadasa & Brown 2015)
- direct shear testing, often under constant normal stiffness (CNS) condition (Cao, Deng, Chen & Fu 2018)

Direct shear testing will be used in this investigation as it is a well-established method, and the ShearTrac2 Shear Apparatus (Figure 13) is available for use through the University of Southern Queensland. The ShearTrac2 uses ‘two force transducers (horizontal and vertical) and two displacement transducers (horizontal and vertical) to offer feedback to provide real-time control by computer’ (Geocomp 2021). The ShearTrac2 also features servo control motor systems facilitating high precision data outcomes. The procedure used is outlined in Section 4.4 of this report, and the results analysed in Section 5.3 to 5.5 of this report.



Figure 13: ShearTrac2 Shear Apparatus

2.3 Joint Failure

In many studies it was found that the asperity angle and sawtooth height were controlling factors for failure conditions. This is due to the changes in contact area between the two parts of the specimen (Cao, Deng, Chen & Fu 2018). Figure 14 shows the three phases of shear stress in relation to shear displacement after normal force is applied during testing. Stage 1 involves increasing shear stress while the displacement remains constant. Stage 2 shows a linear relationship between the increasing shear stress and shear displacement commences causing a sliding action between the sawtooth interface. Stage 3 occurs when the tips of the sawtooth interface interact causing a peak in shear stress before failure occurs.

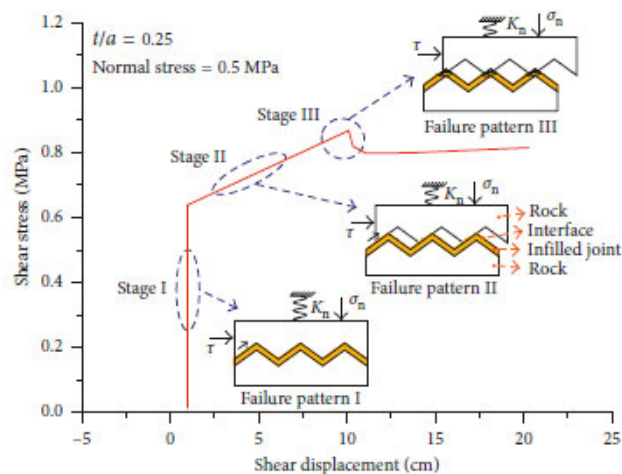


Figure 14: Failure Patterns (Wang, Wang & Zhang 2018)

Failure occurs in three forms: sliding failure, shear failure, and tensile failure (Cao, Deng, Chen & Fu 2018). The asperity angle was found to be a controlling factor in the type of failure mode. Figure 15 shows a sliding failure, which occurs when ‘the specimen slips along the joint surface and the sawtooth tip wears while it is not sheared’ (Cao, Deng, Chen & Fu 2018). Shear failure follows a similar pattern to sliding failure, except the sawtooth tip fails in a horizontal manner due to shear as shown in Figure 16. At asperity angles greater than 55° tensile failure occurs due to increased contact area and resulting frictions (Figure 17). Tensile failure occurs when the friction forces and bending moment result in cracking at the sawtooth base. This form of failure is the most destructive. All three of these failure modes are destructive in nature and as such further research into rock joint failure is key to predicting and minimizing slope failure.

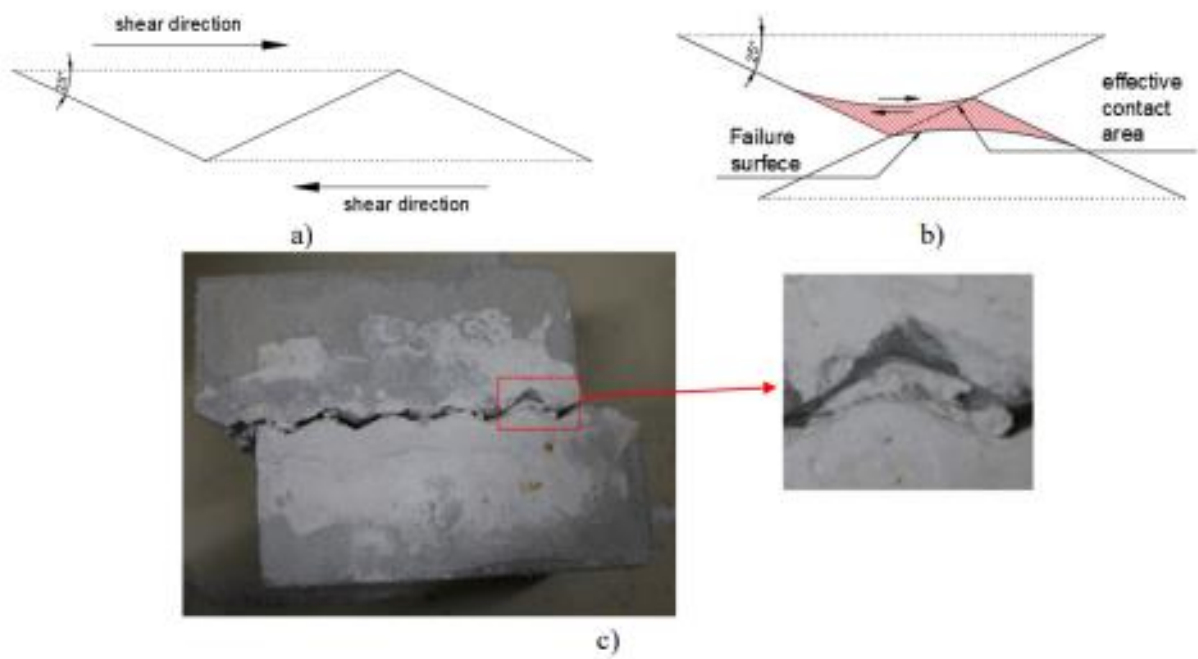


Figure 15: Sliding Failure: a) sawtooth profile b) sliding failure concept c) degraded specimen (Cao, Deng, Chen & Fu 2018)

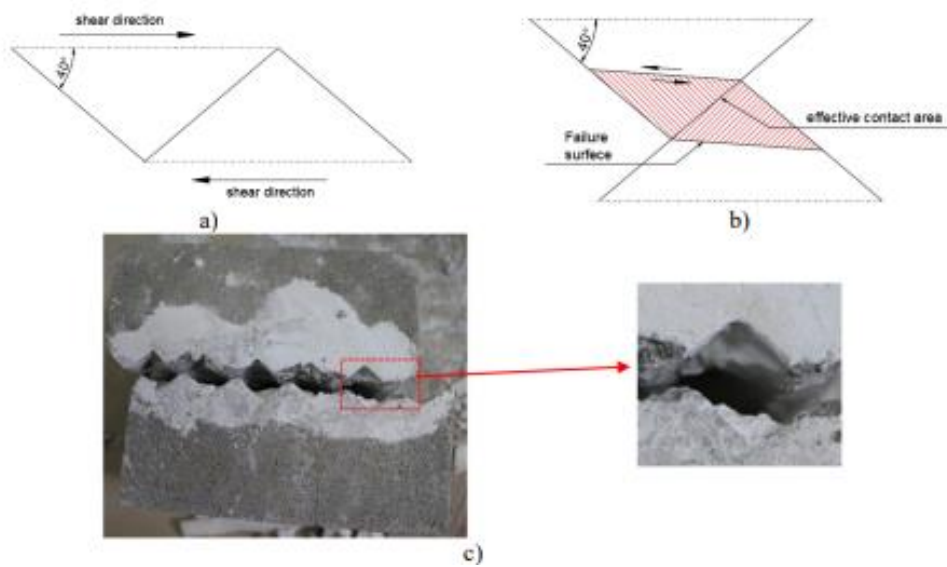


Figure 16: Shear Failure: a) sawtooth profile b) shear failure concept c) degraded specimen (Cao, Deng, Chen & Fu 2018)

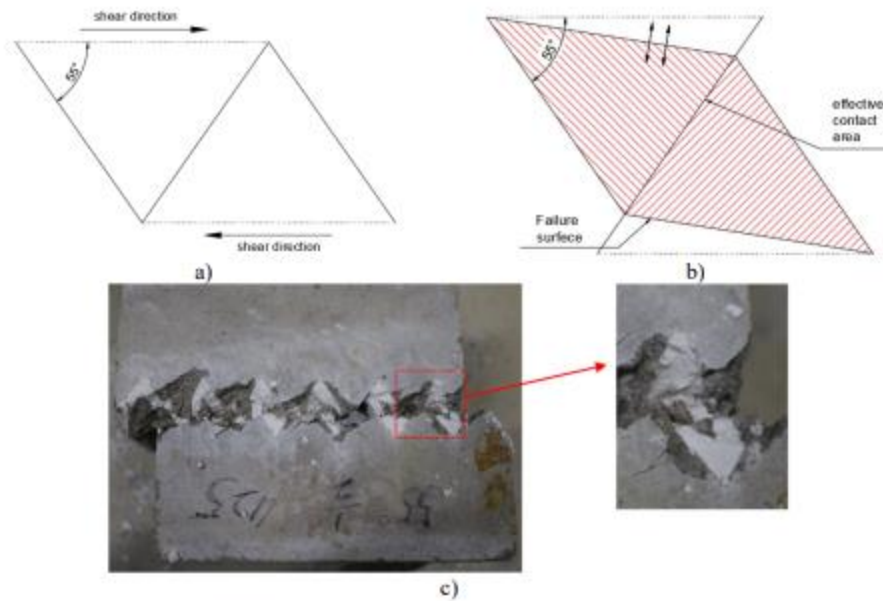


Figure 17: Tensile Failure: a) sawtooth profile b) tensile failure concept c) degraded specimen (Cao, Deng, Chen & Fu 2018)

2.4 Dangers of Idealization

It is crucial to understand the scope, limitations, and applications of this project. As such the results need to be validated due to the dangers of idealization. Unfortunately, laboratory testing results do not always reflect the mechanisms in real world scenarios. Barton (2013) outlines this issue and warns that ‘simplicity is hardly a substitute for reality’. While idealized testing parameters are key to controlling input variables in order to better understand the mechanical relationships, it is important that these relationships are understood in detail before implementation in field practices.

2.5 Knowledge Gap

A review of literature on the topic of shear strength in relation to rock joints shows extensive research has been conducted in this area. However, this research is commonly conducted under idealized conditions considering the worst-case scenario of fully saturated soil. While it is important for critical conditions to be investigated, designing purely based on critical conditions can result in overdesign and increased construction and maintenance costs over the life cycle a project. It is vital to account for the associated risk when selecting a design method and factor of safety. In high risk areas, such as northern South America and Asia, the critical conditions need to be considered. However, in lower risk areas the

engineering costs may be reduced by designing to a more contextually appropriate and necessary factor of safety due to decreased risk of instability occurring. Design needs to further account for not only the risk of the instability occurring, but the impact on the localized and regional communities. As such, continued research into the effect of infill rock joint on shear strength is important.

2.6 Conclusion

As established in Chapter 2 there has been a range of research on the impact of infill on the shear strength properties of rock joints. However, research on the effects of moisture content on the shear strength properties of rock joints has been minimal and focused on fully saturated infill material under critical conditions. While it is important to understand how an infilled rock joint behaves under critical conditions, it does not promote a quantitative understanding of how the moisture content impacts the shear strength parameters of infill with varying moisture contents. As such this project will compare the effects of infill moisture content, infill thickness and normal loading on the shear strength of the rock joint and contextualise these outcomes with those of past research.

CHAPTER 3: PROJECT DEVELOPMENT

3.1 Aims and Objectives

The aim of this project is to quantitatively analyse the effects of soil moisture content and layer thickness on rock joint shear strength properties with a comparison to the shear strength properties of clean rock joints. This will be achieved through experimentation using direct shear testing for a range of normal loadings.

3.2 Limitations

This project focuses on clean and infilled rock joints (with one type of soil, varying moisture content and infill thickness) and so will not provide the depth of data required to develop a generalized model but rather draw conclusion regarding a model for a single infill material and clean rock shear strength only (confined to the properties of the cement grout material). The testing has the potential to be expanded to include various soil and rock types with further research.

3.3 Scope

This research is restricted to investigating the effects on shear strength properties of rock joints under the following conditions:

- clean rock joint (t/a of 0) analysis to provide comparison for infilled rock joint results
- one clay soil type (commercially produced sodium bentonite clay)
- three moisture contents (0%, 10% and 16%)
- three infill thickness conditions (t/a of 0.5, 1.0, and 1.5)
- variety of normal stress values (100, 300, 500 and 700 kPa)
- testing under CNL boundary conditions

3.4 Expected Outcomes

The overarching outcome of this project was to collect testing data for the shear strength of clean rock joints and infilled rock joints (with various thicknesses and moisture contents). The expected outcomes of this research include:

- decreased shear strength as the infill thickness increases (as the thickness of infill increases greater than the asperity height, the shear strength of the infill material will become dominant/controlling)
- decreased shear strength as the moisture content of the infill increases
- the shear strength of the clean rock joint is higher than that of the infilled rock joint
- sufficient and conclusive data that can contribute to the development of a new slope stability model in relation to rock joints

The success of this project will provide information on how the shear strength of clean and infilled rock joints are affected by the moisture content and thickness of infill material as well as the magnitude of the applied normal load, thus contributing to the area of ongoing research.

3.5 Methodology

This project has six main stages:

- 1) Extensive literature review
- 2) Procurement of materials and organization of laboratory facilities
- 3) Three-dimensional moulds and cement grout casting
- 4) Testing of samples
- 5) Data analysis and modelling
- 6) Dissertation report

The aim of the extensive literature review is to investigate the past and current research into the shear strength behaviour of clean and infilled rock joint under a range of conditions, and how this knowledge can be applied in real-world scenarios. By doing so a gap in the current research knowledge available was identified and chosen for expansion in the project. The core conditions investigated include:

- Asperity profile and specimen design
- Infill thickness
- Infill material
- Moisture content
- Normal loading
- Testing techniques
- Joint failure criteria

Procurement of the following supplies was carried out personally, sourcing the materials from direct and retail suppliers for:

- Three-dimensional printing: Anycubic 405-micron UV resin, and methylated spirits (as a cleaning solvent).
- Artificial rock joints creation: polyvinyl chloride (PVC) pipe (nominal diameter of 65 mm), duct tape, painters tape, industrial grease, sand, cement, and 40-grit sandpaper.
- Infill material: sodium bentonite clay.

Laboratory facilities were organised through the University of Southern Queensland in collaboration with the academic project supervisor and university technical officer's. A detailed list of the resources used throughout the testing in the project are listed in the experimental design and procedures outlined in Chapter 4. Civil Materials Laboratory facilities and resources included use of:

- Testing apparatus' (e.g. ShearTrac2, Consolidometer, Cone Penetrometer),
- Curing room,
- General laboratory tools (e.g. heat-resistant and corrosion resistant containers, electric mixer, palette knives, compression testing sample moulds),
- Measuring tools (e.g. digital vernier calipers, balances, measuring cylinders),
- Personal protective equipment (PPE) (e.g. gloves, glasses, hearing protection), and
- Assistance from the laboratory staff.

The three-dimensional design was completed using the student version of *Autodesk Fusion360*. The printing of the asperity profile was conducted on a stereolithography (SLA) printer. This provided a smooth finished surface and minimised interaction between the clay infill material and potential layer lines. The casting and curing of the artificial rock joints were completed in the University of Southern

Queensland’s civil engineering laboratories at the University of Southern Queensland’s Springfield Campus.

The infill testing and direct shear testing of the artificial rock joints was conducted in the University of Southern Queensland’s civil engineering laboratories using a combination of university and personal resources and materials. Testing was conducted in general accordance with Australian (AS) Standards, where possible. In addition, all testing results will be labelled and recorded logically to maximise validity of analysis.

The results and analysis of the data from the abovementioned testing is summarised in Chapter 5. The analysis includes use of tabulated and graphical data to draw conclusions. A summary of the project outcomes is given in Chapter 6.

Table 2 shows a summary of the above tasks.

Table 2: Outline of required steps

Step 1	Extensive literature review
1A	Collection of relevant literary materials
1B	Summarize and analyse the content of relevant materials
1C	Compare and contrast the literary materials
1D	Make concluding decisions on what information and processes will be used in this project.
Step 2	Procurement of materials and organization of laboratory facilities
2A	Select and source testing materials (cement, sand, infill and any additives)
2B	Confirm availability of laboratory and testing resources
2C	Complete all required laboratory safety and induction requirements
Step 3	Three-dimensional moulds and concrete casting
3A	Computer model the three-dimensional moulds
3B	Print three-dimensional moulds
3C	Casting of concrete in printed moulds with a minimum setting time of 24 hours
3D	Curing of concrete for a minimum of 28 days in controlled curing facility
Step 4	Testing of samples
4A	Preparation and preliminary testing of infill material to determine soil characteristics in accordance with AS1289
4B	Preparation of shear testing sample (including infill material between the two halves of the concrete simulated rock joint)
4C	Direct shear testing of clean and infilled rock joints
4D	Collection of data (shear stress, displacement and normal stress)

Step 5	Data analysis and modelling
5A	Collation of all data obtained during testing
5B	Preparation of graphical representations to determine relationship between testing variables
Step 6	Dissertation report
6A	Write up of dissertation report (submission and review by supervisor, adapt based on feedback)
6B	Attend the ENG4903 seminar to present findings, analysis and implications
6C	Complete dissertation report for final submission

3.6 Collection of Data

Data collection is a key component to this study. The data required in this study ranges from preliminary to final results. Preliminary testing will be used to determine infill characteristics including particle size distribution, particle density, moisture content, liquid limit, plastic limit, shrinkage limit, compression index, swell index, angle of internal friction, and cohesion. This data will allow for the appropriate comparison of results and the formation of rational conclusions based on the final data. Dependent variables that need to be controlled for the direct shear testing of the artificial rock joint are moisture content, infill thickness, and applied normal stress. The independent variables of this investigation are shear stress and displacement, and the type of failure mechanism (sliding, shear or tensile) will be noted.

The experimental design and procedures used in this investigation are outlined in Chapter 4:

- 4.1 Mould Design and Formation,
- 4.2 Compression Testing,
- 4.3 Infill Properties, and
- 4.4 Direct Shear Testing of Rock Joints.

The results of the testing procedures are outlined in Chapter 5, and associated Appendices:

- 5.1 Compressive Strength Testing,
- 5.2 Infill Properties,
- 5.3 Direct Shear Testing of Rock Joints (Shear Displacement vs Shear Stress),
- 5.4 Direct Shear Testing of Rock Joints (Shear Displacement vs Normal Stress),
- 5.5 Direct Shear Testing of Rock Joints (Shear Displacement vs Normal Displacement).

3.7 Modelling Procedure

Graphical modelling of the results will be completed using Microsoft Excel. This modelling will incorporate shear stress, normal stress, and normal displacement in relation to the shear displacement of the artificial rock joint. Theoretical modelling of the slope stability implications using UDEC software will be incorporated if time permits. This software will be available through my supervisor (Ali Mirzaghobanali).

3.8 Project Feasibility and Study Justification

Numerous studies on the topic of shear strength of clean and infilled rock joints have been completed. However, these studies largely focus on the variable of infill thickness or type under critical conditions (full saturation). While it is important to understand the critical conditions, not all projects need to be designed to this level and economic impact should be considered. Projects in high-risk areas (such as in South America and Asia) need to be designed based on a factor of safety greater than one. However, in lower risk areas this level of design may not be required, as such a lower factor of safety could be used to achieve a more economically viable outcome (subject to engineering design standards and guidelines). In all projects, a full assessment of the risk level associated with rock joint and slope stability needs to be thoroughly conducted to determine an appropriate factor of safety.

CHAPTER 4: EXPERIMENTAL DESIGN & PROCEDURE

4.1 Mould Design and Formation

4.1.1 Asperity Profile and 3D Modelling

The ShearTrac2 shear apparatus requires specimens to have a diameter of 63 mm and overall height of 36 mm. This diameter will determine the internal diameter of the casting mould, and this overall height must include the top and bottom interlocking cement grout rock joints and the thickness of the infill material.

As the key focus of this project is the impact of moisture content on the shear strength, an asperity angle of less than 30° is used to minimise the impact of joint friction and aim for type 1 sliding failure rather than shear or tensile failure of the rock joint (as discussed in Section 2.1.1 and 2.3). As such, a single uniform triangular (sawtooth) asperity profile will be used, and the parameters of this profile are found in Table 3.

Table 3: Asperity Profile Characteristics

Characteristic	Value
<i>Asperity Height</i>	2 mm
<i>Asperity Length</i>	7 mm
<i>Asperity Angle</i>	29.7°

Autodesk Fusion360 3D CAD program was used to model the interlocking asperity profile within the confines of a 63 mm diameter. The final 3D modelled profile is shown in Figure 18 The profile was printed on the *Anycubic Mono X (4K)* SLA printer using Anycubic's standard grey UV resin at a layer height of 50 microns. The 3D printed profile was then washed in methylated spirits and left to dry before curing in the *Anycubic Wash & Cure Plus* as shown in Figure 19.



Figure 18: 3D model of interlocking sawtooth mould

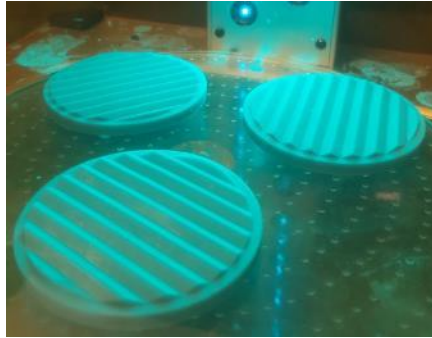


Figure 19: 3D printed asperity profile and Resin Curing Process

4.1.2 Mould Formation and Preparation

Polyvinyl chloride (PVC) Drain waste & Vent (DWV) pipe (nominal diameter of 65 mm (DN65)) was cut at 19 mm lengths using a drop saw to form the vertical component of the mould (Figure 20). The asperity mould was fixed to the end of the 19 mm lengths of PVC pipe, using a combination of duct tape and painters tape, to form the moulds for the cement grout ‘rock joint’ as shown in Figure 21. As this PVC pipe has an internal diameter of 62 mm, the pipe was split vertically (using a rotary tool and cutting disk) to facilitate the 63 mm diameter of the asperity mould due to the specimen size requirements of the ShearTrac2 apparatus. This, in combination with applying all-purpose industrial grease to the internal surfaces of the mould (Figure 22), allowed for easy removal of the cast specimen after an initial setting time. The grease on the internal surfaces of the mould was applied with care to avoid impacting the desired profile of the mould. In addition, five 3-part cubic moulds (each part was 40 mm by 40 mm by 40 mm) were oiled to cast samples to be used for uniaxial compression testing to determine the compressive strength of the cement grout mix as shown in Figure 23



Figure 20: 19mm DN65 DWV PVC pipe lengths

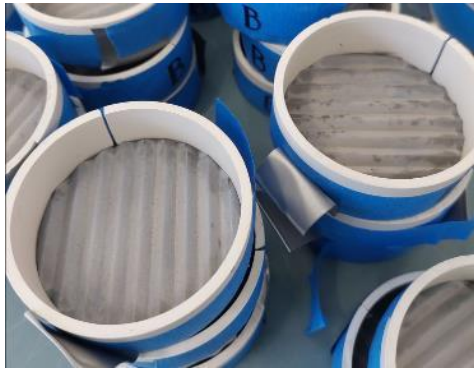


Figure 21: Taped Moulds



Figure 22: Greased Moulds



Figure 23: UCS Sample Moulds

4.1.3 Casting

Initially, a commercially available preblended mix of 20-25% Portland Cement and 75-80% Silica Sand was used. However, this produced a very weak specimen that crumbled when being removed from the moulds as shown in Figure 24. As such a custom mix of sand, cement and water was used as outlined in Table 4 and grease was added to the asperity profile to decrease adhesion of the cement mix to the resin profile.



Figure 24: Demoulding of Initial Cement Grout Mix

Table 4: Custom Cement Grout Mix

Component	Product Used	Characteristics	Amount	Percentage by weight
<i>Sand</i>	Easy Mix Synthetic Turf Infill Sand  (EasyMix 2019)	As per Technical Data Sheet (EasyMix 2020) <ul style="list-style-type: none"> • Double washed to remove clay and silt • 0.2 to 0.6 mm particle size • Kiln dried to remove organic matter • Sieved in accordance with AS1141.11 • sampled in accordance with AS1141.3.1 	900 g	~65.2%
<i>Cement</i>	Bastion Building Materials General Purpose Cement  (Bunnings n.d.)	<ul style="list-style-type: none"> • 100% Portland Cement 	300 g	~21.7%
<i>Water</i>	Potable Tap Water	<ul style="list-style-type: none"> • Room temperature (approximately 24°C) 	180 ml	~13.0%

The above cement grout mixture was thoroughly combined using an electric stand mixer as shown in Figure 25.



Figure 25: Cement Grout Mixing

The cement grout mixture was made in batches to improve workability. Immediately after each batch was poured each mould was manually agitated to release trapped air bubbles and liquify the mixture to allow for easier flow into the asperity profile. Care was taken to not damage the 3D printed mould profile during this process. This process was repeated until all moulds were filled (Figure 26).



Figure 26: Freshly Poured Moulds

The artificial rock joints were left for 36 to 48 hours to set (Figure 27) before being demoulded and labelled '1' (top portion of the joint (Figure 28)) and '2' (bottom portion of the joint (Figure 28)). The cube samples to be used for compressive strength testing were labelled with a day (7, 14, 21 or 28 days) and date to be tested. The samples were then left to cure for 28 days in a temperature and humidity-controlled curing room (Figure 29).



Figure 27: Set Artificial Rock Joints



Figure 28: Demoulded Sample top (left) bottom (right)



Figure 29: Demoulded Samples in curing room

4.2 Compression Testing

Using the 40 mm by 40 mm by 40 mm cubes the uniaxial compressive strength of the cement grout mix was investigated in general accordance with *AS1012.9 Methods of testing concrete – Method 9: Compressive strength tests – Concrete, mortar and grout specimens* (Standards Australia 2014a). Figure 30 shows the set up of the sample prior to testing. The uniaxial compression testing was run at a loading rate of 0.5 kN/s and the maximum compressive strength recorded. This testing was completed at 7, 14, 21 and 28 days, with a minimum of three samples on each occasion to determine to average compressive strength of the cement grout mix. Appendix C shows the images of before the test, after the test, and the results of the test. These results are summarised in Section 5.1.

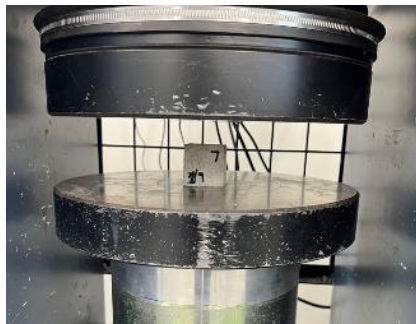


Figure 30: Compression testing set up

4.3 Infill Properties

Preliminary Testing was undertaken in accordance Australian Standards. All general definitions and requirements are as per *AS1289.0 Methods of testing soils for engineering purposes – Part 0: Definitions and general requirements* (Standards Australia 2014b). Sample sizes and preparation were in accordance with *AS1289.1.1 Methods of testing soils for engineering purposes – Method 1.1: Sampling and preparation of soils – Preparation of disturbed soil samples for testing* (Standards Australia 2001), unless otherwise stated. The processes and methods are outlined in this chapter, and the results are summarised in Chapter 5. Risk and hazard control mechanisms were used throughout the tests in this project (e.g. personal protective equipment) as outlined in the Risk Assessment (Appendix B). The infill properties investigated include:

- particle size distribution (d)
- soil particle density (ρ_s)

- moisture content (w)
- liquid limit (w_{CL})
- plastic limit (w_p)
- shrinkage limit (SL)
- compression index (C_c)
- swell index (C_s)
- angle of internal friction (effective) (ϕ')
- cohesion (c')

4.3.1 Infill Particle Size Distribution (d)

The particle size distribution was determined as per *AS1289.3.6.1 Methods of testing soils for engineering purposes – Method 3.6.1: Determination of the particle size distribution of a soil – Standard method of analysis by sieving* (Standards Australia 2009a). As the infill in fine-grained sodium bentonite clay, the procedure for fine sieve analysis in *Section 5.6* of *AS1289.3.6.1* was used (i.e. particles smaller than 2.36 mm) as outlined below. Sieve sizes of 0.045, 0.053, 0.075, 0.15, 0.30, 0.425, 0.60 and 2.36 mm were used for this analysis. While sieve sizes of 0.045 and 0.053 mm are not standard to the analysis as outlined in *AS1289.3.6.1*, these were added due to the fine-grained nature of the clay infill material. As particle size is not a critical attribute of the project and is only used as a descriptive characteristic of the infill material, a hydrometer test was not performed for a detailed fines particle distribution. The results of the sieve analysis are outlined in *Section 5.2.1* of this report.

In accordance with *AS1289.3.6.1* (Standards Australia 2009a) the following equipment was used for the sieve analysis:

- A drying oven in accordance with *AS1289.0* specifications,
- A heat-resistant and corrosion-resistant container,
- A suitable balance within the limit requirements of ± 0.5 g,
- Sieves of required sizes in compliance with *AS1152*. For this analysis sieve sizes of 0.045, 0.053, 0.075, 0.15, 0.30, 0.425, 0.60 and 2.36 mm were used,
- Sieve pan and lid,

- Sieve brushes for cleaning, and
- Mechanical sieve shaker.

The following procedure for determining the particle size distribution of the soil was used in accordance with *AS1289.3.6.1* (Standards Australia 2009a):

1. A 200 g soil sample (m_{total}) was weighed and prepared in accordance with *Section 5.7* of *AS1289.1.1*.
2. The sieves were thoroughly cleaned to remove any past debris.
3. Each sieve and the pan were weighed, and the initial mass of each sieve recorded (m_{initial}).
4. The sieves were stacked in the following order:
 - a. Pan at the bottom
 - b. 0.045 mm
 - c. 0.053 mm
 - d. 0.075 mm
 - e. 0.150 mm
 - f. 0.300 mm
 - g. 0.425 mm
 - h. 0.600 mm
 - i. 2.360 mm
5. The sample was placed on the 2.36 mm sieve, and lid secured on the top.
6. The stack of sieves was placed on the mechanical sieve shaker as shown in Figure 31.



Figure 31: Mechanical Sieving

7. After applying ear protection, the mechanical sieve shaker was turned on for 2 minutes. A longer period was not used to minimise the impact of grinding of the clay particles.
8. The stack of sieves was removed from the sieve shaker.
9. Each compartment was carefully removed, weighed, and mass recorded (m_{final}) from the top sieve to the bottom pan, being careful not to disturb or lose particles caught on the sieve as shown in Figure 32.



Figure 32: Soil particles on sieve

The data collected from the sieve analysis was analysed using the following equations derived from AS1289.3.6.1 (Standards Australia 2009a). The soil mass retained on the sieve was determined using Equation 2.

$$m_{retained} = m_{final} - m_{initial} \quad (2)$$

$m_{retained}$ = mass of soil retained on sieve (g)

$m_{initial}$ = initial mass of sieve (g)

m_{final} = mass of sieve and retained soil after mechanical sieving (g)

The mass passing each sieve was determined using the Equation 3.

$$m_{passing} = m_{previous} - m_{retained} \quad (3)$$

$m_{passing}$ = mass of soil passing through sieve (g)

$m_{previous}$ = mass of soil passing previous sieve (g)

$m_{retained}$ = mass retained on sieve (g)

The percentage passing each sieve was determined using Equation 4 and reported to the nearest 1% as per *AS1289.3.6.1* (Standards Australia 2009a):

$$Passing (\%) = \frac{m_{passing}}{m_{total}} \times 100 \quad (4)$$

$Passing$ = percentage of total soil mass passing sieve (%)

$m_{passing}$ = mass of soil passing through sieve (g)

m_{total} = total soil sample mass (g) = 200 g

4.3.2 Infill Soil Particle Density (ρ_s)

The particle density of the infill was determined in general accordance with *AS1289.3.5.1 Methods of testing soils for engineering purposes – Method 3.5.1: Soil classification tests – Determination of the soil particle density of a soil – Standard method* (Standards Australia 2006). As the infill is fine-grained sodium bentonite clay (particles less than 2.36 mm), the procedure for determining particle density from *Section 5.1* of *AS1289.3.5.1* was used, and results calculated using *Section 6* of *AS1289.3.5.1*. The results of the sieve analysis are outlined in Section 5.2.2 of this report.

In general accordance with *AS1289.3.5.1* (Standards Australia 2006) the following equipment was used for the particle density analysis; however, some equipment needed to be substituted due to available resources:

- A drying oven in accordance with *AS1289.0* specifications,
- A heat-resistant and corrosion-resistant container,
- A suitable balance within the limit requirements of ± 0.05 g,
- Digital pin thermometer with a calibration of a minimum of 1°C steps and variation not exceeding 0.5°C,
- Vacuum pump,
- Two (2) flasks of 500 ml capacity and stoppers,
- Distilled water in wash bottle,
- Constant room temperature, and
- Pressurised air.

The following procedure for determining the particle density of the soil was used in accordance with *AS1289.3.5.1* (Standards Australia 2006):

1. The sample of the soil passing a 2.36 mm sieve was prepared in accordance with *Section 5.5 of AS1289.1.1*.
2. Each flask was washed with water and dried using pressurised air to remove any remaining water or particulates.
3. Each flask was marked, using erasable marker, with different test numbers ('1' & '2').
4. The mass of each flask (with the respective stopper) was record (m_1).
5. Approximately one-third of the volume of each flask with filled with the soil sample, and the mass of the flask, dry soil and stopper recorded (m_2).
6. Water was added to each flask to approximately two-thirds full (Figure 33) and left to soak for a minimum of 24 hours (Figure 34).



Figure 33: Water added to two-thirds full (before 24 hours)

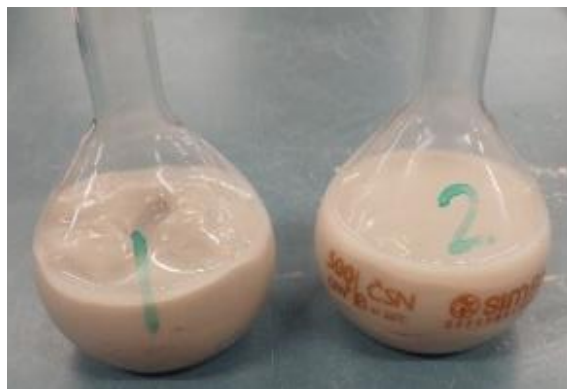


Figure 34: Water and soil mixture (after 24 hours)

7. A partial vacuum was carefully applied to each flask to remove entrapped air for a minimum of 20 minutes (Figure 35), taking care to:
 - a. roll the bottle to assist in releasing trapped air,
 - b. not allow the trapped air to bubble too aggressively, which could lead to soil mass being lost to the vacuum, and
 - c. not build a large negative pressure inside the flask to reduce the risk of flask implosion (the vacuum was periodically removed to allow pressure to normalise inside the flask).
In addition, safety glasses were worn in case of flask implosion.



Figure 35: Applying partial vacuum to remove entrapped air

8. Each flask was filled with water to the 500 ml mark and allowed to reach thermal equilibrium with the room, the final temperature was recorded. During this step water was added when required to maintain the water level at the 500 ml mark.
9. The stopper was added to the flask and the outside of the bottle dried, taking care to not impact the test labelling numbers. The mass of the bottle, stopper and contents was recorded (m_3).
10. The content of each flask was emptied, and the flasks cleaned.
11. Each flask was filled with water to the 500 ml mark and allowed to reach thermal equilibrium with the room to the temperature recorded in Step 8. During this step water was added when required to maintain the water level at the 500 ml mark.
12. The stopper was added to the flask and the outside of the bottle dried, taking care to not impact the test labelling numbers. The mass of the bottle, stopper and water was recorded (m_4).

The particle density of the soil fines sample was determined using Equation 5 (Standards Australia 2006).

$$\rho_f = \frac{(m_2 - m_1)}{(m_4 - m_1) - (m_3 - m_2)} \rho_w \quad (5)$$

ρ_f = particle density of the soil fines passing 2.36 mm sieve (g/cm^3)

$$\begin{aligned}
m_1 &= \text{mass of flask and stopper (g)} \\
m_2 &= \text{mass of flask, stopper and dry soil particles (g)} \\
m_3 &= \text{mass of flask, stopper, soil particles and water (g)} \\
m_4 &= \text{mass of flask, stopper and water (g)} \\
\rho_w &= \text{density of water (g/cm}^3\text{)} = 0.9982 \text{ (at 20}^\circ\text{C), from Table 1 of AS1289.3.5.1}
\end{aligned}$$

The combined soil particle density is given by Equation 6 (Standards Australia 2006).

$$\rho_{st} = \frac{100}{\frac{X}{\rho_f} + \frac{100 - X}{\rho_c}} \quad (6)$$

$$\begin{aligned}
\rho_{st} &= \text{particle density of the total soil sample (g/cm}^3\text{)} \\
\rho_f &= \text{particle density of the soil fines passing 2.36 mm sieve (g/cm}^3\text{)} \\
\rho_c &= \text{particle density of the soil retained on 2.36 mm sieve (g/cm}^3\text{)} \\
X &= \text{percentage by mass of soil passing 2.36 mm sieve} = 100\%
\end{aligned}$$

The particle density of the coarse soil sample (retained on a 2.36 mm sieve) is not applicable as 100% of the soil mass passes the 2.36 mm sieve (from Section 5.2.1 of this report). As such, the final soil particle density is given by Equation 7.

$$\rho_{st} = \rho_f \quad (7)$$

4.3.3 Moisture Content (w)

Infill moisture content was determined in accordance with *AS1289.2.1.1 Methods of testing soils for engineering purposes – Method 2.1.1: Soil moisture content tests – Determination of the moisture content of a soil – Oven drying method (standard method)* (Standards Australia 2005). This procedure was also used in conjunction with other appropriate standards to determine the moisture content for plastic limit, liquid limit, and consolidation tests, in addition to the moisture content of the infill material for the direct shear testing. The result of the initial moisture content test is outlined in Section 5.2.3 of this report and the results of other testing that included moisture content testing are outlined in their respective sections in Chapter 5 of this report.

As outlined in *AS1289.2.1.1* the following equipment is required:

- A drying oven in accordance with *AS1289.0* specifications,
- Three (3) heat-resistant and corrosion-resistant container, and
- A suitable balance within the limit requirements outlined in *Table 1* of *AS1289.2.1.1* (Standards Australia 2005).

The following procedure for determining the moisture content of the soil was used in accordance with *AS1289.2.1.1* (Standards Australia 2005):

1. The soil material sample is prepared in accordance with *AS1289.1.1*.
2. The mass of the clean (and dry) container was recorded (m_a).
3. The sample was placed in the container (Figure 36) and the mass of the container and soil sample was recorded (m_b).



Figure 36: Soil samples (natural state) ready for oven drying

4. The container containing the soil sample was placed in the drying oven at 106.5°C and left to dry until a constant mass was reached.
5. Once the sample was sufficiently dried the container containing the soil sample was removed from the oven and allowed to cool.
6. The mass of the container with soil sample was recorded ($m_{c(i)}$) (Figure 37).



Figure 37: Weighing of dried soil sample

7. The container with soil sample was returned to the oven and the oven was left to recover to 105°C to 110°C.
8. The sample was left for a minimum of 1 hour after the temperature had recovered.
9. Steps 5 to 8 were repeated until the loss in mass of the soil between drying period was less than 0.1% of the initial mass of the wet soil. The last recorded value was used as the mass of the container and dry soil sample (m_c).

The loss in mass as a percentage was determined using Equation 8.

$$\text{Loss in mass}_i = \frac{m_{c(i-1)} - m_{c(i)}}{m_{c(i)}} \times 100 \quad (8)$$

$\text{Loss in mass}_i = \text{percentage loss in mass (\%)}$

$m_{c(i-1)} = \text{previous mass of container and dry soil (g)}$

$m_{c(i)} = \text{current mass of container and dry soil (g)}$

The moisture content (w) of the soil material was determined using Equation 9 (Standards Australia 2005):

$$w = \frac{m_b - m_c}{m_c - m_a} \times 100 \quad (9)$$

$w = \text{moisture content of soil (\%)}$

$m_a = \text{mass of container (g)}$

$m_b = \text{mass of container and wet soil (g)}$

$m_c = \text{mass of container and dry soil (g)}$

In accordance with the reporting requirements of AS1289.2.1.1 the moisture contents reported in Section 5 are reported to the:

- nearest 0.1 where the moisture content is less than 50%;
- nearest 0.5 where the moisture content was between 50 and 100%; and
- nearest 1.0 where the moisture content was greater than 100%

4.3.4 Liquid Limit (w_{CL})

The liquid limit of the infill material was determined in accordance with *AS1289.3.9.1 Methods of testing soils for engineering purposes – Method 3.9.1: Soil classification tests – Determination of the cone liquid limit of a soil* (Standards Australia 2015). The results of the liquid limit analysis are outlined in Section 5.2.4 of this report.

In accordance with *AS1289.3.9.1* (Standards Australia 2015) the following equipment was used for the liquid limit analysis, including the equipment to determine the moisture content in accordance with *AS1289.2.1.1* (Standards Australia 2005) outlined in Section 4.3.3 of this report:

- A drying oven in accordance with *AS1289.0* specifications,
- Six (6) heat-resistant and corrosion-resistant container with lids,
- Non-absorbent container with close fitting lid,
- A suitable balance within the limit requirements outlined in *Table 1* of *AS1289.2.1.1* (Standards Australia 2005),
- Small palette knife,
- Wash bottle with potable water,
- Automatic release penetrometer,
- vernier calipers, and
- A rigid cup of diameter 55.28 mm and 45.33 mm height (Figure 38).

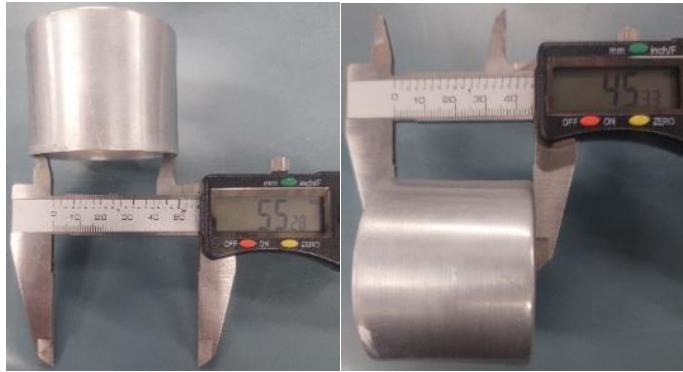


Figure 38: Rigid cup measurements a) diameter b) height

The following procedure for determining the liquid limit of the soil was used in accordance with *AS1289.3.9.1* (Standards Australia 2015):

1. As 100% of the soil passes the 0.425 mm sieve during the particle size distribution test, the natural state clay material was used without further sieving as per *Section 4(a)* of *AS1289.3.9.1*. A 250 g soil sample was weighed in the non-absorbent container with lid.
2. Using the wash bottle, potable water was added to the soil sample incrementally and mixed into a thick homogenous paste (approximately 5 minutes). The sample was covered and left to curing overnight (approximately 24 hours), allowing the water to permeate the clay soil particles. In addition, the six (6) heat-resistant containers were label the initial weight of the container (without lid) recorded.
3. The cured soil sample was remixed for 2 minutes.
4. The rigid cup was incrementally filled with the clay paste until the mixture is above the rim of the cup, taking care to use sufficient pressure to ‘exude the paste outwards to ensure removal of an air from the mixture’(Standards Australia 2015, p. 3).
5. The palette knife was held at a low angle and pushed along the surface of the cup to remove the excess material, leaving a smooth surface at the level of the rim of the cup.
6. The cup was placed under the cone of the penetrometer, and the cone manually lowered until the tip just contacts the surface of the soil sample paste and fixed in position. The dial gauge plunger was lowered to contact the top of the sliding shaft and reading zeroed (Figure 39).



Figure 39: Cone Penetrometer ready for release

7. The cone was released using the automatic release button, which is set to a 5 second release and clamp process.
8. The dial gauge plunger was carefully lowered until it met the top of the sliding shaft (Figure 40), the dial gauge reading was recorded to the nearest 0.1 mm.



Figure 40: Cone Penetrometer after release with penetration reading

9. The cone was raised out of the cup, and the soil paste returned to the bulk paste mixture. Then the cone and cup were thoroughly cleaned.

10. The paste mixture was mixed for 30 seconds, and Steps 4 to 10 repeated until the difference between subsequent tests was not greater than 1.0 mm.
11. The mean penetration of the subsequent tests was calculated, and a sample of approximately 10 g was removed to determine to moisture content of the mix in accordance with *AS1289.2.1.1* as outlined in Section 4.3.3 of this report (Figure 41) making sure to record the weight of the container with the sample. The lid was paced on the container until the end of the cone penetrometer testing to prevent moisture loss. The lids were removed prior to placing all samples in a 106.5°C drying oven.



Figure 41: Liquid Limit samples after oven drying to find moisture content

12. Steps 4 through 11 were repeated five (5) additional times using the cured sample and adding additional water incrementally and mixing for 4 minutes between test cycles (Steps 4 to 11). This provided a comprehensive set of data ranging from 13.4 mm to 25.4 mm penetration to determine the liquid limit of the material.
13. The cone penetration testing data was plotted as Cone Penetration vs Moisture Content, and linear best fit line determined. The equation of this trendline was then used to determine the Liquid Limit (moisture content when the cone penetration equals 20 mm) as shown in Section 5.2.4 of this report.

4.3.5 Plastic Limit (w_p)

The plastic limit of the infill material was determined in accordance with *AS1289.3.2.1 Methods of testing soils for engineering purposes – Method 3.2.1: Soil classification tests – Determination of the plastic limit of a soil* (Standards Australia 2009b). The final value was determined as an average of the results of the moisture contents from testing as per *Section 5* of *AS1289.3.2.1*. The results of the liquid limit analysis are outlined in Section 5.2.5 of this report.

In accordance with *AS1289.3.2.1* (Standards Australia 2009b) the following equipment was used for the plastic limit analysis, including the equipment to determine the moisture content in accordance with *AS1289.2.1.1* (Standards Australia 2005)) outlined in Section 4.3.3 of this report:

- A drying oven in accordance with *AS1289.0* specifications,
- Three (3) heat-resistant and corrosion-resistant containers,
- Non-absorbent container with close fitting lid,
- A suitable balance within the limit requirements outlined in *Table 1* of *AS1289.2.1.1* (Standards Australia 2005),
- Small palette knife,
- 3 mm diameter rod,
- Flat glass plate to roll the threads, and
- Wash bottle with potable water.

The following procedure for determining the plastic limit of the soil was used in accordance with *AS1289.3.2.1* (Standards Australia 2009b):

1. As 100% of the soil passes the 0.425 mm sieve during the particle size distribution test. the natural state clay material was used without further sieving as per *Section 4(a)* of *AS1289.3.2.1*. A 40 g soil sample was weighed in the non-absorbent container with lid.
2. Using the wash bottle, potable water was added to the soil sample incrementally and kneaded into a homogenous and plastic sample, then shaped into a ball. The sample was covered and left to curing overnight (approximately 24 hours), allowing the water to permeate the clay soil particles. The sample was covered and left to curing overnight (approximately 24 hours), allowing the water to permeate the clay soil particles. In addition, the six (6) heat-resistant containers were label the initial weight of the container (without lid) recorded.
3. An approximately 8 g sample of the plastic clay sample was moulded between the fingers, before being rolled into a ball between the palms of the hands until small cracks begin to appear on the surface of the sample. The small cracks ensure that the sample is sufficiently dry.

4. The sample was rolled between the hands and the glass plate to a constant diameter of 3 mm (using the 3 mm rod as a guide), and checked against the following conditions:
 - a. If the sample crumbled into pieces before reaching the 3 mm diameter, a small amount of potable water was added and Steps 3 & 4 repeated.
 - b. If the sample rolled into a 3 mm diameter thread without cracking, the sample was kneaded again between the hands and Steps 3 & 4 repeated.
 - c. If the sample rolled in at thread that crumbled at 3 mm diameter, the sample portions were collected and placed in one (1) of the heat-resistant containers. The weight of the container and sample was recorded, the lid was paced on the container until the end of the plastic limit testing iterations to prevent moisture loss.
5. Steps 3 and 4 were repeated two (2) additional times, making sure to collect a minimum of 5 g of sample after rolling.
6. The lids were removed prior to placing all samples in a 106.5°C drying oven (Figure 42) to determine the moisture content in accordance with *AS1289.2.1.1* as outlined in Section 4.3.3 of this report (Figure 43).



Figure 42: Plastic Limit samples before oven drying to find moisture content



Figure 43: Plastic Limit samples after oven drying to find moisture content

4.3.6 Shrinkage Limit (SL)

The shrinkage limit (was determined using the plastic limit and liquid limit calculated in Chapter 5. Casagrande's Soil Plasticity Chart (Figure 44) was used to find the shrinkage limit of the clay material.

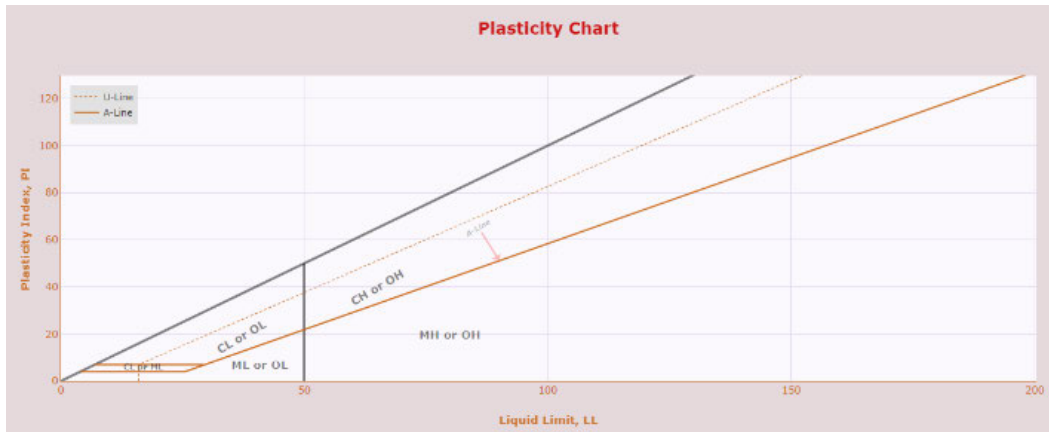


Figure 44: Casagrande's Soil Plasticity Chart (TransCalc 2022)

The A-line is given by Equation 10 (TransCalc 2022).

$$PI = 0.73(LL - 20) \quad (10)$$

$PI = \text{Plasticity Index (\%)}$
 $LL = \text{Liquid Limit (\%)} = w_{CL}$

The U-line is given by Equation 11 (TransCalc 2022).

$$PI = 0.9(LL - 8) \quad (11)$$

$PI = \text{Plasticity Index (\%)}$
 $LL = \text{Liquid Limit (\%)} = w_{CL}$

The plasticity index of the sample soil material is given by Equation 12.

$$PI = LL - PL \quad (12)$$

$PI = \text{Plasticity Index (\%)}$
 $LL = \text{Liquid Limit (\%)} = w_{CL}$
 $PL = \text{Plastic Limit (\%)} = w_p$

The shrinkage limit occurs the x-axis intercept (LL equals zero) for the line that connects the plasticity index of the sample to the intersection of the A-line and U-line. The results of the shrinkage limit calculations can be found in Section 5.2.6 of this report.

4.3.7 Compression Index (C_c) and Swell Index (C_s)

Consolidation testing of the soil infill material was determined in general accordance with *AS1289.6.6.1 Methods of testing soils for engineering purposes – Method 6.6.1: Soil strength and consolidation tests – Determination of the one-dimensional consolidation properties of a soil – Standard Method* (Standards Australia 2020a). The results of the consolidation testing are outlined in Section 5.2.7 of this report.

In accordance with *AS1289.6.6.1* (Standards Australia 2020a) the following equipment was used for the consolidation testing, including the equipment to determine the moisture content in accordance with *AS1289.2.1.1* (Standards Australia 2005) outlined in Section 4.3.3 of this report:

- A drying oven in accordance with *AS1289.0* specifications,
- A heat-resistant and corrosion-resistant container,
- A suitable balance within the limit requirements outlined in *Table 1* of *AS1289.2.1.1* (Standards Australia 2005),
- Oedometer consolidation loading device for applying vertical loading on the specimen capable of long period of loading in accordance with *AS1289.6.6.1* requirements and accompanying weights including:
 - Two (2) 0.5 kg weights,
 - One (1) 1.0 kg weight, and
 - Two (2) 2.0 kg weights.
- Consolidation cell with a porous plate on each face of the specimen in accordance with *AS1289.6.6.1* requirements including a consolidation ring.
- Dial gauge with minimum travel of 5 mm and readable to at least 0.002 mm,
- Palette knife for trimming,
- vernier calipers,
- small level,
- Two (2) 75 mm diameter filter papers, and
- Potable water.

The following procedure for determining the consolidation properties of the soil was used in accordance with *AS1289.6.6.1* (Standards Australia 2020a):

1. The porous plates and filter papers were submerged in water to moisten.
2. The internal diameter and height (H_0) of the cutter ring were measured and recorded (Figure 45), and the mass of the ring recorded (m_0).



Figure 45: Consolidation ring measurements diameter (left) and height (right)

3. The soil sample was prepared. As this is a commercially available product it was treated as a 'disturbed sample'. As such, water was added to a sample of the clay material to form a homogeneous mass at least the height and diameter of the cutter ring.
4. The sample was trimmed using the palette knife and light force until the sample fit in the size of the cutter ring. The ends of the sample were trimmed to be flush with the ring, and residual material carefully removed from the outside of the ring. These trimmings were used to determine the initial moisture content of the sample in accordance with *AS1289.2.1.1* as outlined in Section 4.3.3 of this report.
5. The mass of the ring plus sample (m_1) was recorded, and the initial mass of the sample (m_i) determined.
6. The consolidation cell was constructed in the order of reservoir (consisting of base, o-ring and acrylic cylinder), lower porous stone, filter paper, cutter ring plus sample, clamping ring plus locking nuts, filter paper, upper porous stone, and load pad as shown in (Figure 46).

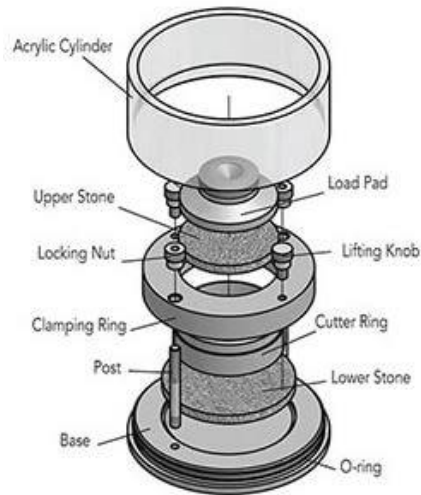


Figure 46: Consolidation Cell (The Constructor 2021)

7. The reservoir was filled with water.
8. Before the loading frame was set in place, the lever loading arm was raised to a level just above the horizontal and the supporting arm raised to hold the weight of the lever arm so that force was not applied to the sample until after the support arm was released. Taking care to keep the loading frame vertical and the load cell bolt only just touching the load pad.
9. The dial gauge was set to read the vertical displacement of the specimen and zeroed, making sure to leave space for movement in positive and negative vertical directions.
10. The first load of 0.5 kg was placed on the weight hanger. As the support arm is still in the locked position this did not apply a load to the sample.
11. The lever loading arm was lowered to horizontal using a small level, by adjusting the support arm.
12. The first load was applied by fully releasing the support arm (Figure 47). Dial gauge readings were recorded (such as Figure 48) for time intervals of:
 - a. 7.5, 15 and 30 seconds,
 - b. 1, 2, 4, 8, 16 and 32 minutes, and
 - c. 1, 2, 4, 8 and 24 hours.



Figure 47: First load applied to sample



Figure 48: Dial gauge reading at 24 hours for 1 kg weight

13. Step 12 was repeated for the weights of 0.5, 1, 2, 4 and 6 kg.
14. Once the 24 hours dial gauge reading was taken, the weights were unloaded in the reverse order waiting a minimum of 30 minutes between removing each weight.
15. Once fully unloaded the cutter ring plus sample, filter papers, porous stones and load pad were carefully removed (Figure 49) from the consolidation cell. The load pad, porous stones and filters were removed from the sample, and the mass of the ring plus sample recorded.



Figure 49: Sample removed from reservoir after unloading

16. The sample was extruded from the cutter ring and cut open for examination (Figure 50), and description of the surfaces recorded.



Figure 50: Extruded and cut sample (post consolidation)

17. The soil test sample was used to determine the final dry mass and moisture content of the sample in accordance with *AS1289.2.1.1* as outlined in Section 4.3.3.

The results of the consolidation testing of the soil fines sample were analysed using a compression versus log-time graph as outlined in *AS1289.6.6.1* (Standards Australia 2020a). Figure 51 shows a typical log-time versus compression graph for consolidation analysis.

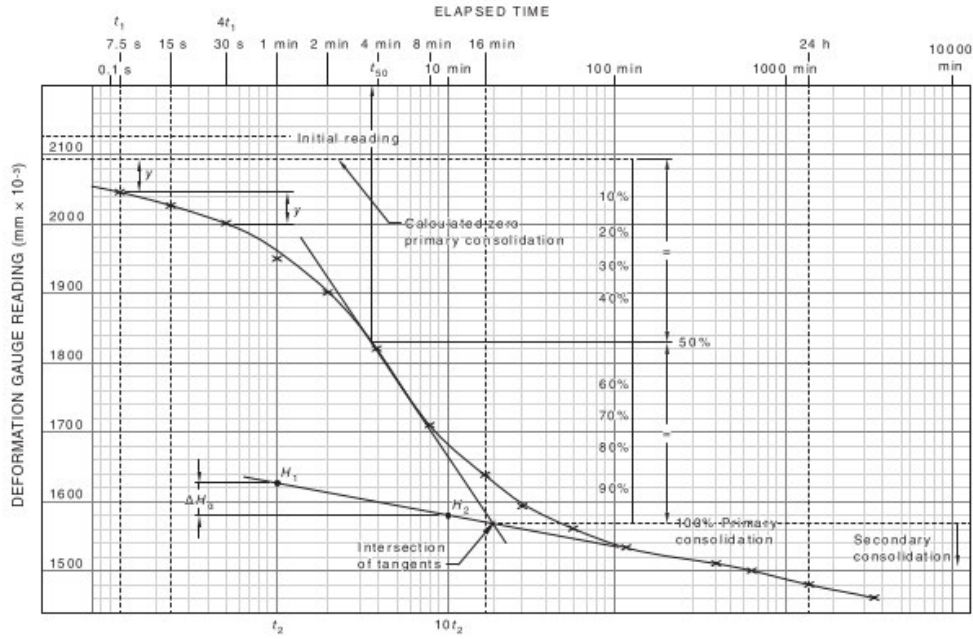


Figure 51: Typical log-time versus compression graph (Standards Australia 2020a)

Figure 52 shows a typical log-effective pressure (σ') versus void ratio (e) graph for determination of the compression index and swell index, where the compression index (C_c) is the slope of the steeper portion of the graph and the swell index (C_s) is the slope of the initial flatter portion of the graph (CIV2403 2015). The void ratio is given by Equation 13 (Standards Australia 2020a).

$$e = \frac{H_0 - H_s}{H_s} \quad (13)$$

e = void ratio

H_0 = initial height of the sample (mm)

$$H_s = \text{equivalent height of solid particles (mm)} = \frac{m_2 \times 1000}{\rho_s \times A}$$

m_2 = dry mass of the sample (g)

ρ_s = soil particle density (g/cm^3)

A = area of sample (mm^2)

The results of the consolidation testing for this project are outlined in Section 5.2.7.

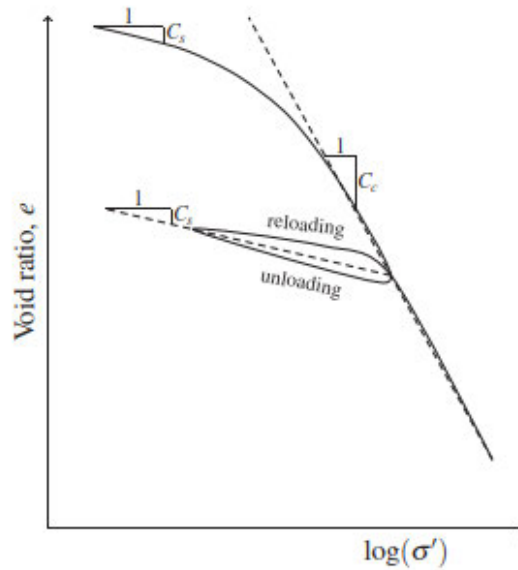


Figure 52: Typical log-effective pressure versus void ratio graph (CIV2403 2015, p. 129)

4.3.8 Friction Angle (ϕ') and Cohesion (c')

The friction angle of the infill material was determined in general accordance with *AS1289.6.2.2 Methods of testing soils for engineering purposes – Method 6.2.2: Soil classification tests – Determination of the shear strength of a soil – Direct shear test using a shear box* (Standards Australia 2020b). The results of the direct shear testing of the soil material analysis are outlined in Section 5.2.8 of this report.

In general accordance with *AS1289.6.2.2* (Standards Australia 2020b) the following equipment was used for the direct shear testing analysis:

- Geocomp ShearTrac2 apparatus with data tracking computer software,
- Circular shear box including the split box, base plate, two (2) porous stones, two (2) shear bolts, load pad, and piston,
- A drying oven in accordance with *AS1289.0* specifications,
- One (1) large heat-resistant and corrosion-resistant container,
- Two (2) small heat-resistant and corrosion-resistant containers,
- Three (3) resealable plastic bags,
- Three (3) resealable airtight containers,

- A suitable balance within the limit requirements outlined in *Table 1* of *AS1289.2.1.1* (Standards Australia 2005),
- rubber tamper,
- small paint brush,
- vernier calipers, and
- Small metal scoop.

The following procedure was used to undertake the direct shear testing of the soil in accordance with *AS1289.6.2.2* (Standards Australia 2020b):

1. The following measurements were recorded (using the vernier calipers):
 - a. Internal diameter (Figure 53) and height (Figure 54) of the top and bottom components of the split box,



Figure 53: Internal diameter of split box top (left) and bottom (right)



Figure 54: Height of split box top (left) and bottom (right)

- b. Diameter and thickness of the porous stones (Figure 55),



Figure 55: Diameter (left) and thickness (right) of porous plate

- c. Internal height of the bottom component of the split box with the base plate installed (Figure 56),



Figure 56: height of bottom split box with base plate installed

- d. Internal height of the bottom component of the split box with the base grid plate and one (1) porous stone installed (Figure 57),



Figure 57: height of bottom split box with base plate and one (1) porous plate installed

- e. Total height of the split box with the base plate and one (1) porous stone installed (Figure 58),



Figure 58: Total height of split box with base plate and one (1) porous stone installed

- f. Total height and diameter of the load pad (Figure 59), and



Figure 59: Dimensions of load pad height (left) and diameter (right)

- g. Height of the base portion of the load pad (Figure 60).



Figure 60: Height of load pad base

2. The three soil samples to be used in the direct shear testing of the infilled rock joints were prepared for testing.
- a. Completely dry state (0% moisture content):
- i. Approximately 800g of the sodium bentonite clay material was placed into a heat-resistant and corrosion-resistant container and placed in the oven (at 106.5°C) for 24 hours.
 - ii. The container was removed and allowed to cool.
 - iii. The mass of the container and clay material was recorded then returned to the oven for 2 hours.
 - iv. The container was removed and allowed to cool, then the mass of the containers and clay material recorded and compared to the previous mass.
 - v. As the two masses were within 0.1% of each other, as previously used in the moisture content testing, the sample was considered dried to a 0% moisture content. If this had not been the case, then Steps ii to iv would have been repeated until a moisture content of 0% was achieved.
 - vi. The material was stored in a sealed plastic bag inside of an airtight container to prevent moisture contamination from the surrounding air.

- b. Intermediate state (10% moisture content):
 - i. Approximately 600 g of the sodium bentonite clay material (in its natural state) and approximately 200 g of the 0% moisture content material from the previous step were sealed in a plastic bag inside an airtight container to prevent external moisture contamination.
 - ii. This mixture was left to cure for approximately 36 hours, allowing the moisture to equalise through the sample.
 - iii. The small heat-resistant and corrosion-resistant containers were labelled and the initial mass recorded.
 - iv. Two (2) subsamples of at least 30 g each were removed and placed in two (2) heat-resistant and corrosion-resistant containers. The mass of each container plus sample were recorded, and placed into an oven (106.5°C) the final moisture content of the sample in accordance with *AS1289.2.1.1* as outlined in Section 4.3.3 of this report.
- c. Natural state (16% moisture content):
 - i. Approximately 600 g of the sodium bentonite clay material was placed into a sealed bag inside an airtight container to minimise moisture exchange to keep a consistent moisture content throughout testing.

3. The shear box was assembled by:

- a. Adjusting the four (4) shear screws (on the top split box) to not protrude past the thickness of the top split box.
- b. Fixing the top and bottom split boxes together using the two (2) shear bolts.
- c. Placing the base plate then one (1) porous stone in the bottom of the shear box.
- d. Placing a subsample of the clay material into the shear box and leveling the sample using the rubber tamper (being careful not to apply excessive pressure).

- e. Three (3) measurements of the height from the level sample to the top of the shear box were taken and compared to the required gap of approximately 13.5 mm (thickness of top porous stone and base of loading pad).
- f. Steps d and e were repeated until the sample was level with a 13.5 mm gap to the top of the shear box (Figure 61).
- g. The porous stone was gently placed on top of the soil sample.
- h. The load pad was gently placed on top of the porous stone.
- i. The piston was gently placed on top of the load pad.
- j. The excess material carefully removed using a small paint brush.



Figure 61: Soil material in shear box

4. The shear box was placed in the ShearTrac2 and the side bolts tightened to fix the shear box in place.
5. The vertical load cell is positioned above the piston, tightly secured, and lowered as required to approximately 1 mm above the piston.
6. The following settings were input into the computerised testing software:
 - a. Project: Project Number, Project Name, Location, Date of Test, Tester, Checker, Test Number and Description.

- b. Test Parameters: Start Phase (Consolidation) and Shear Phase Type (Direct Shear).
 - c. Specimen: Shape (Circular), Initial Diameter (63.3 mm), Initial Height (height of soil sample) and Specific Gravity (as outlined in Section 5.2.2 of this report).
 - d. Consolidation Table: Stress, Step Type (Constant Load), Maximum Duration (1440 minutes), Minimum Duration (2 minutes), T100 Offset (0 minutes) and Read Table (Displacement).
 - e. Shear Table: Delay (0 minutes), Shear Control (Displacement), Rate (0.5/min), Maximum Displacement (15 mm), Maximum Force (2200 N) and Read Table (Time).
 - f. Read Table: Time (0.25-minute steps).
7. The test was set to run, commencing with the consolidation phase.
 8. Once the consolidation phase was completed the shear bolts were removed and the shear screws were rotated one turn clockwise to create a small gap between the top and bottom split boxes. The shear phase of the test was run.
 9. Upon completion of the shear phase the shear box was returned to the starting position (both horizontal and vertical).
 10. The shear box was removed from the ShearTrac2.
 11. The shear box and ShearTrac 2 were cleaned to remove excess clay particles.
 12. Steps 4 through 11 were repeat for each of the three (3) moisture content states (0, 10 and 16%), and at 100, 300, 500 and 700 kPa. Totalling 12 tests.

The angle of internal friction of the soil material was determined using Equation 14 (Craig 2004, p. 91).

$$\tau = c + \sigma_n \tan (\varphi) \tag{14}$$

τ = shear strength of the soil (kPa)

c = cohesion

$$\sigma_n = \text{normal stress (kPa)}$$

$$\varphi = \text{angle of internal friction (}^\circ\text{)}$$

The maximum shear stress of each of the tests was used to construct a Normal Stress versus Shear Stress graph to determine the angle of internal friction and cohesion of the soil material. However, only the 100 and 300 kPa data was used to determine the final angle of internal friction and cohesion as the tests at 500 and 700 kPa aborted once the 2200 N threshold was reached. The angle of internal friction was determined as the angle of the linear trendline, and the cohesion as the y-axis intercept.

4.4 Direct Shear Testing of Rock Joints

Direct shear testing for this project has been undertaken in accordance with *AS1289.6.2.2 Methods of testing soils for engineering purposes - Method 6.2.2: Soil strength and consolidation tests – Determination of shear strength of a soil – Direct shear test using a shear box* (Standards Australia 2020b) as outlined in Section 4.3.9 of this report. The results of the direct shear testing of the soil material analysis are outlined in Section 5.3 to 5.5 of this report.

The key independent variables of interest of this project are the infill thickness to asperity height ratio (t/a), moisture content, and normal loading. The four infill thickness to asperity height ratios of 0 (clean joints), 0.5, 1, and 1.5 are used. The four normal loading conditions of 100, 300, 500 and 700 kPa are used. The three moisture content conditions of 0%, 10% and 16% are used. The asperity angle of 29.7° and asperity base length of 7 mm are held constant throughout testing. Table 5 outlines the testing conditions of this investigation.

Table 5: Testing Conditions

Test Code	Loading (MPa)	t/a Ratio	Infill Thickness (mm)	Moisture Content (%)
<i>CL1</i>	0.1	0	0	Not Applicable (Clean Joint)
<i>CL2</i>	0.3	0	0	
<i>CL3</i>	0.5	0	0	
<i>CL4</i>	0.7	0	0	
<i>111</i>	0.1	0.5	1	Condition 1
<i>211</i>	0.3	0.5	1	Condition 1
<i>311</i>	0.5	0.5	1	Condition 1
<i>411</i>	0.7	0.5	1	Condition 1

112	0.1	0.5	1	Condition 2
212	0.3	0.5	1	Condition 2
312	0.5	0.5	1	Condition 2
412	0.7	0.5	1	Condition 2
113	0.1	0.5	1	Condition 3
213	0.3	0.5	1	Condition 3
313	0.5	0.5	1	Condition 3
413	0.7	0.5	1	Condition 3
121	0.1	1.0	2	Condition 1
221	0.3	1.0	2	Condition 1
321	0.5	1.0	2	Condition 1
421	0.7	1.0	2	Condition 1
122	0.1	1.0	2	Condition 2
222	0.3	1.0	2	Condition 2
322	0.5	1.0	2	Condition 2
422	0.7	1.0	2	Condition 2
123	0.1	1.0	2	Condition 3
223	0.3	1.0	2	Condition 3
323	0.5	1.0	2	Condition 3
423	0.7	1.0	2	Condition 3
131	0.1	1.5	3	Condition 1
231	0.3	1.5	3	Condition 1
331	0.5	1.5	3	Condition 1
431	0.7	1.5	3	Condition 1
132	0.1	1.5	3	Condition 2
232	0.3	1.5	3	Condition 2
332	0.5	1.5	3	Condition 2
432	0.7	1.5	3	Condition 2
133	0.1	1.5	3	Condition 3
233	0.3	1.5	3	Condition 3
333	0.5	1.5	3	Condition 3
433	0.7	1.5	3	Condition 3
<i>Test Code (1st number is the loading case, 2nd number is the t/a ratio case & 3rd number is the moisture content case, and CL is clean joints)</i>				

As Steps 1 & 2 in the direct shear testing procedure outlined in Section 4.3.9 have already been completed, the procedure outlined below will describe the requirements for the testing of the artificial rock joints. 40 grit sandpaper was required in addition to the equipment outlined in Section 4.3.9. The

following procedure was used to undertake direct shear testing of the clean and infilled artificial rock joints based on AS1289.6.2.2 (Standards Australia 2020b):

1. The joint profiles were paired and both halves were labelled with the appropriate test code from Table 5, as shown in Figure 62.



Figure 62: Artificial rock joints with test codes

2. The bottom half of each artificial rock joint profile was sanded using 40 grit sandpaper until the top of the asperity sat flush with the top of the bottom half of the split box (with the base plate was installed (no porous stone)). Care was taken to apply even pressure to result in a horizontal surface. This height was recorded.
3. The top half of each artificial rock joint profile was sanded using 40 grit sandpaper to the appropriate height leaving a 7 mm gap from the top of the joint to the top of the shear box (given by Equations 15 to 18). This height was recorded, and a line added along the flat surface of the top joint indicating the direction of the joint profile to allow for easier alignment when constructing the sample for testing (Figure 63).
 - a. Clean joints: approximately 19.4 mm

$$H_{top,CL} = H_{box,t} - H_{pad,base} + a \quad (15)$$

$$H_{top,CL} = \text{desired height of top portion of clean joint (mm)}$$

$$H_{box,t} = \text{Height of top portion of split box} = 24.4 \text{ mm}$$

$$H_{pad,base} = \text{Height of base of load pad} = 7 \text{ mm}$$

$$a = \text{asperity height} = 2 \text{ mm}$$

$$H_{top,CL} = 24.4 - 7 + 2 = 19.4 \text{ mm}$$

- b. Infill ratio of 0.5 (1 mm infill thickness): approximately 18.4 mm

$$H_{top,t=1} = H_{box,t} - H_{pad,base} + a - t \quad (16)$$

$H_{top,t=1}$ = desired height of top portion of joint with 1 mm infill (mm)

t = infill thickness = 1 mm

a = asperity height = 2 mm

$$H_{top,t=1} = 24.4 - 7 + 2 - 1 = 18.4 \text{ mm}$$

- c. Infill ratio of 1.0 (2 mm infill thickness): approximately 17.4 mm

$$H_{top,t=2} = H_{box,t} - H_{pad,base} + a - t \quad (17)$$

$H_{top,t=2}$ = desired height of top portion of joint with 2 mm infill (mm)

t = infill thickness = 2 mm

a = asperity height = 2 mm

$$H_{top,t=2} = 24.4 - 7 + 2 - 2 = 17.4 \text{ mm}$$

- d. Infill ratio of 1.5 (3 mm infill thickness): approximately 17.4 mm

$$H_{top,t=3} = H_{box,t} - H_{pad,base} + a - t \quad (18)$$

$H_{top,t=3}$ = desired height of top portion of joint with 3 mm infill (mm)

t = infill thickness = 3 mm

a = asperity height = 2 mm

$$H_{top,t=3} = 24.4 - 7 + 2 - 3 = 17.4 \text{ mm}$$

4. The joint pairs for infilled joint testing were arranged in sets of 12 for each of the three (3) infill moisture conditions (Figure 63). This facilitated easy progress tracking throughout testing.



Figure 63: Joint Preparation

5. The shear box was assembled by the following steps where Steps e to h were omitted for clean joint testing:
 - a. Adjusting the four (4) shear screws (on the top split box) to not protrude past the thickness of the top split box.
 - b. Fixing the top and bottom split boxes together using the two (2) shear bolts.
 - c. Placing the base plate in the bottom of the shear box (no porous stone was used).
 - d. Placing the bottom portion of the joint in the shear box (making sure to align the asperity profile parallel to the direction of shear (Figure 64)).



Figure 64: Alignment of bottom joint in shear box

- e. Recording the height from the top of the asperity profile of the bottom joint to the top of the shear box (H_a).
- f. Placing a subsample of the appropriate clay material into the shear box and leveling the sample using the rubber tamper (being careful not to apply excessive pressure or twist the tamper so that the alignment of the bottom joint was not impacted).
- g. Three (3) measurements of the height from the level sample to the top of the shear box were taken and compared to the required height (H_r) as given by Equations 19 to 21.

- i. Infill ratio of 0.5 (1 mm infill thickness):

$$H_{r,t=1} = H_a \quad (19)$$

$H_{r,t=1}$ = height required from top of infill to top of shear box for 1 mm infill(mm)
 H_a = height from top of asperity profile of bottom joint to top of the shear box (mm)

- ii. Infill ratio of 1.0 (2 mm infill thickness):

$$H_{r,t=2} = H_a - 1 \quad (20)$$

$H_{r,t=2}$ = height required from top of infill to top of shear box for 2 mm infill(mm)

- iii. Infill ratio of 1.5 (3 mm infill thickness):

$$H_{r,t=3} = H_a - 2 \quad (21)$$

$H_{r,t=3}$ = height required from top of infill to top of shear box for 3 mm infill(mm)

- h. Steps f and g were repeated until the sample was the appropriate level. Figure 65 shows a sample being prepared for an infill ratio of 0.5 (1 mm infill thickness).

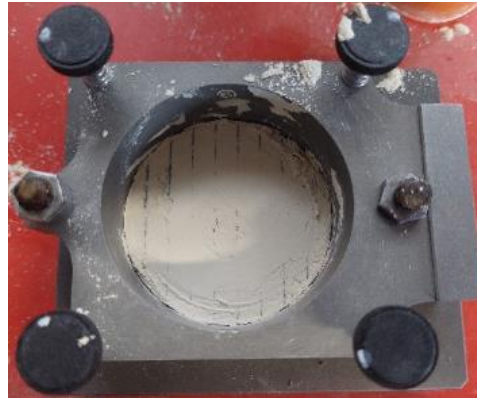


Figure 65: Preparation of sample with 1 mm infill thickness

- i. The top of the joint was gently placed on top of the soil sample (making sure to align the asperity profile parallel to the shear direction as indicated by the line), and with small, gentle movements carefully manoeuvred into the final interlocking alignment,
 - j. The load pad was gently placed on top of the joint,
 - k. The piston was gently placed on top of the load pad, and
 - l. The excess material carefully removed using a small paint brush.
6. The shear box was placed in the ShearTrac2 and the side bolts tightened to fix the shear box in place.
 7. The vertical load cell is positioned above the piston, tightly secured, and lowered as required to approximately 1 mm above the piston.
 8. The following settings were input into the computerised testing software:
 - a. Project: Project Number, Project Name, Location, Date of Test, Tester, Checker, Test Number and Description.
 - b. Test Parameters: Start Phase (Consolidation) and Shear Phase Type (Direct Shear).
 - c. Specimen: Shape (Circular), Initial Diameter (63.3 mm), Initial Height (height of the two joint components plus infill minus one 2 mm asperity height) and Specific Gravity (as outlined in Section 5.2.2 of this report).

- d. Consolidation Table: Stress, Step Type (Constant Load), Maximum Duration (1440 minutes), Minimum Duration (2 minutes), T100 Offset (0 minutes) and Read Table (Displacement).
 - e. Shear Table: Delay (0 minutes), Shear Control (Displacement), Rate (0.5/min), Maximum Displacement (15 mm), Maximum Force (2200 N) and Read Table (Time).
 - f. Read Table: Time (0.25 minute steps).
9. The test was set to run, commencing with the consolidation phase.
 10. Once the consolidation phase was completed the shear bolts were removed and the shear screws were rotated one turn clockwise to create a small gap between the top and bottom split boxes. The shear phase of the test was run. Due to the limitations of the machine in use the aborted once a threshold of 2200 N (shear or normal) or 15 mm horizontal moment was reached
 11. Upon completion of the shear phase the shear box was returned to the starting position (both horizontal and vertical).
 12. The shear box was removed from the ShearTrac2.
 13. The sample was carefully removed, inspected and place back into its place in the testing set.
 14. The shear box and ShearTrac 2 were cleaned to remove excess clay particles.
 15. Steps 5 through 14 were repeat for each of combination of the following variables, totalling 40 tests as outlined in Table 5.
 - a. Infill moisture content (0, 10 and 16%) for infilled joints,
 - b. Normal loading of 100, 300, 500 and 700 kPa, and
 - c. Infill thickness (1, 2 and 3 mm) and clean joints.

4.4.1 Direct Shear Testing Data Collation

1. As there is a large volume of raw data, the text (.txt) files were imported into excel as shown in Figure 66, where:

- a. Phase 1 indicates the consolidation phase
- b. Phase 2 indicates the shear phase
- c. ‘V’ denotes the vertical (normal) direction
- d. ‘H’ denotes the horizontal (shear) direction

Clean	Joint	-	CL1	-	100kPa			Clean	Joint	-	CL2	-	300kPa		
Phase:	1							Phase:	1						
Step:	0							Step:	0						
	Time	V-Load	V-Disp	H-Load	H-Disp	V-Motor	H-Motor		Time	V-Load	V-Disp	H-Load	H-Disp	V-Motor	H-Motor
	msec	N	mm	N	mm				msec	N	mm	N	mm		
	0	11.76	-14.02	-14.062	11.237	0	0		0	20.939	-15.221	-15.076	11.174	0	0
	13528	67.55	-13.763	5.2188	11.23	64621	0		6264	38.293	-14.935	-8.698	11.164	60788	0
	143533	311.94	-13.536	17.396	11.235	92718	0		9019	138.54	-14.71	9.1329	11.156	89231	0
Phase:	2								12026	345.78	-14.455	22.615	11.147	119820	0
Step:	0								15537	505.55	-14.198	28.848	11.146	147143	0
									23303	904.83	-13.95	43.49	11.118	176578	0
	Time	V-Load	V-Disp	H-Load	H-Disp	V-Motor	H-Motor		144810	936.38	-13.913	41.46	11.112	179876	0
	msec	N	mm	N	mm			Phase:	2						
	0	311.22	-13.521	-11.307	11.26	93181	0	Step:	0						
	15036	311.79	-13.52	9.4228	11.28	93447	12166		Time	V-Load	V-Disp	H-Load	H-Disp	V-Motor	H-Motor
	30071	311.94	-13.52	11.162	11.282	93516	24544		msec	N	mm	N	mm		
	45101	311.79	-13.52	18.701	11.287	93589	36715		0	936.38	-13.901	45.519	11.104	180151	0
	60133	310.65	-13.524	57.986	11.338	93842	49093		15035	936.38	-13.901	37.836	11.102	180197	12158
	75166	311.79	-13.522	110.32	11.46	94170	61267		30067	936.38	-13.901	41.46	11.103	180231	24542
	90205	311.94	-13.522	206	11.577	94227	73650		45094	925.91	-13.892	263.98	11.178	181150	36719
	105235	311.51	-13.522	189.33	11.69	94391	85825		60127	933.23	-13.848	413.01	11.287	184975	48898
	120016	311.94	-13.522	178.16	11.809	94501	97999		75157	925.48	-13.805	487.38	11.403	188640	61285
	135049	311.94	-13.523	175.99	11.936	94491	110171		90191	934.66	-13.771	481.58	11.524	192563	73664
	150075	312.37	-13.523	175.55	12.069	94424	122549		105226	932.8	-13.742	495.93	11.645	195359	85838
	165106	311.79	-13.523	176.28	12.187	94439	134721		120009	931.94	-13.707	510.14	11.776	198203	98020
	180139	311.08	-13.522	364.73	12.308	94558	147106		135049	933.94	-13.670	514.7	11.895	200833	110103

Figure 66: Raw Data (example)

2. The key Phase 2 data (displacement and load) was collated and the appropriate corrections to the normal and shear displacement values (Figure 67). The correction factor was taken as the reading when time is zero. The bulk collated data is included in Appendix H. The forces in the normal and shear directions were to stress values using Equation 22.

$$P = \frac{F}{A} \times 10^{-3} \quad (22)$$

P = stress in the normal (σ) or shear (τ) direction (kPa)

F = load in the normal or shear direction (N)

- normal effective stress ranges from:
 - 0 to 800 kPa for clean joints only,
 - 90 to 110 kPa for samples subjected to an applied normal stress of 100 kPa,
 - 290 to 310 kPa for samples subjected to an applied normal stress of 300 kPa,
 - 490 to 510 kPa for samples subjected to an applied normal stress of 500 kPa, and
 - 690 to 710 kPa for samples subjected to an applied normal stress of 700 kPa.
- normal displacement ranges from -1.3 to 0.7 mm. Where negative displacement values are indicative of movement upwards, and positive displacement values are indicative on movement downwards. As such, the negative and positive axes for the normal displacement are inverted in Section 5.5.

CHAPTER 5: RESULTS & DISCUSSION

5.1 Compressive Strength Testing

Uniaxial compression testing was undertaken in general accordance with *AS1012.9* as outlined in Section 4.2 of this report. The results of the uniaxial compression testing at 7, 14, 21 and 28 days is shown in Table 6 with the average compressive strengths of 15.583, 12.604, 15.922 and 16.325 MPa respectively. As the uniaxial compressive strength of the artificial rock specimen is less than 20 MPa, it is classed as a ‘soft rock’ (Agustawijaya 2007). Agustawijaya’s (2007) investigation into ‘soft rocks’ included the impact of the mineral content, weathering, and saturation. While these factors regarding the rock joint material are outside the scope of this project, future investigation into impacts of such factors on rock joint behaviour would further expand the understanding of the shear behaviour of rock joints. The impact of saturation and weathering on rock joint behaviour, in combination with moisture variant infill properties, would be a future consideration to build on the research carried out in this project.

Table 6: Compressive Strength Results Summary

Day's Cured	Sample	Maximum Load (kN)	Compressive Strength (MPa)
7	<i>Sample 1</i>	29.3	18.312
	<i>Sample 2</i>	23.4	14.625
	<i>Sample 3</i>	22.1	13.812
	<i>Average</i>	-	15.583
14	<i>Sample 1</i>	24.1	15.062
	<i>Sample 2</i>	12.5	7.812
	<i>Sample 3</i>	23.9	14.937
	<i>Average</i>	-	12.604
21	<i>Sample 1</i>	27.3	17.062
	<i>Sample 2</i>	20.9	13.062
	<i>Sample 3</i>	23.8	14.875
	<i>Sample 4</i>	29.9	18.687
	<i>Average</i>	-	15.922
28	<i>Sample 1</i>	25.4	15.875
	<i>Sample 2</i>	26.9	16.812
	<i>Sample 3</i>	25.0	15.625
	<i>Sample 4</i>	26.3	16.437
	<i>Sample 5</i>	27.0	16.875
	<i>Average</i>	-	16.325

5.2 Infill Properties

5.2.1 Particle Size Distribution (d)

The particle size distribution of the clay material, determined in accordance with *AS1289.3.6.1 Methods of testing soils for engineering purposes – Method 3.6.1: Determination of the particle size distribution of a soil – Standard method of analysis by sieving* (Standards Australia 2009a) as outlined in Section 4.3.1, as is shown in Table 7 and Figure 68. As per *AS1289.3.6.1*, sieve sizes of 0.075, 0.15, 0.30, 0.425, 0.60 and 2.36 mm were used. In addition, 0.053 and 0.045 mm sieves were added due to the fine-grained nature of the material.

Table 7: Sieve Analysis Results

Sieve Size (mm)	Initial Mass of Sieve (g)	Mass of Sieve and Retained Soil (g)	Mass Retained on Sieve (g)	Mass Passing Sieve (g)	Percent Passing (%)
2.36	540.7	541	0.3	199.7	100
0.6	309.6	309.8	0.2	199.5	100
0.425	292.1	292.4	0.3	199.2	100
0.3	280.3	280.6	0.3	198.9	99
0.15	266.7	270.9	4.2	194.7	97
0.075	396.4	499.4	103	91.7	46
0.053	253.8	319	65.2	26.5	13
0.045	254.3	276.6	22.3	4.2	2
Pan	495.1	499.3	4.2	0	0
Total			200		

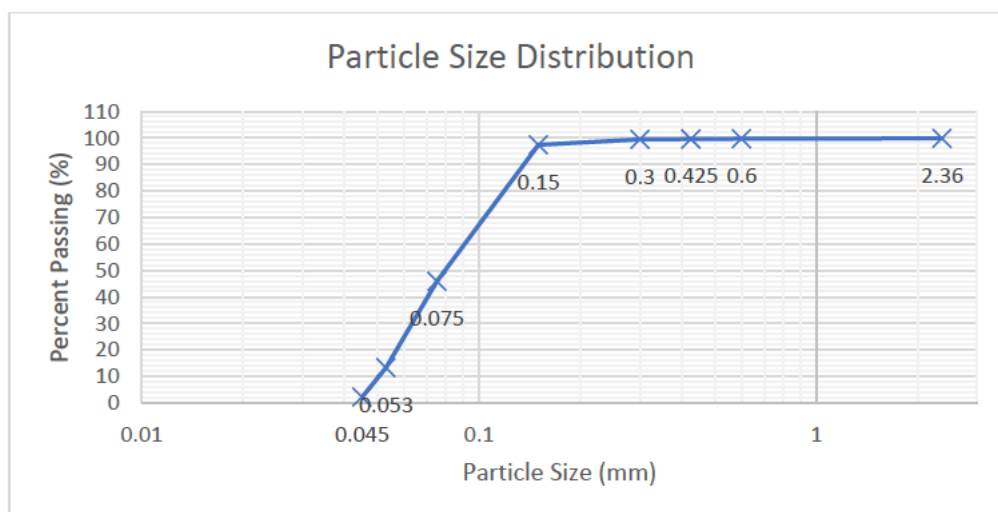


Figure 68: Particle Size Distribution Chart

To determine the particle size distribution of the fines, where over 10% of the clay material is passing through the 75 micron sieve, AS1289.3.6.1 refers to the hydrometer method of determining the distribution as per AS1289.3.6.3 *Methods of testing soils for engineering purposes – Method 3.6.3: Determination of the particle size distribution of a soil – Standard method of fine analysis using a hydrometer* (Standards Australia 2020a). Table 7 shows that 46% of the material passes through the 75 micron sieve. However, as the particle size distribution is not critical to the project outcomes the hydrometer method of determining particle size distribution was not completed due to time constraints.

5.2.2 Infill Soil Particle Density (ρ_s)

The particle density of the infill material was determined in accordance with AS1289.3.5.1 *Methods of testing soils for engineering purposes – Method 3.5.1: Soil classification tests – Determination of the soil particle density of a soil – Standard method* (Standards Australia 2006) as outlined in Section 4.3.2. To improve the accuracy of the determined particle density two samples were tested and the average taken as the final particle density value as outlined in Table 8. The particle density of the clay soil material is 2125 kg/m³ and has a specific gravity of 2.13.

Table 8: Particle Density Results

	Test 1	Test 2
Weight of bottle and stopper (g) (m_1)	136.74	134.70
Weight of bottle, stopper and soil (g) (m_2)	264.10	265.89
Weight of bottle, stopper, soil and water (g) (m_3)	703.61	701.44
Weight of bottle, stopper and water (g) (m_4)	635.46	632.53
Temperature of water (°C)	20	20
Density of water at 20°C (g/cm³)	0.9982	0.9982
Density of fines (g/cm³) (ρ_f)	2.15	2.10
Density of coarse (g/cm³) (ρ_c)	0	0
Percentage of fines (%)	100	100
Soil Density (g/cm³)	2.15	2.10
Soil Density (kg/m³)	2150	2100
Average Soil Density (kg/m³)	2125	
Specific Gravity	2.13	

5.2.3 Moisture Content (w)

The moisture content of the clay soil material was determined in accordance with *AS1289.2.1.1 Methods of testing soils for engineering purposes – Method 2.1.1: Soil moisture content tests – Determination of the moisture content of a soil – Oven drying method (standard method)* (Standards Australia 2005) as outlined in Section 4.3.3. The moisture content of the initial clay material was calculated as outlined in Section 4.3.3 of this report. To improve the accuracy of the determined moisture content three samples were tested and the mean taken as the final moisture content value as outlined in Table 9. For further details on the testing results see Appendix D. The initial moisture content of the clay soil material is 16.1%.

Table 9: Initial Moisture Content Results

Sample	Empty Weight of Container (g)	Weight of container & wet soil (g)	Final weight of container & dry soil (g)	Moisture Content (%)
1	36.90	71.04	66.31	16.1
2	36.88	70.08	65.47	16.1
3	36.31	70.22	65.53	16.1
			<i>Average</i>	16.1

5.2.4 Cone Liquid Limit (w_{CL})

Table 10 shows the outcomes of the cone penetration tests used to determine the liquid limit of the clay soil material in accordance with *AS1289.3.9.1 Methods of testing soils for engineering purposes – Method 3.9.1: Soil classification tests – Determination of the cone liquid limit of a soil* (Standards Australia 2015) as outlined in Section 4.3.4 and *AS1289.2.1.1 Methods of testing soils for engineering purposes – Method 2.1.1: Soil moisture content tests – Determination of the moisture content of a soil – Oven drying method (standard method)* (Standards Australia 2005) as outlined in Section 4.3.3. As per *AS1289.3.9.1*, the penetration readings are recorded to the nearest 0.1 mm. As per *AS1289.2.1.1*, the moisture contents are recorded to the nearest 1% for values above 100%. For further details on the testing results see Appendix E.

Table 10: Liquid Limit Cone Penetrometer Results

Test	Iteration	Penetration Reading (mm)	Difference (mm)	Average Penetration (mm)	Moisture Content (w) (%)
1	1	13.5	0.20	13.4	149
	2	13.3			
2	1	17.8	0.20	17.9	161
	2	18.0			
3	1	19.7	0.50	19.5	165
	2	19.2			
4	1	21.4	1.00	21.9	174
	2	22.4			
5	1	24.2	0.20	24.3	180
	2	24.4			
6	1	25.6	0.40	25.4	184
	2	25.2			

Figure 69 shows a graphical representation of the average penetration corresponding moisture content as per Table 10. As shown below, the linear regression model has a strong fit to the data set as represented by the R-squared value of 0.9968 (or 99.68% of the variance in moisture content is explained by the cone penetration value).

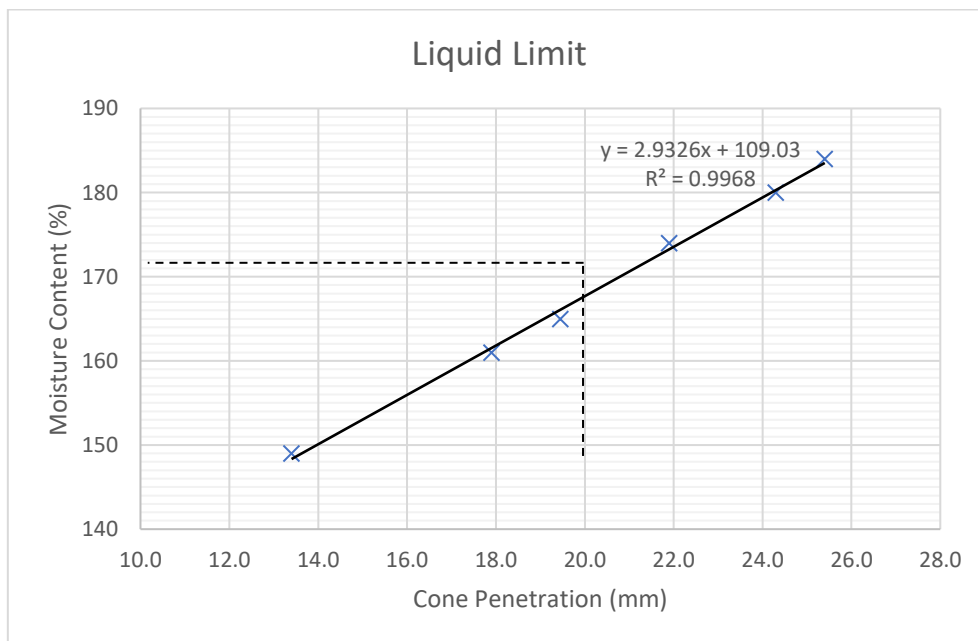


Figure 69: Liquid Limit as per Cone Penetration Test

As per Figure 69, the linear representation of the relationship between cone penetration and moisture content is given by Equation 23.

$$y = 2.9326x + 109.03 \quad (23)$$

Liquid limit of the clay soil occurs at a cone penetration of 20 mm. As such:

$$w_{CL} = 2.9326(20) + 109.03$$

$$w_{CL} = 167.7\% = 168\%$$

The liquid limit of this clay soil material occurs at 168% moisture content.

5.2.5 Plastic Limit (w_p)

The plastic limit of the clay soil material is determined in accordance with *AS1289.3.2.1 Methods of testing soils for engineering purposes – Method 3.2.1: Soil classification tests – Determination of the plastic limit of a soil* (Standards Australia 2009b) as outlined in Section 4.3.5 and *AS1289.2.1.1 Methods of testing soils for engineering purposes – Method 2.1.1: Soil moisture content tests – Determination of the moisture content of a soil – Oven drying method (standard method)* (Standards Australia 2005) as outlined in Section 4.3.3. To improve the accuracy of the determined plastic limit three samples were tested and the average taken as the final moisture content value as outlined in Table 11. For further details on the testing results see Appendix F. The plastic limit of this clay soil material occurs at 89.5% moisture content.

Table 11: Plastic Limit Results

Sample	Empty Weight of Container (g)	Weight of container & wet soil (g)	Final weight of container & dry soil (g)	Moisture Content (%)
1	31.25	38.69	35.24	86.5
2	37.54	44.06	40.93	92.5
3	37.10	43.53	40.49	89.5
			<i>Average</i>	89.5

5.2.6 Shrinkage Limit (SL)

The shrinkage limit has been determined using the liquid limit of 168 (Section 5.2.4), the plastic limit of 89.5 (Section 5.2.5), and Casagrande’s Plasticity Chart as outlined in Section 4.3.6. As such the plasticity index of the clay soil material is calculated to be 78.5, which is used to determine the location of the clay material on the Plasticity Chart in Figure 70.

$$PI = LL - PL$$

PI = Plasticity Index (%)

LL = Liquid Limit = 168%

PL = Plastic Limit = 89.5%

PI = 168 – 89.5 = 78.5 %

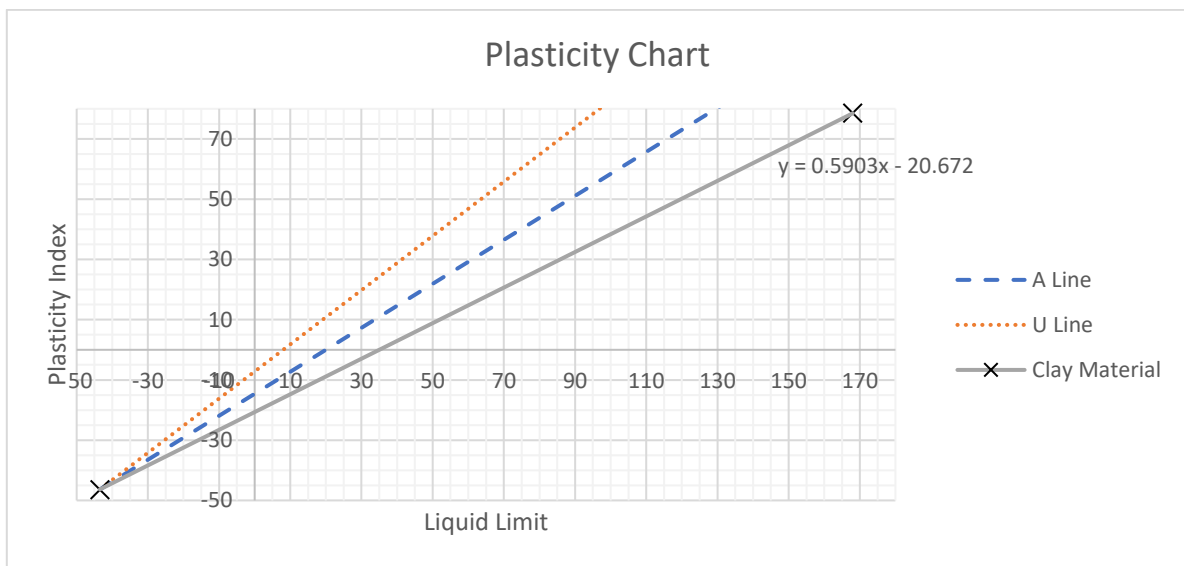


Figure 70: Plasticity Chart Results

Based on the above figure, the linear relationship between the clay materials liquid and plastic limit properties and the intersection with the A-line and U-line of the Plasticity Chart is given by Equation 24.

$$y = 0.5903x - 20.672 \tag{24}$$

The shrinkage limit of the material is given as the moisture content when the plasticity index is zero, i.e. the intersection between the equation representing the clay soil material and the x-axis.

$$0 = 0.5903x - 20.672$$

$$0.5903x = 20.672$$

$$x = \frac{20.672}{0.5903} = 35.02$$

The shrinkage limit of this clay soil material occurs at 35.0% moisture content.

5.2.7 Compression Index (C_c) and Swell Index (C_s)

Consolidation testing was undertaken in general accordance with *AS1289.6.6.1 Methods of testing soils for engineering purposes: Method 6.6.1: Soil strength and consolidation tests – Determination of the one-dimensional consolidation properties of a soil – Standard method* (Standards Australia 2020a) as outlined in Section 4.3.7. Figure 71 shows the results of the consolidation test data outlined in Table 12).

Table 12: Consolidation Results

Time Interval (minutes)	Dial Gauge Reading (×10 ⁻³ mm)				
	0.5 kg	1.0 kg	2.0 kg	4.0 kg	6.0 kg
0.1	5000	4480	4196	3224	2160
0.125	5000	4474	4190	1608	1069
0.25	5000	4472	4184	1603	1067
0.5	5000	4468	4176	1598	1065
1	5000	4464	4164	1589	1061
2	5000	4460	4146	1575	1055
4	5006	4454	4124	1558	1048
8	5006	4444	4088	1532	1036
16	5006	4430	4032	1493	1019
32	4928	4412	3950	1437	992
60	4800	4392	3854	1445	958
120	4614	4364	3674	1355	899

240	4488	4330	3550	1259	843
480	4460	4294	3424	1176	705
1440	4488	4236	3274	1083	685

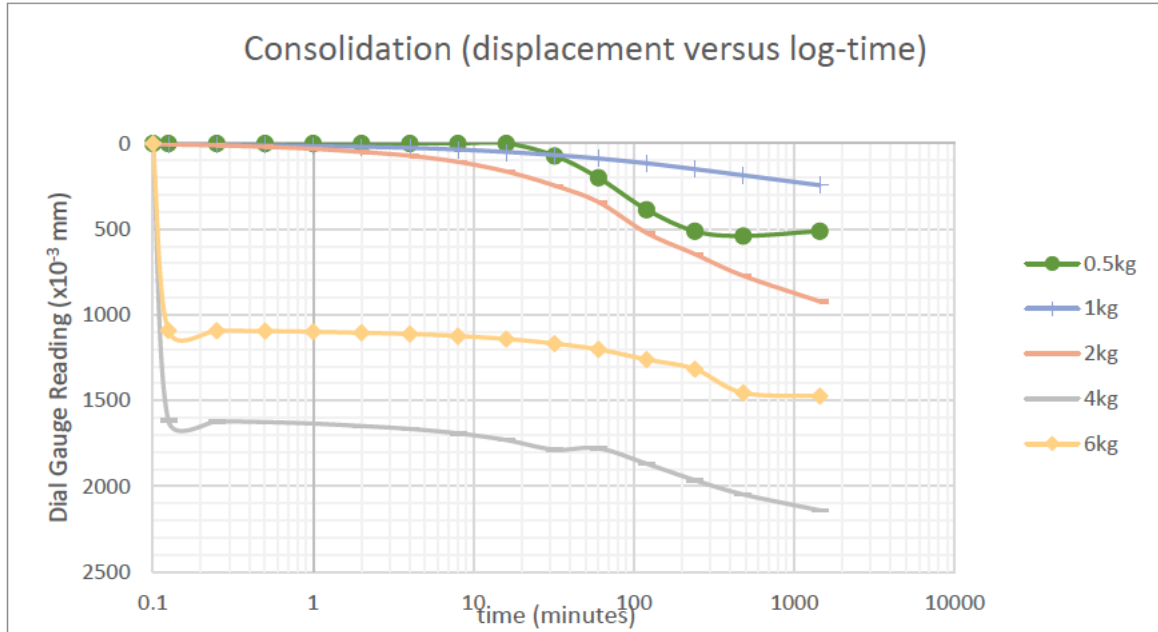


Figure 71: Consolidation (log-time versus displacement)

The compression index (C_c) is the slope of the steeper portion of the log-effective pressure (σ') versus void ratio (e) graph (Figure 72) and the swell index (C_s) is the slope of the initial flatter portion of the graph. The void ratio is given by the following equation (Standards Australia 2020a) as outlined in Section 4.3.7 and Table 13 shows the calculated values.

$$e = \frac{H_o - H_s}{H_s}$$

H_o = initial height of the sample (mm)

m_2 = dry mass of the sample (g) = 69.29 g

$$\rho_s = \text{soil particle density (g/cm}^3\text{)} = \frac{2125}{1000} = 2.125 \text{ g/cm}^3$$

$$A = \text{area of sample (mm}^2\text{)} = \pi r^2 = \pi \times \left(\frac{74.78}{2}\right)^2 = 4392 \text{ mm}^2$$

$$H_s = \text{equivalent height of solid particles (mm)} = \frac{69.29 \times 1000}{2.125 \times 4392} = 7.425 \text{ mm}$$

Table 13: Void Ratio Calculations

Effective Pressure (σ') (kPa)	Change from 18.85 mm	H _o (mm)	Void Ratio (e)
11	0.512	18.338	1.470
22	0.764	18.086	1.436
44	1.726	17.124	1.306
89	2.834	16.016	1.157
133	3.630	15.220	1.050

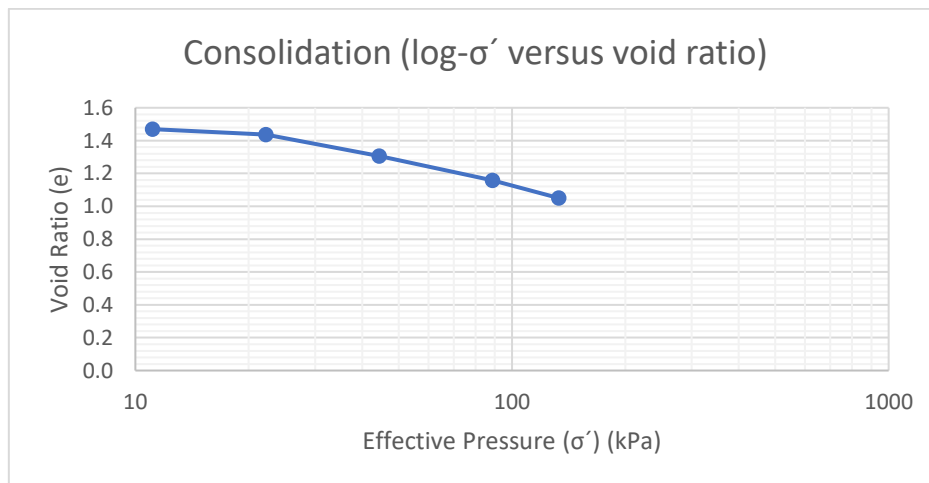


Figure 72: Consolidation (log-effective pressure versus void ratio)

The swell index is given by the slope of the line connecting the first two readings.

$$(\log(11), 1.470)$$

$$(\log(22), 1.436)$$

$$\text{Slope} = \frac{1.436 - 1.470}{\log(22) - \log(11)} = -0.113$$

$$C_s = 0.113$$

Due to the limited results achieved using the masses readily available, further testing is required to confirm that the compression index is representative of the sample. If so, the compression index is given by the slope of the line connecting the last two readings.

$$(\log(89), 1.157)$$

$$(\log(133), 1.050)$$

$$Slope = \frac{1.050 - 1.157}{\log(133) - \log(89)} = -0.609$$

$$C_s = 0.609$$

The compression index and swell index on the infill material are 0.609 and 0.113 respectively. This occurs at a moisture content of 127.4% as shown in Table 14.

Table 14: Moisture Content Test Results from Consolidation Test

Sample	Empty Weight of Container (g)	Weight of container & wet soil (g)	Final weight of container & dry soil (g)	Moisture Content (%)
1	31.20	117.81	69.29	127.4

5.2.8 Friction Angle (ϕ') and Cohesion (c')

The friction angle of the infill material was determined as per AS1289.6.2.2 *Methods of testing soils for engineering purposes – Method 6.2.2: Soil strength and consolidations tests – Determination of shear strength of a soil – Direct shear test using a shear box* (Standards Australia 2020b) as outlined in Section 4.3.8. A summary of the results is shown below in Table 15 and Figure 73, and the maximum shear stress for each of the normal stresses (100, 300, 500 and 700 kPa) and each of the moisture contents as outlined in the main project scope. Figure 73 shows that as the moisture content of the infill material increases, the angle of internal friction (slope of the trend) decreases and the cohesion increases. However, due to the limitations of the bounds of the ShearTrac2 apparatus being used, the horizontal moment is limited to 15 mm and the maximum shear force is limited to 2200 N, only the shear stresses corresponding to the normal stresses of 100 and 300 kPa are used to determine the friction angle (ϕ) and cohesion (c).

The friction angle of the infill material at the moisture content of 16% is 86°, with the corresponding cohesion of 14.632. For further details on the testing results see Appendix G.

Table 15: Summary of normal and shear stress results for determination of friction angle and cohesion

Normal Stress (kPa)	Maximum Shear Force (N)	Maximum Shear Stress (kPa)
Moisture content of 0% (fully dried)		
100	519.41	166.62
300	1612.30	517.22
500	2200.00	705.75
700	2200.90	706.04
Moisture content of 10%		
100	505.79	162.26
300	1482.30	475.52
500	2200.60	705.94
700	2200.00	705.75
Moisture content of 16% (natural state)		
100	511.44	164.07
300	1443.10	462.94
500	2200.00	705.75
700	2200.60	705.94

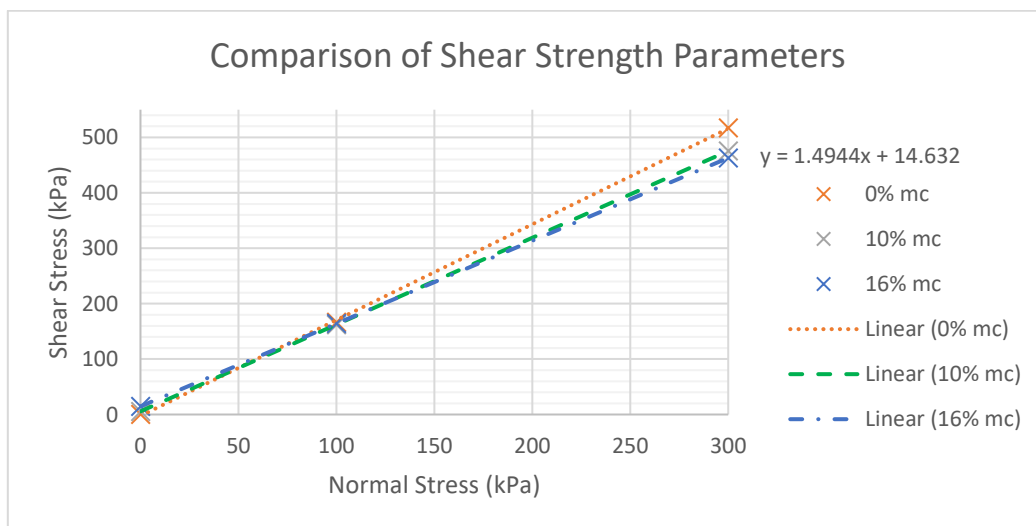


Figure 73: Normal vs shear stress for determination of friction angle and cohesion

5.2.9 Summary of Soil Properties

A summary of the soil property values determined in Sections 5.2.1 to 5.2.8 is found in Table 16.

Table 16: Infill Material Properties Results Summary

Infill Property	Result	Relevant Standard
<i>Particle Size Distribution (d)</i>	45 microns	AS1289.3.6.1-2009
<i>Infill Particle Density (ρ_s)</i>	2125 kg/m ³	AS1289.3.5.1-2006
<i>Moisture Content (w_L)</i>	16.1%	AS1289.2.1.1-2005
<i>Liquid Limit (LL)</i>	168	AS1289.3.9.1-2015
<i>Plastic Limit (PL)</i>	89.5	AS1289.3.2.1-2009
<i>Shrinkage Limit (SL)</i>	35.0	From Plasticity Chart
<i>Compression Index (C_c)</i>	0.609 (at 127.4% moisture content)	AS1289.6.6.1-2020
<i>Swell Index (C_s)</i>	0.113 (at 127.4% moisture content)	AS1289.6.6.1-2020
<i>Friction Angle (ϕ')</i>	86°	AS1289.6.2.2-2020
<i>Cohesion (c')</i>	14.632 kN/m ²	AS1289.6.2.2-2020

5.3 Direct Shear Testing of Rock Joints (Shear Displacement vs Shear Stress)

This section outlines the graphical summaries of the results from the direct shear testing of the clean and infilled rock joints with regards to the shear displacement and shear stress variables. The process for this testing and general data collation is outlined in Section 4.4. The bulk collated data used to produce these graphs is given in Appendix H.

5.3.1 Clean Joints at normal stresses of 100 kPa, 300 kPa, 500 kPa, and 700 kPa

Figure 75 shows a comparison of shear displacement and shear stress in the clean rock joints at the applied normal stresses of 100, 300, 500 and 700 kPa. When subjected to 100 kPa of normal stress the test runs for the full shear displacement of 15 mm. At 100 kPa the shear stress profile follows a repetitive wave pattern with peaks and troughs approximately 7 mm in wavelength, with a maximum peak of 442.02 kPa. As the asperity base length is 7 mm this indicates that the asperity profile controls the general behaviour of the shear stress of this clean rock joint. However, when the clean rock joints

are subject to the higher normal stresses of 300, 500 and 700 kPa the upper limit of 2200 N (approximately 700 kPa) was reached before 3 mm of shear displacement could occur. As such, the general peak-trough behaviour linked to asperity profile cannot be extended to the higher normal stress values. Although, as discussed in Chapter 2, it is likely that this peak-trough pattern would apply where the infill thickness is less than the asperity height. The initial plateau for 100, 300 and 700 kPa indicates that when the second phase of the direct shear testing (shear phase) occurred there was up to 1 mm misalignment between the top and bottom joint components. Taking this into account when comparing the impact of the increasing normal loading on the shear stress, the relationship shows that as the applied normal stress increases the shear stress increases. This is also reflected in the decreasing slope of the initial linear portion of the data as the normal stress decreases.

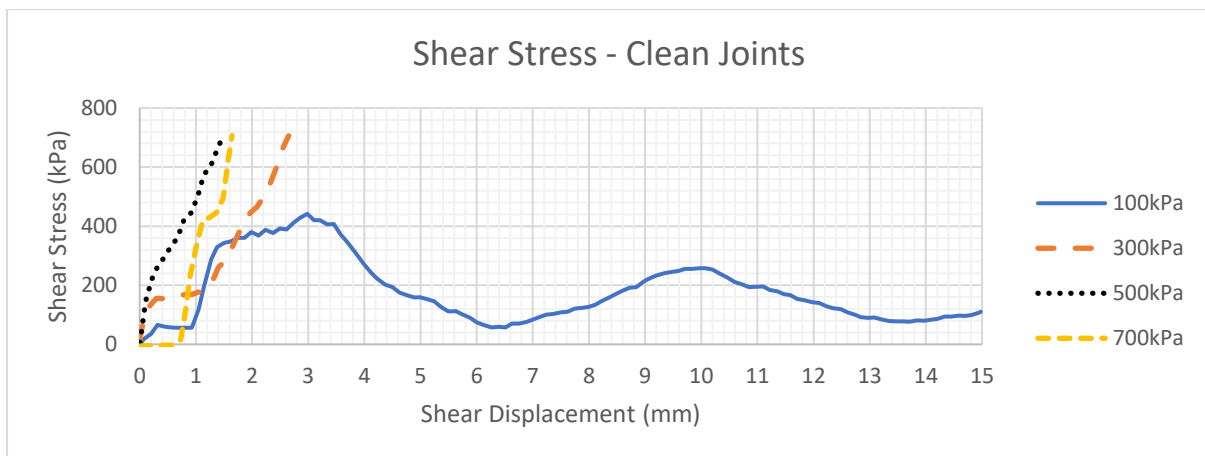


Figure 74: Clean Joint Results ($t/a=0$) (Shear Displacement vs Shear Stress)

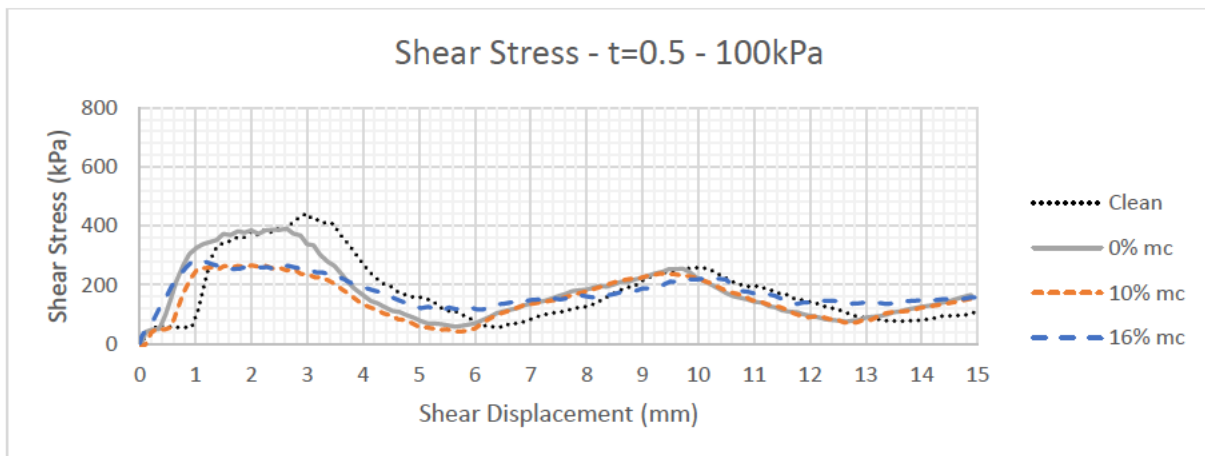
5.3.2 Infilled Joints with normal stress of 100 kPa

Figure 76 shows a comparison of shear displacement and shear stress in the clean and infilled rock joints at the applied normal stresses of 100 kPa with moisture contents 0, 10 and 16%. Where the thickness of the infill was less than the asperity height (Figure 76a), the asperity profile controls the general behaviour of the shear stress as discussed in Section 5.3.1. In Figure 76b, where the infill thickness is equal to the asperity height the pattern reflected in Figure 76a is flattened. This suggests that the infill material is a controlling factor of the shear stress, and the asperity profile does still contribute but to a lesser degree than in Figure 76a. Figure 76c shows a convergence on 200 kPa for all moisture contents. The maximum shear stress of the infill material (at all three moisture conditions and

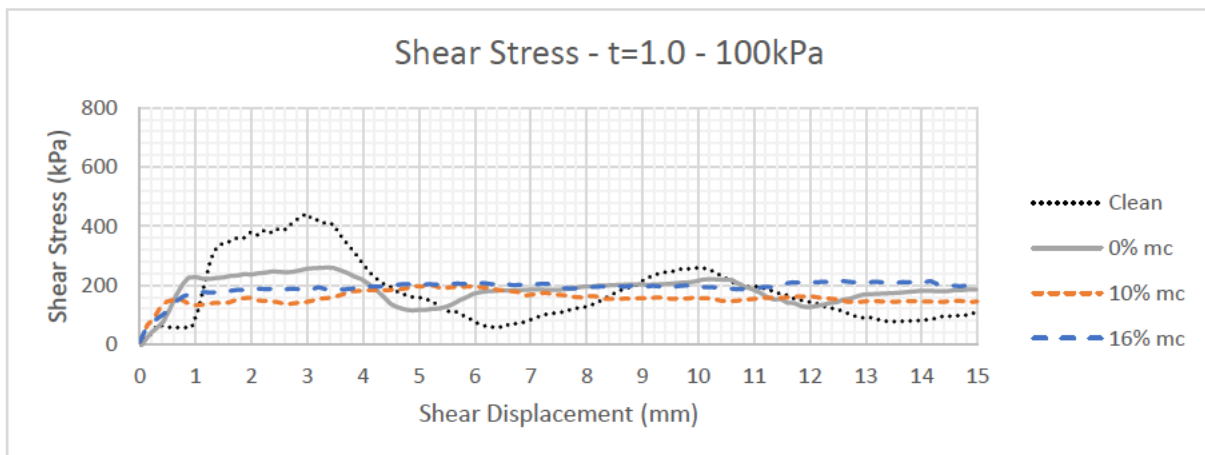
a normal stress of 100 kPa) was approximately 165 kPa (Table 15), this suggests that the infill material is the dominant controlling factor when the infill thickness is greater than the asperity height. Table 17 shows that as the moisture content increased the amplitude of each wave decreased in Figure 76a (e.g. decreasing amplitude of the first wave of 332.55, 217.08 and 153.47). This trend is also reflected in Figure 76b to a lesser extent. In addition, there is a decreasing amplitude from the first wave to the second wave within the data for each moisture content. This is due to the decreasing surface contact as each sawtooth moves beyond the initial sample location.

Table 17: Peaks, troughs, and amplitudes of Figure 76a

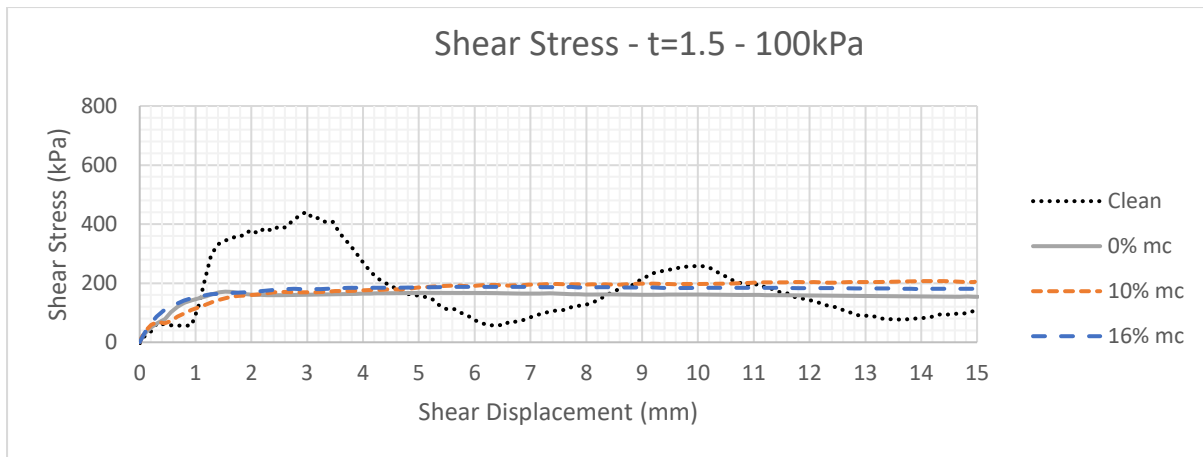
Moisture Content (%)	First Peak (kPa)	First Trough (kPa)	Second Peak (kPa)	Second Trough (kPa)	Amplitude 1 (kPa)	Amplitude 2 (kPa)
0	390.54	57.99	255.03	75.89	332.55	179.14
10	258.75	41.67	238.8	69.85	217.08	168.95
16	264.94	111.47	222.43	135.61	153.47	86.82



(a)



(b)



(c)

Figure 75: Shear Testing Results for 100 kPa (Shear Displacement vs Shear Stress)

a) $t/a=0.5$ b) $t/a=1.0$ c) $t/a=1.5$

5.3.3 Infilled Joints with normal stress of 300 kPa

Figure 77 shows a comparison of shear displacement and shear stress in the clean and infilled rock joints at the applied normal stresses of 300 kPa with moisture contents 0, 10 and 16%. Where the thickness of the infill was less than the asperity height (Figure 77a), the increase in normal stress has resulted in an increase of shear stress in comparison with Figure 76a. This has resulted in all samples reaching upper limit of 2200 N before 3 mm of shear displacement could occur. As a result, it is not possible to determine from this data if the same peak-trough pattern reflected in Figure 76a would occur. As the shear stress values for the three moisture conditions are not significantly different, the data set would need to be extended in order to be able to draw any definitive conclusions. In Figure 77b, where the infill thickness is equal to the asperity height peak-trough pattern reoccurs for the moisture content of 10%, and mildly for the moisture content of 16%. However, at 0% the limit of 2200 N is reached after approximately 1 mm. This suggests that the asperity profile is contributing to the shear stress, but less pronounced than that in Figure 76a, which shows that the infill material is the main contributing factor (as was also reflected when comparing Figure 76a to Figure 76b in Section 5.3.2). Figure 77c shows a convergence on 530 kPa for all moisture contents; however, at 0% the convergence is not as clustered as 10% and 16%. The maximum shear stress of the infill material (at all three moisture conditions and an applied normal stress of 300 kPa) was approximately 475 kPa (Table 15), this suggests that the infill material is the dominant controlling factor when the infill thickness is greater than the asperity height. A comparison of Figure 77b and Figure 77c shows that the shear stress convergence rate increases as the moisture content increases.

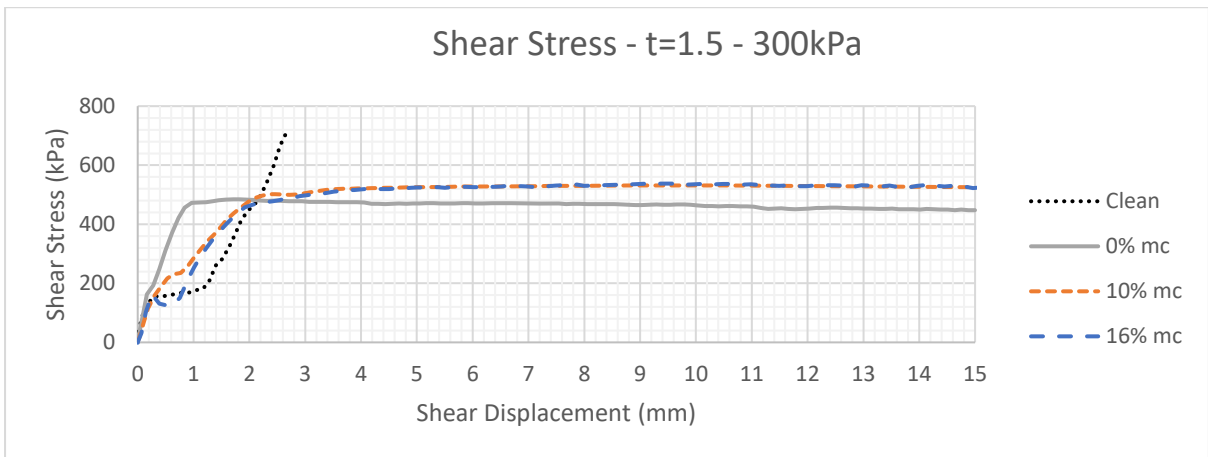
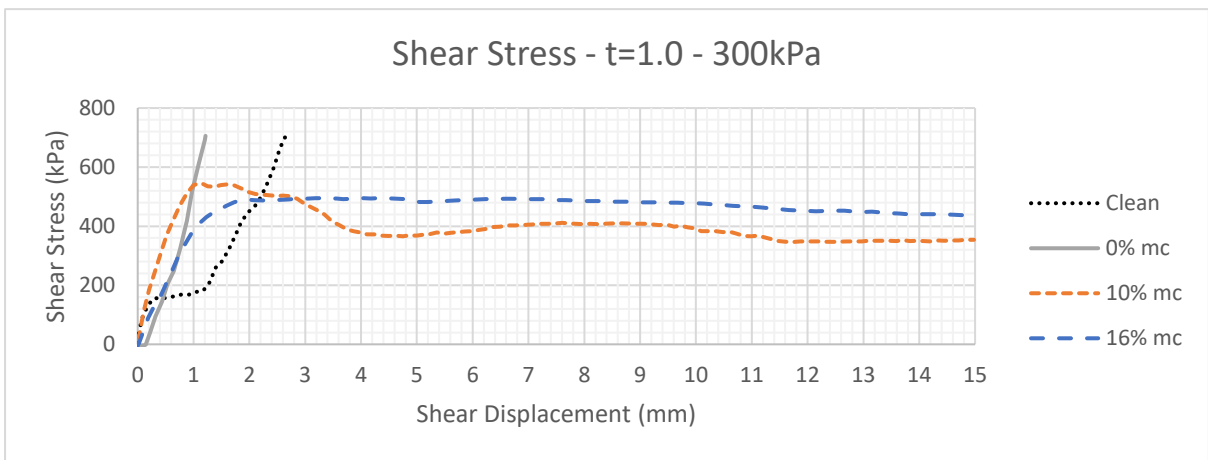
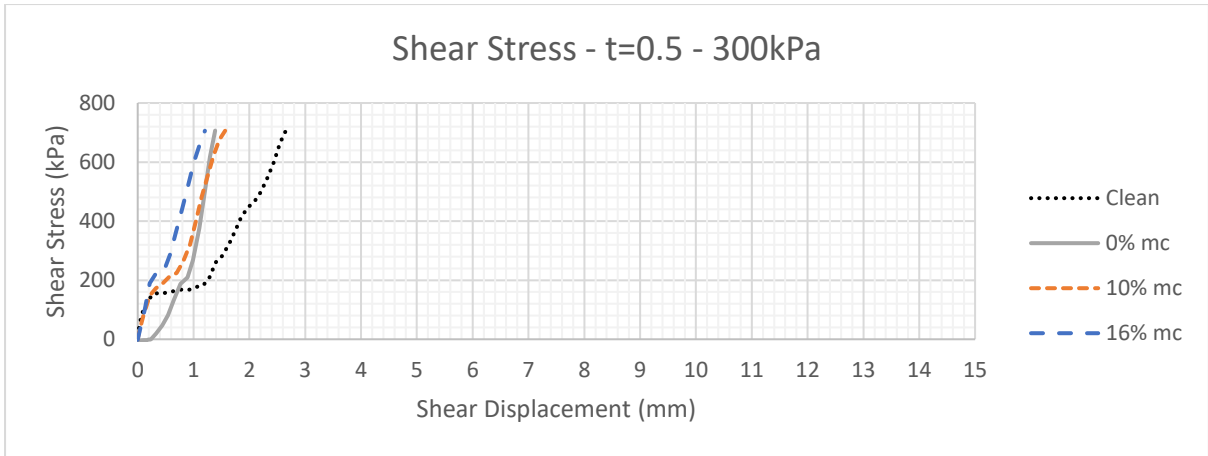
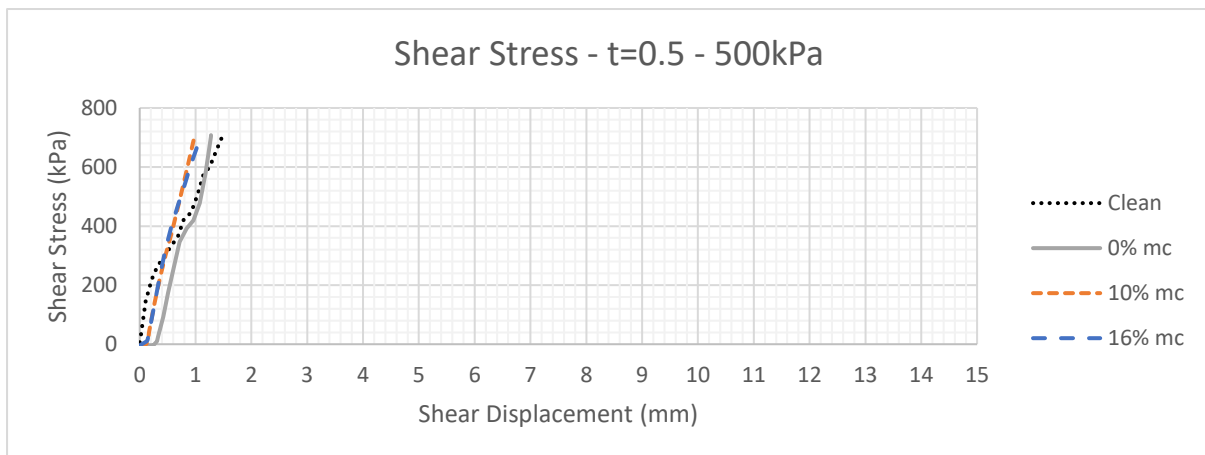


Figure 76: Shear Testing Results for 300 kPa (Shear Displacement vs Shear Stress)

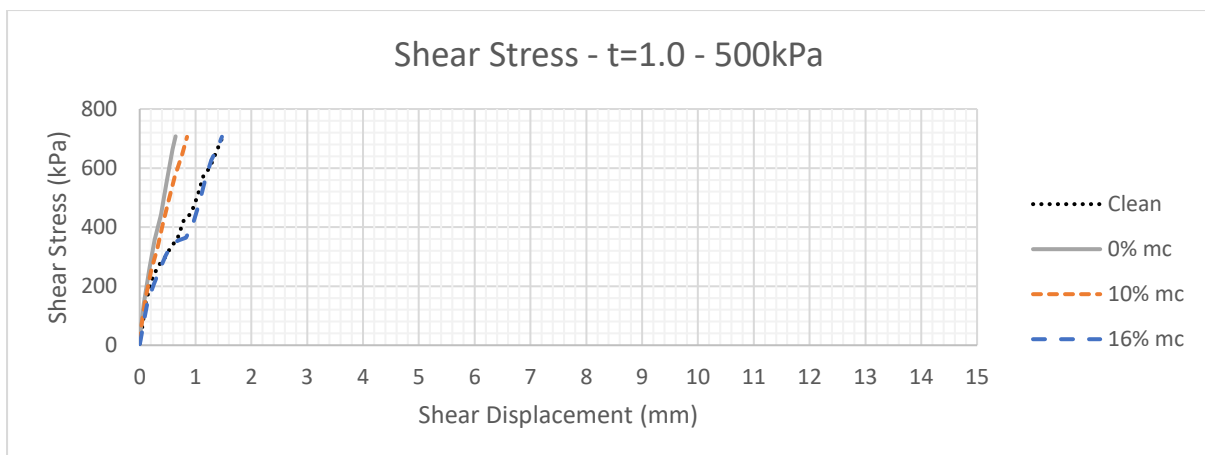
a) $t/a=0.5$ b) $t/a=1.0$ c) $t/a=1.5$

5.3.4 Infilled Joints with normal stress of 500 kPa

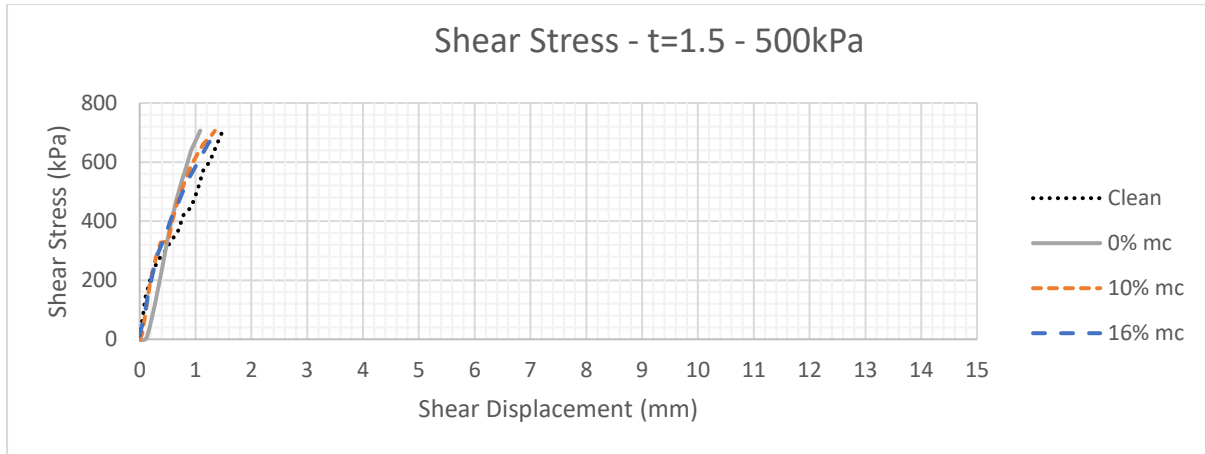
Figure 78 shows a comparison of shear displacement and shear stress in the clean and infilled rock joints at the applied normal stresses of 500 kPa with moisture contents 0, 10 and 16%. For all infill thickness the samples reached the upper limit of 2200 N before approximately 1.5 mm of shear displacement could occur, thus ending the test. As a result, it is not possible to determine from this data if the same peak-trough pattern reflected in Figure 76a would occur. However, in comparison with Figure 77a, Figure 78a shows a more tightly grouped dataset for the three moisture contents. Moisture contents of 10% and 16% are virtually identical, and the moisture content of 0% closely aligning with the clean joint behaviour. However, Figure 78b shows a divergence of the behaviour of the three moisture contents. Based on the behaviour seen in Section 5.3.3 this could be indicative of a faster convergence to the true peak shear stress as the moisture content increases, which is further supported by the reconvergence of the 0% and 10% conditions to the trend of the 16% condition (from Figure 78b) in Figure 78c. As the maximum shear stress of the infill material (at all three moisture conditions and an applied normal stress of 500 kPa) was determined as 700 kPa (upper limit of testing) (Table 15), it cannot be confirmed that the infill material is the dominant controlling factor when the infill thickness is greater than the asperity height under these conditions.



(a)



(b)



(c)

Figure 77: Shear Testing Results for 500 kPa (Shear Displacement vs Shear Stress)

a) $t/a=0.5$ b) $t/a=1.0$ c) $t/a=1.5$

5.3.5 Infilled Joints with normal stress of 700 kPa

Figure 79 shows a comparison of shear displacement and shear stress in the clean and infilled rock joints at the applied normal stresses of 700 kPa with moisture contents 0, 10 and 16%. Where the thickness of the infill was less than the asperity height (Figure 79a), the increase in normal stress has resulted in an increase of shear stress in comparison with Figure 76a. This has resulted in all samples reaching upper limit of 2200 N before approximately 1 mm of shear displacement could occur, apart from 16% moisture content in Figure 79c where peak shear stress was reached at approximately 1.5 mm. As a result, it is not possible to determine from this data if the same peak-trough pattern reflected in Figure 76a would occur. However, the general slope of the data shown in Figure 79 has increased from Figure 78 which increased from Figure 77. As the normal stress increased, the upper limit of shear stress is reached at a lesser shear displacement. Figure 79a and Figure 79b show tightly grouped datasets for all moisture conditions. However, Figure 79c shows a divergence of the behaviour of the 16% moisture content. Based on the behaviour seen in Sections 5.3.2 to 5.3.4 this could be indicative of a faster convergence on the peak true shear stress with increasing moisture content. As the maximum shear stress of the infill material (at all three moisture conditions and an applied normal stress of 700 kPa) was determined as 700 kPa (upper limit of testing) (Table 15), it cannot be confirmed that the infill material is the dominant controlling factor when the infill thickness is greater than the asperity height under these conditions.

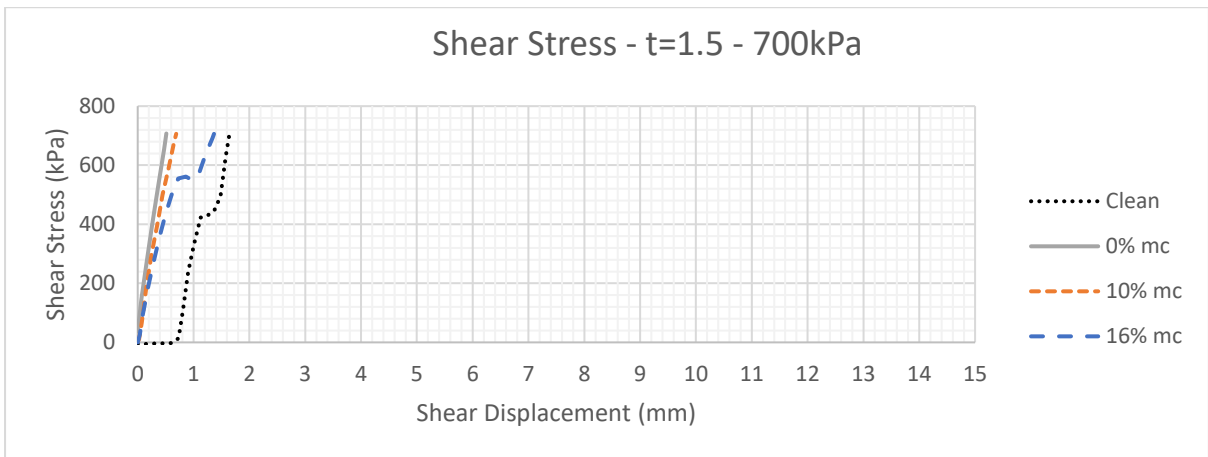
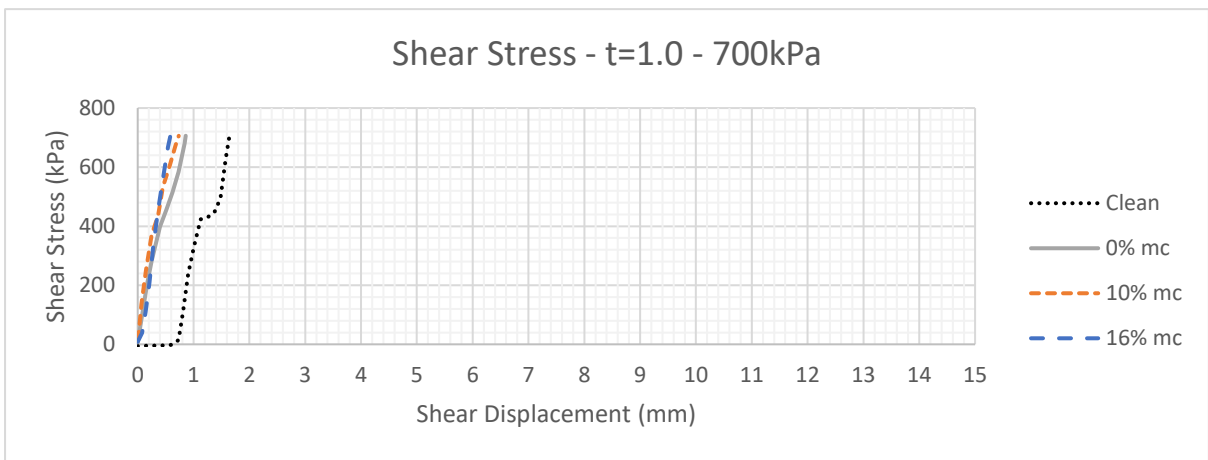
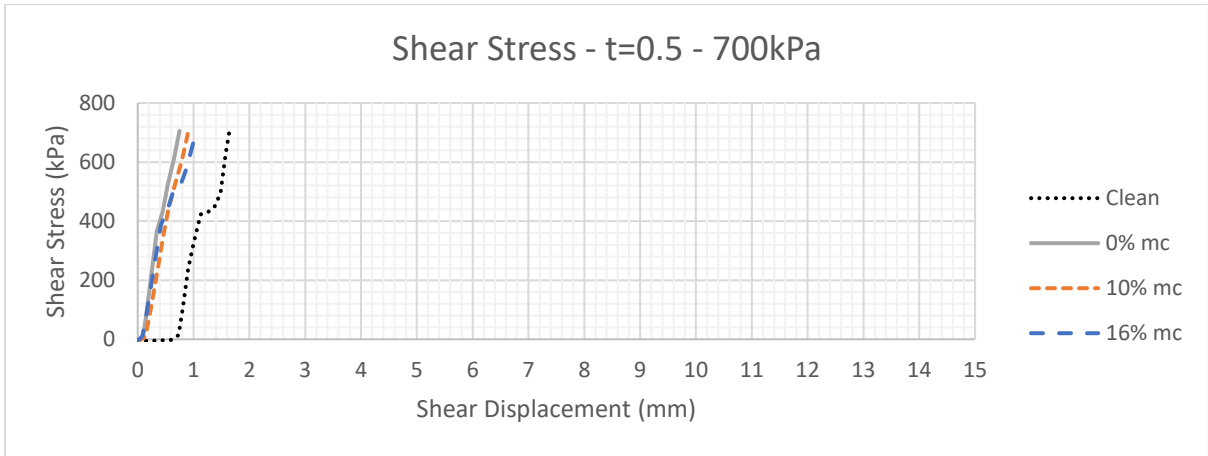


Figure 78: Shear Testing Results for 700 kPa (Shear Displacement vs Shear Stress)

a) $t/a=0.5$ b) $t/a=1.0$ c) $t/a=1.5$

5.3.6 Summary

The peak-trough behaviour with a wavelength approximately equal to the asperity base length of 7 mm (Sections 5.3.1 and 5.3.2) supports the expected outcomes (as based on previous research outlined in Chapter 2) for clean joints and joints where the infill thickness is less than the asperity height. In addition, this data also reflected the expected outcome that as the infill thickness increase to equal or greater than the asperity height, the infill properties would become the dominant controlling factor. In Section 5.3.2, as the moisture content increased the convergence rate of the shear stress increased as shown by the decreasing amplitude. In addition, the magnitude of the amplitude decreased with increasing shear displacement (due to the decrease in surface contact area as each sawtooth passed beyond the confine of the initial 63 mm cylindrical sample). This could not be directly reflected in the trends of the data for higher applied normal stress due to limiting conditions (increasing normal stress resulting in increasing shear stress that quickly reaching to upper testing limit). However, there were indicators throughout the analysis that could support this trend regardless of the applied normal stress. As such, a key conclusion can be drawn that, as the moisture content increases, the rate of convergence to the trending shear stress increases and the trending shear stress is generally reflective of the maximum shear stress of the infill material (thus the convergence is more pronounced when the infill thickness is greater than the asperity height). However, the magnitude of this convergent shear stress appears to be largely unaffected by the moisture content or infill thickness conditions, but rather controlled by the applied normal stress. Further testing at normal stresses lower than 300 kPa with a wider variety of moisture contents could prove to validate these results.

5.4 Direct Shear Testing of Rock Joints (Shear Displacement vs Normal Stress)

This section outlines the graphical summaries of the results from the direct shear testing of the clean and infilled rock joints with regards to the shear displacement and normal stress variables. The process for this testing and general data collation is outlined in Section 4.4. The bulk collated data used to produce these graphs is given in Appendix H.

5.4.1 Clean Joints at normal stresses of 100 kPa, 300 kPa, 500 kPa, and 700 kPa

Figure 80 shows a comparison of shear displacement and normal stress in the clean rock joints at the applied normal stresses of 100, 300, 500 and 700 kPa. When subjected to 100 kPa of normal stress the test runs for the full shear displacement of 15 mm. However, when the clean rock joints are subject to the higher normal stress of 300, 500 and 700 kPa the upper limit of 2200 N (approximately 700 kPa) was reached before 3 mm of shear displacement could occur. As such, the general peak-trough behaviour linked to the asperity profile cannot be automatically extended to the higher normal stress values. The consistency of these normal stresses to remain approximately equal to the applied normal stress validates that the testing was conducted under CNL conditions.

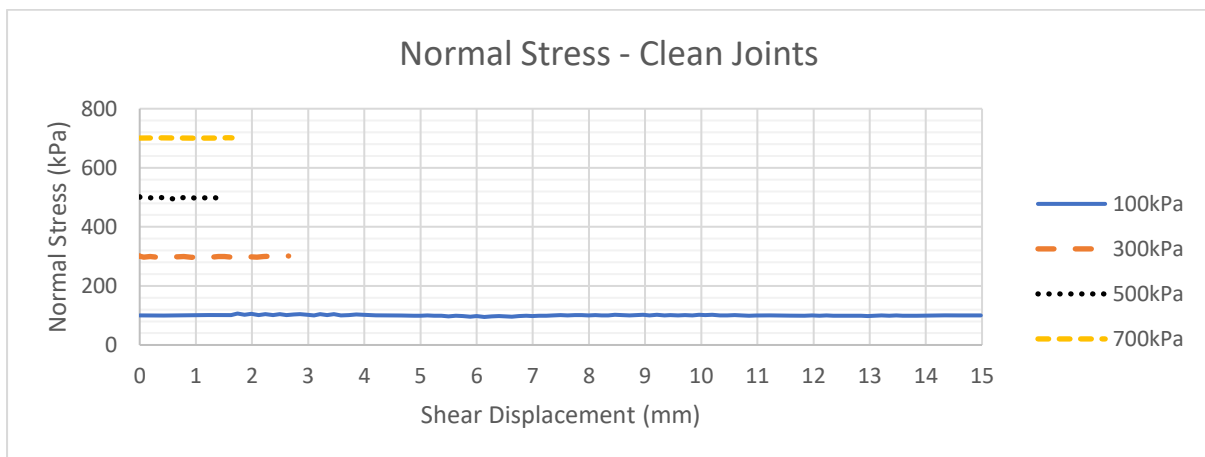
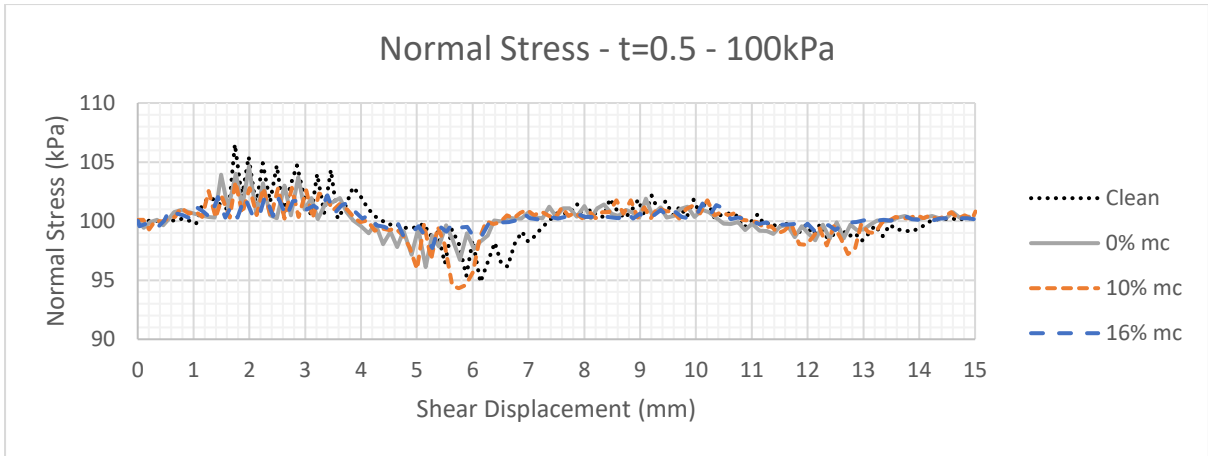


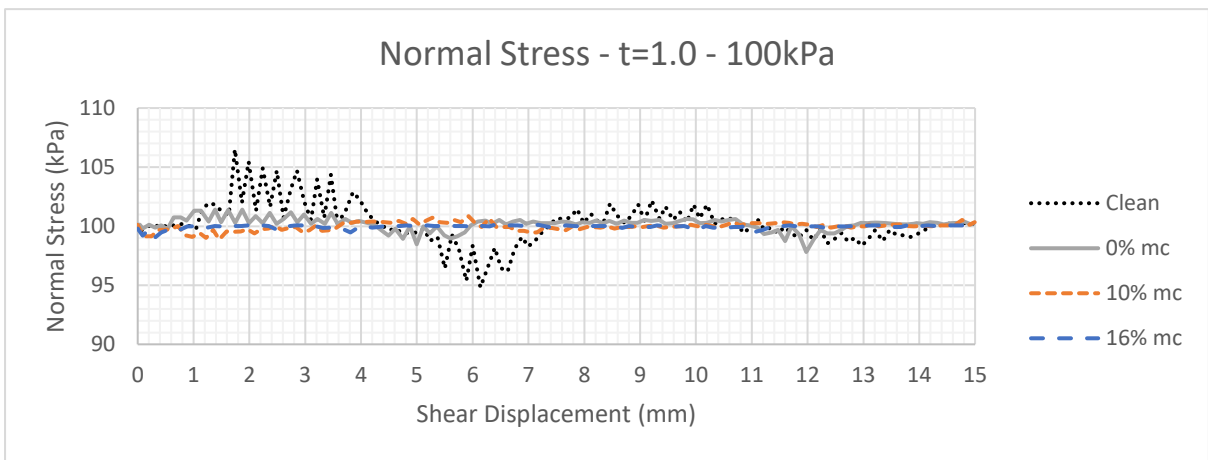
Figure 79: Clean Joint Results ($t/a=0$) (Shear Displacement vs Normal Stress)

5.4.2 Infilled Joints with normal stress of 100 kPa

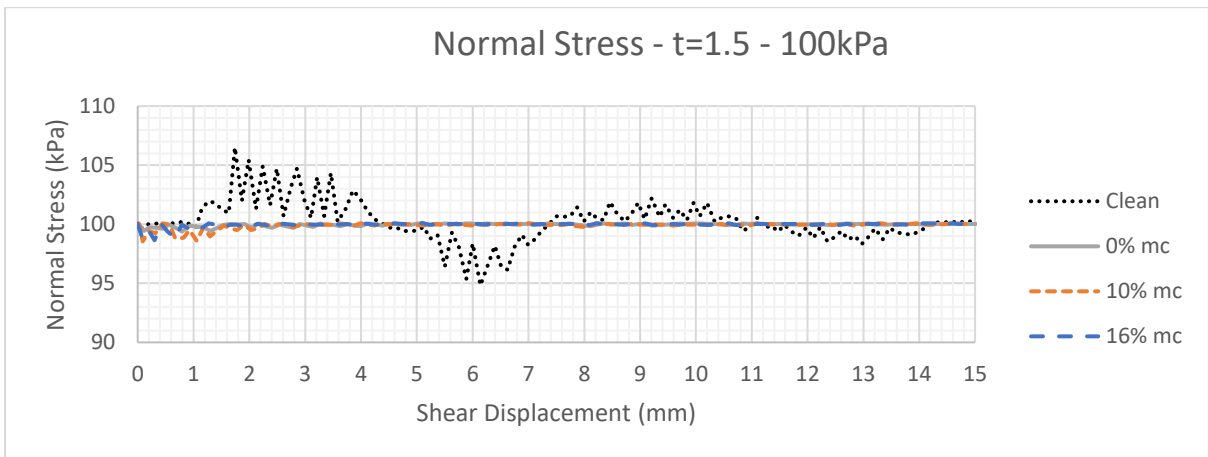
Figure 81 shows a comparison of shear displacement and normal stress in the clean and infilled rock joints at the applied normal stresses of 100 kPa with moisture contents 0, 10 and 16%. Where the thickness of the infill was less than the asperity height (Figure 81a), the normal stress profile follows a repetitive wave pattern with peaks and troughs approximately 7 mm in wavelength. As the asperity base length is 7 mm this indicates that the asperity profile controls the general behaviour of the normal stress (in combination with the applied normal loading condition) of these clean and infilled rock joint. The location of the peaks and troughs in the wave form align with those from Section 5.3.2 relating to shear stress, further reinforcing that there is a direct relationship between the shear stress and normal stress of rock joints. However, the amplitude of the normal stress waves is significantly lower than those from Section 5.3.2 and stay within approximate ± 5 kPa of the input applied normal pressure. This supports that the testing was completed under CNL conditions. In Figure 81b, where the infill thickness is equal to the asperity height the pattern reflected in Figure 81a is flattened. This suggests that the infill material is a controlling factor of the shear stress, and the asperity profile still contributes but to a lesser degree than in Figure 81a. Figure 81c shows a convergence on 100 kPa for all moisture contents, which is reflective of the applied normal loading condition. The general behaviour of the normal stress trends follows those outlined in Section 5.3 regarding shear stress, but due to the decreased magnitude of the fluctuations the impact is minor under CNL boundary conditions. A comparison of Figure 81a, Figure 81b and Figure 81c shows that, as the moisture content increases, the rate of convergence to the trending applied normal stress increases. This is generally reflected by the decreasing variation from the applied normal stress value as the moisture content increased. There are instances that do not reflect this, such as at approximately 5.8 and 12.8 mm shear displacement, where the variance of the normal stress of the 10% sample is greater than that of the 0% sample. However, due to the small stress fluctuations of up to approximately ± 5 kPa further testing with a wider range of moisture contents at a low applied normal stress (e.g. 100 kPa), with targeted analysis of the normal stress trends could show the trends more conclusively. In addition, testing under CNS conditions with varying moisture contents would provide better insight into the impact of moisture content on the normal stress of rock joint subjected to shear.



(a)



(b)



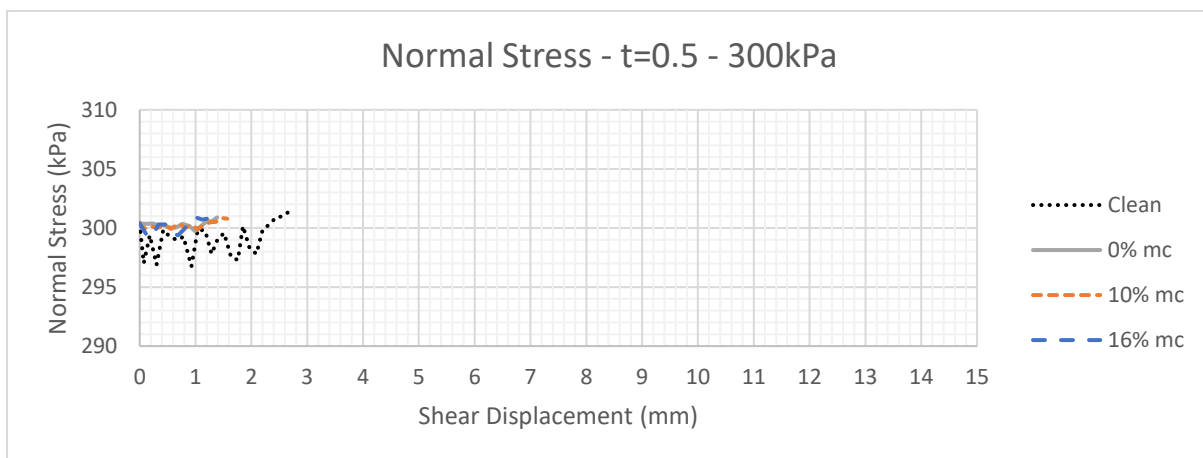
(c)

Figure 80: Shear Testing Results for 100 kPa (Shear Displacement vs Normal Stress)

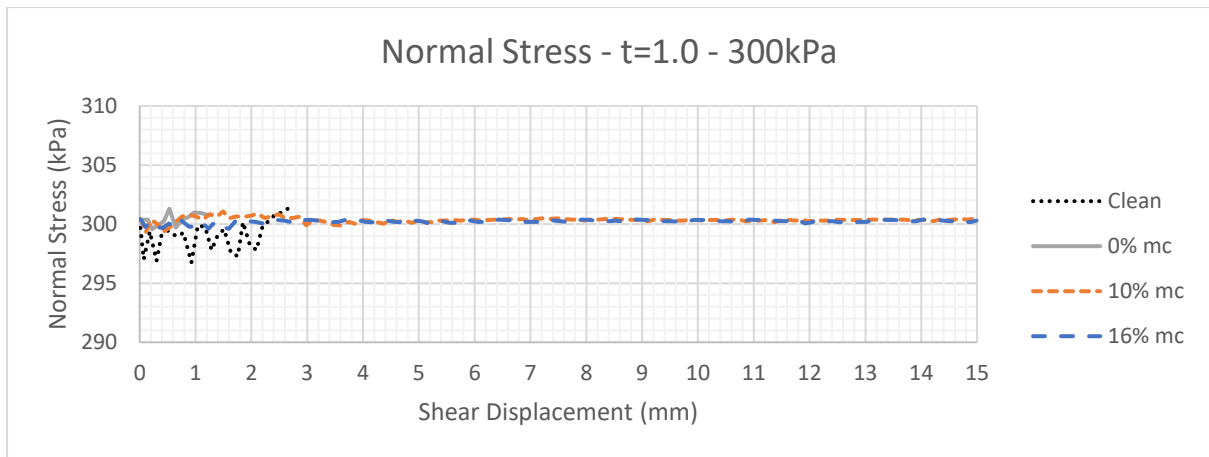
a) $t/a=0.5$ b) $t/a=1.0$ c) $t/a=1.5$

5.4.3 Infilled Joints with normal stress of 300 kPa

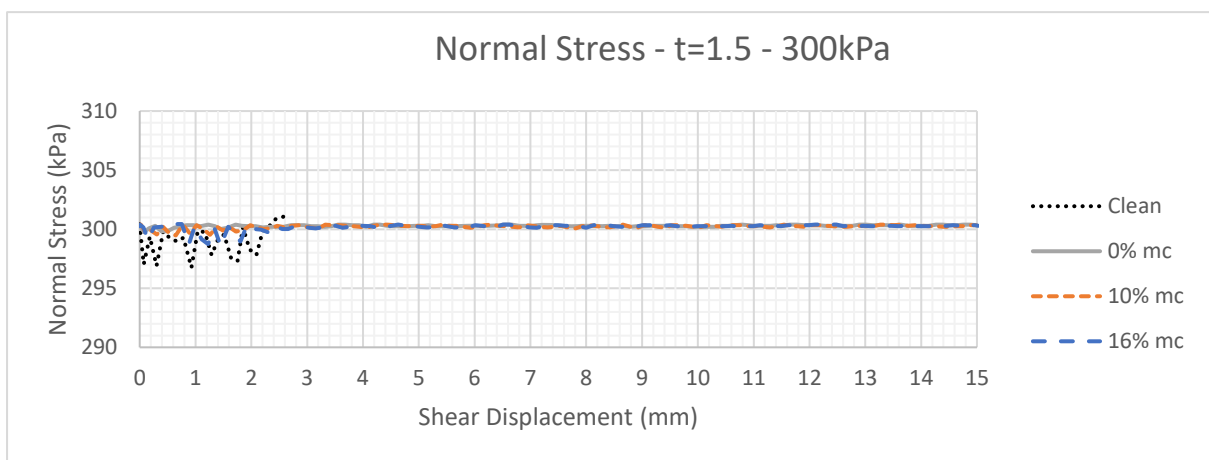
Figure 82 shows a comparison of shear displacement and normal stress in the clean and infilled rock joints at the applied normal stresses of 300 kPa with moisture contents 0, 10 and 16%. Where the thickness of the infill was less than the asperity height (Figure 82a), data regarding the normal stress behaviour of the joint is limited as the shear stress reached the upper testing limit of 2200 N (as outlined in Section 5.3.3), thus ending the test before 3 mm of shear displacement could occur. As a result, it is not possible to determine from this data if the same peak-trough pattern reflected in Figure 81a would occur. As the normal stress values for the three moisture conditions are not significantly different, the data set would need to be extended in order to be able to draw any definitive conclusions. In Figure 82b, where the infill thickness is equal to the asperity height, the peak-trough pattern mildly reoccurs for the moisture content of 10% and 16%. However, at 0% the limit of 2200 N is reached at approximately 1 mm. The extended data (to the full 15 mm shear displacement) for 10% and 16% is available as the increase in infill thickness is now a key contributing factor to the shear strength properties of the joint and thus did not reach to upper normal loading limit of 2200 N. The location of the peaks and troughs in the wave form align with those from Section 5.3.3 relating to shear stress, further reinforcing that there is a direct relationship between the shear stress and normal stress of rock joints. However, the amplitude of the normal stress waves is significantly lower than those from Section 5.3.3 and stay within approximate ± 2 kPa of the input applied normal pressure. This demonstrates that the testing was completed under CNL conditions. Figure 81c shows a convergence on 300 kPa for all moisture contents, which is reflective of the applied normal loading condition. The general behaviour of the normal stress trends follows those outlined in Section 5.3 regarding shear stress, but due to the decreased magnitude of the fluctuations the impact is minor under CNL boundary conditions.



(a)



(b)



(c)

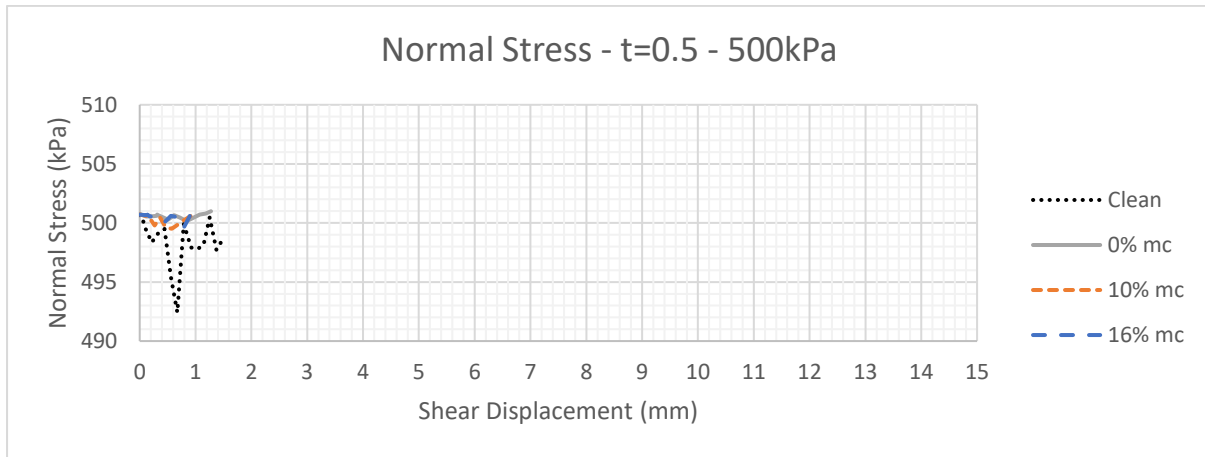
Figure 81: Shear Testing Results for 300 kPa (Shear Displacement vs Normal Stress)

a) $t/a=0.5$ b) $t/a=1.0$ c) $t/a=1.5$

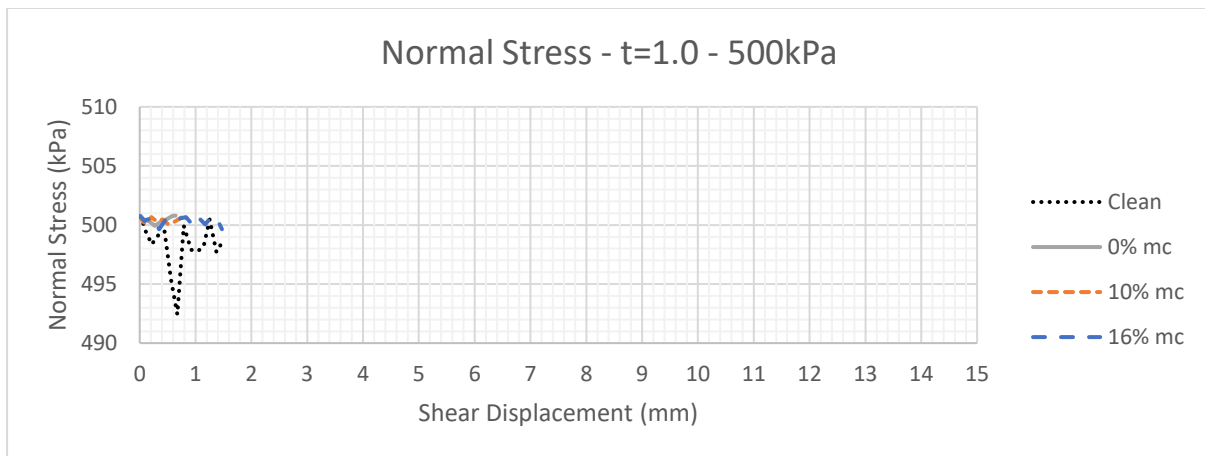
5.4.4 Infilled Joints with normal stress of 500 kPa

Figure 83 shows a comparison of shear displacement and normal stress in the clean and infilled rock joints at the applied normal stresses of 500 kPa with moisture contents 0, 10 and 16%. For all infill thickness the samples shear stresses reached the upper limit of 2200 N before approximately 1.5 mm of shear displacement could occur (from Section 5.3.4), thus ending the test. As a result, it is not possible to determine from this data if the same peak-trough pattern reflected in Figure 81 and 82b would occur. As the normal stress values for the three moisture conditions are not significantly different, the data set would need be extended in order to be able to draw any definitive conclusions. Based on the available data, the amplitude of the normal stress waves within approximate ± 1 kPa of the input applied normal pressure, which is negligible given the magnitude and scope of the test. Figure 83 shows a general trend to converge on 500 kPa for all moisture contents, which is reflective of the applied normal loading

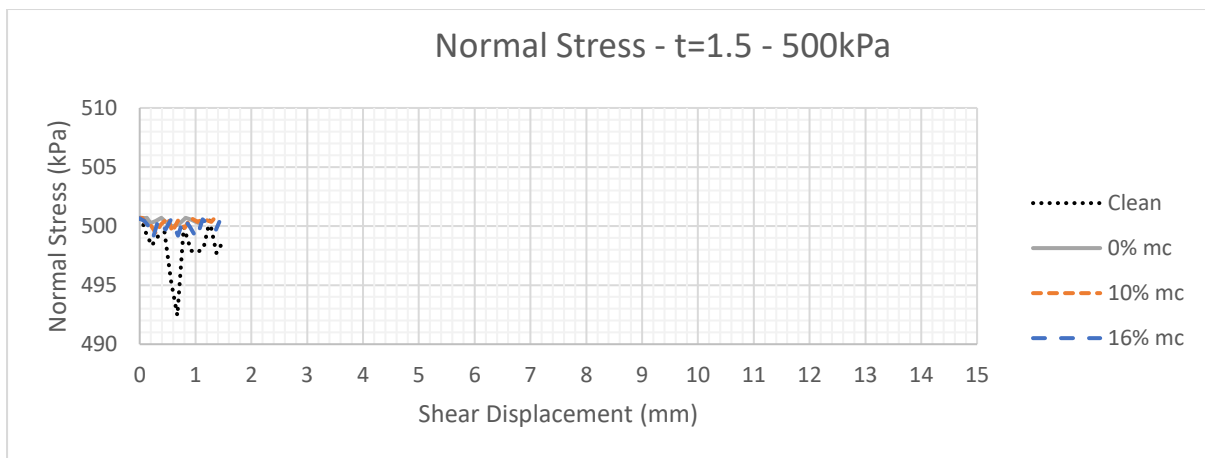
condition. This supports that the testing was completed under CNL conditions. Due to the lack of data available regarding the normal stress behaviour and trends cannot be definitively determined.



(a)



(b)



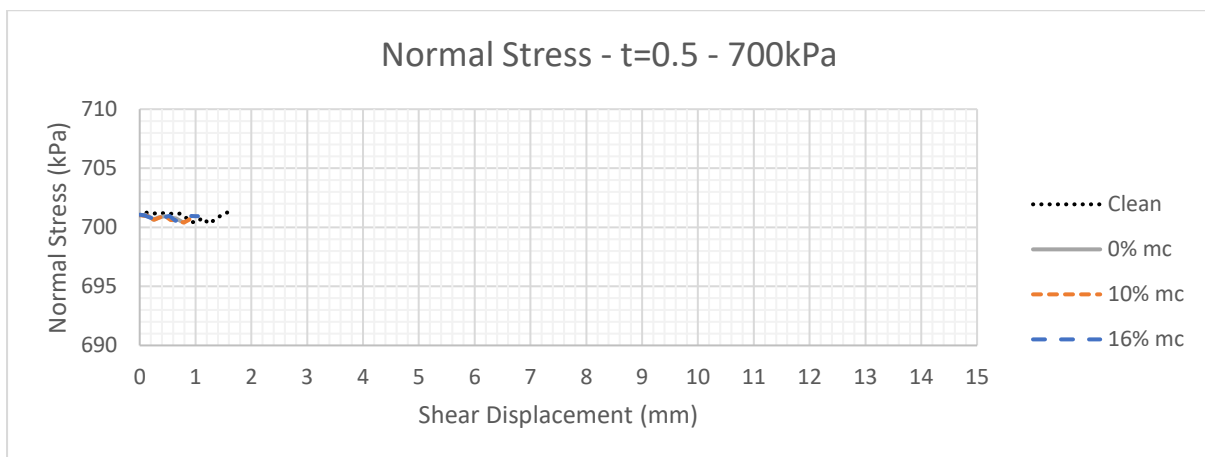
(c)

Figure 82: Shear Testing Results for 500 kPa (Shear Displacement vs Normal Stress)

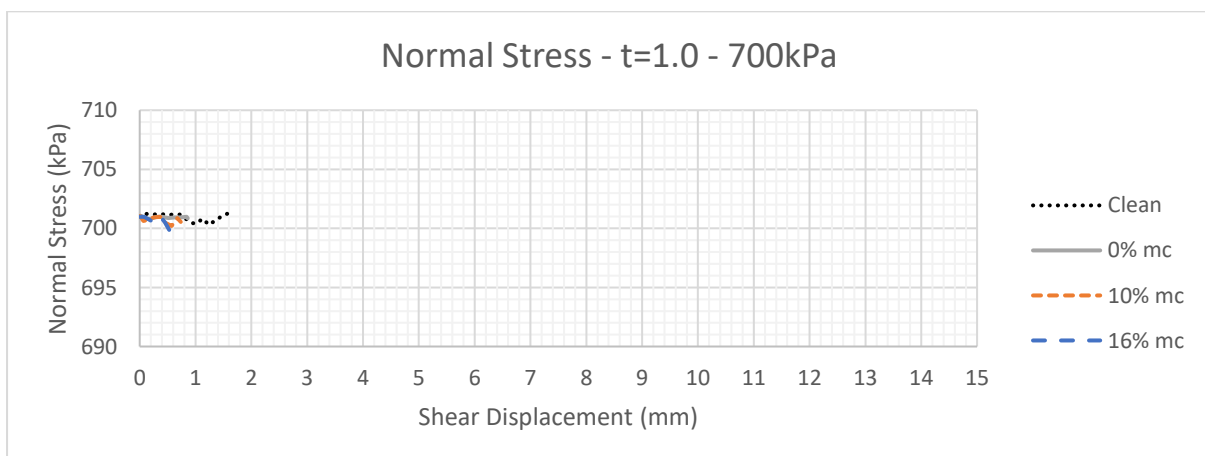
a) $t/a=0.5$ b) $t/a=1.0$ c) $t/a=1.5$

5.4.5 Infilled Joints with normal stress of 700 kPa

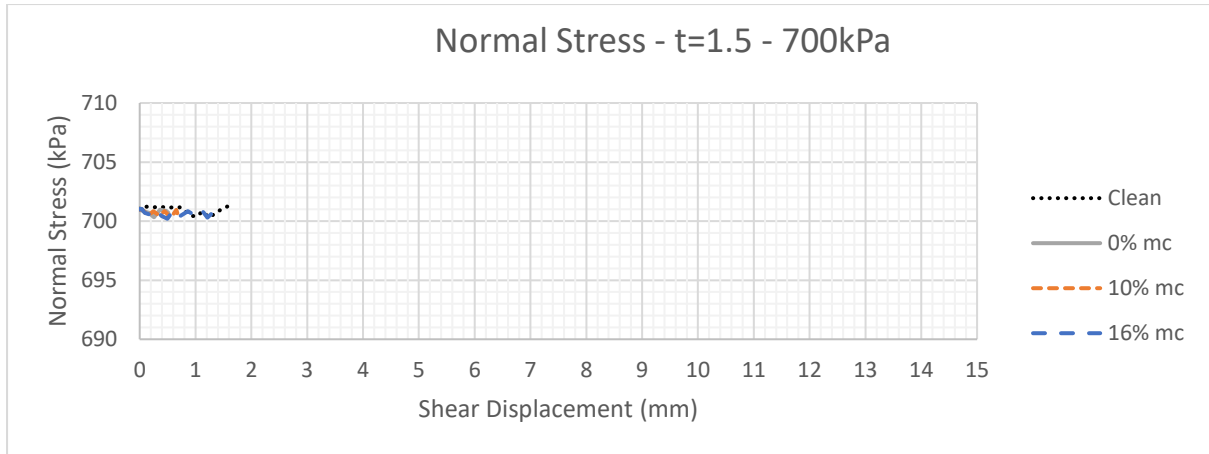
Figure 84 shows a comparison of shear displacement and normal stress in the clean and infilled rock joints at the applied normal stresses of 700 kPa with moisture contents 0, 10 and 16%. For all infill thickness the samples shear stresses reached the upper limit of 2200 N before approximately 1.5 mm of shear displacement could occur (from Section 5.3.5), thus ending the test. As a result, it is not possible to determine from this data if the same peak-trough pattern reflected in Figure 81 and 82b would occur. As the normal stress values for the three moisture conditions are not significantly different, the data set would need be extended in order to be able to draw any definitive conclusions. Based on the available data, the amplitude of the normal stress waves within approximate ± 1 kPa of the input applied normal pressure, which is negligible given the magnitude and scope of the test. Figure 83 shows a general trend to converge on 500 kPa for all moisture contents, which is reflective of the applied normal loading condition. This supports that the testing was completed under CNL conditions. Due to the lack of data available regarding the normal stress the behaviour and trends cannot be definitively determined.



(a)



(b)



(c)

Figure 83: Shear Testing Results for 700 kPa (Shear Displacement vs Normal Stress)

a) $t/a=0.5$ b) $t/a=1.0$ c) $t/a=1.5$

5.4.6 Summary

The peak-trough behaviour with a wavelength approximately equal to the asperity base length of 7 mm (Section 5.4.1 and Section 5.4.2) supports the expected outcomes (as based on previous research outlined in Chapter 2) for clean joints and joints where the infill thickness is less than the asperity height. In addition, this data also reflected the expected outcome that as the infill thickness increase to equal or greater than the asperity height, the infill properties would become the dominate controlling factor. In Section 5.4.2, as the moisture content increased the convergence rate of the normal stress increased as shown by the decreasing amplitude. Where the magnitude of the amplitude decreased with increasing shear displacement in Section 5.3 with regards to shear stress, this does not occur in the normal stress data in Section 5.4 as the normal stress applied is constant due to CNL boundary conditions and servo controlled by the ShearTrac2. In Section 5.4, this is also reflected in the trends of the data for higher applied normal stress. Based on the data available in Section 5.4.2 (to a lesser extent Section 5.4.3), the conclusion can be drawn that as the moisture content increases, the rate of convergence to the applied normal stress increases, which is more pronounced when the infill thickness is greater than the asperity height. However, due to the small stress fluctuations of up to approximately ± 5 kPa further testing with a wider range of moisture contents at a low applied normal stress (e.g. 100 kPa), with targeted analysis of the normal stress trends could show the trends more conclusively. In addition, testing under CNS conditions with varying moisture contents would provide better insight, into the impact of moisture content on the normal stress of rock joint subjected to shear, due to the release of normal stress as a fixed boundary condition.

5.5 Direct Shear Testing of Rock Joints (Shear Displacement vs Normal Displacement)

This section outlines the graphical summaries of the results from the direct shear testing of the clean and infilled rock joints with regards to the shear displacement and normal displacement variables. The process for this testing and general data collation is outlined in Section 4.4. The bulk collated data used to produce these graphs is given in Appendix H.

5.5.1 Clean Joints at normal stresses of 100 kPa, 300 kPa, 500 kPa, and 700 kPa

Figure 84 shows a comparison of shear displacement and normal displacement in the clean rock joints at the applied normal stresses of 100, 300, 500 and 700 kPa. When subjected to 100 kPa of normal stress the test runs for the full shear displacement of 15 mm. At 100 kPa the normal displacement profile follows a repetitive wave pattern with peaks and troughs approximately 7 mm in wavelength, with a maximum peak of -1.23 mm. This pattern is representation of the dilation curve for this sample. As the asperity base length is 7 mm this indicates that the asperity profile controls the general behaviour of the shear stress of this clean rock joint. However, as the asperity height was 2 mm this shows a difference of 0.77 mm between the maximum normal displacement and the asperity height. This indicated that failure on the joint profile occurred. Figure 85 shows the failure of Sample CL1 (Clean Joint 1 subjected to 100 kPa normal stress). When compared to the types of failure outlined in Section 2.3 this joint has failure through Type 1 sliding failure, which reflects the expected failure mode due to the low asperity angle of less than 30° . This sliding failure wears on the joint material, which in turn decreases the height of the asperity (but not asperity angle) and causes excess material to gather in the valley of the asperity profile. This effect explains the decrease in from the peak normal displacement of -1.23 mm to the second crest of -0.988 mm. When the clean rock joints are subject to the higher normal stresses of 300, 500 and 700 kPa the shear stress reached the upper limit of 2200 N before 3 mm of shear displacement could occur. As such, the general peak-trough behaviour linked to asperity profile cannot be extended to the higher normal stress values. However, investigation of the joint surface profile of CL2 (Clean Joint 2 subjected to 300 kPa normal stress) (Figure 86) indicates that this joint also underwent sliding failure. Comparatively the joint surface profiles of CL3 (Clean Joint 3 subjected to 500 kPa normal stress) (Figure 87) and CL4 (Clean Joint 4 subjected to 700 kPa normal stress) (Figure 88) show minimal damage due to shearing. As it would be expected that the damage to the joint profile would increase as the normal loading increases (and as such the shear stress increases), this may indicate that there was an inconsistency between these samples' materials. On further inspection, Figure 85 and Figure 86 appear to have a greater proportion of sand particles that settled in the tip of the asperity

profile than in Figure 85 and 86. Based on this, additional consideration to the scale of asperity profile (allowing for easier settlement of material), cement grout mixture (or another joint material), and casting of the artificial rock joint should be given in future research.

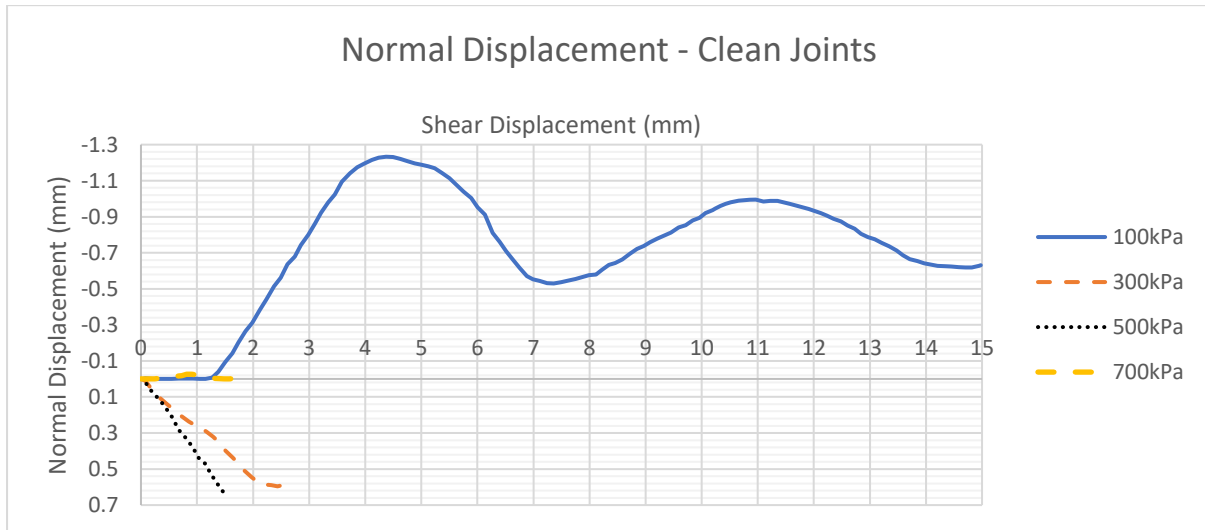


Figure 84: Clean Joint Results ($t/a=0$) (Shear Displacement vs Normal Displacement)



Figure 85: Joint Failure on Sample CL1



Figure 86: Joint Failure of Sample CL2



Figure 87: Joint CL3 (after testing)



Figure 88: Joint CL4 (after testing)

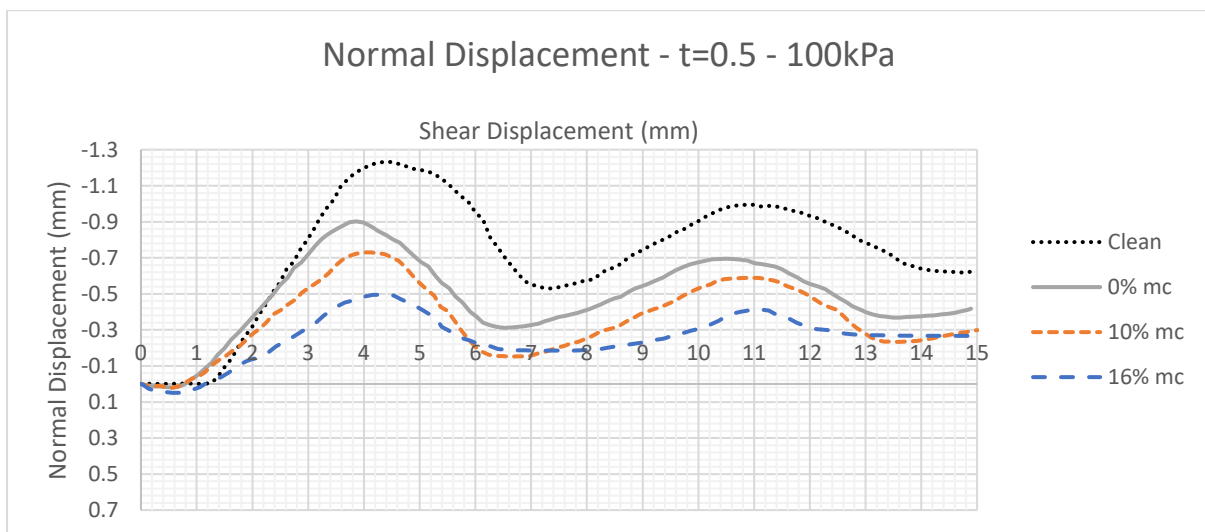
5.5.2 Infilled Joints with normal stress of 100 kPa

Figure 89 shows a comparison of shear displacement and normal displacement in the clean and infilled rock joints at the applied normal stresses of 100 kPa with moisture contents 0, 10 and 16%. Where the thickness of the infill was less than the asperity height (Figure 89a), the normal displacement profile follows a repetitive wave pattern with peaks and troughs approximately 7 mm in wavelength. As the asperity base length is 7 mm this indicates that the asperity profile controls the general behaviour of the normal displacement (in combination with the applied normal loading condition) of these clean and infilled rock joint. The location of the peaks and troughs in the wave form align with those from Section 5.3.2 relating to shear stress and Section 5.4.2 relating to normal stress. In Section 5.2.8, Figure 73 showed that as the moisture content of the infill material increases, the angle of internal friction (slope of the trend) decreases and the cohesion increases. This trend is reflected in the results outlined in Table 18 and Figure 89 where it shows that as the moisture content of the infill material increases, the normal displacement decreases. This is likely due to the lubricating effect of moisture in the infill material. With decreased moisture content the angle of internal friction of the infill increases, thus the friction forces acting on the infill soil particles increases. However, when the moisture content increases the

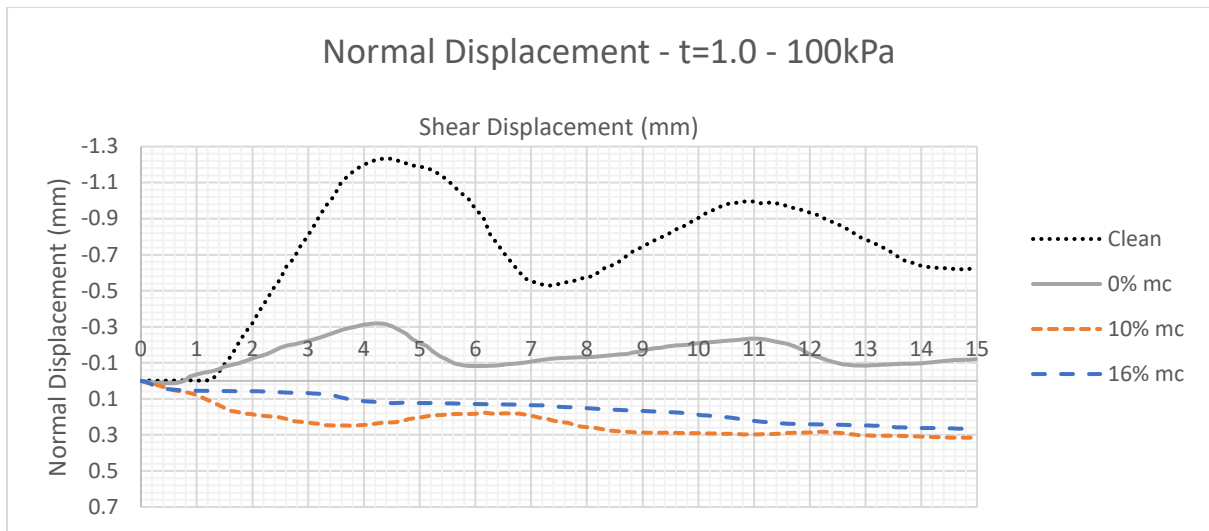
particles can more easily slide past each other. As the infill thickness increases in Figure 89b this peak-trough behaviour is flattened as was reflected in Section 5.3.2 and 5.4.2, before converging at approximately 0.3 mm contraction in Figure 89c. In Figure 89b the amplitude of the waveform decreases as the moisture content increases. A comparison of the infill conditions shows that when the infill is greater than or equal to the asperity height, the characteristics of the infill material dominate the behaviour of the rock joint. This is also supported by the occurrence of contraction rather than dilation. With increasing infill thickness, the impact of moisture content becomes more apparent, and as the moisture content increases the convergence rate of the trend to approximately 0.3 mm contraction increases.

Table 18: Peak normal displacement under 100 kPa normal pressure at $t/a=0.5$

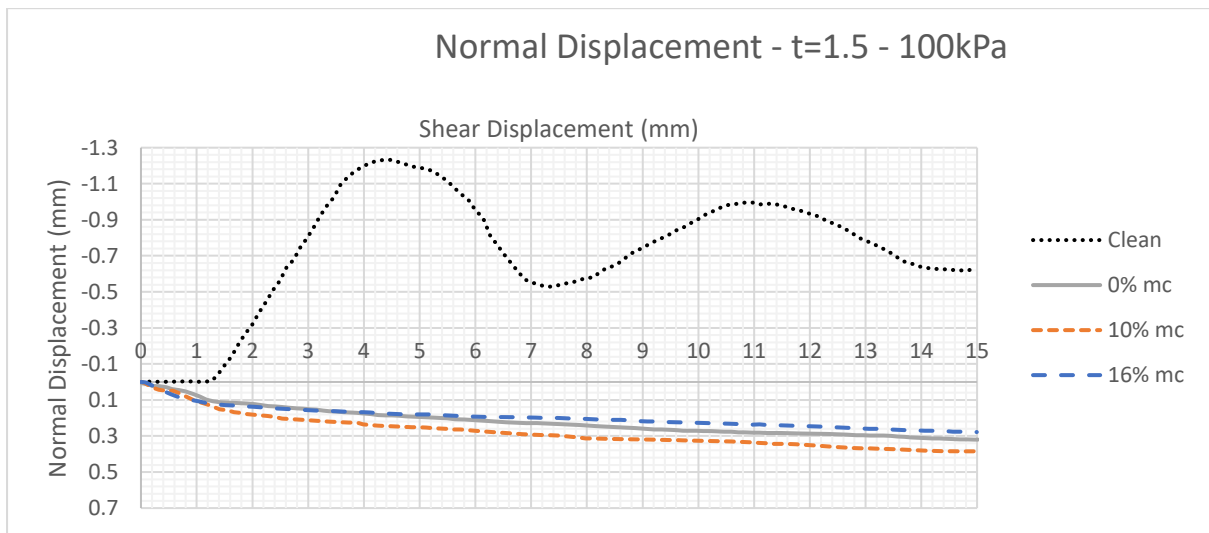
Moisture Content	First Peak Normal Displacement (maximum) (mm)	Second Peak Normal Displacement (mm)
Clean	-1.23	-0.99
0%	-0.902	-0.695
10%	-0.729	-0.589
16%	-0.495	-0.413



(a)



(b)



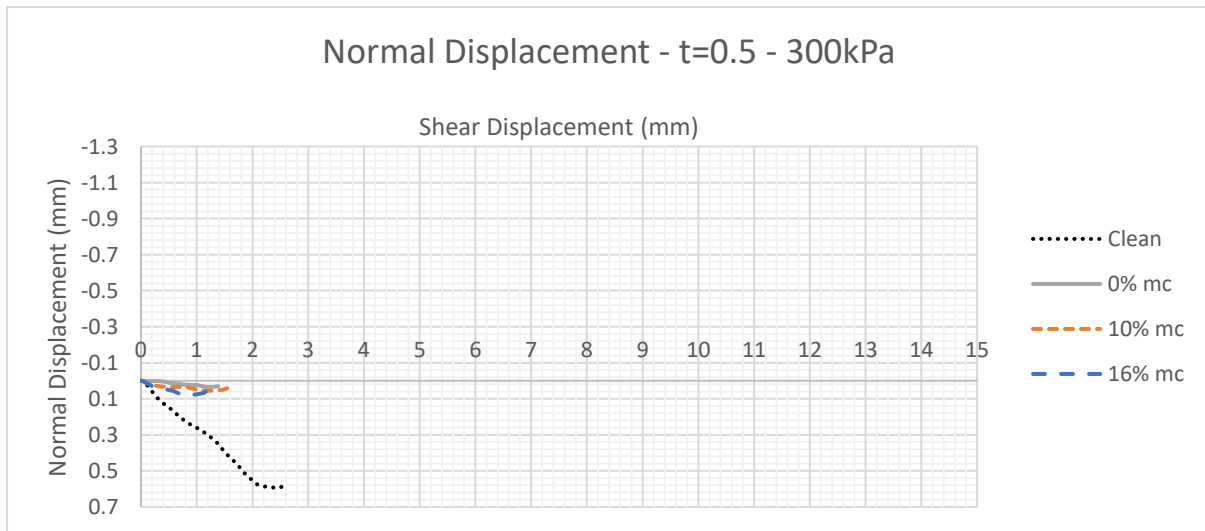
(c)

Figure 89: Shear Testing Results for 100 kPa (Shear Displacement vs Normal Displacement)
 a) $t/a=0.5$ b) $t/a=1.0$ c) $t/a=1.5$

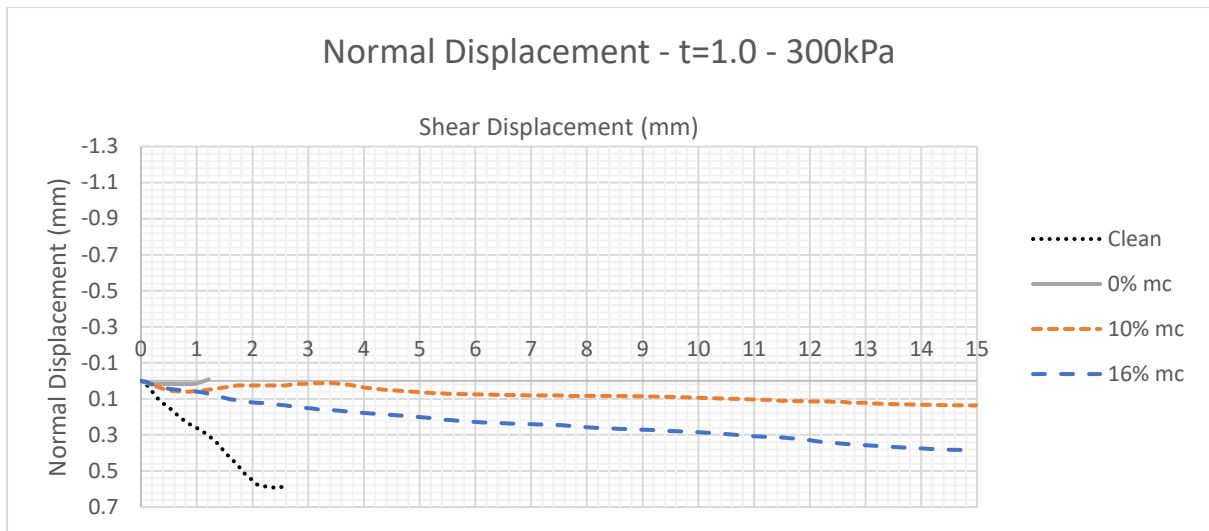
5.5.3 Infilled Joints with normal stress of 300 kPa

Figure 90 shows a comparison of shear displacement and normal displacement in the clean and infilled rock joints at the applied normal stresses of 300 kPa with moisture contents 0, 10 and 16%. Where the thickness of the infill was less than the asperity height (Figure 90a), data regarding the normal stress behaviour of the joint is limited as the shear stress reached the upper testing limit of 2200 N (as outlined in Section 5.3.3 and Section 5.4.3), thus ending the test before 3 mm of shear displacement could occur. As a result, it is not possible to determine from this data if the same peak-trough pattern reflected in Figure 89a would occur. In Figure 90b, where the infill thickness is equal to the asperity height peak-

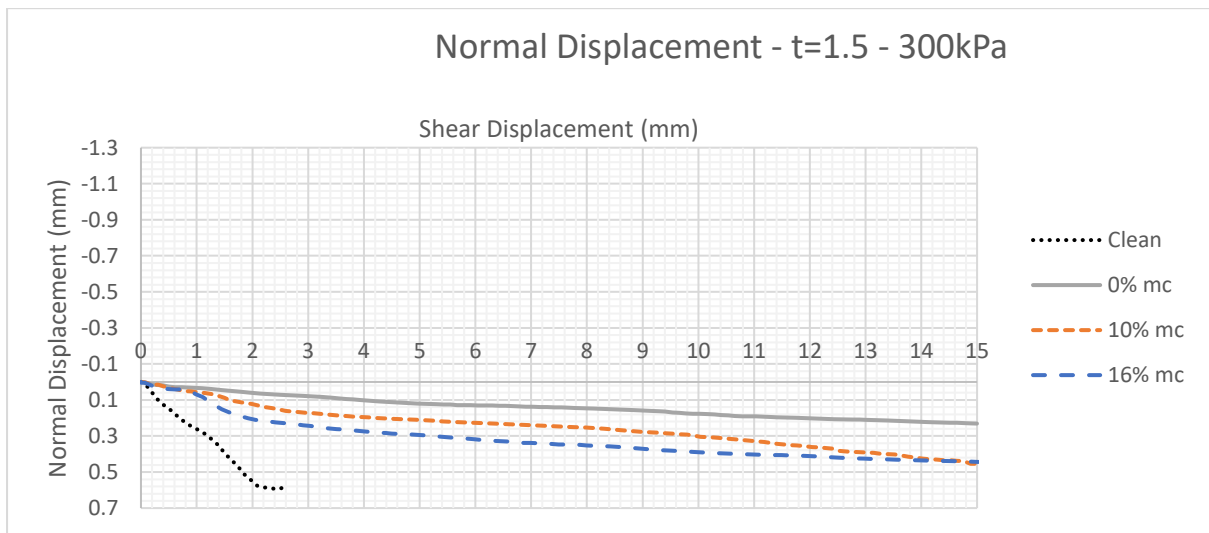
trough pattern mildly reoccurs for the moisture content of 10% and 16%. However, at 0% the limit of 2200 N is reached before approximately 3 mm of shear displacement. The extended data (to the full 15 mm shear displacement) for 10% and 16% is available as the increase in infill thickness is now a key contributing factor to the shear strength properties of the joint and thus did not reach to upper normal loading limit of 2200 N. The location of the peaks and troughs in the wave form align with those from Section 5.3.3 relating to shear stress and Section 5.4.3 relating to normal stress, further reinforcing that there is a direct relationship between the shear stress and normal stress of rock joints. Figure 90 shows that as the moisture content of the infill material increases, the contraction of the normal displacement increases. As outlined in Section 5.5.2, this is likely due to the lubricating effect of moisture in the infill material. With decreased moisture content the angle of internal friction of the infill increases, thus the friction forces acting on the infill soil particles increases. However, when the moisture content increases the particles can more easily slide past each other, thus leading to increased contraction. As the infill thickness increases in Figure 90c this peak-trough behaviour is flattened as was reflected in Section 5.3.3 and 5.4.3, before converging at approximately 0.4 mm contraction. While subtle, the amplitude of the waveform decreases as the moisture content increases in Figure 90b. A comparison of the infill conditions shows that when the infill is greater than or equal to the asperity height, the characteristics of the infill material dominate the behaviour of the rock joint. This is also supported by Section 5.5.2 where dilation occurred at the lower infill thickness versus contraction in thicker infill conditions. With increasing infill thickness, the impact of moisture content becomes more apparent, and as the moisture content increases the convergence rate of the trend to approximately 0.4 mm contraction increases.



(a)



(b)



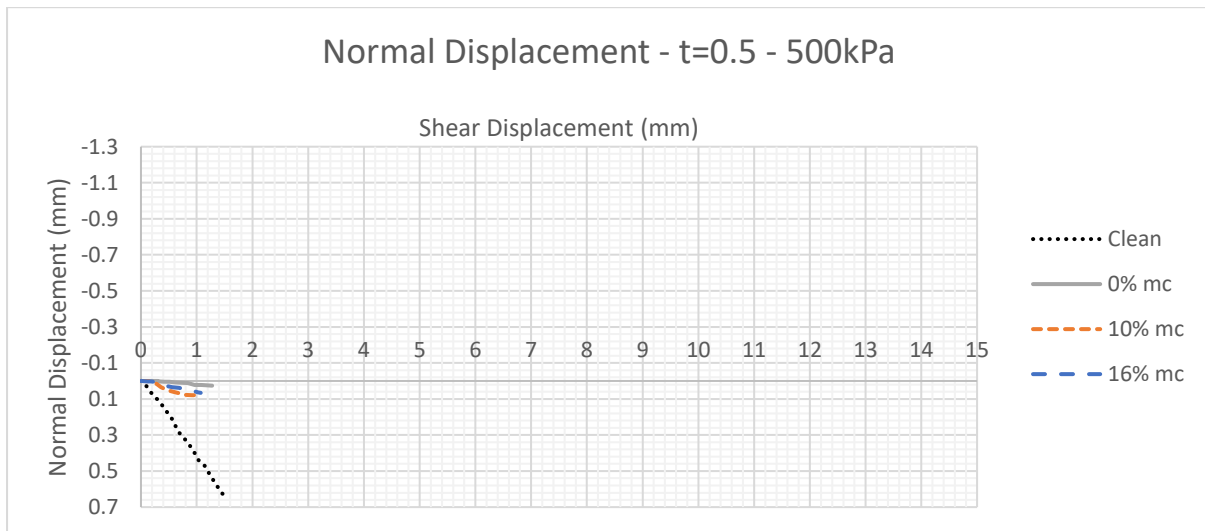
(c)

Figure 90: Shear Testing Results for 300 kPa (Shear Displacement vs Normal Displacement)
 a) $t/a=0.5$ b) $t/a=1.0$ c) $t/a=1.5$

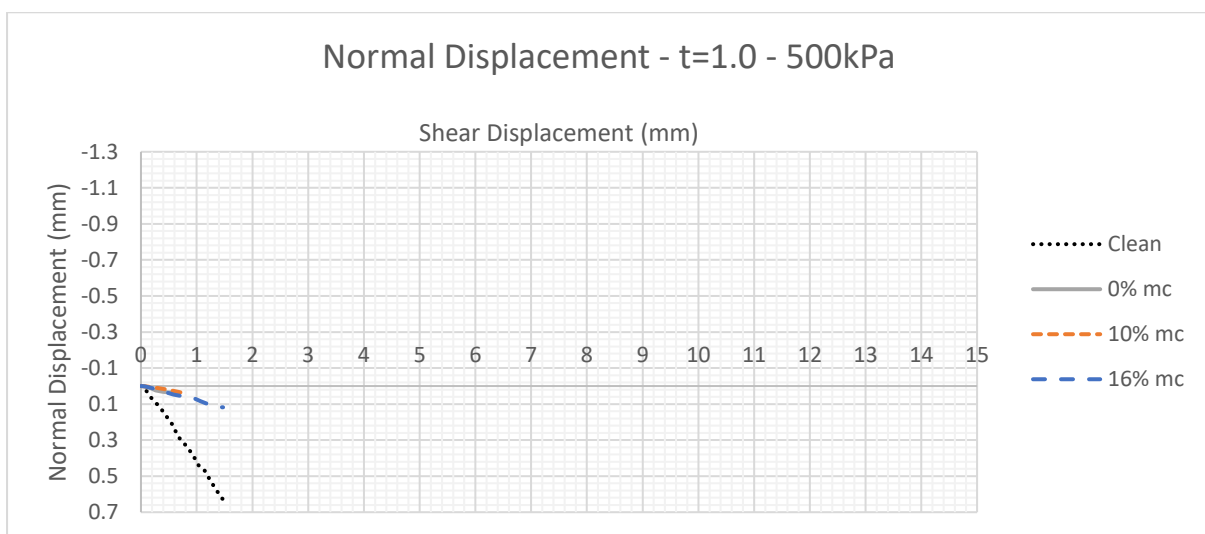
5.5.4 Infilled Joints with normal stress of 500 kPa

Figure 91 shows a comparison of shear displacement and normal displacement in the clean and infilled rock joints at the applied normal stresses of 500 kPa with moisture contents 0, 10 and 16%. For all infill thickness the samples shear stresses reached the upper limit of 2200 N before approximately 1.5 mm of shear displacement could occur (from Section 5.3.4), thus ending the test. As a result, it is not possible to determine from this data if the same peak-trough pattern reflected in Figure 89 and 90b would occur. From the limited data available, Figure 91 shows that as the moisture content of the infill material increases, the contraction of the normal displacement increases. This comparison of the infill conditions also shows that when the infill is greater than or equal to the asperity height, the characteristics of the

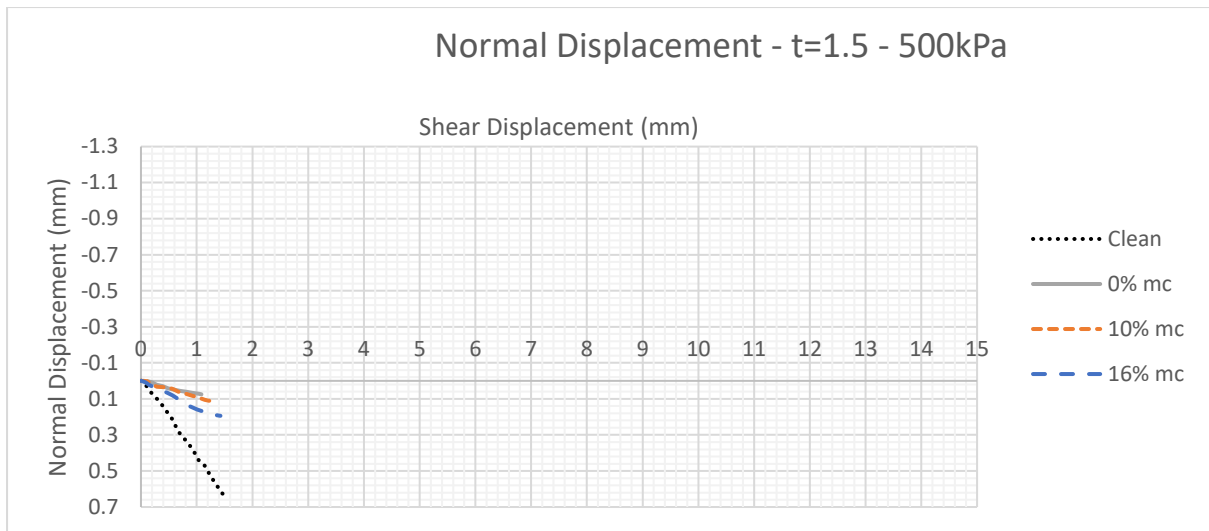
infill material dominate the behaviour of the rock joint allowing for increased contraction. This is also supported by Section 5.5.2 where dilation occurred at the lower infill thickness versus contraction in thicker infill conditions. With increasing infill thickness, the impact of moisture content becomes more apparent. Based on the data outlined in Section 5.5.2 and Section 5.5.3 it would be expected that as the moisture content increases the rate of convergence to a set contraction (positive normal displacement) would occur. With decreased moisture content the angle of internal friction of the infill increases, thus the friction forces acting on the infill soil particles increases. However, when the moisture content increases the particles can more easily slide past each other, thus facilitating increased contraction. However, due to the lack of data available regarding the normal displacement behaviour and trends cannot be definitively determined.



(a)



(b)



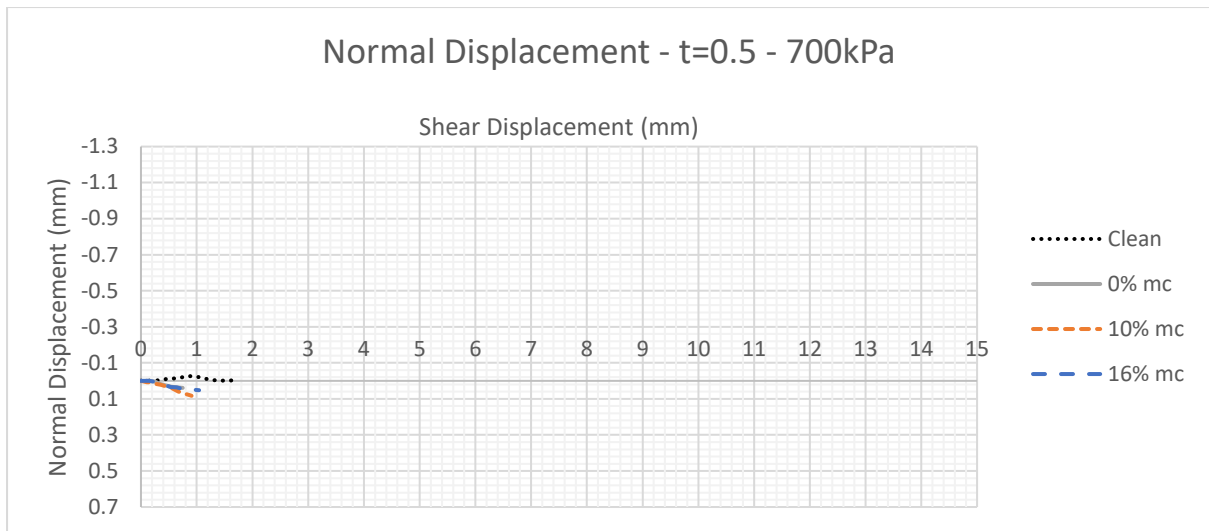
(c)

Figure 91: Shear Testing Results for 500 kPa (Shear Displacement vs Normal Displacement)

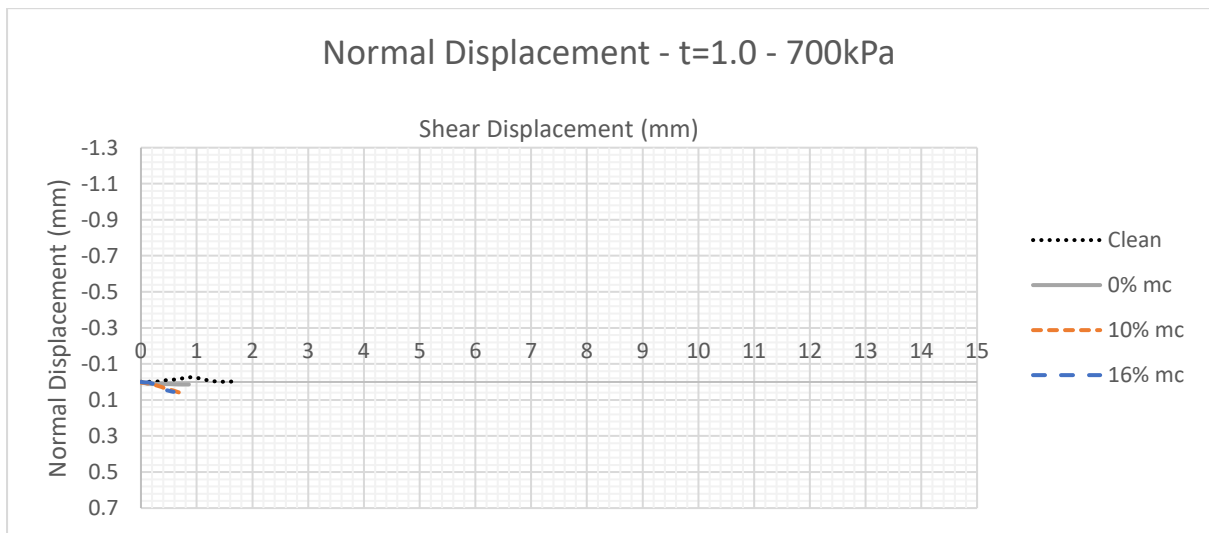
a) $t/a=0.5$ b) $t/a=1.0$ c) $t/a=1.5$

5.5.5 Infilled Joints with normal stress of 700 kPa

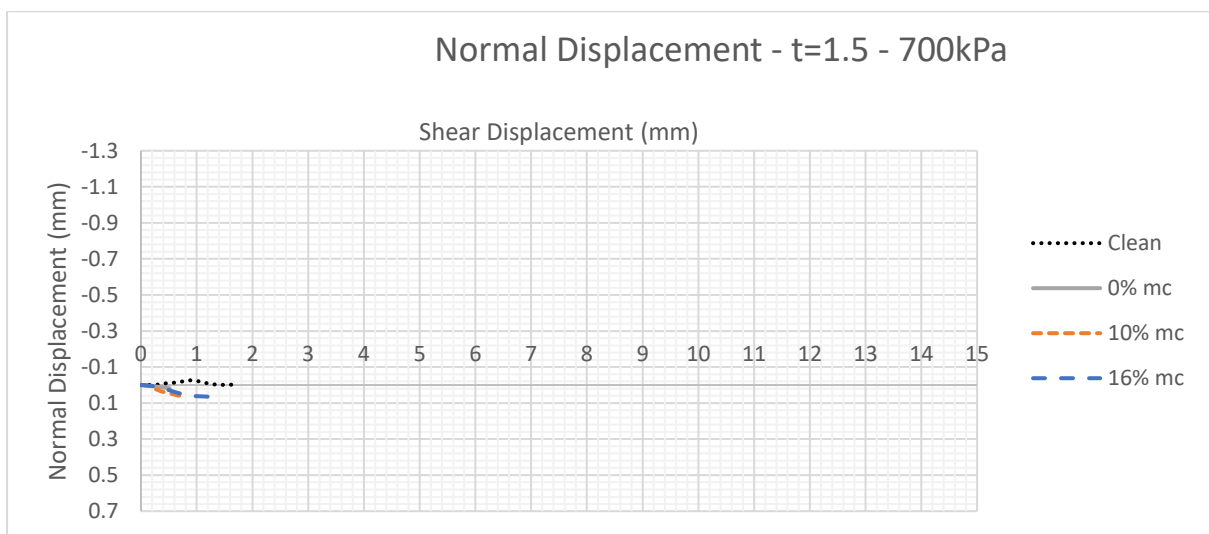
Figure 92 shows a comparison of shear displacement and normal displacement in the clean and infilled rock joints at the applied normal stresses of 700 kPa with moisture contents 0, 10 and 16%. For all infill thickness the samples shear stresses reached the upper limit of 2200 N by approximately 1.5 mm of shear displacement could occur (from Section 5.3.4), thus ending the test. As a result, it is not possible to determine from this data if the same peak-trough pattern reflected in Figure 89 and 90b would occur. From the limited data available, Figure 92 shows that with increasing infill thickness, the impact of moisture content becomes more apparent. Based on the data outlined in Section 5.5.2 and Section 5.5.3 it would be expected that as the moisture content increases the rate of convergence to a set contraction (positive normal displacement) would occur, which is mildly shown in Figure 92c. With decreased moisture content the angle of internal friction of the infill increases, thus the friction forces acting on the infill soil particles increases. However, when the moisture content increases the particles can more easily slide past each other, thus leading to increased contraction. However, due to the lack of data available regarding the normal displacement behaviour and trends cannot be definitively determined.



(a)



(b)



(c)

*Figure 92: Shear Testing Results for 700 kPa (Shear Displacement vs Normal Displacement)
a) t/a=0.5 b) t/a=1.0 c) t/a=1.5*

5.5.6 Summary

The peak-trough behaviour with a wavelength approximately equal to the asperity base length of 7 mm (Section 5.5.1 and 5.5.2) supports the expected outcomes (as based on previous research outlined in Chapter 2) for clean joints and joints where the infill thickness is less than the asperity height. In addition, this data also reflected the expected outcome that as the infill thickness increase to equal or greater than the asperity height, the infill properties would become the dominate controlling factor. In Section 5.5.2, as the moisture content increased the convergence rate of the normal displacement increased as shown by the decreasing amplitude. Also, the amplitude decreased with increasing shear displacement in Section 5.5.2 indicating that with each asperity step sliding failure (as shown in Section 5.5.1) occurred thus reducing the asperity height and infilling the valleys of the asperity profile with failed rock joint material. In Section 5.5.3, where the infill thickness is equal to the asperity height peak-trough pattern mildly reoccurs for the moisture content of 10% and 16% (Figure 90b), before starting to converge on a common contraction value in Figure 90c. Based on the data available in Section 5.5.2 (to a lesser extent Section 5.5.3), the conclusion can be drawn that as the moisture content increases, the rate of convergence to the normal displacement trend increases, which is more pronounced when the infill thickness is greater than the asperity height. An addition conclusion is that as the infill thickness increases (causing infill dominated control of shear strength parameters), contraction rather than dilation occurs. Dilation trends only occurred when the surface friction between the joint surfaces, and the soil particles, is highest (clean joints and at 0% moisture content combined with low infill thickness). This is likely due to the lubricating effect of moisture in the infill material. With decreased moisture content the angle of internal friction of the infill increased, thus the friction forces acting on the infill soil particles increased. However, when the moisture content increases the particles can more easily slide past each other, thus facilitating increased contraction.

5.6 UDEC and International Coal Operators' Conference

The two additional components of this project to incorporate the results of the study into UDEC for geotechnical implementation and present the findings of this study at the International Coal Operator's Conference (as outlined in Appendix A) were not undertaken due to time constraints, but are a future consideration.

CHAPTER 6: CONCLUSION

This project has analysed the effects of sodium bentonite clay infill at 0%, 10% and 16% moisture conditions, and various infill layer thickness, on the shear strength characteristics of clean and infilled rock joints subjected to Constant Normal Loading (CNL) boundary conditions to expand on previous geotechnical research knowledge into rock joints and slope stability. One of the original goals of the project was to inform on the impact of variable moisture contents on shear strength of rock joints with the aim to potentially decrease construction and maintenance costs. However, the key findings concluded that, while the various samples did show different behaviour based on moisture content, the magnitude of the shear strength of the rock joints was not controlled by the moisture content but rather:

- the joint profile when the infill thickness was less than the asperity height (highest in clean rock joints),
- the joint profile and infill material shear strength properties when the infill thickness was equal to the asperity height, and
- infill material shear strength properties principally controlled when the infill thickness was greater than the asperity height.

While the magnitude of the shear strength of the joint was not found to be impacted by the moisture content, the rate of convergence of the shear stress, normal stress and normal displacement trends increased as the moisture content increased when subjected to lower applied normal pressure of 100 and 300 kPa. This is likely due to the lubricating effect of moisture in the infill material. With decreased moisture content the angle of internal friction of the infill increased, resulting in increased friction forces acting on the infill soil particles. However, when the moisture content increased the soil particles could more easily slide past each other facilitating decreased variance in shear stress, normal stress, and normal displacement (including increased contraction). This decreased variance allows the material to more readily achieve equilibrium with the trending magnitude of the shear stress, normal stress or normal displacement.

However, due to the limiting loading of 2200 N of the direct shear apparatus used, the data at higher applied normal loadings is generally inconclusive. Due to limited data set at higher applied normal stresses, further research should investigate the impact of variable moisture conditions on the shear strength properties of clay infilled rock joints by narrowing the scope to include more moisture content conditions tested at relatively low applied normal stresses (up to 300 kPa). In addition, testing under CNS conditions should be investigated to determine the impact of infill moisture content on the shear behaviour of deeper rock joints.

LIST OF REFERENCES

Agustawijaya, DS 2007, 'The Uniaxial Compressive Strength of Soft Rock', *Civil Engineering Dimension*, vol. 9, no. 1, pp. 9-14.

Barton, N & Choubey, V 1977, 'The shear strength of rock joints in theory and practice', *Rock Mechanicals and Rock Engineering*, vol. 10, no. 1, pp.1-54.

Barton, N 2013, 'Shear strength criteria for rock, rock joints, rockfill and rock masses: Problems and some solutions', *Journal of Rock Mechanics and Geotechnical Engineering*, vol. 5, no. 4, pp. 249-261.

Brodnig, G & Prasad, V 2010, *A View from the Top: Vulnerability in Mountain Systems*, ResearchGate, Berlin, Germany, viewed 1 October 2019, <https://www.researchgate.net/publication/278000364_A_View_from_the_Top_Vulnerability_in_Mountain_Systems>.

Bunnings n.d., *Bastion GP Cement*, digital image of Bastion GP Cement, viewed 5 November 2022, <https://www.bunnings.com.au/bastion-20kg-general-purpose-cement_p0760330>.

Cao, P, Deng, H, Chen, Y & Fu, N 2018, 'The shear characteristic and failure mechanism study of infilled rock joints with constant normal load', *Journal of Vibroengineering*, vol. 21, no. 4, pp. 940-951.

CIV2403 Geology and Geomechanics: Study Book 2 2015, University of Southern Queensland, Toowoomba, viewed 1 October 2022, <<http://usqstudydesk.usq.edu.au>>.

Craig, RF 2004, *Craig's Soil Mechanics*, 7th edn, Chapman & Hall, London.

Dafalla, M 2012, 'Effects of Clay and Moisture Content on Direct Shear Tests for Clay-Sand Mixtures', *Advances in Materials Science and Engineering*, vol. 1, pp. 1-8.

EasyMix 2019, *Easy Mix Synthetic Turf Infill Sand*, digital image of Easy Mix Synthetic Turf Infill Sand, EasyMix, Brisbane, Australia, viewed 5 November 2022, <<https://www.easymixsales.com.au/product/sand-gravel/synthetic-turf-sand/>>.

EasyMix 2020, *Easy Mix Construction & Synthetic Turf Sand*, Data Sheet March 2020, <<https://www.easymixsales.com.au/wp-content/uploads/2022/10/Easy-Mix-Construction-Synthetic-Turf-Sand-TDS.pdf>>.

El Dorado Weather 2019, *The World Average Annual Precipitation*, El Dorado Weather, Placerville, California, United States of America, viewed 1 October 2019, <<https://eldoradoweather.com/climate/world-maps/world-annual-precip-map.html>>.

Geocomp 2021, *ShearTrac II Shear Apparatus*, Geocomp Corporation, Massachusetts, United States of America, viewed 8 February 2022, <<https://www.geocomp.com/Products/LabSystems/ShearTrac-II>>.

Han, G, Jing, H, Jiang, Y, Liu, R & Wu, J 2019), 'Effect of Cyclic Loading on the Shear Behaviours of Both Unfilled and Infilled Rough Rock Joints Under Constant Normal Stiffness Conditions', *Rock Mechanics and Rock Engineering*, vol. 53, pp. 31-57.

Indraratna, B, Jayanathan, M & Brown, T 2008, 'Shear strength model for overconsolidated clay-infilled idealised rock joints', Paper, University of Wollongong, Wollongong, New South Wales, Australia.

Indraratna, B, Welideniya, H & Brown, E 2005, 'A shear strength model for idealised infilled joints under constant normal stiffness', *Géotechnique*, vol. 55, no. 3, pp. 215-226.

Indraratna, B, Premadasa, W & Brown, T 2015, 'Shear behaviour of rock joints with unsaturated infill', *Géotechnique*, vol. 63. No. 15, pp. 1356-1360.

Jahanian, H & Sadaghiani, M 2015, 'Experimental Study on the Shear Strength of Sandy Clay Infilled Regular Rough Rock Joints', *Rock Mechanics and Rock Engineering*, vol. 48, no. 3, pp. 907-922.

Lei, D, Lin, H & Wang, Y 2022, 'Damage characteristics of shear strength of joints under freeze-thaw cycles', *Archive of Applied Mechanics*, vol. 92, pp. 1615-1631.

Liu, X, Zhu, W & Li, L 2020, 'Numerical Shear Tests on the Scale Effect of Rock Joints under CNL and CND Conditions', *Advances in Civil Engineering*, vol. 2020.

Philipp, S, Afsar, F & Gudmundsson, A 2013, 'Effects of mechanical layering on hydrofracture emplacement and fluid transport in reservoirs', *Frontiers in Earth Science*, vol. 1, December, pp. 1-19.

Ray, P 2016, *Introduction to Structural Geology*, The University of Sydney, Sydney, Australia, viewed 1 October 2019, <https://www.researchgate.net/publication/299135987_Introduction_to_Structural_Geology>.

Shrivastava, A & Rao, S 2015, 'Shear Behaviour of Rock Joints Under CNL and CNS Boundary Conditions', *Geotechnical and Geological Engineering*, vol. 33, October.

Shrivastava, A & Rao, S 2017, 'Physical Modelling of Shear Behaviour of Infilled Rock Joints Under CNL and CNS Boundary Conditions', *Rock Mechanics and Rock Engineering*, vol. 51, September, pp. 101-118.

Standards Australia 2001, *Methods of testing soils for engineering purposes – Method 1.1: Sampling and preparation of soils – Preparation of disturbed soil samples for testing*, AS1289.1.1-2001, Standards Australia, Sydney, viewed 25 August 2022, <<https://au.i2.saiglobal.com/>>.

Standards Australia 2005, *Methods of testing soils for engineering purposes – Method 2.1.1: Soil moisture content tests – Determination of the moisture content of a soil – Oven drying method (standard method)*, AS1289.2.1.1-2005, Standards Australia, Sydney, viewed 22 February 2022, <<https://au.i2.saiglobal.com/>>.

Standards Australia 2006, *Methods of testing soils for engineering purposes – Method 3.5.1: Soil classification tests – Determination of the soil particle density of a soil – Standard method*, AS1289.3.5.1-2006, Standards Australia, Sydney, viewed 23 August 2022, <<https://au.i2.saiglobal.com/>>.

Standards Australia 2009a, *Methods of testing soils for engineering purposes – Method 3.6.1: Determination of the particle size distribution of a soil – Standard method of analysis by sieving*, AS1289.3.6.1-2009, Standards Australia, Sydney, viewed 23 August 2022, <<https://au.i2.saiglobal.com/>>.

Standards Australia 2009b, *Methods of testing soils for engineering purposes – Method 3.2.1: Soil classification tests – Determination of the plastic limit of a soil*, AS1289.3.2.1-2009, Standards Australia, Sydney, viewed 23 August 2022, <<https://au.i2.saiglobal.com/>>.

Standards Australia 2014a, *Methods of testing concrete – Method 9: Compressive strength tests – Concrete, mortar and grout specimens*, AS1012.9-2014, Standards Australia, Sydney, viewed 25 August 2022, <<https://au.i2.saiglobal.com/>>.

Standards Australia 2014b, *Methods of testing soils for engineering purposes – Part 0: Definitions and general requirements*, AS1289.0-2014, Standards Australia, Sydney, viewed 18 February 2022, <<https://au.i2.saiglobal.com/>>.

Standards Australia 2015, *Methods of testing soils for engineering purposes – Method 3.9.1: Soil classification tests – Determination of the cone liquid limit of a soil*, AS1289.3.9.1-2015, Standards Australia, Sydney, viewed 29 August 2022, <<https://au.i2.saiglobal.com/>>.

Standards Australia 2020a, *Methods of testing soils for engineering purposes – Method 6.6.1: Soil strength and consolidation tests – Determination of the one-dimensional consolidation properties of a soil – Standard Method*, AS1289.6.6.1-2020, Standards Australia, Sydney, viewed 29 August 2022, <<https://au.i2.saiglobal.com/>>.

Standards Australia 2020b, *Methods of testing soils for engineering purposes - Method 6.2.2: Soil strength and consolidation tests – Determination of shear strength of a soil – Direct shear test using a shear box*, AS1289.6.2.2-2020, Standards Australia, Sydney, viewed 8 February 2022, <<https://au.i2.saiglobal.com/>>.

Tang, ZC & Wong LNY 2015, 'Influences of Normal Loading Rate and Shear Velocity on the Shear Behaviour of Artificial Rock Joints', *Rock Mechanics and Rock Engineering*, vol. 49, pp. 2165-2172.

The Constructor 2021, *Arrangement of Consolidometer Parts*, digital image of Consolidation Cell, viewed 7 October 2022, <<https://theconstructor.org/geotechnical/soil-consolidation-test/3054/>>.

The Engineering Community 2018, *Deadliest Landslides In Recorded History*, The Engineering Community, viewed 1 October 2019, <<https://www.theengineeringcommunity.org/deadliest-landslides-in-recorded-history/>>.

TransCalc 2022, *Casagrande's Plasticity Soil Chart*, digital image of Casagrande's Plasticity Soil Chart, viewed 7 October 2022, <<http://www.transcalc.com/plasticitychartastm>>

Wang, X, Wang, R & Zhang, Z 2018, 'Numerical Analysis Method of Shear Properties of Infilled Joints under Constant Normal Stiffness Condition', *Advances in Civil Engineering*, vol. 2018, no. 3, pp. 1-13.

World Population Review 2022, *2022 World Population by Country*, World Population Review, viewed 29 August 2022, <<https://worldpopulationreview.com/>>.

Zohaib, M, Mirzaghobanali, A, Helwig, A, Azzia, N, Gregor, P, Rastegarmanesh, A & McDougall, K 2020, 'Shear Strength Properties of Artificial Rock Joints', *2020 Coal Operators Conference*, 12-14 February 2020, University of Wollongong, Wollongong, New South Wales, Australia.

Zydroń, T, Wojciechowska-Dymańska, M, Gruchot, A & Zalewski, T 2017, 'Influence of moisture content of cohesive soils on their shear strength', *Transportation Overview – Przegląd Komunikacyjny*, May, pp. 10-19.

Appendix A – Project Specification

ENG4111/4112 Research Project

Project Specification

For: Elizabeth Downing
Title: Shear Strength Properties of Clean and Clay Infilled Rock Joints: An analysis of the impact of moisture content under CNL conditions
Major: Civil Engineering
Supervisors: Dr Ali Mirzaghobanali
Enrolment: ENG4111 ONC SF S1, 2021
ENG4112 ONC SF S2, 2022
Project Aim: To investigate the effects of normal loading, infill thickness and infill moisture content on the shear strength properties of clay infilled rock joints, and compare and contrast these properties to the shear strength properties of clean rock joints.

Programme: Version 1, 17th March 2021

1. Review existing literature on past studies on shear strength of rock joints
2. Evaluate testing methods used in past studies
3. Model rock material and joints using three-dimensional printed moulds and concrete casting.
4. Investigate experimentally the effects of normal loading on the shear strength properties of clean and infilled rock joints.
5. Investigate experimentally the effects of infill thickness on the shear strength properties of infilled rock joints.
6. Investigate experimentally the effects of infill moisture content on the shear strength properties of infilled rock joints.
7. Compare and contrast the effect of normal loading on the shear strength properties of clean and infilled rock joints
 - a. Clean rock joints contrasted with infilled rock joints with respect to normal loading
 - b. Infilled rock joints contrasted with respect to infill thickness
 - c. Infilled rock joints contrasted with respect to infill moisture content

If time and resources permit (or future considerations)

8. Incorporate the results of the study into UDEC for further Geotechnical implementation.
9. Present the findings at the International Coal Operators' Conference.

Appendix B – Risk Assessment

1527		RISK DESCRIPTION			TREND	CURRENT	RESIDUAL
		Shear strength of clean and clay infilled rock joints				Low	Low
RISK OWNER		RISK IDENTIFIED ON		LAST REVIEWED ON		NEXT SCHEDULED REVIEW	
Elizabeth Downing		19/08/2022		19/08/2022		19/08/2023	
RISK FACTOR(S)	EXISTING CONTROL(S)	CURRENT	PROPOSED CONTROL(S)	TREATMENT OWNER	DUE DATE	RESIDUAL	
Manual handling of materials (20kg bags of mortar mix, and sample preparation and storage)	Control: Follow safe manual handling and ergonomic procedures. Wearing SafetyBoots (dropped items).	Low	No Control:			Low	
Exposure to cement dust from Mortar mix and heat during mixing. Irritation to eyes, nose, throat and upper respiratory tract.	Control: Wear dust mask during mixing, wear gloves and glasses.	Low	No Control:			Low	
Use of electrical equipment (mixer and ShearTrac) with materials mixed with water.	Control: Machine is maintained Control: Clean up of spilled water	Low	No Control:			Low	
Operation of mixer and ShearTrac (e.g. pinching, dropped parts)	Control: Operation of equipment in accordance with safe working procedures and assistance of Lab Staff. Control: Safety boots, and gloves where appropriate	Low	No Control:			Low	
COVID19	Control: Following UniSQ's COVIDSafe Plans - if unwell or flu like symptoms stay at home and postpone laboratory work.	Low	No Control:			Low	
Breakage and/or removal of samples resulting in potential sharp and/or flying debris.	Control: Glove, Glasses, safety boots.	Low					
ATTACHMENTS							
RiskManagementPlans - RMP_2020_4316.pdf RiskManagementPlans - RMP_2018_2502.pdf							

powered by riskware.com.au

commercial in confidence

RiskManagementPlans - RMP_2021_5322.pdf RiskManagementPlans - RMP_2018_2569.pdf Shear behavior of clayey infilled rock joints having triangular a.pdf Top Mould Profile.png Bottom Mould Profile.png
--

powered by riskware.com.au

commercial in confidence

Appendix C – Uniaxial Compression Testing Summary

C.1 7 Day Compression Testing

Before Testing (All Samples):



Figure 93: 7 Day Compression Testing Samples (Before Testing)

Sample 1:

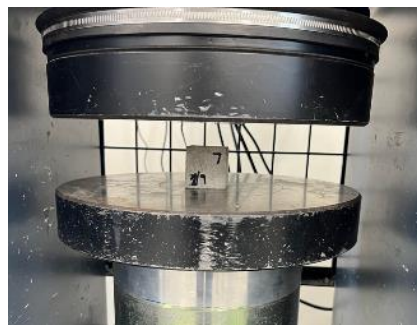


Figure 94: 7 Day Compression Testing Sample 1 (Before Testing)

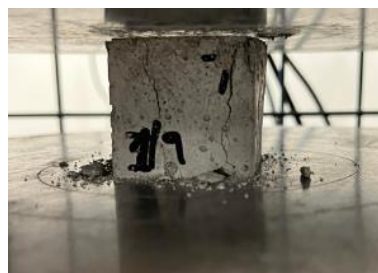


Figure 95: 7 Day Compression Testing Sample 1 (After Testing)



Figure 96: 7 Day Compression Testing Sample 1 (Results)

Sample 2:



Figure 97: 7 Day Compression Testing Sample 2 (Before Testing)



Figure 98: 7 Day Compression Testing Sample 2 (After Testing)

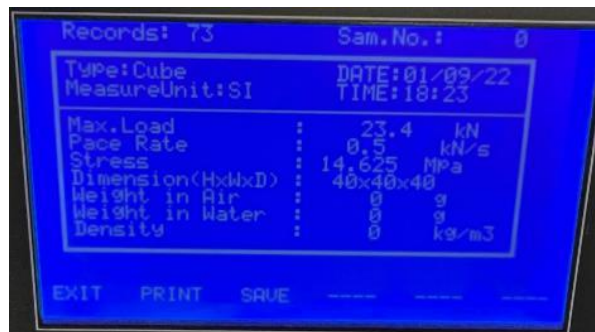


Figure 99: 7 Day Compression Testing Sample 2 (Results)

Sample 3:



Figure 100: 7 Day Compression Testing Sample 3 (Before Testing)

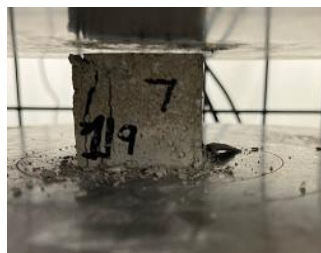


Figure 101: 7 Day Compression Testing Sample 3 (After Testing)



Figure 102: 7 Day Compression Testing Sample 3 (Results)

Post Testing (All Samples):



Figure 103: 7 Day Compression Testing Samples (After Testing)

C.2 14 Day Compression Testing

Before Testing (All Samples):



Figure 104: 14 Day Compression Testing Samples (Before Testing)

Sample 1:

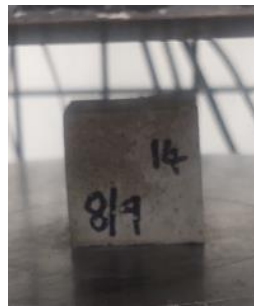


Figure 105: 14 Day Compression Testing Sample 1 (Before Testing)

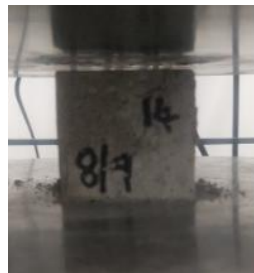


Figure 106: 14 Day Compression Testing Sample 1 (After Testing)



Figure 107: 14 Day Compression Testing Sample 1 (Results)

Sample 2:



Figure 108: 14 Day Compression Testing Sample 2 (Before Testing)

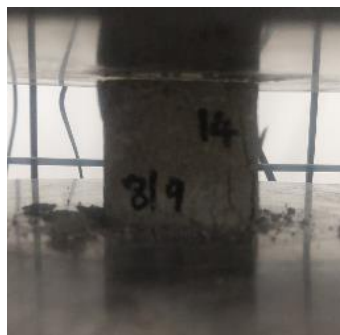


Figure 109: 14 Day Compression Testing Sample 2 (After Testing)

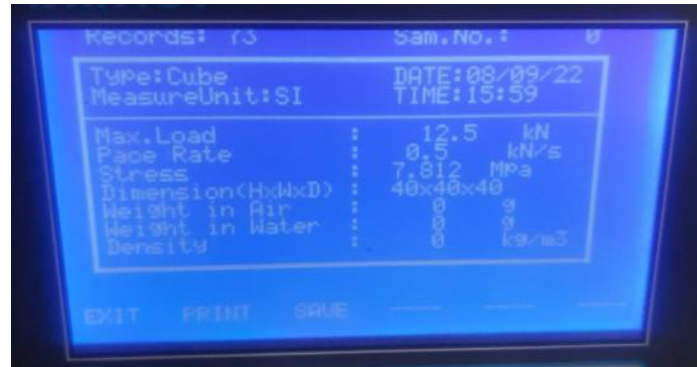


Figure 110: 14 Day Compression Testing Sample 2 (Results)

Sample 3:



Figure 111: 14 Day Compression Testing Sample 3 (Before Testing)



Figure 112: 14 Day Compression Testing Sample 3 (After Testing)



Figure 113: 14 Day Compression Testing Sample 3 (Results)

Post Testing (All Samples):

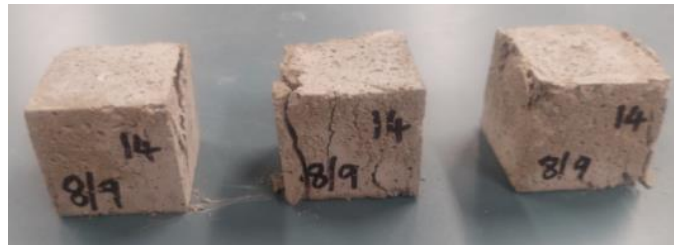


Figure 114: 14 Day Compression Testing Samples (After Testing)

C.3 21 Day Compression Testing

Before Testing (All Samples):



Figure 115: 21 Day Compression Testing Samples (Before Testing)

Sample 1:

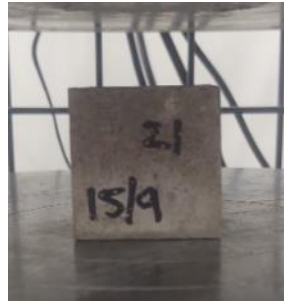


Figure 116: 21 Day Compression Testing Sample 1 (Before Testing)



Figure 117: 21 Day Compression Testing Sample 1 (After Testing)



Figure 118: 21 Day Compression Testing Sample 1 (Results)

Sample 2:



Figure 119: 21 Day Compression Testing Sample 2 (Before Testing)



Figure 120: 21 Day Compression Testing Sample 2 (After Testing)



Figure 121: 21 Day Compression Testing Sample 2 (Results)

Sample 3:

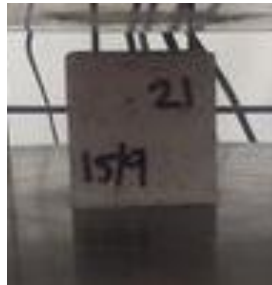


Figure 122: 21 Day Compression Testing Sample 3 (Before Testing)



Figure 123: 21 Day Compression Testing Sample 3 (After Testing)



Figure 124: 21 Day Compression Testing Sample 3 (Results)

Sample 4:

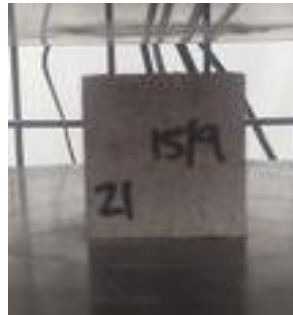


Figure 125: 21 Day Compression Testing Sample 4 (Before Testing)



Figure 126: 21 Day Compression Testing Sample 4 (After Testing)



Figure 127: 21 Day Compression Testing Sample 4 (Results)

Post Testing (All Samples):



Figure 128: 21 Day Compression Testing Samples (After Testing)

C.4 28 Day Compression Testing

Before Testing (All Samples):



Figure 129: 28 Day Compression Testing Samples (Before Testing)

Sample 1:



Figure 130: 28 Day Compression Testing Sample 1 (Before Testing)



Figure 131: 28 Day Compression Testing Sample 1 (After Testing)



Figure 132: 28 Day Compression Testing Sample 1 (Results)

Sample 2:



Figure 133: 28 Day Compression Testing Sample 2 (Before Testing)



Figure 134: 28 Day Compression Testing Sample 2 (After Testing)



Figure 135: 28 Day Compression Testing Sample 2 (Results)

Sample 3:



Figure 136: 28 Day Compression Testing Sample 3 (Before Testing)



Figure 137: 28 Day Compression Testing Sample 3 (After Testing)



Figure 138: 28 Day Compression Testing Sample 3 (Results)

Sample 4:



Figure 139: 28 Day Compression Testing Sample 4 (Before Testing)



Figure 140: 28 Day Compression Testing Sample 4 (After Testing)



Figure 141: 28 Day Compression Testing Sample 4 (Results)

Sample 5:



Figure 142: 28 Day Compression Testing Sample 5 (Before Testing)



Figure 143: 28 Day Compression Testing Sample 5 (After Testing)



Figure 144: 28 Day Compression Testing Sample 5 (Results)

Post Testing (All Samples):



Figure 145: 28 Day Compression Testing Samples (After Testing)

Appendix D – Moisture Content Results

Sample	Empty weight of container (g)	Weight of container & wet soil (g)	Time in oven 1	Weight of container & dry soil 1 (g)	Time in oven 2	Weight of container & dry soil 2 (g)	Difference (%)*	Time in oven 3	Weight of container & dry soil 3 (g)	Difference (%)*	Moisture Content (%)#
<i>1</i>	36.90	71.04	18 hours & 15 minutes	66.25	1 hour & 20 minutes	66.32	0.11	1 hour & 20 minutes	66.31	0.02	16.1
<i>2</i>	36.88	70.08		65.41		65.53	0.18		65.47	0.09	16.1
<i>3</i>	36.31	70.22		65.46		65.56	0.15		65.53	0.05	16.1
*must be <0.1% as per AS1289.2.1.1-2005										<i>Average</i>	16.1
#rounded to nearest 0.1 as per AS1289.2.1.1-2005 for values less than 50%											

Appendix E – Cone Liquid Limit Results

Test	Iteration	Penetration Reading (mm)	Difference (mm)	Average Penetration (mm)	Empty weight of container (g)	Weight of container & wet soil (g)	Time in oven 1	Weight of container & dry soil 1 (g)	Time in oven 2	Weight of container & dry soil 2 (g)	Difference (%)*	Moisture Content (w) (%)		
1	1	13.5	0.20	13.4	31.64	45.18	21 hours & 30 minutes	37.10	1 hour & 40 minutes	37.08	0.05	149		
	2	13.3						36.55		36.54	0.03	161		
2	1	17.8	0.20	17.9	31.83	44.14		36.08		36.08	0.00	165		
	2	18.0						37.32		37.33	0.03	174		
3	1	19.7	0.50	19.5	31.16	44.20		35.74		35.75	0.03	180		
	2	19.2						37.41		37.39	0.05	184		
4	1	21.4	1.00	21.9	31.55	47.40								
	2	22.4												
5	1	24.2	0.20	24.3	31.28	43.80								
	2	24.4												
6	1	25.6	0.40	25.4	31.75	47.75								
	2	25.2												

*must be <0.1% as per AS1289.2.1.1-2005
#rounded to nearest 1.0 as per AS1289.2.1.1-2005 for values greater than 100%

Appendix F – Plastic Limit Results

Sample	Empty weight of container (g)	Weight of container & wet soil (g)	Time in oven 1	Weight of container & dry soil 1 (g)	Time in oven 2	Weight of container & dry soil 2 (g)	Difference (%)*	Time in oven 3	Weight of container & dry soil 3 (g)	Difference (%)*	Moisture Content (%)#
<i>1</i>	31.25	38.69		35.24		35.26	0.06		35.24	0.06	86.5
<i>2</i>	37.54	44.06		40.91		40.95	0.10		40.93	0.05	92.5
<i>3</i>	37.10	43.53		40.47		40.52	0.12		40.49	0.07	89.5
*must be <0.1% as per AS1289.2.1.1-2005										<i>Average</i>	89.5
#rounded to nearest 0.5 as per AS1289.2.1.1-2005 for values between 50 and 100%											

Appendix G – Collated Direct Shear Testing Results (Soil Only)

G.1 Moisture Content 1 (16%)

Applied Normal Stress of 100 kPa

Shear Displacement (mm)	Shear Force (N)	Shear Stress (kPa)
0.000	33.922	10.88
0.053	120.76	38.74
0.177	164.54	52.78
0.285	193.82	62.18
0.407	214.98	68.96
0.518	234.41	75.20
0.898	298.78	95.85
1.013	312.55	100.26
1.143	324.43	104.08
1.257	336.76	108.03
1.383	347.92	111.61
1.511	359.08	115.19
1.623	367.49	117.89
1.751	379.67	121.80
1.867	385.46	123.65
1.994	395.32	126.82
2.114	403.59	129.47
2.242	411.27	131.93
2.369	416.63	133.65
2.485	423.16	135.75
2.617	430.4	138.07
2.728	436.06	139.89
2.859	443.6	142.31
2.977	446.5	143.24
3.087	454.03	145.65
3.209	458.82	147.19
3.330	463.75	148.77
3.446	469.69	150.67
3.582	473.31	151.84
3.707	476.5	152.86
3.808	479.4	153.79
3.933	482.16	154.68
4.068	484.48	155.42
4.187	484.33	155.37
4.324	484.77	155.51
4.445	486.07	155.93
4.567	488.54	156.72
4.686	492.74	158.07
4.814	493.75	158.39
4.945	494.91	158.77
5.063	496.07	159.14

5.187	498.97	160.07
5.309	501.15	160.77
5.440	501.58	160.90
5.557	502.45	161.18
5.682	503.47	161.51
5.814	502.74	161.28
5.939	503.32	161.46
6.060	504.34	161.79
6.192	504.63	161.88
6.306	505.35	162.11
6.436	506.08	162.35
6.556	507.09	162.67
6.685	506.66	162.53
6.802	507.82	162.91
6.937	507.53	162.81
7.061	507.82	162.91
7.188	507.09	162.67
7.305	507.09	162.67
7.438	506.95	162.63
7.558	507.96	162.95
7.672	508.11	163.00
7.803	507.82	162.91
7.933	509.56	163.46
8.044	509.12	163.32
8.168	510.86	163.88
8.286	509.56	163.46
8.427	510.72	163.84
8.536	511.44	164.07
8.674	511.44	164.07
8.796	510.72	163.84
8.914	510.28	163.70
9.043	510.57	163.79
9.177	511.15	163.97
9.300	508.83	163.23
9.424	509.41	163.42
9.550	509.41	163.42
9.676	509.12	163.32
9.799	508.98	163.28
9.917	509.12	163.32
10.047	508.98	163.28
10.170	508.4	163.09
10.294	508.25	163.04
10.421	507.96	162.95
10.551	505.06	162.02
10.674	505.35	162.11
10.804	504.92	161.98
10.929	504.19	161.74
11.054	502.74	161.28
11.185	503.76	161.60
11.297	502.02	161.05
11.411	502.74	161.28
11.538	502.89	161.33
11.682	502.02	161.05

11.801	502.16	161.09
11.912	503.32	161.46
12.040	502.74	161.28
12.170	502.74	161.28
12.297	501.15	160.77
12.416	500.28	160.49
12.544	498.97	160.07
12.669	499.26	160.16
12.788	498.97	160.07
12.914	498.68	159.97
13.032	498.25	159.84
13.159	498.1	159.79
13.282	498.39	159.88
13.403	497.52	159.60
13.534	495.35	158.91
13.657	495.06	158.81
13.785	492.01	157.83
13.904	494.19	158.53
14.025	493.03	158.16
14.156	491.43	157.65
14.283	491.72	157.74
14.412	491.87	157.79
14.528	490.42	157.32
14.656	489.7	157.09
14.783	488.68	156.77
14.909	488.97	156.86
14.988	489.55	157.05

Applied Normal Stress of 300 kPa

Shear Displacement (mm)	Shear Force (N)	Shear Stress (kPa)
0.000	80.746	25.90
0.051	262.82	84.31
0.154	398.95	127.98
0.270	480.56	154.16
0.395	552.18	177.14
0.507	612.19	196.39
0.885	761.07	244.15
1.000	800.36	256.75
1.119	839.5	269.31
1.236	871.68	279.63
1.371	905.17	290.37
1.500	933	299.30
1.598	959.39	307.77
1.715	987.51	316.79
1.848	1011.4	324.45
1.968	1037.8	332.92
2.089	1058.4	339.53
2.214	1080.1	346.49
2.344	1099.7	352.78
2.454	1120.7	359.52

2.587	1138.9	365.35
2.699	1156.5	371.00
2.828	1176.8	377.51
2.939	1191.9	382.36
3.062	1205.7	386.78
3.175	1220.6	391.56
3.308	1229.7	394.48
3.430	1239.3	397.56
3.560	1245.1	399.42
3.675	1261.2	404.59
3.797	1276.7	409.56
3.926	1292.4	414.60
4.052	1309.5	420.08
4.185	1322.7	424.32
4.295	1336.2	428.65
4.426	1347.7	432.34
4.548	1355.7	434.90
4.680	1362.4	437.05
4.799	1372	440.13
4.920	1376.5	441.58
5.047	1387.6	445.14
5.156	1395.9	447.80
5.286	1402.1	449.79
5.419	1411.4	452.77
5.540	1419.2	455.27
5.664	1423.6	456.69
5.791	1429.5	458.58
5.900	1427.3	457.87
6.032	1428.8	458.35
6.163	1433.1	459.73
6.290	1431.7	459.28
6.403	1431.5	459.22
6.520	1435.2	460.41
6.649	1438.9	461.59
6.777	1439.4	461.75
6.895	1441.1	462.30
7.013	1442.6	462.78
7.137	1443.1	462.94
7.274	1442.4	462.72
7.404	1442.3	462.68
7.532	1436.9	460.95
7.654	1438.2	461.37
7.774	1437.9	461.27
7.901	1436.5	460.82
8.031	1433.3	459.80
8.148	1433.7	459.93
8.268	1433.9	459.99
8.395	1433.1	459.73
8.523	1431.7	459.28
8.656	1431.4	459.19
8.769	1423.9	456.78
8.899	1430.1	458.77
9.005	1431.4	459.19

9.131	1433	459.70
9.273	1429.2	458.48
9.393	1423.7	456.72
9.521	1422.8	456.43
9.639	1421.7	456.08
9.763	1418.2	454.95
9.891	1417.8	454.82
10.014	1416.2	454.31
10.147	1413.7	453.51
10.266	1412.7	453.19
10.399	1414.6	453.80
10.521	1413.1	453.32
10.634	1411.5	452.80
10.774	1408.1	451.71
10.894	1407.5	451.52
11.026	1405.7	450.94
11.148	1402.4	449.88
11.278	1400.1	449.15
11.393	1397.2	448.22
11.521	1395.9	447.80
11.634	1394	447.19
11.758	1391.5	446.39
11.890	1390.8	446.16
12.018	1389.8	445.84
12.147	1388.2	445.33
12.265	1387.2	445.01
12.390	1384.6	444.17
12.509	1381.4	443.15
12.632	1379.9	442.67
12.753	1379.2	442.44
12.878	1377.2	441.80
12.994	1375.6	441.29
13.119	1373.8	440.71
13.256	1371.7	440.04
13.380	1371.1	439.84
13.499	1369.8	439.43
13.620	1366.7	438.43
13.750	1364.6	437.76
13.882	1360.2	436.35
13.997	1359.8	436.22
14.118	1359.1	435.99
14.245	1356.4	435.13
14.369	1355.3	434.77
14.496	1354.6	434.55
14.623	1352.4	433.84
14.750	1351.2	433.46
14.876	1350.1	433.11
15.003	1346.4	431.92

Applied Normal Stress of 500 kPa

Shear Displacement (mm)	Shear Force (N)	Shear Stress (kPa)
0.000	93.793	30.09
0.053	383	122.86
0.152	593.35	190.34
0.254	737.01	236.43
0.363	860.37	276.00
0.480	966.63	310.09
0.814	1223.4	392.46
0.923	1288.6	413.38
1.039	1350.9	433.36
1.155	1413.9	453.57
1.290	1468.4	471.06
1.416	1521.6	488.12
1.520	1567.7	502.91
1.647	1611.6	516.99
1.770	1649.7	529.22
1.903	1676.7	537.88
2.026	1713.5	549.68
2.154	1749.7	561.30
2.285	1791.6	574.74
2.401	1825.4	585.58
2.529	1857.7	595.94
2.640	1884.4	604.51
2.767	1908.9	612.37
2.876	1936	621.06
2.990	1957.9	628.09
3.097	1985	636.78
3.230	2006.6	643.71
3.348	2031.6	651.73
3.475	2051.4	658.08
3.590	2072.1	664.72
3.710	2093.9	671.71
3.834	2111	677.20
3.960	2131.3	683.71
4.091	2148.1	689.10
4.202	2162.5	693.72
4.333	2179.4	699.14
4.454	2184.8	700.88
4.589	2185.7	701.16
4.711	2200	705.75

Applied Normal Stress of 700 kPa

Shear Displacement (mm)	Shear Force (N)	Shear Stress (kPa)
0.000	58.711	18.83
0.006	105.83	33.95
0.071	509.99	163.60
0.179	760.35	243.92
0.284	957.79	307.26
0.395	1140.9	366.00
0.745	1579.3	506.63
0.872	1701.5	545.83
0.983	1814.7	582.15
1.115	1913.8	613.94
1.222	2001	641.91
1.333	2084	668.54
1.461	2163.2	693.95
1.507	2200.6	705.94

G.2 Moisture Content 2 (0%)

Applied Normal Stress of 100 kPa

Shear Displacement (mm)	Shear Force (N)	Shear Stress (kPa)
0.00	12.32	3.95
0.08	96.55	30.97
0.21	145.55	46.69
0.33	183.96	59.01
0.44	229.48	73.62
0.56	255.58	81.99
0.69	275.00	88.22
0.82	292.25	93.75
0.92	306.89	98.45
1.06	321.68	103.19
1.17	332.99	106.82
1.31	346.03	111.01
1.42	355.17	113.94
1.53	367.05	117.75
1.66	374.74	120.22
1.80	384.16	123.24
1.92	393.00	126.07
2.03	398.66	127.89
2.16	406.92	130.54
2.28	412.14	132.21
2.40	419.68	134.63
2.53	425.62	136.54
2.66	434.03	139.24
2.79	440.41	141.28
2.90	448.24	143.79

3.02	454.47	145.79
3.15	459.40	147.37
3.26	466.07	149.51
3.39	470.56	150.95
3.51	476.36	152.81
3.62	481.00	154.30
3.75	487.96	156.54
3.88	492.74	158.07
4.00	497.38	159.56
4.13	500.57	160.58
4.25	502.89	161.33
4.38	503.03	161.37
4.50	500.57	160.58
4.62	500.71	160.63
4.75	498.68	159.97
4.87	498.68	159.97
5.00	501.73	160.95
5.11	505.50	162.16
5.24	507.96	162.95
5.37	508.69	163.19
5.49	509.56	163.46
5.61	508.54	163.14
5.73	508.54	163.14
5.87	510.43	163.74
5.99	511.15	163.97
6.11	512.89	164.53
6.24	513.47	164.72
6.37	514.77	165.14
6.49	515.50	165.37
6.62	516.80	165.79
6.74	517.82	166.11
6.87	518.83	166.44
6.98	519.12	166.53
7.11	519.41	166.62
7.24	518.83	166.44
7.35	518.69	166.39
7.49	517.67	166.07
7.61	517.38	165.97
7.74	517.24	165.93
7.87	517.38	165.97
7.99	517.38	165.97
8.12	516.95	165.84
8.23	517.09	165.88
8.35	516.51	165.69
8.47	515.50	165.37
8.59	515.64	165.42
8.73	515.93	165.51
8.86	516.37	165.65
8.98	516.51	165.69
9.09	516.08	165.56
9.22	515.79	165.46
9.36	515.50	165.37
9.47	515.21	165.28

9.60	515.06	165.23
9.73	514.77	165.14
9.86	514.92	165.18
9.98	514.63	165.09
10.09	514.63	165.09
10.22	514.34	165.00
10.36	513.76	164.81
10.48	513.32	164.67
10.61	513.18	164.63
10.73	512.89	164.53
10.86	511.59	164.12
10.98	511.59	164.12
11.11	511.59	164.12
11.23	510.86	163.88
11.36	510.28	163.70
11.48	510.14	163.65
11.59	509.85	163.56
11.72	509.99	163.60
11.84	510.28	163.70
11.98	509.99	163.60
12.10	508.98	163.28
12.23	508.83	163.23
12.35	509.27	163.37
12.47	508.83	163.23
12.60	508.69	163.19
12.72	508.54	163.14
12.84	509.12	163.32
12.96	509.12	163.32
13.09	508.98	163.28
13.21	508.54	163.14
13.33	507.67	162.86
13.46	507.38	162.77
13.58	507.53	162.81
13.70	507.53	162.81
13.84	507.82	162.91
13.96	506.37	162.44
14.09	506.37	162.44
14.21	506.08	162.35
14.34	505.50	162.16
14.46	504.92	161.98
14.59	504.19	161.74
14.71	503.90	161.65
14.83	504.34	161.79
14.95	504.34	161.79
15.00	504.48	161.84

Applied Normal Stress of 300 kPa

Shear Displacement (mm)	Shear Force (N)	Shear Stress (kPa)
0.00	47.11	15.11
0.02	117.13	37.57
0.13	264.42	84.82
0.23	373.72	119.89
0.34	504.77	161.93
0.46	611.32	196.11
0.58	709.61	227.64
0.71	789.63	253.31
0.82	850.37	272.80
0.95	902.70	289.58
1.06	951.99	305.39
1.20	992.58	318.42
1.31	1030.10	330.45
1.42	1064.90	341.62
1.55	1097.70	352.14
1.67	1128.70	362.08
1.80	1155.40	370.65
1.92	1182.20	379.25
2.04	1209.20	387.91
2.16	1234.20	395.93
2.29	1258.50	403.72
2.41	1279.50	410.46
2.53	1299.90	417.00
2.66	1322.20	424.16
2.76	1341.40	430.32
2.90	1357.90	435.61
3.02	1378.90	442.35
3.13	1405.30	450.81
3.27	1425.50	457.29
3.38	1444.70	463.45
3.49	1465.60	470.16
3.63	1479.50	474.62
3.75	1493.40	479.08
3.86	1507.20	483.50
3.99	1517.10	486.68
4.12	1523.20	488.64
4.24	1521.40	488.06
4.38	1515.80	486.26
4.50	1523.70	488.80
4.61	1539.70	493.93
4.73	1553.30	498.29
4.87	1564.20	501.79
4.99	1572.40	504.42
5.12	1577.70	506.12
5.24	1584.90	508.43
5.35	1594.00	511.35
5.49	1600.90	513.56
5.60	1607.20	515.58
5.73	1612.30	517.22

5.86	1609.60	516.35
5.99	1609.70	516.39
6.10	1604.90	514.85
6.23	1601.60	513.79
6.35	1601.40	513.72
6.49	1599.10	512.98
6.60	1589.60	509.94
6.73	1591.90	510.68
6.85	1593.60	511.22
6.98	1596.40	512.12
7.11	1596.80	512.25
7.23	1600.30	513.37
7.35	1602.90	514.20
7.48	1604.50	514.72
7.61	1604.90	514.85
7.72	1606.40	515.33
7.86	1607.70	515.74
7.98	1608.10	515.87
8.09	1606.90	515.49
8.21	1604.20	514.62
8.34	1599.70	513.18
8.48	1596.80	512.25
8.59	1594.80	511.61
8.73	1593.50	511.19
8.84	1592.90	511.00
8.97	1593.80	511.28
9.09	1593.30	511.12
9.23	1592.90	511.00
9.34	1593.30	511.12
9.47	1592.00	510.71
9.59	1591.60	510.58
9.72	1591.10	510.42
9.84	1590.10	510.10
9.96	1588.10	509.46
10.08	1587.40	509.23
10.21	1586.40	508.91
10.34	1585.10	508.49
10.47	1583.80	508.08
10.60	1581.40	507.31
10.72	1579.70	506.76
10.85	1577.20	505.96
10.98	1576.10	505.61
11.10	1575.50	505.41
11.23	1574.30	505.03
11.34	1573.50	504.77
11.46	1575.30	505.35
11.59	1574.20	505.00
11.72	1572.40	504.42
11.85	1571.30	504.07
11.96	1569.40	503.46
12.09	1568.50	503.17
12.22	1565.80	502.30
12.34	1564.50	501.89

12.47	1563.00	501.40
12.59	1561.70	500.99
12.71	1561.30	500.86
12.83	1560.30	500.54
12.96	1560.00	500.44
13.08	1559.30	500.22
13.20	1556.90	499.45
13.32	1556.50	499.32
13.45	1556.40	499.29
13.58	1554.90	498.81
13.70	1554.20	498.58
13.83	1551.90	497.84
13.95	1549.50	497.07
14.07	1547.10	496.30
14.20	1546.40	496.08
14.33	1546.10	495.98
14.46	1546.10	495.98
14.57	1544.30	495.41
14.70	1543.70	495.21
14.82	1543.50	495.15
14.95	1542.70	494.89
14.96	1542.70	494.89

Applied Normal Stress of 500 kPa

Shear Displacement (mm)	Shear Force (N)	Shear Stress (kPa)
0.00	42.33	13.58
0.01	45.66	14.65
0.01	50.01	16.04
0.02	125.69	40.32
0.10	343.86	110.31
0.21	518.25	166.25
0.33	713.52	228.89
0.43	868.35	278.56
0.55	992.87	318.51
0.65	1111.50	356.56
0.79	1222.20	392.08
0.90	1305.30	418.74
1.03	1374.60	440.97
1.14	1440.50	462.11
1.26	1502.10	481.87
1.37	1559.70	500.35
1.49	1609.80	516.42
1.62	1657.10	531.59
1.73	1702.80	546.25
1.85	1745.40	559.92
1.98	1789.00	573.90
2.10	1822.70	584.71
2.22	1856.30	595.49
2.34	1888.80	605.92
2.47	1929.80	619.07

2.58	1960.70	628.98
2.72	1988.40	637.87
2.83	2014.20	646.15
2.96	2039.80	654.36
3.07	2071.10	664.40
3.19	2097.70	672.93
3.31	2127.40	682.46
3.44	2156.90	691.93
3.56	2184.30	700.71
3.62	2200.00	705.75

Applied Normal Stress of 700 kPa

Shear Displacement (mm)	Shear Force (N)	Shear Stress (kPa)
0.00	71.61	22.97
0.07	469.26	150.54
0.17	739.76	237.31
0.27	952.86	305.67
0.38	1158.30	371.58
0.50	1339.90	429.83
0.63	1505.50	482.96
0.73	1646.20	528.09
0.86	1765.10	566.24
0.97	1871.10	600.24
1.09	1975.20	633.64
1.20	2069.50	663.89
1.33	2159.10	692.63
1.36	2200.90	706.04

G.3 Moisture Content 3 (10%)

Applied Normal Stress of 100 kPa

Shear Displacement (mm)	Shear Force (N)	Shear Stress (kPa)
0.00	12.90	4.14
0.01	16.82	5.39
0.01	20.15	6.46
0.01	25.08	8.05
0.11	77.85	24.97
0.21	116.55	37.39
0.33	152.79	49.01
0.45	185.99	59.66
0.56	220.64	70.78
0.67	240.35	77.10
0.80	258.04	82.78
0.93	275.15	88.27
1.04	288.92	92.68
1.18	302.83	97.15

1.29	313.13	100.45
1.42	324.43	104.08
1.54	333.86	107.10
1.64	343.28	110.12
1.77	351.25	112.68
1.92	358.94	115.15
2.03	366.91	117.70
2.15	373.72	119.89
2.27	380.68	122.12
2.39	385.75	123.75
2.51	393.44	126.21
2.64	397.35	127.47
2.76	404.17	129.66
2.89	408.51	131.05
3.01	415.47	133.28
3.13	420.11	134.77
3.26	425.33	136.44
3.37	430.11	137.98
3.50	435.04	139.56
3.63	439.68	141.05
3.73	442.00	141.79
3.86	446.06	143.09
3.99	450.84	144.63
4.12	456.21	146.35
4.24	458.38	147.05
4.36	462.88	148.49
4.49	464.76	149.09
4.61	468.97	150.44
4.74	469.83	150.72
4.86	469.55	150.63
4.99	471.72	151.33
5.11	473.60	151.93
5.23	477.08	153.05
5.35	480.42	154.12
5.48	482.59	154.81
5.60	485.20	155.65
5.72	486.07	155.93
5.85	488.10	156.58
5.98	490.13	157.23
6.09	491.72	157.74
6.22	494.19	158.53
6.35	495.49	158.95
6.48	495.78	159.04
6.60	498.10	159.79
6.73	499.41	160.21
6.85	499.41	160.21
6.98	500.13	160.44
7.09	498.54	159.93
7.22	497.52	159.60
7.35	496.94	159.42
7.46	496.36	159.23
7.60	495.78	159.04
7.72	495.49	158.95

7.85	495.93	159.09
7.98	495.78	159.04
8.10	496.65	159.32
8.23	496.36	159.23
8.34	497.23	159.51
8.46	498.39	159.88
8.58	498.83	160.02
8.71	499.70	160.30
8.85	499.12	160.12
8.97	499.55	160.25
9.09	499.84	160.35
9.20	500.28	160.49
9.33	501.00	160.72
9.47	501.44	160.86
9.58	502.02	161.05
9.72	502.31	161.14
9.84	502.45	161.18
9.96	502.89	161.33
10.08	503.03	161.37
10.20	503.18	161.42
10.33	503.76	161.60
10.46	503.76	161.60
10.59	503.76	161.60
10.71	504.48	161.84
10.84	504.77	161.93
10.97	504.48	161.84
11.09	504.77	161.93
11.22	505.06	162.02
11.34	505.06	162.02
11.47	505.21	162.07
11.59	505.35	162.11
11.71	505.21	162.07
11.82	505.79	162.26
11.95	504.92	161.98
12.09	504.63	161.88
12.21	504.05	161.70
12.33	503.61	161.56
12.45	503.47	161.51
12.57	503.76	161.60
12.71	503.76	161.60
12.83	503.32	161.46
12.95	503.32	161.46
13.07	502.74	161.28
13.19	503.32	161.46
13.31	502.74	161.28
13.44	502.60	161.23
13.57	502.60	161.23
13.68	502.02	161.05
13.81	501.87	161.00
13.94	501.29	160.81
14.07	501.87	161.00
14.19	502.02	161.05
14.31	501.87	161.00

14.45	501.73	160.95
14.56	501.44	160.86
14.70	501.29	160.81
14.82	501.29	160.81
14.93	501.00	160.72
14.99	501.00	160.72

Applied Normal Stress of 300 kPa

Shear Displacement (mm)	Shear Force (N)	Shear Stress (kPa)
0.00	47.55	15.25
0.00	48.13	15.44
0.00	52.33	16.79
0.03	120.76	38.74
0.11	273.26	87.66
0.22	387.93	124.45
0.34	475.05	152.39
0.45	553.63	177.60
0.57	623.21	199.92
0.68	676.70	217.08
0.82	726.42	233.03
0.93	772.09	247.68
1.06	812.10	260.52
1.18	850.37	272.80
1.30	883.28	283.35
1.41	915.03	293.54
1.55	945.32	303.25
1.67	971.85	311.77
1.78	998.09	320.18
1.90	1018.70	326.79
2.02	1044.50	335.07
2.15	1065.80	341.90
2.27	1088.10	349.06
2.40	1105.90	354.77
2.53	1122.60	360.13
2.64	1139.30	365.48
2.76	1155.20	370.58
2.87	1174.80	376.87
3.01	1189.00	381.43
3.12	1207.90	387.49
3.24	1221.50	391.85
3.36	1236.70	396.73
3.49	1250.80	401.25
3.61	1263.80	405.42
3.74	1278.70	410.20
3.86	1290.20	413.89
3.97	1301.80	417.61
4.10	1309.00	419.92
4.22	1320.80	423.71
4.35	1335.60	428.46
4.48	1346.40	431.92

4.59	1359.50	436.12
4.72	1370.40	439.62
4.85	1377.20	441.80
4.97	1385.40	444.43
5.09	1392.30	446.64
5.21	1398.50	448.63
5.34	1405.30	450.81
5.46	1405.00	450.72
5.59	1408.80	451.94
5.71	1415.60	454.12
5.83	1425.60	457.33
5.97	1433.00	459.70
6.09	1441.00	462.27
6.21	1446.90	464.16
6.34	1447.50	464.35
6.46	1439.40	461.75
6.58	1436.90	460.95
6.70	1440.80	462.20
6.84	1447.20	464.26
6.95	1452.70	466.02
7.08	1455.90	467.05
7.21	1461.50	468.84
7.33	1465.80	470.22
7.45	1467.10	470.64
7.58	1467.20	470.67
7.70	1467.60	470.80
7.82	1467.60	470.80
7.95	1467.10	470.64
8.09	1468.50	471.09
8.19	1470.40	471.70
8.31	1471.40	472.02
8.44	1473.70	472.76
8.57	1474.40	472.98
8.69	1476.60	473.69
8.83	1478.10	474.17
8.95	1478.10	474.17
9.07	1478.80	474.39
9.19	1477.60	474.01
9.31	1476.90	473.78
9.45	1477.30	473.91
9.58	1477.20	473.88
9.70	1477.10	473.85
9.82	1477.60	474.01
9.94	1477.30	473.91
10.06	1478.80	474.39
10.20	1478.80	474.39
10.32	1480.10	474.81
10.45	1480.00	474.78
10.57	1480.70	475.00
10.70	1482.00	475.42
10.82	1482.30	475.52
10.95	1482.00	475.42
11.08	1480.50	474.94

11.21	1480.00	474.78
11.33	1480.00	474.78
11.45	1478.40	474.26
11.56	1479.10	474.49
11.69	1480.10	474.81
11.83	1478.80	474.39
11.95	1478.70	474.36
12.06	1478.10	474.17
12.19	1478.80	474.39
12.32	1478.50	474.30
12.44	1477.20	473.88
12.56	1477.60	474.01
12.69	1478.40	474.26
12.81	1478.20	474.20
12.93	1477.20	473.88
13.06	1475.80	473.43
13.17	1475.60	473.37
13.30	1475.30	473.27
13.43	1474.60	473.05
13.55	1473.60	472.73
13.68	1472.60	472.40
13.80	1470.80	471.83
13.93	1469.50	471.41
14.05	1467.90	470.90
14.17	1466.30	470.38
14.30	1465.50	470.13
14.42	1465.30	470.06
14.55	1464.00	469.65
14.68	1463.70	469.55
14.80	1463.00	469.32
14.93	1462.70	469.23
14.98	1461.50	468.84

Applied Normal Stress of 500 kPa

Shear Displacement (mm)	Shear Force (N)	Shear Stress (kPa)
0.00	18.41	5.91
0.02	121.48	38.97
0.11	374.16	120.03
0.22	559.13	179.37
0.32	711.93	228.38
0.44	841.67	270.00
0.56	967.79	310.46
0.68	1065.50	341.81
0.79	1144.20	367.05
0.92	1215.50	389.93
1.04	1283.70	411.81
1.17	1343.50	430.99
1.28	1401.80	449.69
1.39	1451.00	465.48
1.52	1503.30	482.25
1.63	1549.50	497.07

1.76	1593.30	511.12
1.87	1633.00	523.86
2.00	1670.20	535.79
2.12	1712.80	549.46
2.25	1748.40	560.88
2.37	1786.00	572.94
2.48	1819.00	583.53
2.61	1849.80	593.41
2.72	1879.90	603.06
2.85	1905.30	611.21
2.97	1934.90	620.71
3.08	1955.20	627.22
3.21	1975.50	633.73
3.33	2001.50	642.07
3.45	2024.30	649.39
3.58	2043.60	655.58
3.71	2067.10	663.12
3.80	2086.80	669.44
3.94	2106.50	675.76
4.07	2127.20	682.40
4.19	2142.70	687.37
4.32	2161.90	693.53
4.44	2176.10	698.08
4.56	2194.80	704.08
4.61	2200.60	705.94

Applied Normal Stress of 700 kPa

Shear Displacement (mm)	Shear Force (N)	Shear Stress (kPa)
0.00	0.58	0.19
0.03	126.41	40.55
0.12	433.16	138.96
0.23	627.12	201.18
0.33	813.26	260.89
0.44	995.34	319.30
0.56	1159.10	371.83
0.69	1287.90	413.15
0.79	1406.90	451.33
0.92	1524.80	489.15
1.04	1639.70	526.01
1.16	1734.20	556.32
1.27	1817.40	583.01
1.39	1896.20	608.29
1.52	1972.80	632.87
1.62	2047.20	656.73
1.73	2110.90	677.17
1.86	2177.00	698.37
1.91	2200.00	705.75

Appendix H – Collated Rock Joint Direct Shear Testing Results

H.1 Clean Rock Joints

Clean Joint CL1 at 100 kPa:

Shear Displacement (mm)	Shear Force (N)	Shear Stress (kPa)	Normal Displacement (mm)	Normal Force (N)	Normal Stress (kPa)
0.00	-11.31	-3.63	0.00	311.22	99.84
0.02	9.42	3.02	0.00	311.79	100.02
0.02	11.16	3.58	0.00	311.94	100.07
0.03	18.70	6.00	0.00	311.79	100.02
0.08	57.99	18.60	0.00	310.65	99.66
0.20	110.32	35.39	0.00	311.79	100.02
0.32	206.00	66.08	0.00	311.94	100.07
0.43	189.33	60.74	0.00	311.51	99.93
0.55	178.16	57.15	0.00	311.94	100.07
0.68	175.99	56.46	0.00	311.94	100.07
0.81	175.55	56.32	0.00	312.37	100.21
0.93	176.28	56.55	0.00	311.79	100.02
1.05	364.73	117.00	0.00	311.08	99.79
1.15	619.29	198.67	0.00	315.95	101.36
1.27	899.22	288.47	-0.01	317.82	101.96
1.38	1025.60	329.01	-0.04	317.39	101.82
1.50	1071.20	343.64	-0.09	315.67	101.27
1.63	1087.00	348.71	-0.14	314.66	100.94
1.74	1124.60	360.77	-0.20	332.02	106.51
1.87	1124.10	360.61	-0.26	317.96	102.00
1.99	1185.00	380.14	-0.31	328.72	105.45
2.12	1149.00	368.59	-0.38	315.81	101.31
2.24	1207.70	387.43	-0.44	327.00	104.90
2.37	1175.40	377.06	-0.51	316.81	101.63
2.49	1223.90	392.62	-0.56	326.42	104.71
2.61	1211.30	388.58	-0.64	313.94	100.71
2.75	1287.40	412.99	-0.68	321.55	103.15
2.85	1333.30	427.72	-0.74	326.42	104.71
2.98	1377.90	442.02	-0.80	318.10	102.05
3.10	1308.90	419.89	-0.86	313.37	100.53
3.21	1311.40	420.69	-0.92	324.13	103.98
3.34	1265.70	406.03	-0.98	313.94	100.71
3.46	1269.50	407.25	-1.02	325.27	104.35
3.58	1153.80	370.13	-1.10	312.37	100.21
3.72	1053.00	337.80	-1.14	315.81	101.31
3.86	958.66	307.53	-1.17	320.69	102.88
3.98	860.37	276.00	-1.19	318.68	102.23
4.12	757.45	242.99	-1.22	315.24	101.13
4.24	689.02	221.03	-1.23	313.08	100.43
4.37	632.49	202.90	-1.23	311.94	100.07
4.50	602.91	193.41	-1.23	310.79	99.70
4.63	547.97	175.79	-1.22	310.93	99.75
4.75	520.28	166.90	-1.21	309.93	99.42
4.88	496.94	159.42	-1.20	309.93	99.42
5.00	494.77	158.72	-1.19	310.07	99.47
5.12	475.78	152.63	-1.18	311.08	99.79
5.24	455.05	145.98	-1.17	307.92	98.78

5.37	389.81	125.05	-1.14	308.92	99.10
5.50	347.34	111.43	-1.11	300.61	96.43
5.63	351.83	112.87	-1.08	309.50	99.29
5.75	311.82	100.03	-1.04	305.63	98.04
5.89	278.91	89.47	-1.00	297.31	95.38
6.00	232.24	74.50	-0.95	306.63	98.37
6.14	200.63	64.36	-0.91	295.59	94.82
6.27	177.44	56.92	-0.81	300.89	96.52
6.40	185.99	59.66	-0.76	306.06	98.18
6.51	176.86	56.74	-0.71	300.61	96.43
6.63	218.90	70.22	-0.66	299.75	96.16
6.75	217.59	69.80	-0.62	305.77	98.09
6.88	235.71	75.61	-0.57	308.92	99.10
6.99	259.20	83.15	-0.55	306.34	98.27
7.11	286.31	91.85	-0.54	307.78	98.73
7.24	311.82	100.03	-0.53	310.07	99.47
7.36	321.10	103.01	-0.53	311.65	99.98
7.50	337.19	108.17	-0.54	313.80	100.67
7.62	343.13	110.07	-0.55	313.66	100.62
7.75	376.04	120.63	-0.55	313.94	100.71
7.87	383.87	123.14	-0.57	316.24	101.45
7.99	394.89	126.68	-0.58	312.51	100.25
8.12	419.10	134.45	-0.58	314.95	101.03
8.22	453.89	145.61	-0.61	313.23	100.48
8.35	490.42	157.32	-0.63	312.80	100.35
8.46	527.82	169.32	-0.64	317.67	101.91
8.59	562.61	180.48	-0.66	314.52	100.90
8.72	597.26	191.60	-0.69	312.51	100.25
8.85	604.94	194.06	-0.72	314.52	100.90
8.96	657.71	210.99	-0.74	317.39	101.82
9.08	694.10	222.66	-0.76	313.08	100.43
9.21	730.05	234.20	-0.78	318.53	102.18
9.35	749.76	240.52	-0.80	313.66	100.62
9.45	763.83	245.03	-0.81	316.96	101.68
9.59	773.25	248.06	-0.84	313.37	100.53
9.71	797.17	255.73	-0.85	315.52	101.22
9.84	796.88	255.64	-0.88	312.80	100.35
9.96	805.00	258.24	-0.89	317.39	101.82
10.07	803.98	257.91	-0.92	313.80	100.67
10.20	790.06	253.45	-0.94	317.39	101.82
10.33	744.55	238.85	-0.96	312.37	100.21
10.46	707.00	226.80	-0.98	313.51	100.57
10.60	658.00	211.08	-0.99	313.80	100.67
10.72	634.81	203.64	-0.99	313.23	100.48
10.85	604.36	193.88	-0.99	309.93	99.42
10.96	608.57	195.23	-0.99	311.22	99.84
11.10	610.16	195.74	-0.98	313.51	100.57
11.22	572.76	183.74	-0.99	310.79	99.70
11.35	561.60	180.16	-0.99	311.36	99.88
11.47	527.97	169.37	-0.98	309.79	99.38
11.59	519.27	166.58	-0.97	311.51	99.93
11.71	479.69	153.88	-0.96	309.79	99.38
11.84	465.34	149.28	-0.95	308.64	99.01
11.98	446.64	143.28	-0.93	310.79	99.70
12.10	433.45	139.05	-0.92	308.06	98.82
12.23	402.86	129.24	-0.91	310.93	99.75
12.35	382.28	122.63	-0.89	307.20	98.55
12.49	369.66	118.59	-0.87	308.35	98.92

12.60	337.63	108.31	-0.85	309.93	99.42
12.73	313.85	100.68	-0.83	307.63	98.69
12.85	285.87	91.71	-0.81	308.64	99.01
12.97	278.33	89.29	-0.79	306.49	98.32
13.09	282.97	90.78	-0.77	308.35	98.92
13.21	262.24	84.13	-0.76	310.65	99.66
13.35	245.14	78.64	-0.73	307.78	98.73
13.48	241.95	77.62	-0.71	310.79	99.70
13.59	241.80	77.57	-0.69	309.50	99.29
13.71	240.06	77.01	-0.66	309.36	99.24
13.85	251.37	80.64	-0.65	308.92	99.10
13.97	250.65	80.41	-0.64	309.64	99.33
14.09	259.49	83.24	-0.63	310.65	99.66
14.21	269.64	86.50	-0.63	311.79	100.02
14.34	293.12	94.03	-0.63	312.22	100.16
14.45	292.40	93.80	-0.62	312.22	100.16
14.58	301.67	96.77	-0.62	312.51	100.25
14.71	300.95	96.54	-0.62	311.94	100.07
14.82	309.21	99.19	-0.62	312.65	100.30
14.94	332.84	106.77	-0.63	312.37	100.21
14.98	342.55	109.89	-0.63	312.37	100.21

Clean Joint CL2 at 300 kPa:

Shear Displacement (mm)	Shear Force (N)	Shear Stress (kPa)	Normal Displacement (mm)	Normal Force (N)	Normal Stress (kPa)
0.00	45.52	14.60	0.00	936.38	300.39
0.00	37.84	12.14	0.00	936.38	300.39
0.00	41.46	13.30	0.00	936.38	300.39
0.07	263.98	84.68	0.01	925.91	297.03
0.18	413.01	132.49	0.05	933.23	299.38
0.30	487.38	156.35	0.10	925.48	296.89
0.42	481.58	154.49	0.13	934.66	299.84
0.54	495.93	159.09	0.16	932.80	299.24
0.67	510.14	163.65	0.19	931.94	298.96
0.78	524.20	168.16	0.22	932.94	299.28
0.93	525.36	168.53	0.25	925.05	296.75
1.04	551.02	176.77	0.27	934.81	299.88
1.17	567.69	182.11	0.29	934.38	299.75
1.29	654.23	209.87	0.32	928.35	297.81
1.40	810.51	260.01	0.35	932.22	299.05
1.51	878.35	281.77	0.40	933.80	299.56
1.64	1008.20	323.43	0.44	927.49	297.54
1.76	1160.30	372.22	0.48	926.77	297.30
1.85	1284.80	412.16	0.51	935.67	300.16
1.97	1388.90	445.55	0.55	929.79	298.27
2.09	1452.40	465.92	0.58	928.35	297.81
2.21	1553.90	498.48	0.59	934.81	299.88
2.33	1705.50	547.12	0.59	936.10	300.30
2.44	1871.80	600.47	0.60	937.96	300.89
2.55	2073.00	665.01	0.59	938.25	300.99
2.65	2201.00	706.07	0.58	939.25	301.31

Clean Joint CL3 at 500 kPa:

Shear Displacement (mm)	Shear Force (N)	Shear Stress (kPa)	Normal Displacement (mm)	Normal Force (N)	Normal Stress (kPa)
0.00	18.41	5.91	0.00	1560.70	500.67
0.01	32.47	10.42	0.00	1560.80	500.70
0.01	39.72	12.74	0.00	1560.70	500.67
0.04	185.99	59.66	0.00	1560.00	500.44
0.11	454.47	145.79	0.03	1557.00	499.48
0.22	685.54	219.92	0.08	1553.50	498.36
0.33	832.25	266.98	0.11	1555.80	499.09
0.44	919.95	295.12	0.16	1557.00	499.48
0.56	1039.40	333.44	0.21	1544.30	495.41
0.67	1121.20	359.68	0.28	1535.00	492.42
0.79	1317.50	422.65	0.32	1558.40	499.93
0.92	1392.10	446.58	0.38	1552.10	497.91
1.04	1575.60	505.45	0.44	1551.70	497.78
1.14	1794.80	575.76	0.47	1552.90	498.16
1.26	1870.80	600.15	0.53	1560.10	500.47
1.37	2044.90	656.00	0.58	1551.50	497.72
1.48	2196.80	704.72	0.63	1554.20	498.58
1.48	2202.20	706.46	0.64	1554.10	498.55

Clean Joint CL4 at 700 kPa:

Shear Displacement (mm)	Shear Force (N)	Shear Stress (kPa)	Normal Displacement (mm)	Normal Force (N)	Normal Stress (kPa)
0.00	-20.15	-6.46	0.00	2185.30	701.04
0.01	-18.41	-5.91	0.00	2185.70	701.16
0.12	-15.51	-4.98	0.00	2185.90	701.23
0.24	-15.08	-4.84	0.00	2185.70	701.16
0.37	-11.89	-3.81	-0.01	2185.90	701.23
0.48	-10.87	-3.49	-0.01	2185.60	701.13
0.61	-5.80	-1.86	-0.01	2185.70	701.16
0.73	43.93	14.09	-0.02	2185.70	701.16
0.81	344.15	110.40	-0.03	2184.80	700.88
0.90	741.94	238.01	-0.03	2183.60	700.49
1.01	1029.00	330.10	-0.02	2183.30	700.39
1.13	1318.20	422.87	-0.02	2184.60	700.81
1.24	1336.00	428.58	0.00	2183.00	700.30
1.37	1394.60	447.38	0.00	2184.40	700.75
1.49	1541.30	494.44	0.00	2185.40	701.07
1.58	1952.50	626.35	0.00	2186.00	701.26
1.64	2203.80	706.97	0.00	2186.40	701.39

H.2 Rock Joints with Moisture Condition 1 (16%)

Infilled Joint 111 (100 kPa, $t/a=0.5$, MC1):

Shear Displacement (mm)	Shear Force (N)	Shear Stress (kPa)	Normal Displacement (mm)	Normal Force (N)	Normal Stress (kPa)
0.00	5.51	1.77	0.00	311.79	100.02
0.00	15.08	4.84	0.00	311.79	100.02
0.03	76.11	24.41	0.00	310.36	99.56
0.13	177.87	57.06	0.03	310.93	99.75
0.26	268.04	85.99	0.04	309.93	99.42
0.35	374.74	120.22	0.04	309.93	99.42
0.47	497.09	159.46	0.05	311.79	100.02
0.57	610.74	195.92	0.05	314.81	100.99
0.69	704.82	226.10	0.05	313.80	100.67
0.82	799.05	256.33	0.04	313.23	100.48
0.94	876.32	281.12	0.03	312.37	100.21
1.06	861.97	276.52	0.02	315.38	101.17
1.18	867.19	278.19	-0.01	314.23	100.80
1.30	842.69	270.33	-0.02	312.65	100.30
1.44	818.48	262.57	-0.04	318.10	102.05
1.57	784.12	251.54	-0.06	312.65	100.30
1.67	788.91	253.08	-0.08	315.52	101.22
1.79	794.56	254.89	-0.11	312.65	100.30
1.92	816.59	261.96	-0.13	318.10	102.05
2.05	817.75	262.33	-0.14	313.51	100.57
2.16	807.17	258.94	-0.16	312.51	100.25
2.29	811.66	260.38	-0.18	318.53	102.18
2.42	788.47	252.94	-0.21	313.08	100.43
2.53	825.73	264.89	-0.23	317.67	101.91
2.66	825.87	264.94	-0.25	312.80	100.35
2.78	806.88	258.84	-0.27	316.96	101.68
2.92	790.79	253.68	-0.30	317.24	101.77
3.03	786.44	252.29	-0.32	314.81	100.99
3.15	757.74	243.08	-0.34	315.81	101.31
3.28	753.10	241.59	-0.38	314.52	100.90
3.40	734.54	235.64	-0.41	318.53	102.18
3.52	719.47	230.80	-0.43	313.66	100.62
3.65	682.65	218.99	-0.45	315.95	101.36
3.79	641.47	205.78	-0.46	316.67	101.59
3.89	615.38	197.41	-0.47	314.37	100.85
4.02	595.67	191.09	-0.49	312.37	100.21
4.15	570.59	183.04	-0.49	313.37	100.53
4.28	549.42	176.25	-0.50	310.65	99.66
4.42	503.47	161.51	-0.50	310.22	99.52
4.54	484.91	155.56	-0.49	309.36	99.24
4.66	455.19	146.02	-0.47	311.22	99.84
4.77	433.01	138.91	-0.46	307.49	98.64
4.91	397.64	127.56	-0.43	308.78	99.06
5.03	379.81	121.84	-0.41	310.36	99.56
5.16	392.28	125.84	-0.39	307.63	98.69
5.28	375.75	120.54	-0.37	304.62	97.72

5.40	347.48	111.47	-0.32	310.50	99.61
5.53	383.29	122.96	-0.30	308.92	99.10
5.65	369.66	118.59	-0.27	311.22	99.84
5.78	373.29	119.75	-0.25	310.07	99.47
5.91	388.80	124.73	-0.24	310.22	99.52
6.03	364.59	116.96	-0.22	307.20	98.55
6.15	366.18	117.47	-0.22	307.49	98.64
6.28	403.88	129.56	-0.21	310.93	99.75
6.40	419.24	134.49	-0.19	311.79	100.02
6.53	427.07	137.00	-0.19	311.36	99.88
6.65	438.52	140.68	-0.19	311.51	99.93
6.77	427.50	137.14	-0.19	311.94	100.07
6.89	453.02	145.33	-0.19	313.94	100.71
7.03	467.66	150.02	-0.19	312.51	100.25
7.15	469.11	150.49	-0.19	312.22	100.16
7.27	453.60	145.51	-0.19	312.08	100.11
7.39	481.72	154.53	-0.19	312.80	100.35
7.53	468.97	150.44	-0.19	312.37	100.21
7.65	481.87	154.58	-0.19	312.80	100.35
7.76	512.17	164.30	-0.19	312.94	100.39
7.89	512.89	164.53	-0.19	313.51	100.57
8.02	498.68	159.97	-0.19	312.80	100.35
8.13	490.71	157.42	-0.19	312.80	100.35
8.25	523.47	167.93	-0.19	313.23	100.48
8.37	512.45	164.39	-0.20	312.94	100.39
8.51	528.69	169.60	-0.21	312.65	100.30
8.62	547.10	175.51	-0.21	312.51	100.25
8.75	563.77	180.86	-0.22	314.09	100.76
8.87	560.44	179.79	-0.23	312.37	100.21
9.00	584.79	187.60	-0.23	313.66	100.62
9.12	588.71	188.86	-0.24	312.22	100.16
9.25	595.96	191.18	-0.25	313.37	100.53
9.37	626.11	200.85	-0.25	314.66	100.94
9.49	659.74	211.64	-0.26	312.94	100.39
9.62	654.96	210.11	-0.27	314.37	100.85
9.75	669.16	214.66	-0.29	312.80	100.35
9.87	681.05	218.48	-0.30	312.51	100.25
9.99	681.92	218.76	-0.31	312.65	100.30
10.12	693.37	222.43	-0.31	316.38	101.49
10.24	690.47	221.50	-0.33	313.08	100.43
10.36	689.75	221.27	-0.35	315.95	101.36
10.49	680.18	218.20	-0.37	315.09	101.08
10.63	619.44	198.71	-0.39	312.22	100.16
10.75	560.15	179.69	-0.40	312.65	100.30
10.88	550.29	176.53	-0.41	312.37	100.21
11.02	529.56	169.88	-0.41	311.65	99.98
11.13	534.49	171.46	-0.41	310.93	99.75
11.26	524.92	168.39	-0.41	311.36	99.88
11.38	507.82	162.91	-0.39	310.22	99.52
11.50	473.89	152.02	-0.37	310.79	99.70
11.63	453.16	145.37	-0.36	310.79	99.70
11.76	422.29	135.47	-0.34	310.93	99.75
11.88	439.10	140.86	-0.33	309.36	99.24

12.00	436.78	140.12	-0.31	311.08	99.79
12.12	441.28	141.56	-0.31	309.21	99.19
12.26	457.22	146.67	-0.30	310.79	99.70
12.38	457.22	146.67	-0.30	310.65	99.66
12.50	453.60	145.51	-0.29	309.36	99.24
12.63	440.84	141.42	-0.28	310.79	99.70
12.75	425.62	136.54	-0.28	311.36	99.88
12.87	428.08	137.33	-0.27	311.51	99.93
13.00	437.80	140.44	-0.27	311.94	100.07
13.12	440.12	141.19	-0.27	312.22	100.16
13.25	431.13	138.30	-0.27	311.94	100.07
13.37	422.72	135.61	-0.27	312.08	100.11
13.49	427.21	137.05	-0.27	311.94	100.07
13.62	433.16	138.96	-0.27	312.22	100.16
13.74	453.45	145.46	-0.27	313.08	100.43
13.87	457.37	146.72	-0.27	312.22	100.16
13.99	463.02	148.53	-0.27	312.08	100.11
14.11	464.33	148.96	-0.27	312.22	100.16
14.24	462.30	148.30	-0.27	311.94	100.07
14.37	474.18	152.12	-0.27	312.37	100.21
14.50	471.86	151.37	-0.27	312.51	100.25
14.61	475.20	152.44	-0.27	312.51	100.25
14.74	477.23	153.09	-0.27	312.51	100.25
14.86	490.42	157.32	-0.27	312.51	100.25
14.98	491.00	157.51	-0.27	312.22	100.16

Infilled Joint 211 (300 kPa, t/a=0.5, MC1):

Shear Displacement (mm)	Shear Force (N)	Shear Stress (kPa)	Normal Displacement (mm)	Normal Force (N)	Normal Stress (kPa)
0.00	-6.67	-2.14	0.00	936.38	300.39
0.03	78.14	25.07	0.00	935.52	300.11
0.13	321.53	103.15	0.02	933.23	299.38
0.22	591.32	189.69	0.03	932.80	299.24
0.34	703.52	225.69	0.04	936.10	300.30
0.46	710.77	228.01	0.05	936.10	300.30
0.58	898.35	288.19	0.06	933.95	299.61
0.68	1131.90	363.11	0.07	933.23	299.38
0.80	1384.40	444.11	0.08	934.95	299.93
0.90	1626.80	521.87	0.08	936.67	300.48
1.01	1868.50	599.41	0.07	937.96	300.89
1.12	2074.20	665.40	0.07	937.39	300.71
1.20	2200.90	706.04	0.05	937.67	300.80

Infilled Joint 311 (500 kPa, t/a=0.5, MC1):

Shear Displacement (mm)	Shear Force (N)	Shear Stress (kPa)	Normal Displacement (mm)	Normal Force (N)	Normal Stress (kPa)
0.00	-12.61	-4.05	0.00	1560.80	500.70
0.13	33.05	10.60	0.00	1560.70	500.67
0.14	40.45	12.97	0.00	1560.80	500.70
0.14	45.23	14.51	0.00	1560.80	500.70
0.18	162.36	52.08	0.00	1560.30	500.54
0.26	409.96	131.51	0.01	1560.30	500.54
0.36	713.81	228.99	0.02	1560.10	500.47
0.46	989.39	317.39	0.03	1559.00	500.12
0.56	1223.80	392.59	0.03	1560.50	500.60
0.68	1468.50	471.09	0.04	1560.10	500.47
0.79	1650.40	529.44	0.05	1557.40	499.61
0.91	1885.30	604.80	0.05	1560.80	500.70
1.02	2068.10	663.44	0.06	1559.40	500.25
1.07	2200.90	706.04	0.07	1558.70	500.02

Infilled Joint 411 (700 kPa, t/a=0.5, MC1):

Shear Displacement (mm)	Shear Force (N)	Shear Stress (kPa)	Normal Displacement (mm)	Normal Force (N)	Normal Stress (kPa)
0.00	-11.31	-3.63	0.00	2185.40	701.07
0.07	22.47	7.21	0.00	2185.30	701.04
0.08	26.53	8.51	0.00	2185.30	701.04
0.08	32.62	10.46	0.00	2185.30	701.04
0.15	226.87	72.78	0.00	2184.80	700.88
0.23	537.24	172.34	0.00	2184.40	700.75
0.32	879.80	282.24	0.02	2185.10	700.97
0.42	1210.90	388.45	0.02	2184.60	700.81
0.53	1361.40	436.73	0.03	2185.10	700.97
0.64	1564.20	501.79	0.04	2183.80	700.55
0.77	1627.20	522.00	0.05	2184.40	700.75
0.88	1806.30	579.45	0.05	2185.10	700.97
0.99	2073.40	665.14	0.05	2185.00	700.94
1.04	2203.00	706.71	0.05	2185.00	700.94

Infilled Joint 121 (100 kPa, t/a=1.0, MC1):

Shear Displacement (mm)	Shear Force (N)	Shear Stress (kPa)	Normal Displacement (mm)	Normal Force (N)	Normal Stress (kPa)
0.00	22.04	7.07	0.00	311.08	99.79
0.09	140.76	45.16	0.00	309.21	99.19
0.19	208.17	66.78	0.02	310.79	99.70
0.30	266.88	85.61	0.03	308.64	99.01
0.42	315.01	101.05	0.04	310.07	99.47
0.55	381.41	122.35	0.05	310.79	99.70
0.65	454.47	145.79	0.05	310.22	99.52
0.78	504.05	161.70	0.05	310.93	99.75
0.89	529.85	169.97	0.05	311.65	99.98
1.01	539.85	173.18	0.05	311.65	99.98
1.12	551.16	176.81	0.05	311.51	99.93
1.25	546.38	175.28	0.05	311.36	99.88
1.38	549.28	176.21	0.06	311.79	100.02
1.48	553.34	177.51	0.06	311.65	99.98
1.60	560.44	179.79	0.06	311.51	99.93
1.73	572.76	183.74	0.06	311.79	100.02
1.86	571.89	183.46	0.06	311.79	100.02
1.98	579.57	185.92	0.06	311.94	100.07
2.10	584.36	187.46	0.06	311.94	100.07
2.23	581.46	186.53	0.06	311.94	100.07
2.35	583.92	187.32	0.06	311.79	100.02
2.48	580.59	186.25	0.06	310.93	99.75
2.59	578.27	185.51	0.06	311.94	100.07
2.72	585.23	187.74	0.07	311.79	100.02
2.83	583.49	187.18	0.07	311.94	100.07
2.95	581.46	186.53	0.07	311.94	100.07
3.07	575.23	184.53	0.07	311.36	99.88
3.20	603.93	193.74	0.07	311.65	99.98
3.32	583.05	187.04	0.07	311.22	99.84
3.45	580.44	186.20	0.08	311.36	99.88
3.57	580.15	186.11	0.09	310.93	99.75
3.68	577.40	185.23	0.10	310.93	99.75
3.81	589.58	189.13	0.11	310.07	99.47
3.94	605.09	194.11	0.11	311.22	99.84
4.06	609.29	195.46	0.11	311.79	100.02
4.20	610.45	195.83	0.12	311.36	99.88
4.32	609.87	195.64	0.12	311.51	99.93
4.45	623.93	200.15	0.12	311.79	100.02
4.57	622.77	199.78	0.12	311.79	100.02
4.69	632.49	202.90	0.12	311.79	100.02
4.82	633.79	203.32	0.12	311.94	100.07

4.94	628.43	201.60	0.12	311.79	100.02
5.06	628.28	201.55	0.12	311.79	100.02
5.19	631.76	202.67	0.12	311.94	100.07
5.31	628.14	201.50	0.12	311.79	100.02
5.43	635.24	203.78	0.13	311.79	100.02
5.55	638.00	204.67	0.13	311.94	100.07
5.69	640.60	205.50	0.13	311.79	100.02
5.81	637.27	204.43	0.13	311.79	100.02
5.94	642.05	205.97	0.13	311.65	99.98
6.06	642.20	206.02	0.13	312.08	100.11
6.18	642.49	206.11	0.13	311.79	100.02
6.31	632.49	202.90	0.13	311.65	99.98
6.42	651.19	208.90	0.13	312.22	100.16
6.56	638.00	204.67	0.13	311.94	100.07
6.67	623.79	200.11	0.13	311.94	100.07
6.80	626.83	201.08	0.13	311.94	100.07
6.93	635.82	203.97	0.14	311.79	100.02
7.05	629.30	201.88	0.14	311.79	100.02
7.17	634.95	203.69	0.14	312.08	100.11
7.31	635.10	203.74	0.14	311.65	99.98
7.43	604.22	193.83	0.14	311.36	99.88
7.55	592.77	190.16	0.14	311.65	99.98
7.68	588.85	188.90	0.15	311.94	100.07
7.81	589.14	188.99	0.15	311.79	100.02
7.92	591.75	189.83	0.15	311.65	99.98
8.04	601.17	192.85	0.15	311.79	100.02
8.17	607.70	194.95	0.15	311.79	100.02
8.31	610.45	195.83	0.16	311.79	100.02
8.42	605.81	194.34	0.16	311.79	100.02
8.56	611.90	196.30	0.16	311.79	100.02
8.68	607.70	194.95	0.16	311.22	99.84
8.80	614.80	197.23	0.16	311.79	100.02
8.92	609.44	195.51	0.17	311.51	99.93
9.06	607.70	194.95	0.17	311.51	99.93
9.18	617.70	198.16	0.17	311.51	99.93
9.31	609.29	195.46	0.17	311.94	100.07
9.42	606.68	194.62	0.17	311.79	100.02
9.55	604.65	193.97	0.18	311.51	99.93
9.68	614.80	197.23	0.18	311.65	99.98
9.79	618.14	198.30	0.18	311.79	100.02
9.93	603.06	193.46	0.18	311.08	99.79
10.05	604.22	193.83	0.19	310.93	99.75
10.18	602.62	193.32	0.19	311.79	100.02
10.30	598.71	192.06	0.20	311.36	99.88

10.43	592.77	190.16	0.20	311.22	99.84
10.55	588.85	188.90	0.20	311.36	99.88
10.68	580.15	186.11	0.21	311.51	99.93
10.80	582.47	186.85	0.21	311.51	99.93
10.93	580.44	186.20	0.22	311.94	100.07
11.06	591.17	189.65	0.22	310.22	99.52
11.18	604.51	193.92	0.23	310.65	99.66
11.30	603.64	193.65	0.23	311.22	99.84
11.43	618.57	198.43	0.23	311.79	100.02
11.56	640.60	205.50	0.24	311.79	100.02
11.68	653.65	209.69	0.24	311.94	100.07
11.80	648.72	208.11	0.24	311.65	99.98
11.93	650.75	208.76	0.24	311.65	99.98
12.06	652.49	209.32	0.24	311.65	99.98
12.18	657.71	210.99	0.24	311.65	99.98
12.30	657.86	211.04	0.24	311.36	99.88
12.43	660.47	211.88	0.24	311.79	100.02
12.55	669.16	214.66	0.24	311.65	99.98
12.67	661.19	212.11	0.24	311.65	99.98
12.80	654.09	209.83	0.24	311.65	99.98
12.91	649.59	208.39	0.25	311.79	100.02
13.05	654.38	209.92	0.25	311.94	100.07
13.17	659.89	211.69	0.25	311.94	100.07
13.29	652.64	209.36	0.25	311.94	100.07
13.42	653.22	209.55	0.25	311.36	99.88
13.54	645.97	207.22	0.26	311.51	99.93
13.67	655.39	210.25	0.26	311.51	99.93
13.79	653.65	209.69	0.26	311.94	100.07
13.90	662.20	212.43	0.26	311.65	99.98
14.03	652.35	209.27	0.26	311.79	100.02
14.16	665.39	213.45	0.26	311.94	100.07
14.29	629.44	201.92	0.26	311.79	100.02
14.42	617.85	198.20	0.26	311.94	100.07
14.54	617.99	198.25	0.26	311.94	100.07
14.67	613.50	196.81	0.27	311.94	100.07
14.80	614.51	197.13	0.27	311.94	100.07
14.91	613.93	196.95	0.27	311.65	99.98
14.99	614.08	196.99	0.27	311.94	100.07

Infilled Joint 221 (300 kPa, t/a=1.0, MC1):

Shear Displacement (mm)	Shear Force (N)	Shear Stress (kPa)	Normal Displacement (mm)	Normal Force (N)	Normal Stress (kPa)
0.00	-13.92	-4.46	0.00	936.38	300.39
0.01	3.04	0.98	0.00	936.38	300.39
0.02	5.80	1.86	0.00	936.38	300.39
0.02	9.86	3.16	0.00	936.38	300.39
0.10	137.72	44.18	0.01	934.38	299.75
0.19	279.64	89.71	0.02	935.67	300.16
0.30	410.11	131.56	0.03	934.23	299.70
0.42	527.10	169.09	0.04	934.23	299.70
0.52	660.03	211.74	0.04	935.38	300.07
0.64	809.20	259.59	0.05	934.23	299.70
0.75	958.66	307.53	0.05	936.10	300.30
0.88	1089.40	349.48	0.05	934.52	299.79
0.99	1199.30	384.73	0.06	934.52	299.79
1.12	1281.80	411.20	0.06	935.67	300.16
1.23	1343.00	430.83	0.07	933.95	299.61
1.35	1389.40	445.71	0.09	935.81	300.20
1.46	1424.00	456.81	0.09	934.38	299.75
1.60	1463.40	469.45	0.10	933.95	299.61
1.72	1499.70	481.10	0.11	936.10	300.30
1.82	1520.40	487.74	0.11	936.24	300.34
1.95	1528.70	490.40	0.12	935.95	300.25
2.07	1523.90	488.86	0.12	935.81	300.20
2.21	1520.00	487.61	0.12	935.38	300.07
2.33	1520.40	487.74	0.13	935.67	300.16
2.45	1523.90	488.86	0.13	936.24	300.34
2.58	1525.90	489.50	0.14	936.10	300.30
2.70	1528.20	490.24	0.14	935.81	300.20
2.83	1534.20	492.17	0.14	935.52	300.11
2.94	1537.40	493.19	0.15	936.24	300.34
3.08	1537.70	493.29	0.15	936.24	300.34
3.19	1541.60	494.54	0.16	936.10	300.30
3.31	1542.60	494.86	0.16	935.95	300.25
3.44	1540.70	494.25	0.16	935.67	300.16
3.56	1538.10	493.42	0.17	935.81	300.20
3.68	1532.60	491.65	0.17	936.24	300.34
3.81	1534.60	492.29	0.17	936.10	300.30
3.95	1540.60	494.22	0.18	936.10	300.30
4.04	1541.60	494.54	0.18	935.81	300.20
4.17	1540.40	494.15	0.18	935.67	300.16
4.31	1542.70	494.89	0.19	936.38	300.39
4.43	1541.60	494.54	0.19	936.10	300.30

4.56	1540.30	494.12	0.19	935.81	300.20
4.68	1536.60	492.94	0.19	935.67	300.16
4.81	1531.30	491.23	0.20	935.67	300.16
4.92	1512.90	485.33	0.20	936.10	300.30
5.05	1503.00	482.16	0.20	935.95	300.25
5.18	1503.70	482.38	0.21	935.38	300.07
5.30	1503.90	482.45	0.21	936.10	300.30
5.43	1509.40	484.21	0.22	935.95	300.25
5.55	1510.80	484.66	0.22	935.52	300.11
5.68	1517.90	486.94	0.22	935.52	300.11
5.80	1521.90	488.22	0.22	936.24	300.34
5.92	1527.20	489.92	0.23	936.10	300.30
6.05	1528.70	490.40	0.23	935.81	300.20
6.18	1531.90	491.43	0.23	935.81	300.20
6.29	1532.40	491.59	0.23	935.67	300.16
6.43	1534.30	492.20	0.23	936.38	300.39
6.55	1534.30	492.20	0.24	936.24	300.34
6.68	1535.20	492.49	0.24	936.10	300.30
6.80	1534.80	492.36	0.24	936.10	300.30
6.92	1532.90	491.75	0.24	935.81	300.20
7.04	1531.60	491.33	0.24	935.81	300.20
7.18	1531.70	491.36	0.24	935.81	300.20
7.30	1531.30	491.23	0.24	936.38	300.39
7.43	1525.80	489.47	0.24	936.10	300.30
7.55	1523.20	488.64	0.24	935.95	300.25
7.68	1521.10	487.96	0.25	935.67	300.16
7.80	1518.40	487.10	0.25	935.81	300.20
7.92	1515.00	486.01	0.26	936.38	300.39
8.04	1513.00	485.36	0.26	936.24	300.34
8.17	1512.40	485.17	0.26	936.10	300.30
8.28	1511.70	484.95	0.26	936.10	300.30
8.41	1507.90	483.73	0.26	935.95	300.25
8.53	1505.20	482.86	0.27	936.10	300.30
8.67	1505.90	483.09	0.27	935.81	300.20
8.78	1504.50	482.64	0.27	936.38	300.39
8.92	1503.90	482.45	0.27	936.38	300.39
9.03	1500.30	481.29	0.27	936.24	300.34
9.16	1500.30	481.29	0.27	936.24	300.34
9.28	1499.20	480.94	0.28	935.95	300.25
9.42	1501.30	481.61	0.28	935.95	300.25
9.54	1496.60	480.10	0.28	935.95	300.25
9.66	1494.00	479.27	0.28	935.81	300.20
9.79	1491.40	478.44	0.28	935.81	300.20
9.92	1488.50	477.50	0.28	936.24	300.34

10.04	1487.60	477.22	0.29	936.24	300.34
10.15	1486.80	476.96	0.29	936.24	300.34
10.28	1480.00	474.78	0.29	935.95	300.25
10.41	1474.30	472.95	0.29	935.95	300.25
10.54	1468.70	471.15	0.30	935.95	300.25
10.66	1462.00	469.00	0.30	935.81	300.20
10.79	1458.80	467.98	0.30	935.81	300.20
10.91	1453.60	466.31	0.31	936.38	300.39
11.04	1451.40	465.60	0.31	936.24	300.34
11.18	1446.00	463.87	0.31	936.24	300.34
11.29	1436.90	460.95	0.31	936.10	300.30
11.42	1431.20	459.12	0.31	936.10	300.30
11.54	1424.60	457.01	0.32	935.95	300.25
11.65	1416.20	454.31	0.32	935.95	300.25
11.78	1414.10	453.64	0.32	936.38	300.39
11.92	1399.90	449.08	0.33	935.38	300.07
12.04	1407.60	451.55	0.33	935.67	300.16
12.15	1405.20	450.78	0.34	936.24	300.34
12.28	1407.90	451.65	0.34	935.95	300.25
12.42	1410.20	452.39	0.34	935.95	300.25
12.54	1410.40	452.45	0.35	935.67	300.16
12.66	1409.40	452.13	0.35	935.81	300.20
12.79	1405.20	450.78	0.35	935.67	300.16
12.91	1403.40	450.21	0.36	935.81	300.20
13.03	1398.30	448.57	0.36	935.81	300.20
13.15	1399.10	448.83	0.36	936.38	300.39
13.28	1394.70	447.41	0.36	936.38	300.39
13.40	1390.10	445.94	0.36	936.24	300.34
13.52	1384.40	444.11	0.37	936.24	300.34
13.65	1380.70	442.92	0.37	936.10	300.30
13.78	1374.60	440.97	0.37	935.95	300.25
13.90	1379.40	442.51	0.37	935.95	300.25
14.03	1374.60	440.97	0.38	936.38	300.39
14.15	1373.70	440.68	0.38	936.24	300.34
14.27	1374.00	440.77	0.38	936.24	300.34
14.40	1370.70	439.72	0.38	936.10	300.30
14.53	1369.60	439.36	0.38	935.95	300.25
14.65	1366.40	438.34	0.38	936.10	300.30
14.77	1363.70	437.47	0.39	935.67	300.16
14.90	1362.70	437.15	0.39	935.81	300.20
14.99	1356.40	435.13	0.39	936.10	300.30

Infilled Joint 321 (500 kPa, t/a=1.0, MC1):

Shear Displacement (mm)	Shear Force (N)	Shear Stress (kPa)	Normal Displacement (mm)	Normal Force (N)	Normal Stress (kPa)
0.00	11.31	3.63	0.00	1560.80	500.70
0.00	17.25	5.53	0.00	1560.80	500.70
0.01	51.61	16.56	0.00	1561.00	500.76
0.09	280.80	90.08	0.00	1559.70	500.35
0.14	455.34	146.07	0.01	1560.10	500.47
0.25	639.16	205.04	0.02	1560.40	500.57
0.35	785.43	251.96	0.03	1557.50	499.64
0.47	951.12	305.12	0.04	1560.10	500.47
0.58	1076.40	345.30	0.05	1559.80	500.38
0.70	1108.10	355.47	0.05	1560.30	500.54
0.83	1134.20	363.85	0.06	1560.70	500.67
0.96	1284.10	411.93	0.07	1558.50	499.96
1.07	1507.40	483.57	0.08	1560.40	500.57
1.17	1748.30	560.85	0.10	1558.80	500.06
1.28	1953.00	626.51	0.11	1560.80	500.70
1.41	2103.30	674.73	0.12	1559.50	500.28
1.47	2201.00	706.07	0.12	1557.50	499.64

Infilled Joint 421 (700 kPa, t/a=1.0, MC1):

Shear Displacement (mm)	Shear Force (N)	Shear Stress (kPa)	Normal Displacement (mm)	Normal Force (N)	Normal Stress (kPa)
0.00	26.67	8.56	0.00	2185.10	700.97
0.07	121.48	38.97	0.00	2185.10	700.97
0.14	340.09	109.10	0.00	2184.60	700.81
0.21	646.98	207.55	0.01	2184.00	700.62
0.28	1034.20	331.77	0.03	2184.00	700.62
0.36	1414.10	453.64	0.04	2185.30	701.04
0.45	1742.20	558.89	0.05	2183.70	700.52
0.54	2082.70	668.12	0.05	2181.30	699.75
0.59	2203.60	706.91	0.05	2183.00	700.30

Infilled Joint 131 (100 kPa, t/a=1.5, MC1):

Shear Displacement (mm)	Shear Force (N)	Shear Stress (kPa)	Normal Displacement (mm)	Normal Force (N)	Normal Stress (kPa)
0.00	0.58	0.19	0.00	311.79	100.02
0.08	94.95	30.46	0.00	308.06	98.82
0.19	193.82	62.18	0.02	310.22	99.52
0.30	269.93	86.59	0.03	307.49	98.64

0.42	331.54	106.36	0.05	311.79	100.02
0.54	373.58	119.84	0.07	309.79	99.38
0.67	409.09	131.23	0.08	308.06	98.82
0.79	439.54	141.00	0.09	311.65	99.98
0.91	461.72	148.12	0.10	310.50	99.61
1.03	480.27	154.07	0.11	310.07	99.47
1.16	492.59	158.02	0.12	310.79	99.70
1.27	507.24	162.72	0.12	311.94	100.07
1.39	509.99	163.60	0.13	311.65	99.98
1.51	514.48	165.04	0.13	310.93	99.75
1.65	521.44	167.28	0.13	311.51	99.93
1.77	525.21	168.49	0.13	311.65	99.98
1.89	526.95	169.04	0.14	311.22	99.84
2.01	530.87	170.30	0.14	310.93	99.75
2.14	537.97	172.58	0.14	311.79	100.02
2.26	543.62	174.39	0.14	311.65	99.98
2.38	550.29	176.53	0.15	311.22	99.84
2.52	554.93	178.02	0.15	311.94	100.07
2.63	560.29	179.74	0.15	311.79	100.02
2.77	562.90	180.58	0.15	311.65	99.98
2.88	560.15	179.69	0.16	311.36	99.88
3.00	560.87	179.92	0.16	311.79	100.02
3.11	560.44	179.79	0.16	311.65	99.98
3.25	561.89	180.25	0.16	311.65	99.98
3.37	564.64	181.13	0.16	311.65	99.98
3.49	568.12	182.25	0.16	311.94	100.07
3.61	570.88	183.14	0.17	311.65	99.98
3.73	573.20	183.88	0.17	311.79	100.02
3.86	573.49	183.97	0.17	311.51	99.93
3.99	574.36	184.25	0.17	312.08	100.11
4.12	574.65	184.35	0.17	311.79	100.02
4.23	575.81	184.72	0.17	311.65	99.98
4.36	576.82	185.04	0.18	311.65	99.98
4.49	575.66	184.67	0.18	311.94	100.07
4.62	577.54	185.27	0.18	311.94	100.07
4.74	579.57	185.92	0.18	311.79	100.02
4.86	576.24	184.86	0.18	311.79	100.02
4.99	578.41	185.55	0.18	311.79	100.02
5.10	580.30	186.16	0.18	312.08	100.11
5.23	579.28	185.83	0.18	311.51	99.93
5.36	581.89	186.67	0.18	311.79	100.02
5.48	583.34	187.13	0.19	311.79	100.02
5.61	583.63	187.23	0.19	311.79	100.02
5.74	584.07	187.37	0.19	311.79	100.02

5.85	581.89	186.67	0.19	311.79	100.02
5.98	583.63	187.23	0.19	311.94	100.07
6.11	583.63	187.23	0.19	311.79	100.02
6.24	585.66	187.88	0.19	311.65	99.98
6.35	584.79	187.60	0.20	311.94	100.07
6.47	584.36	187.46	0.20	311.79	100.02
6.60	585.66	187.88	0.20	311.79	100.02
6.72	585.08	187.69	0.20	311.79	100.02
6.84	585.52	187.83	0.20	311.94	100.07
6.96	583.34	187.13	0.20	311.79	100.02
7.09	584.21	187.41	0.20	311.65	99.98
7.22	582.04	186.72	0.20	311.79	100.02
7.36	582.76	186.95	0.20	311.65	99.98
7.48	582.04	186.72	0.20	311.79	100.02
7.61	582.18	186.76	0.20	311.79	100.02
7.73	584.36	187.46	0.20	311.79	100.02
7.85	579.72	185.97	0.20	311.79	100.02
7.98	580.59	186.25	0.21	311.65	99.98
8.10	579.57	185.92	0.21	311.51	99.93
8.22	580.01	186.06	0.21	311.94	100.07
8.34	580.44	186.20	0.21	311.79	100.02
8.47	580.15	186.11	0.21	311.94	100.07
8.61	578.99	185.74	0.21	311.65	99.98
8.72	578.56	185.60	0.21	311.65	99.98
8.85	578.99	185.74	0.22	311.79	100.02
8.95	579.14	185.79	0.22	311.79	100.02
9.08	580.15	186.11	0.22	311.94	100.07
9.22	576.39	184.90	0.22	311.51	99.93
9.34	573.92	184.11	0.22	311.36	99.88
9.47	572.33	183.60	0.22	311.65	99.98
9.59	572.47	183.65	0.22	311.79	100.02
9.71	574.36	184.25	0.23	311.65	99.98
9.84	573.34	183.93	0.23	311.79	100.02
9.96	572.91	183.79	0.23	311.65	99.98
10.10	573.78	184.07	0.23	311.65	99.98
10.21	574.65	184.35	0.23	311.51	99.93
10.35	573.49	183.97	0.23	311.65	99.98
10.47	573.78	184.07	0.23	311.79	100.02
10.59	574.65	184.35	0.23	311.94	100.07
10.72	574.50	184.30	0.23	311.51	99.93
10.85	575.66	184.67	0.24	311.36	99.88
10.97	573.92	184.11	0.24	311.65	99.98
11.10	574.65	184.35	0.24	311.79	100.02
11.23	574.94	184.44	0.24	311.79	100.02

11.34	574.36	184.25	0.24	311.65	99.98
11.47	573.20	183.88	0.24	311.79	100.02
11.58	573.20	183.88	0.24	311.79	100.02
11.70	572.47	183.65	0.24	311.79	100.02
11.84	572.18	183.55	0.24	311.79	100.02
11.96	571.89	183.46	0.24	311.65	99.98
12.09	571.75	183.42	0.25	311.51	99.93
12.21	571.17	183.23	0.25	311.65	99.98
12.34	570.30	182.95	0.25	311.94	100.07
12.45	569.86	182.81	0.25	311.51	99.93
12.58	569.86	182.81	0.25	311.51	99.93
12.70	570.01	182.86	0.26	311.79	100.02
12.82	569.28	182.62	0.26	311.65	99.98
12.94	569.57	182.72	0.26	311.79	100.02
13.06	568.56	182.39	0.26	311.79	100.02
13.20	568.56	182.39	0.26	311.79	100.02
13.32	568.12	182.25	0.26	311.79	100.02
13.44	567.54	182.06	0.26	311.65	99.98
13.56	566.67	181.79	0.27	311.65	99.98
13.70	566.09	181.60	0.27	311.65	99.98
13.83	562.90	180.58	0.27	311.65	99.98
13.94	560.87	179.92	0.27	311.65	99.98
14.06	563.48	180.76	0.27	311.94	100.07
14.19	564.35	181.04	0.27	311.94	100.07
14.31	564.50	181.09	0.27	311.94	100.07
14.44	564.93	181.23	0.27	311.22	99.84
14.57	565.66	181.46	0.28	311.94	100.07
14.70	565.66	181.46	0.28	311.79	100.02
14.82	565.95	181.55	0.28	311.79	100.02
14.96	565.66	181.46	0.28	311.79	100.02
15.00	565.37	181.37	0.28	311.79	100.02

Infilled Joint 231 (300 kPa, t/a=1.5, MC1):

Shear Displacement (mm)	Shear Force (N)	Shear Stress (kPa)	Normal Displacement (mm)	Normal Force (N)	Normal Stress (kPa)
0.00	-3.91	-1.26	0.00	935.95	300.25
0.00	1.45	0.47	0.00	936.24	300.34
0.00	8.12	2.60	0.00	936.38	300.39
0.07	98.87	31.72	0.01	935.67	300.16
0.14	319.94	102.64	0.01	932.51	299.15
0.25	507.53	162.81	0.03	935.67	300.16
0.39	409.09	131.23	0.04	935.81	300.20
0.51	391.26	125.51	0.04	936.38	300.39

0.64	402.43	129.10	0.04	936.53	300.44
0.75	468.68	150.35	0.04	936.53	300.44
0.88	637.71	204.57	0.05	931.22	298.73
0.98	768.18	246.43	0.07	935.81	300.20
1.11	887.19	284.61	0.08	932.51	299.15
1.22	991.57	318.09	0.11	931.22	298.73
1.34	1084.20	347.81	0.13	935.38	300.07
1.45	1163.80	373.34	0.15	930.79	298.59
1.59	1245.70	399.62	0.17	935.81	300.20
1.71	1320.10	423.48	0.18	933.95	299.61
1.80	1370.40	439.62	0.19	931.94	298.96
1.92	1424.70	457.04	0.20	936.10	300.30
2.06	1452.70	466.02	0.21	935.24	300.02
2.18	1474.40	472.98	0.22	935.09	299.97
2.30	1480.70	475.00	0.22	934.38	299.75
2.42	1490.00	477.99	0.23	936.10	300.30
2.55	1505.20	482.86	0.23	935.24	300.02
2.66	1519.40	487.42	0.23	935.24	300.02
2.80	1526.90	489.82	0.24	936.10	300.30
2.91	1543.60	495.18	0.24	935.95	300.25
3.04	1554.30	498.61	0.25	935.52	300.11
3.15	1563.00	501.40	0.25	935.38	300.07
3.27	1568.70	503.23	0.26	935.67	300.16
3.38	1576.90	505.86	0.26	936.24	300.34
3.52	1590.70	510.29	0.26	936.10	300.30
3.64	1599.40	513.08	0.26	935.52	300.11
3.76	1606.90	515.49	0.27	935.81	300.20
3.88	1609.10	516.19	0.27	936.38	300.39
4.00	1614.60	517.96	0.28	936.10	300.30
4.13	1620.90	519.98	0.28	935.95	300.25
4.26	1619.60	519.56	0.28	935.52	300.11
4.39	1619.30	519.47	0.28	935.52	300.11
4.50	1617.00	518.73	0.29	936.10	300.30
4.63	1626.80	521.87	0.29	936.38	300.39
4.76	1626.40	521.74	0.29	936.10	300.30
4.89	1630.60	523.09	0.29	936.10	300.30
5.01	1636.20	524.89	0.30	935.81	300.20
5.14	1636.20	524.89	0.30	935.67	300.16
5.26	1638.70	525.69	0.30	935.67	300.16
5.37	1638.00	525.46	0.30	936.38	300.39
5.50	1631.90	523.51	0.31	935.95	300.25
5.63	1639.60	525.98	0.31	935.67	300.16
5.75	1642.30	526.84	0.31	935.67	300.16
5.88	1641.00	526.43	0.32	935.67	300.16

6.01	1640.30	526.20	0.32	936.24	300.34
6.12	1640.40	526.23	0.32	936.10	300.30
6.25	1643.20	527.13	0.32	935.81	300.20
6.38	1643.60	527.26	0.33	935.67	300.16
6.51	1644.30	527.48	0.33	936.38	300.39
6.62	1651.30	529.73	0.33	936.38	300.39
6.74	1650.30	529.41	0.34	936.10	300.30
6.87	1649.70	529.22	0.34	935.95	300.25
6.99	1645.20	527.77	0.34	935.67	300.16
7.12	1640.00	526.11	0.34	935.52	300.11
7.23	1639.70	526.01	0.34	935.95	300.25
7.36	1648.80	528.93	0.34	936.24	300.34
7.49	1657.30	531.66	0.35	936.24	300.34
7.62	1660.40	532.65	0.35	936.10	300.30
7.75	1666.50	534.61	0.35	936.10	300.30
7.87	1664.20	533.87	0.35	935.95	300.25
8.00	1651.90	529.92	0.35	935.52	300.11
8.13	1651.70	529.86	0.35	936.24	300.34
8.25	1659.10	532.23	0.36	936.38	300.39
8.37	1660.20	532.59	0.36	936.24	300.34
8.49	1660.70	532.75	0.36	935.95	300.25
8.62	1664.40	533.93	0.36	935.81	300.20
8.75	1666.50	534.61	0.36	935.81	300.20
8.88	1670.60	535.92	0.37	935.81	300.20
9.00	1672.80	536.63	0.37	936.24	300.34
9.12	1675.70	537.56	0.37	936.24	300.34
9.23	1675.40	537.46	0.38	936.24	300.34
9.36	1674.40	537.14	0.38	936.10	300.30
9.50	1676.10	537.69	0.38	936.24	300.34
9.62	1675.20	537.40	0.38	935.95	300.25
9.74	1671.30	536.15	0.39	935.81	300.20
9.86	1666.50	534.61	0.39	935.81	300.20
9.98	1669.30	535.50	0.39	935.95	300.25
10.11	1673.10	536.72	0.39	935.95	300.25
10.24	1668.80	535.34	0.40	935.95	300.25
10.37	1668.30	535.18	0.40	935.95	300.25
10.48	1672.80	536.63	0.40	935.95	300.25
10.61	1672.00	536.37	0.40	936.10	300.30
10.74	1665.70	534.35	0.40	935.81	300.20
10.85	1665.70	534.35	0.40	935.95	300.25
10.99	1668.70	535.31	0.40	935.95	300.25
11.11	1662.60	533.36	0.40	936.24	300.34
11.24	1664.60	534.00	0.40	936.10	300.30
11.36	1657.00	531.56	0.41	936.10	300.30

11.49	1652.50	530.12	0.41	935.95	300.25
11.61	1656.40	531.37	0.41	936.24	300.34
11.74	1659.90	532.49	0.41	936.24	300.34
11.86	1649.10	529.02	0.41	936.24	300.34
11.98	1650.10	529.35	0.41	936.24	300.34
12.11	1654.90	530.89	0.41	936.38	300.39
12.24	1653.90	530.56	0.42	936.38	300.39
12.36	1659.00	532.20	0.42	936.38	300.39
12.48	1658.00	531.88	0.42	936.38	300.39
12.61	1655.40	531.05	0.42	935.95	300.25
12.73	1651.20	529.70	0.42	936.10	300.30
12.85	1646.10	528.06	0.43	935.95	300.25
12.97	1659.60	532.39	0.43	936.10	300.30
13.10	1655.70	531.14	0.43	935.95	300.25
13.21	1657.50	531.72	0.43	935.95	300.25
13.33	1645.50	527.87	0.43	936.10	300.30
13.47	1654.40	530.72	0.43	936.10	300.30
13.59	1642.80	527.00	0.43	935.95	300.25
13.71	1652.80	530.21	0.43	936.10	300.30
13.84	1638.80	525.72	0.43	935.95	300.25
13.96	1653.60	530.47	0.43	935.95	300.25
14.09	1658.00	531.88	0.44	935.95	300.25
14.21	1648.30	528.77	0.44	935.95	300.25
14.33	1653.00	530.28	0.44	935.95	300.25
14.46	1644.10	527.42	0.44	936.10	300.30
14.58	1651.20	529.70	0.44	936.24	300.34
14.71	1639.00	525.78	0.44	936.10	300.30
14.83	1643.30	527.16	0.44	936.24	300.34
14.96	1627.70	522.16	0.44	936.24	300.34
15.02	1630.90	523.19	0.44	936.10	300.30

Infilled Joint 331 (500 kPa, t/a=1.5, MC1):

Shear Displacement (mm)	Shear Force (N)	Shear Stress (kPa)	Normal Displacement (mm)	Normal Force (N)	Normal Stress (kPa)
0.00	41.75	13.39	0.00	1560.50	500.60
0.00	36.97	11.86	0.00	1560.70	500.67
0.02	82.20	26.37	0.00	1560.50	500.60
0.08	245.28	78.68	0.01	1560.00	500.44
0.15	481.72	154.53	0.02	1558.70	500.02
0.24	704.97	226.15	0.04	1555.50	499.00
0.34	918.50	294.65	0.05	1560.40	500.57
0.46	1101.90	353.49	0.06	1557.70	499.70
0.57	1277.70	409.88	0.08	1560.50	500.60

0.68	1433.70	459.93	0.10	1556.10	499.19
0.79	1582.30	507.60	0.13	1560.70	500.67
0.90	1716.50	550.65	0.15	1558.50	499.96
1.02	1843.40	591.36	0.16	1555.40	498.97
1.13	1959.90	628.73	0.17	1560.40	500.57
1.23	2067.20	663.15	0.18	1559.00	500.12
1.36	2158.80	692.53	0.19	1557.40	499.61
1.43	2200.90	706.04	0.19	1559.70	500.35

Infilled Joint 431 (700 kPa, t/a=1.5, MC1):

Shear Displacement (mm)	Shear Force (N)	Shear Stress (kPa)	Normal Displacement (mm)	Normal Force (N)	Normal Stress (kPa)
0.00	-0.14	-0.05	0.00	2185.10	700.97
0.01	15.66	5.02	0.00	2185.10	700.97
0.01	19.86	6.37	0.00	2185.30	701.04
0.04	80.89	25.95	0.00	2185.30	701.04
0.09	288.63	92.59	0.00	2184.30	700.71
0.19	584.79	187.60	0.00	2183.80	700.55
0.29	860.52	276.05	0.01	2185.00	700.94
0.39	1118.30	358.75	0.02	2183.40	700.43
0.50	1348.50	432.59	0.03	2182.70	700.20
0.60	1555.90	499.13	0.04	2185.00	700.94
0.72	1730.90	555.27	0.05	2183.40	700.43
0.86	1749.70	561.30	0.06	2184.70	700.84
0.97	1712.20	549.27	0.06	2183.70	700.52
1.10	1793.50	575.35	0.06	2185.10	700.97
1.21	1979.50	635.02	0.06	2183.00	700.30
1.34	2156.90	691.93	0.08	2184.80	700.88
1.37	2201.50	706.23	0.08	2185.10	700.97

H.3 Rock Joints with Moisture Condition 2 (0%)

Infilled Joint 112 (100 kPa, $t/a=0.5$, MC2):

Shear Displacement (mm)	Shear Force (N)	Shear Stress (kPa)	Normal Displacement (mm)	Normal Force (N)	Normal Stress (kPa)
0.000	-15.221	-4.88	0	311.79	100.02
0.034	7.2483	2.33	0.001	311.94	100.07
0.104	128.15	41.11	0.007	309.93	99.42
0.220	150.33	48.23	0.013	311.51	99.93
0.345	157.72	50.60	0.014	312.08	100.11
0.456	302.54	97.05	0.018	310.65	99.66
0.552	474.62	152.26	0.02	312.22	100.16
0.651	659.31	211.50	0.018	314.09	100.76
0.778	829.5	266.10	0.003	314.66	100.94
0.884	948.95	304.42	-0.021	314.23	100.80
1.016	1017.5	326.41	-0.048	313.66	100.62
1.132	1053.2	337.86	-0.081	313.23	100.48
1.265	1078.5	345.98	-0.117	312.8	100.35
1.377	1099.4	352.68	-0.162	312.65	100.30
1.492	1161.5	372.60	-0.195	323.98	103.93
1.620	1147.8	368.21	-0.246	314.95	101.03
1.756	1189.6	381.62	-0.286	324.27	104.02
1.872	1174.1	376.65	-0.324	315.38	101.17
1.995	1199.7	384.86	-0.372	326.14	104.62
2.127	1162.6	372.96	-0.415	313.8	100.67
2.247	1199.4	384.76	-0.455	321.69	103.20
2.374	1205.1	386.59	-0.499	313.23	100.48
2.489	1202.5	385.76	-0.547	312.51	100.25
2.627	1217.4	390.54	-0.589	321.12	103.01
2.744	1165.5	373.89	-0.644	313.23	100.48
2.876	1146.1	367.66	-0.674	323.27	103.70
2.993	1052.5	337.64	-0.717	314.81	100.99
3.111	1041.3	334.04	-0.761	317.82	101.96
3.228	942.13	302.23	-0.8	312.22	100.16
3.365	867.77	278.38	-0.832	316.38	101.49
3.485	822.83	263.96	-0.854	316.67	101.59
3.621	729.18	233.92	-0.878	317.82	101.96
3.742	641.76	205.87	-0.897	314.09	100.76
3.863	574.79	184.39	-0.902	311.94	100.07
3.993	515.5	165.37	-0.895	310.5	99.61
4.136	452.87	145.28	-0.873	308.49	98.96
4.258	429.53	137.79	-0.847	311.08	99.79
4.397	384.16	123.24	-0.827	305.63	98.04
4.526	347.05	111.33	-0.801	308.92	99.10

4.646	337.77	108.36	-0.784	304.91	97.81
4.764	305.73	98.08	-0.749	309.07	99.15
4.904	276.02	88.55	-0.709	302.9	97.17
5.026	242.09	77.66	-0.676	309.79	99.38
5.156	216	69.29	-0.652	299.6	96.11
5.273	216	69.29	-0.603	307.92	98.78
5.391	209.33	67.15	-0.561	305.05	97.86
5.526	196.14	62.92	-0.531	310.65	99.66
5.644	180.77	57.99	-0.486	306.63	98.37
5.772	192.8	61.85	-0.451	301.47	96.71
5.900	204.26	65.53	-0.401	308.49	98.96
6.025	222.96	71.52	-0.372	304.34	97.63
6.137	251.81	80.78	-0.339	306.34	98.27
6.269	286.89	92.03	-0.326	307.92	98.78
6.385	322.4	103.42	-0.316	311.94	100.07
6.514	345.89	110.96	-0.312	311.65	99.98
6.632	360.24	115.56	-0.313	312.65	100.30
6.758	377.93	121.24	-0.316	312.37	100.21
6.871	407.64	130.77	-0.321	312.37	100.21
7.005	424.46	136.17	-0.327	314.09	100.76
7.128	441.28	141.56	-0.335	312.65	100.30
7.249	457.22	146.67	-0.348	312.51	100.25
7.371	479.69	153.88	-0.359	315.52	101.22
7.496	506.8	162.58	-0.372	312.8	100.35
7.620	525.36	168.53	-0.379	315.09	101.08
7.737	557.39	178.81	-0.386	315.09	101.08
7.866	566.67	181.79	-0.398	312.94	100.39
8.002	575.66	184.67	-0.41	315.67	101.27
8.114	594.8	190.81	-0.425	312.51	100.25
8.232	610.31	195.79	-0.437	315.09	101.08
8.352	604.07	193.78	-0.457	316.1	101.40
8.489	627.99	201.46	-0.474	313.66	100.62
8.608	655.25	210.20	-0.484	313.08	100.43
8.746	656.12	210.48	-0.511	314.66	100.94
8.865	682.79	219.04	-0.529	313.94	100.71
8.984	695.4	223.08	-0.543	312.65	100.30
9.103	721.06	231.31	-0.556	317.67	101.91
9.219	742.81	238.29	-0.572	313.23	100.48
9.364	764.26	245.17	-0.591	315.38	101.17
9.478	790.64	253.63	-0.612	312.65	100.30
9.604	792.09	254.10	-0.633	313.08	100.43
9.725	794.99	255.03	-0.648	314.95	101.03
9.849	756.58	242.71	-0.663	315.52	101.22
9.976	695.84	223.22	-0.674	312.8	100.35

10.112	661.91	212.34	-0.682	314.66	100.94
10.235	623.64	200.06	-0.691	314.09	100.76
10.368	582.18	186.76	-0.693	312.51	100.25
10.498	536.08	171.97	-0.695	311.08	99.79
10.628	501.87	161.00	-0.693	310.93	99.75
10.753	487.52	156.39	-0.689	311.51	99.93
10.883	470.7	151.00	-0.684	309.36	99.24
11.009	445.48	142.91	-0.67	311.08	99.79
11.136	435.33	139.65	-0.664	309.21	99.19
11.270	399.53	128.17	-0.658	309.07	99.15
11.385	385.9	123.80	-0.65	308.35	98.92
11.501	353.57	113.42	-0.637	310.22	99.52
11.629	341.54	109.56	-0.613	310.79	99.70
11.770	334.58	107.33	-0.592	307.49	98.64
11.893	310.52	99.61	-0.568	310.36	99.56
12.007	296.89	95.24	-0.554	308.64	99.01
12.136	283.7	91.01	-0.543	306.63	98.37
12.274	260.79	83.66	-0.526	310.79	99.70
12.396	254.42	81.62	-0.502	307.06	98.50
12.518	247.89	79.52	-0.478	311.36	99.88
12.646	236.58	75.89	-0.455	307.2	98.55
12.768	245.43	78.73	-0.43	310.79	99.70
12.881	252.68	81.06	-0.416	309.36	99.24
13.002	278.77	89.43	-0.398	309.5	99.29
13.123	287.76	92.31	-0.385	310.79	99.70
13.249	293.7	94.22	-0.377	311.94	100.07
13.368	312.11	100.12	-0.373	311.65	99.98
13.492	333.57	107.01	-0.369	311.79	100.02
13.620	343.13	110.07	-0.369	312.65	100.30
13.741	363.28	116.54	-0.372	313.08	100.43
13.868	376.48	120.77	-0.374	312.37	100.21
13.982	392.86	126.03	-0.375	312.22	100.16
14.101	401.85	128.91	-0.378	312.65	100.30
14.231	410.4	131.65	-0.38	313.08	100.43
14.355	436.2	139.93	-0.385	312.51	100.25
14.482	448.38	143.84	-0.389	312.51	100.25
14.603	473.75	151.98	-0.394	314.09	100.76
14.723	494.19	158.53	-0.404	312.65	100.30
14.850	512.31	164.35	-0.413	312.8	100.35
14.890	517.82	166.11	-0.417	312.94	100.39

Infilled Joint 212 (300 kPa, t/a=0.5, MC2):

Shear Displacement (mm)	Shear Force (N)	Shear Stress (kPa)	Normal Displacement (mm)	Normal Force (N)	Normal Stress (kPa)
0.000	-18.266	-5.86	0	936.38	300.39
0.106	-11.597	-3.72	0.002	936.24	300.34
0.165	-8.408	-2.70	0.002	936.24	300.34
0.195	-4.7839	-1.53	0.002	936.38	300.39
0.219	-3.1893	-1.02	0.002	936.24	300.34
0.237	1.7396	0.56	0.002	936.38	300.39
0.330	61.756	19.81	0.001	935.95	300.25
0.438	146.42	46.97	0.008	935.95	300.25
0.540	254.13	81.52	0.012	935.24	300.02
0.648	412.86	132.44	0.015	935.24	300.02
0.765	583.49	187.18	0.021	936.24	300.34
0.893	653.22	209.55	0.023	935.67	300.16
0.989	835.44	268.01	0.024	934.38	299.75
1.104	1173.4	376.42	0.03	935.81	300.20
1.201	1556.1	499.19	0.034	936.96	300.57
1.291	1923.3	616.99	0.034	936.96	300.57
1.387	2202.2	706.46	0.03	937.96	300.89

Infilled Joint 312 (500 kPa, t/a=0.5, MC2):

Shear Displacement (mm)	Shear Force (N)	Shear Stress (kPa)	Normal Displacement (mm)	Normal Force (N)	Normal Stress (kPa)
0.000	-17.251	-5.53	0	1561	500.76
0.117	-13.482	-4.32	0	1560.3	500.54
0.243	-12.612	-4.05	0	1560.4	500.57
0.300	25.659	8.23	0	1560.5	500.60
0.310	36.531	11.72	0.002	1560.7	500.67
0.314	40.156	12.88	0.002	1560.8	500.70
0.329	82.776	26.55	0.002	1560.7	500.67
0.419	289.93	93.01	0.004	1560.1	500.47
0.510	543.77	174.44	0.005	1559.5	500.28
0.615	826.89	265.26	0.008	1560.7	500.67
0.712	1081.4	346.91	0.01	1560.1	500.47
0.841	1222.8	392.27	0.012	1559.1	500.15
0.960	1305	418.64	0.023	1560	500.44
1.077	1490	477.99	0.023	1560.8	500.70
1.178	1801.5	577.91	0.024	1561.1	500.79
1.274	2192.6	703.38	0.026	1561.7	500.99
1.277	2206.8	707.93	0.026	1561.7	500.99

Infilled Joint 412 (700 kPa, t/a=0.5, MC2):

<i>Shear Displacement (mm)</i>	<i>Shear Force (N)</i>	<i>Shear Stress (kPa)</i>	<i>Normal Displacement (mm)</i>	<i>Normal Force (N)</i>	<i>Normal Stress (kPa)</i>
0.000	-17.831	-5.72	0	2185.4	701.07
0.090	15.511	4.98	0	2185.1	700.97
0.096	29.138	9.35	0	2185.3	701.04
0.097	34.212	10.98	-0.001	2185.4	701.07
0.102	40.446	12.97	-0.001	2185.3	701.04
0.158	277.61	89.06	0	2185	700.94
0.250	705.98	226.48	0.005	2184.1	700.65
0.339	1137.8	365.00	0.017	2184.7	700.84
0.445	1340.8	430.12	0.025	2185	700.94
0.545	1640.9	526.39	0.033	2184.7	700.84
0.652	1910.2	612.78	0.037	2184.4	700.75
0.749	2200.6	705.94	0.039	2183.6	700.49

Infilled Joint 122 (100 kPa, t/a=1.0, MC2):

Shear Displacement (mm)	Shear Force (N)	Shear Stress (kPa)	Normal Displacement (mm)	Normal Force (N)	Normal Stress (kPa)
0.000	-16.671	-5.35	0	311.94	100.07
0.023	-9.8577	-3.16	0.004	312.08	100.11
0.035	-5.5087	-1.77	0.003	312.08	100.11
0.088	36.821	11.81	0.005	311.08	99.79
0.202	124.09	39.81	0.009	312.08	100.11
0.312	175.7	56.36	0.013	311.36	99.88
0.422	236.73	75.94	0.013	311.94	100.07
0.530	364.01	116.77	0.013	310.93	99.75
0.647	511.01	163.93	0.012	314.09	100.76
0.772	637.42	204.48	0	314.09	100.76
0.876	702.65	225.41	-0.024	313.23	100.48
1.012	708.16	227.17	-0.037	315.81	101.31
1.130	691.78	221.92	-0.045	315.81	101.31
1.268	690.76	221.59	-0.052	312.94	100.39
1.385	700.19	224.62	-0.064	316.1	101.40
1.496	703.67	225.73	-0.079	312.8	100.35
1.621	719.9	230.94	-0.088	315.95	101.36
1.747	724.98	232.57	-0.097	312.65	100.30
1.870	740.92	237.68	-0.11	316.1	101.40
1.993	736.14	236.15	-0.123	312.51	100.25
2.116	747.01	239.64	-0.136	314.37	100.85
2.237	755.13	242.24	-0.147	312.51	100.25
2.365	769.33	246.80	-0.162	315.24	101.13
2.486	765.13	245.45	-0.182	312.37	100.21

2.611	756.87	242.80	-0.194	313.66	100.62
2.742	765.71	245.64	-0.201	315.38	101.17
2.860	777.45	249.40	-0.211	312.8	100.35
2.979	795.57	255.22	-0.22	314.81	100.99
3.107	803.69	257.82	-0.23	312.37	100.21
3.220	806.01	258.56	-0.241	313.66	100.62
3.349	809.35	259.64	-0.255	312.37	100.21
3.464	805.43	258.38	-0.267	315.24	101.13
3.583	782.67	251.08	-0.281	312.37	100.21
3.716	749.91	240.57	-0.291	313.66	100.62
3.842	715.84	229.64	-0.3	312.65	100.30
3.968	687.86	220.66	-0.31	313.08	100.43
4.101	633.5	203.22	-0.315	312.65	100.30
4.230	576.39	184.90	-0.319	312.22	100.16
4.356	503.61	161.56	-0.316	310.79	99.70
4.492	424.32	136.12	-0.304	309.21	99.19
4.614	389.81	125.05	-0.286	311.08	99.79
4.752	365.46	117.24	-0.263	308.35	98.92
4.876	357.05	114.54	-0.23	311.65	99.98
4.998	361.98	116.12	-0.209	306.92	98.46
5.120	364.15	116.82	-0.194	311.65	99.98
5.232	372.71	119.56	-0.164	309.79	99.38
5.357	376.04	120.63	-0.138	311.65	99.98
5.488	397.79	127.61	-0.118	309.36	99.24
5.608	425.04	136.35	-0.099	308.49	98.96
5.728	463.31	148.63	-0.089	309.07	99.15
5.856	498.97	160.07	-0.084	310.07	99.47
5.966	531.3	170.44	-0.081	311.94	100.07
6.093	549.57	176.30	-0.082	312.94	100.39
6.228	560.29	179.74	-0.082	313.23	100.48
6.350	562.9	180.58	-0.085	312.37	100.21
6.475	567.98	182.21	-0.088	313.37	100.53
6.595	563.92	180.90	-0.093	312.22	100.16
6.722	567.25	181.97	-0.096	312.94	100.39
6.851	572.04	183.51	-0.101	313.37	100.53
6.960	574.5	184.30	-0.105	312.37	100.21
7.087	578.41	185.55	-0.111	312.94	100.39
7.216	575.66	184.67	-0.117	312.51	100.25
7.334	572.47	183.65	-0.121	312.51	100.25
7.470	571.6	183.37	-0.126	312.51	100.25
7.597	578.41	185.55	-0.127	312.94	100.39
7.727	589	188.95	-0.129	312.8	100.35
7.848	599.87	192.44	-0.13	312.22	100.16
7.968	608.28	195.13	-0.131	312.8	100.35

8.099	609.87	195.64	-0.132	312.65	100.30
8.209	618.28	198.34	-0.136	313.23	100.48
8.334	621.03	199.22	-0.139	312.51	100.25
8.450	623.35	199.97	-0.142	313.08	100.43
8.579	627.12	201.18	-0.146	312.37	100.21
8.714	629.88	202.06	-0.149	313.23	100.48
8.837	629.01	201.78	-0.157	312.65	100.30
8.956	631.76	202.67	-0.162	312.65	100.30
9.073	626.83	201.08	-0.174	313.37	100.53
9.203	629.15	201.83	-0.18	313.08	100.43
9.343	632.2	202.81	-0.184	313.37	100.53
9.453	635.68	203.92	-0.191	312.37	100.21
9.592	644.08	206.62	-0.196	312.51	100.25
9.713	651.33	208.94	-0.199	313.08	100.43
9.838	654.23	209.87	-0.202	313.66	100.62
9.954	662.2	212.43	-0.207	313.51	100.57
10.068	679.89	218.11	-0.211	312.51	100.25
10.200	686.85	220.34	-0.215	312.65	100.30
10.338	683.95	219.41	-0.218	313.37	100.53
10.456	682.07	218.81	-0.221	312.94	100.39
10.586	680.76	218.39	-0.224	313.37	100.53
10.708	641.62	205.83	-0.228	313.66	100.62
10.842	603.64	193.65	-0.232	312.22	100.16
10.959	583.2	187.09	-0.233	311.94	100.07
11.098	544.06	174.53	-0.233	311.36	99.88
11.219	502.02	161.05	-0.228	309.64	99.33
11.356	471.72	151.33	-0.22	310.07	99.47
11.470	479.11	153.70	-0.213	310.79	99.70
11.596	436.64	140.07	-0.205	307.78	98.73
11.714	434.75	139.47	-0.193	311.65	99.98
11.845	400.69	128.54	-0.176	309.64	99.33
11.976	389.38	124.91	-0.15	304.91	97.81
12.106	404.17	129.66	-0.136	308.21	98.87
12.232	415.18	133.19	-0.123	310.79	99.70
12.346	433.74	139.14	-0.111	309.79	99.38
12.479	444.61	142.63	-0.101	309.79	99.38
12.593	472.3	151.51	-0.092	310.65	99.66
12.716	481.72	154.53	-0.088	311.79	100.02
12.833	503.76	161.60	-0.085	311.94	100.07
12.954	524.34	168.21	-0.085	312.65	100.30
13.075	528.26	169.46	-0.086	312.51	100.25
13.195	532.9	170.95	-0.087	312.65	100.30
13.320	533.62	171.18	-0.09	312.65	100.30
13.452	536.95	172.25	-0.091	312.51	100.25

13.565	542.03	173.88	-0.093	312.37	100.21
13.693	547.25	175.56	-0.095	312.22	100.16
13.820	554.06	177.74	-0.096	312.22	100.16
13.952	560.44	179.79	-0.097	312.51	100.25
14.070	563.34	180.72	-0.099	312.37	100.21
14.190	563.05	180.62	-0.102	312.8	100.35
14.322	558.99	179.32	-0.107	312.65	100.30
14.436	560	179.65	-0.112	312.22	100.16
14.568	569.14	182.58	-0.114	312.51	100.25
14.694	569.57	182.72	-0.116	312.65	100.30
14.804	575.66	184.67	-0.117	312.94	100.39
14.930	577.54	185.27	-0.119	312.22	100.16
14.975	577.54	185.27	-0.12	312.65	100.30

Infilled Joint 222 (300 kPa, t/a=1.0, MC2):

Shear Displacement (mm)	Shear Force (N)	Shear Stress (kPa)	Normal Displacement (mm)	Normal Force (N)	Normal Stress (kPa)
0.000	-17.396	-5.58	0	936.38	300.39
0.111	-13.482	-4.32	0.014	936.38	300.39
0.138	-5.0738	-1.63	0.015	936.24	300.34
0.143	-2.3195	-0.74	0.016	936.38	300.39
0.148	2.7544	0.88	0.015	936.38	300.39
0.221	123.08	39.48	0.016	933.8	299.56
0.321	296.02	94.96	0.016	934.81	299.88
0.431	448.09	143.75	0.018	935.95	300.25
0.530	633.21	203.13	0.017	939.25	301.31
0.645	770.49	247.17	0.018	934.23	299.70
0.759	1009.4	323.81	0.018	936.38	300.39
0.878	1301.8	417.61	0.018	937.1	300.62
0.970	1610.9	516.77	0.017	938.25	300.99
1.091	1904.4	610.92	0.006	938.11	300.94
1.200	2155.1	691.35	-0.006	937.67	300.80
1.215	2200.1	705.78	-0.009	937.53	300.76

Infilled Joint 322 (500 kPa, t/a=1.0, MC2):

Shear Displacement (mm)	Shear Force (N)	Shear Stress (kPa)	Normal Displacement (mm)	Normal Force (N)	Normal Stress (kPa)
0.000	76.977	24.69	0	1560.7	500.67
0.073	433.45	139.05	0.002	1560.1	500.47
0.177	813.55	260.98	0.012	1559.5	500.28
0.265	1110.6	356.28	0.024	1558.4	499.93
0.382	1379.9	442.67	0.032	1559.5	500.28

0.478	1713.9	549.81	0.034	1560.1	500.47
0.586	2069.2	663.79	0.036	1561	500.76
0.643	2205.2	707.42	0.037	1561.1	500.79

Infilled Joint 422 (700 kPa, t/a=1.0, MC2):

Shear Displacement (mm)	Shear Force (N)	Shear Stress (kPa)	Normal Displacement (mm)	Normal Force (N)	Normal Stress (kPa)
0.000	21.455	6.88	0	2185.1	700.97
0.003	30.588	9.81	0.001	2185.1	700.97
0.005	35.372	11.35	0.001	2185.3	701.04
0.022	98.577	31.62	0.002	2185.4	701.07
0.108	411.85	132.12	0.009	2184.6	700.81
0.193	716.13	229.73	0.012	2184.6	700.81
0.299	1003.7	321.98	0.012	2185.1	700.97
0.400	1243.1	398.78	0.012	2185.1	700.97
0.512	1419.9	455.50	0.012	2184.8	700.88
0.621	1604.6	514.75	0.013	2185	700.94
0.734	1818.5	583.37	0.014	2185	700.94
0.842	2119	679.77	0.014	2185.1	700.97
0.860	2201.5	706.23	0.014	2184.7	700.84

Infilled Joint 132 (100 kPa, t/a=1.5, MC2):

Shear Displacement (mm)	Shear Force (N)	Shear Stress (kPa)	Normal Displacement (mm)	Normal Force (N)	Normal Stress (kPa)
0.000	24.644	7.91	0	311.94	100.07
0.003	22.76	7.30	0.003	311.94	100.07
0.009	26.529	8.51	0.006	311.79	100.02
0.011	35.227	11.30	0.006	311.79	100.02
0.114	106.12	34.04	0.014	309.93	99.42
0.212	160.33	51.43	0.022	310.93	99.75
0.332	205.71	65.99	0.024	310.79	99.70
0.449	242.67	77.85	0.03	310.5	99.61
0.559	317.48	101.85	0.039	311.65	99.98
0.680	375.75	120.54	0.046	310.79	99.70
0.797	417.21	133.84	0.052	309.79	99.38
0.934	442.73	142.03	0.066	311.36	99.88
1.055	463.89	148.81	0.081	311.08	99.79
1.176	484.91	155.56	0.098	310.93	99.75
1.298	508.4	163.09	0.108	309.93	99.42
1.425	527.1	169.09	0.113	310.79	99.70
1.534	534.34	171.41	0.115	311.51	99.93
1.666	531.3	170.44	0.117	311.79	100.02

1.788	516.8	165.79	0.118	311.65	99.98
1.913	506.37	162.44	0.12	311.79	100.02
2.043	499.41	160.21	0.124	310.79	99.70
2.165	498.83	160.02	0.129	311.94	100.07
2.283	497.09	159.46	0.134	311.22	99.84
2.408	496.07	159.14	0.135	310.79	99.70
2.543	496.94	159.42	0.139	311.65	99.98
2.650	497.81	159.70	0.143	311.22	99.84
2.789	498.68	159.97	0.146	310.79	99.70
2.905	500.71	160.63	0.148	311.79	100.02
3.033	501.29	160.81	0.151	311.36	99.88
3.147	502.31	161.14	0.154	311.08	99.79
3.267	504.63	161.88	0.159	311.94	100.07
3.376	506.08	162.35	0.162	311.65	99.98
3.505	507.38	162.77	0.165	311.51	99.93
3.630	508.69	163.19	0.167	311.22	99.84
3.751	510.57	163.79	0.169	311.79	100.02
3.871	511.59	164.12	0.171	311.36	99.88
3.996	513.18	164.63	0.175	311.22	99.84
4.127	515.06	165.23	0.179	311.94	100.07
4.254	515.64	165.42	0.183	311.65	99.98
4.389	517.24	165.93	0.185	311.36	99.88
4.498	518.25	166.25	0.186	311.79	100.02
4.629	519.7	166.72	0.188	311.79	100.02
4.754	520.57	167.00	0.19	311.65	99.98
4.887	520.86	167.09	0.193	311.51	99.93
5.008	522.02	167.46	0.195	311.94	100.07
5.129	521.88	167.42	0.197	311.79	100.02
5.254	521.01	167.14	0.198	311.65	99.98
5.364	521.01	167.14	0.199	311.65	99.98
5.491	521.59	167.32	0.202	311.94	100.07
5.626	521.44	167.28	0.206	311.79	100.02
5.745	520.86	167.09	0.207	311.65	99.98
5.871	521.88	167.42	0.209	311.94	100.07
6.002	521.15	167.18	0.212	311.94	100.07
6.111	520.72	167.04	0.215	311.65	99.98
6.244	520.28	166.90	0.218	311.94	100.07
6.372	518.11	166.21	0.22	311.79	100.02
6.500	517.53	166.02	0.223	311.79	100.02
6.611	515.79	165.46	0.224	311.94	100.07
6.728	515.5	165.37	0.227	311.65	99.98
6.859	515.5	165.37	0.228	311.79	100.02
6.982	515.21	165.28	0.229	311.79	100.02
7.104	515.21	165.28	0.229	311.65	99.98

7.219	515.5	165.37	0.23	311.65	99.98
7.346	515.64	165.42	0.232	311.94	100.07
7.481	512.6	164.44	0.233	311.79	100.02
7.610	509.56	163.46	0.235	311.65	99.98
7.735	506.22	162.39	0.237	311.94	100.07
7.859	506.22	162.39	0.239	311.65	99.98
7.980	504.05	161.70	0.242	311.36	99.88
8.113	505.06	162.02	0.244	311.22	99.84
8.232	505.64	162.21	0.246	311.65	99.98
8.351	503.9	161.65	0.248	311.94	100.07
8.471	504.05	161.70	0.25	311.65	99.98
8.598	503.61	161.56	0.252	311.79	100.02
8.726	502.74	161.28	0.254	311.94	100.07
8.861	502.45	161.18	0.257	311.51	99.93
8.975	501.73	160.95	0.259	311.79	100.02
9.101	501.29	160.81	0.261	311.65	99.98
9.211	501	160.72	0.263	311.36	99.88
9.337	502.31	161.14	0.264	311.51	99.93
9.477	503.03	161.37	0.266	311.65	99.98
9.595	504.34	161.79	0.268	311.79	100.02
9.724	504.48	161.84	0.27	311.94	100.07
9.843	504.48	161.84	0.27	311.79	100.02
9.966	503.76	161.60	0.271	311.94	100.07
10.090	504.05	161.70	0.272	311.94	100.07
10.219	503.32	161.46	0.273	311.79	100.02
10.345	501.87	161.00	0.274	311.79	100.02
10.463	501.73	160.95	0.276	311.65	99.98
10.593	501.58	160.90	0.277	311.51	99.93
10.719	500.28	160.49	0.279	311.51	99.93
10.832	499.84	160.35	0.279	311.94	100.07
10.976	498.83	160.02	0.281	311.79	100.02
11.095	499.12	160.12	0.281	311.94	100.07
11.225	497.52	159.60	0.283	311.79	100.02
11.345	497.09	159.46	0.283	311.65	99.98
11.476	496.07	159.14	0.283	311.79	100.02
11.591	495.49	158.95	0.284	311.79	100.02
11.719	495.64	159.00	0.285	311.65	99.98
11.831	494.48	158.63	0.286	311.65	99.98
11.958	493.75	158.39	0.286	311.65	99.98
12.087	492.59	158.02	0.287	311.79	100.02
12.219	492.74	158.07	0.288	311.79	100.02
12.344	492.3	157.93	0.288	311.51	99.93
12.464	489.99	157.19	0.289	311.51	99.93
12.592	489.55	157.05	0.292	311.79	100.02

12.707	490.86	157.47	0.294	311.94	100.07
12.833	488.68	156.77	0.295	311.79	100.02
12.954	487.67	156.44	0.296	311.79	100.02
13.081	489.26	156.95	0.297	311.94	100.07
13.192	487.81	156.49	0.297	311.65	99.98
13.319	485.93	155.88	0.298	311.65	99.98
13.455	485.49	155.74	0.3	311.65	99.98
13.576	485.35	155.70	0.302	311.79	100.02
13.698	484.77	155.51	0.304	311.79	100.02
13.823	483.61	155.14	0.308	311.79	100.02
13.948	482.16	154.68	0.31	311.79	100.02
14.079	482.74	154.86	0.311	311.65	99.98
14.194	481.87	154.58	0.313	311.51	99.93
14.320	479.11	153.70	0.314	311.79	100.02
14.438	482.45	154.77	0.316	311.79	100.02
14.564	480.13	154.02	0.317	311.94	100.07
14.693	479.84	153.93	0.318	311.79	100.02
14.818	482.45	154.77	0.319	311.79	100.02
14.942	481.43	154.44	0.32	311.79	100.02
15.012	481.29	154.40	0.32	311.79	100.02

Infilled Joint 232 (300 kPa, t/a=1.5, MC2):

Shear Displacement (mm)	Shear Force (N)	Shear Stress (kPa)	Normal Displacement (mm)	Normal Force (N)	Normal Stress (kPa)
0.000	22.18	7.12	0	936.24	300.34
0.075	244.12	78.31	0.003	934.38	299.75
0.166	506.95	162.63	0.011	935.38	300.07
0.280	600.45	192.62	0.016	936.1	300.30
0.388	775.28	248.71	0.019	934.66	299.84
0.496	968.81	310.79	0.026	934.66	299.84
0.614	1160.2	372.19	0.029	935.52	300.11
0.733	1315.6	422.04	0.03	935.95	300.25
0.841	1422.6	456.36	0.031	936.24	300.34
0.969	1472.1	472.24	0.032	936.24	300.34
1.091	1477.6	474.01	0.035	935.95	300.25
1.229	1480.7	475.00	0.038	936.38	300.39
1.343	1488.8	477.60	0.041	935.95	300.25
1.450	1499.2	480.94	0.046	935.24	300.02
1.576	1508.4	483.89	0.048	935.52	300.11
1.715	1509.2	484.15	0.053	936.38	300.39
1.833	1510.1	484.43	0.056	936.1	300.30
1.951	1507.9	483.73	0.06	935.95	300.25
2.076	1504	482.48	0.063	935.95	300.25

2.204	1498.2	480.62	0.066	935.67	300.16
2.324	1494.7	479.49	0.068	935.81	300.20
2.453	1495.5	479.75	0.07	935.81	300.20
2.576	1492.7	478.85	0.072	935.81	300.20
2.708	1490	477.99	0.075	936.24	300.34
2.827	1490.7	478.21	0.076	936.24	300.34
2.944	1489.8	477.92	0.078	936.24	300.34
3.069	1483	475.74	0.08	935.95	300.25
3.185	1482.4	475.55	0.083	935.95	300.25
3.315	1484	476.06	0.085	935.81	300.20
3.439	1482.6	475.61	0.088	935.95	300.25
3.553	1479.7	474.68	0.091	936.38	300.39
3.682	1480.4	474.91	0.095	936.38	300.39
3.803	1480.8	475.03	0.097	936.24	300.34
3.932	1478.8	474.39	0.1	936.24	300.34
4.058	1475.6	473.37	0.102	935.81	300.20
4.188	1463.3	469.42	0.106	936.38	300.39
4.307	1462	469.00	0.109	936.38	300.39
4.435	1458.4	467.85	0.111	936.1	300.30
4.556	1463	469.32	0.115	935.95	300.25
4.682	1464.9	469.93	0.116	935.95	300.25
4.815	1462.3	469.10	0.118	935.95	300.25
4.930	1465.8	470.22	0.119	936.1	300.30
5.056	1465.8	470.22	0.12	936.1	300.30
5.170	1468.1	470.96	0.121	936.24	300.34
5.302	1468.8	471.19	0.124	935.95	300.25
5.427	1467.6	470.80	0.125	935.95	300.25
5.552	1466	470.29	0.126	936.1	300.30
5.673	1467.1	470.64	0.128	935.95	300.25
5.806	1468.8	471.19	0.128	936.1	300.30
5.914	1468.5	471.09	0.129	936.1	300.30
6.045	1467.6	470.80	0.13	936.1	300.30
6.180	1467.5	470.77	0.13	936.1	300.30
6.302	1468.2	470.99	0.131	936.1	300.30
6.421	1468.1	470.96	0.132	936.24	300.34
6.541	1469.1	471.28	0.133	936.38	300.39
6.667	1469.7	471.47	0.134	936.38	300.39
6.799	1467.3	470.70	0.136	936.1	300.30
6.908	1466.6	470.48	0.137	936.1	300.30
7.033	1468.5	471.09	0.138	936.1	300.30
7.161	1467.9	470.90	0.139	936.24	300.34
7.285	1467.6	470.80	0.14	936.38	300.39
7.416	1464.7	469.87	0.142	936.24	300.34
7.543	1465.3	470.06	0.142	936.1	300.30

7.673	1460.4	468.49	0.143	935.95	300.25
7.793	1462.1	469.04	0.144	935.95	300.25
7.913	1462	469.00	0.146	936.1	300.30
8.052	1460.8	468.62	0.147	936.1	300.30
8.164	1461	468.68	0.148	936.1	300.30
8.283	1458.1	467.75	0.149	935.95	300.25
8.405	1459.5	468.20	0.151	936.1	300.30
8.535	1458.2	467.78	0.153	935.95	300.25
8.675	1456.5	467.24	0.154	936.1	300.30
8.789	1454.3	466.53	0.155	935.81	300.20
8.916	1450.4	465.28	0.157	935.95	300.25
9.023	1450.8	465.41	0.159	935.95	300.25
9.153	1452.3	465.89	0.161	936.1	300.30
9.290	1454.6	466.63	0.163	936.1	300.30
9.407	1452.8	466.05	0.165	936.1	300.30
9.539	1453.3	466.21	0.169	935.95	300.25
9.658	1455	466.76	0.171	935.95	300.25
9.783	1455.7	466.98	0.174	935.95	300.25
9.905	1453.1	466.15	0.176	935.81	300.20
10.020	1446.6	464.06	0.177	935.81	300.20
10.166	1440.2	462.01	0.178	935.81	300.20
10.289	1437.9	461.27	0.18	935.81	300.20
10.412	1437.6	461.18	0.184	936.1	300.30
10.540	1438.6	461.50	0.185	936.1	300.30
10.655	1439.4	461.75	0.189	936.24	300.34
10.789	1435.3	460.44	0.19	936.38	300.39
10.908	1435	460.34	0.191	936.24	300.34
11.037	1433.6	459.89	0.191	936.1	300.30
11.160	1420.7	455.75	0.193	936.1	300.30
11.295	1408.1	451.71	0.195	936.1	300.30
11.410	1413.9	453.57	0.196	936.24	300.34
11.526	1414.3	453.70	0.197	936.1	300.30
11.647	1410.4	452.45	0.198	936.38	300.39
11.773	1407.2	451.42	0.199	936.38	300.39
11.907	1410.5	452.48	0.201	936.24	300.34
12.035	1413.9	453.57	0.201	936.24	300.34
12.165	1418.6	455.08	0.204	936.24	300.34
12.276	1420.7	455.75	0.205	936.1	300.30
12.411	1421	455.85	0.206	936.1	300.30
12.527	1420.8	455.79	0.207	936.1	300.30
12.649	1418.6	455.08	0.208	936.1	300.30
12.768	1416.2	454.31	0.209	936.1	300.30
12.892	1415.6	454.12	0.209	936.38	300.39
13.016	1412.7	453.19	0.211	936.38	300.39

13.134	1411.8	452.90	0.212	936.24	300.34
13.274	1409.9	452.29	0.213	936.24	300.34
13.399	1409.5	452.16	0.214	936.24	300.34
13.510	1411.2	452.71	0.215	936.24	300.34
13.633	1407.2	451.42	0.217	936.38	300.39
13.772	1406.5	451.20	0.218	936.1	300.30
13.895	1405.7	450.94	0.22	936.1	300.30
14.015	1402.1	449.79	0.222	936.1	300.30
14.134	1407.9	451.65	0.222	936.1	300.30
14.265	1405	450.72	0.224	936.38	300.39
14.382	1401.8	449.69	0.225	936.38	300.39
14.512	1401.8	449.69	0.226	936.24	300.34
14.637	1396.7	448.06	0.227	936.24	300.34
14.753	1400.8	449.37	0.228	936.38	300.39
14.883	1396.3	447.93	0.23	936.38	300.39
14.998	1395	447.51	0.231	936.24	300.34

Infilled Joint 332 (500 kPa, t/a=1.5, MC2):

Shear Displacement (mm)	Shear Force (N)	Shear Stress (kPa)	Normal Displacement (mm)	Normal Force (N)	Normal Stress (kPa)
0.000	-17.831	-5.72	0	1560.8	500.70
0.100	-3.9141	-1.26	0.004	1560.7	500.67
0.118	12.177	3.91	0.004	1560.7	500.67
0.123	14.932	4.79	0.004	1560.8	500.70
0.127	20.15	6.46	0.003	1560.8	500.70
0.195	168.31	53.99	0.008	1559.4	500.25
0.288	414.75	133.05	0.022	1560	500.44
0.388	706.13	226.52	0.03	1560.8	500.70
0.486	1006.5	322.88	0.042	1559.5	500.28
0.589	1303.2	418.06	0.048	1558.5	499.96
0.702	1569	503.33	0.055	1559.1	500.15
0.823	1797	576.47	0.061	1560.8	500.70
0.918	1995	639.99	0.066	1560.3	500.54
1.046	2153.3	690.77	0.071	1559.5	500.28
1.085	2202.3	706.49	0.075	1559.4	500.25

Infilled Joint 432 (700 kPa, t/a=1.5, MC2):

Shear Displacement (mm)	Shear Force (N)	Shear Stress (kPa)	Normal Displacement (mm)	Normal Force (N)	Normal Stress (kPa)
0.000	114.67	36.79	0	2185.1	700.97
0.068	458.38	147.05	0.002	2184.7	700.84
0.162	862.4	276.65	0.006	2184.3	700.71

0.256	1230.8	394.84	0.008	2183.1	700.33
0.363	1643.6	527.26	0.012	2185.1	700.97
0.475	2040.5	654.58	0.016	2184.8	700.88
0.513	2205.1	707.39	0.017	2184.3	700.71

H.4 Rock Joints with Moisture Condition 3 (10%)

Infilled Joint 113 (100 kPa, t/a=0.5, MC3):

Shear Displacement (mm)	Shear Force (N)	Shear Stress (kPa)	Normal Displacement (mm)	Normal Force (N)	Normal Stress (kPa)
0.000	-18.411	-5.91	0	311.94	100.07
-0.007	-19.28	-6.18	0	311.94	100.07
0.002	-17.686	-5.67	0	311.94	100.07
0.015	-16.526	-5.30	0.001	312.08	100.11
0.100	-5.9436	-1.91	0.008	312.08	100.11
0.202	120.47	38.65	0.013	309.5	99.29
0.312	161.93	51.95	0.011	311.79	100.02
0.439	151.78	48.69	0.016	311.65	99.98
0.560	174.39	55.94	0.021	312.51	100.25
0.666	356.62	114.40	0.013	312.8	100.35
0.780	537.39	172.39	-0.004	315.24	101.13
0.913	696.42	223.41	-0.028	313.66	100.62
1.034	793.25	254.47	-0.042	314.23	100.80
1.154	799.05	256.33	-0.067	312.8	100.35
1.273	806.59	258.75	-0.103	319.68	102.55
1.394	783.83	251.45	-0.131	312.65	100.30
1.513	824.42	264.47	-0.154	317.96	102.00
1.647	806.88	258.84	-0.185	312.65	100.30
1.754	825.29	264.75	-0.207	322.12	103.33
1.874	810.8	260.10	-0.241	313.8	100.67
2.007	829.79	266.19	-0.279	320.4	102.78
2.130	812.82	260.75	-0.306	313.37	100.53
2.249	822.83	263.96	-0.342	320.4	102.78
2.383	797.89	255.96	-0.388	312.8	100.35
2.515	800.07	256.66	-0.41	320.4	102.78
2.630	775.71	248.84	-0.439	312.37	100.21
2.764	785.57	252.01	-0.467	320.54	102.83
2.884	741.21	237.78	-0.506	312.8	100.35
3.017	732.66	235.03	-0.535	319.82	102.60
3.134	702.07	225.22	-0.559	312.51	100.25
3.248	702.07	225.22	-0.583	318.96	102.32
3.369	671.05	215.27	-0.615	318.39	102.14

3.495	632.92	203.04	-0.658	314.52	100.90
3.616	579.14	185.79	-0.69	316.24	101.45
3.752	522.89	167.74	-0.711	314.81	100.99
3.883	462.3	148.30	-0.725	312.51	100.25
3.986	418.37	134.21	-0.728	311.51	99.93
4.112	387.35	124.26	-0.729	311.94	100.07
4.245	358.5	115.01	-0.727	309.21	99.19
4.371	321.39	103.10	-0.72	309.79	99.38
4.504	301.82	96.82	-0.702	309.36	99.24
4.627	260.5	83.57	-0.682	309.79	99.38
4.750	252.97	81.15	-0.645	307.92	98.78
4.871	218.46	70.08	-0.601	304.77	97.77
5.003	178.16	57.15	-0.558	299.03	95.93
5.132	174.39	55.94	-0.523	310.93	99.75
5.256	163.52	52.46	-0.49	301.61	96.76
5.377	148.45	47.62	-0.427	310.22	99.52
5.498	153.81	49.34	-0.405	305.63	98.04
5.632	130.76	41.95	-0.349	294.73	94.55
5.750	129.89	41.67	-0.296	294.01	94.32
5.877	141.49	45.39	-0.245	294.87	94.59
6.004	164.54	52.78	-0.204	298.31	95.70
6.126	219.91	70.55	-0.178	307.35	98.60
6.240	261.23	83.80	-0.162	311.65	99.98
6.371	302.54	97.05	-0.155	310.93	99.75
6.486	328.35	105.33	-0.155	311.36	99.88
6.615	350.24	112.36	-0.152	313.23	100.48
6.735	376.62	120.82	-0.153	312.51	100.25
6.858	405.33	130.03	-0.154	313.94	100.71
6.975	418.23	134.17	-0.155	314.66	100.94
7.101	431.42	138.40	-0.167	313.23	100.48
7.229	442.58	141.98	-0.177	314.23	100.80
7.349	455.77	146.21	-0.189	313.23	100.48
7.470	465.78	149.42	-0.202	312.37	100.21
7.601	490.42	157.32	-0.211	315.38	101.17
7.717	509.41	163.42	-0.226	313.08	100.43
7.838	531.88	170.63	-0.233	313.94	100.71
7.960	549.13	176.16	-0.248	312.51	100.25
8.098	572.91	183.79	-0.267	314.09	100.76
8.202	595.81	191.13	-0.284	312.51	100.25
8.324	616.25	197.69	-0.298	314.09	100.76
8.446	640.6	205.50	-0.308	314.09	100.76
8.576	664.52	213.18	-0.322	317.24	101.77
8.699	678.44	217.64	-0.345	313.66	100.62
8.835	690.76	221.59	-0.366	317.24	101.77

8.954	696.27	223.36	-0.387	312.65	100.30
9.073	717.15	230.06	-0.4	315.38	101.17
9.189	726.13	232.94	-0.414	312.37	100.21
9.310	744.4	238.80	-0.425	315.24	101.13
9.456	736.43	236.24	-0.444	314.37	100.85
9.578	735.27	235.87	-0.46	314.23	100.80
9.700	721.5	231.45	-0.485	312.37	100.21
9.825	715.55	229.55	-0.505	314.95	101.03
9.945	700.48	224.71	-0.522	315.81	101.31
10.070	672.93	215.87	-0.538	313.8	100.67
10.206	644.95	206.90	-0.551	317.24	101.77
10.330	607.55	194.90	-0.571	313.23	100.48
10.460	569.28	182.62	-0.581	314.09	100.76
10.587	544.06	174.53	-0.585	313.23	100.48
10.709	526.37	168.86	-0.587	313.94	100.71
10.836	499.12	160.12	-0.588	312.08	100.11
10.967	460.85	147.84	-0.589	311.79	100.02
11.092	453.74	145.56	-0.588	311.51	99.93
11.220	423.01	135.70	-0.582	309.93	99.42
11.351	400.54	128.49	-0.574	310.36	99.56
11.463	388.22	124.54	-0.563	308.49	98.96
11.581	360.39	115.61	-0.544	309.21	99.19
11.706	324.14	103.98	-0.53	310.93	99.75
11.851	293.27	94.08	-0.512	305.63	98.04
11.969	280.36	89.94	-0.492	305.48	98.00
12.085	289.93	93.01	-0.469	307.35	98.60
12.210	287.03	92.08	-0.444	309.93	99.42
12.343	263.4	84.50	-0.427	305.34	97.95
12.471	261.37	83.85	-0.412	310.36	99.56
12.594	230.35	73.90	-0.38	307.2	98.55
12.720	217.74	69.85	-0.342	303.04	97.21
12.845	230.79	74.04	-0.309	304.34	97.63
12.964	255.87	82.08	-0.287	311.08	99.79
13.086	254.42	81.62	-0.26	308.78	99.06
13.206	290.95	93.34	-0.243	308.64	99.01
13.333	320.81	102.91	-0.234	311.36	99.88
13.455	334.29	107.24	-0.235	311.79	100.02
13.577	340.82	109.33	-0.233	312.8	100.35
13.702	344.87	110.63	-0.235	312.51	100.25
13.827	358.79	115.10	-0.236	312.51	100.25
13.953	376.62	120.82	-0.241	313.37	100.53
14.073	392.42	125.89	-0.248	312.51	100.25
14.193	402.43	129.10	-0.252	313.23	100.48
14.323	415.04	133.14	-0.26	312.22	100.16

14.447	425.33	136.44	-0.27	312.94	100.39
14.575	440.26	141.23	-0.276	314.09	100.76
14.695	454.9	145.93	-0.285	312.37	100.21
14.812	468.39	150.26	-0.289	313.23	100.48
14.943	485.2	155.65	-0.297	312.22	100.16
15.007	498.68	159.97	-0.298	314.23	100.80

Infilled Joint 213 (300 kPa, t/a=0.5, MC3):

Shear Displacement (mm)	Shear Force (N)	Shear Stress (kPa)	Normal Displacement (mm)	Normal Force (N)	Normal Stress (kPa)
0.000	-0.57986	-0.19	0	936.53	300.44
0.026	77.702	24.93	0	935.81	300.20
0.109	261.37	83.85	0.014	934.95	299.93
0.217	460.41	147.70	0.025	935.52	300.11
0.324	537.39	172.39	0.031	935.24	300.02
0.453	590.74	189.51	0.033	935.81	300.20
0.561	654.38	209.92	0.036	934.95	299.93
0.699	698.45	224.06	0.033	936.38	300.39
0.813	817.17	262.14	0.033	935.24	300.02
0.936	1000.1	320.83	0.042	935.95	300.25
1.043	1244	399.07	0.051	934.81	299.88
1.144	1502.1	481.87	0.055	935.95	300.25
1.262	1746.3	560.21	0.054	936.67	300.48
1.363	1946.7	624.49	0.054	936.81	300.52
1.466	2109.7	676.78	0.049	937.82	300.85
1.566	2201.3	706.17	0.039	937.67	300.80

Infilled Joint 313 (500 kPa, t/a=0.5, MC3):

Shear Displacement (mm)	Shear Force (N)	Shear Stress (kPa)	Normal Displacement (mm)	Normal Force (N)	Normal Stress (kPa)
0.000	-17.686	-5.67	0	1560.8	500.70
0.113	-2.8993	-0.93	0.001	1560.5	500.60
0.138	21.745	6.98	0.001	1560.7	500.67
0.143	25.514	8.18	0.001	1560.8	500.70
0.144	31.313	10.05	0.001	1560.8	500.70
0.169	138.3	44.37	0.001	1560.1	500.47
0.266	436.78	140.12	0.014	1558	499.80
0.362	704.68	226.06	0.035	1560.1	500.47
0.470	950.4	304.88	0.051	1557.4	499.61
0.575	1182.8	379.44	0.06	1557.1	499.51
0.686	1448.9	464.80	0.069	1558.2	499.86
0.798	1731.8	555.55	0.078	1559.4	500.25

0.917	2021.1	648.36	0.079	1560.5	500.60
0.984	2202.8	706.65	0.079	1561.1	500.79

Infilled Joint 413 (700 kPa, t/a=0.5, MC3):

Shear Displacement (mm)	Shear Force (N)	Shear Stress (kPa)	Normal Displacement (mm)	Normal Force (N)	Normal Stress (kPa)
0.000	-18.121	-5.81	0	2185.3	701.04
0.106	10.003	3.21	0.007	2185.1	700.97
0.139	42.04	13.49	0.008	2185.1	700.97
0.145	45.954	14.74	0.008	2185.3	701.04
0.147	51.463	16.51	0.008	2185.1	700.97
0.175	135.25	43.39	0.008	2184.4	700.75
0.263	406.48	130.40	0.016	2184.1	700.65
0.361	739.04	237.08	0.022	2184.7	700.84
0.454	1086.2	348.45	0.031	2185	700.94
0.552	1381.2	443.08	0.039	2184	700.62
0.668	1636.1	524.85	0.06	2184	700.62
0.790	1884	604.38	0.071	2183.3	700.39
0.889	2139.3	686.28	0.081	2184.1	700.65
0.908	2200.6	705.94	0.083	2184.7	700.84

Infilled Joint 123 (100 kPa, t/a=1.0, MC3):

Shear Displacement (mm)	Shear Force (N)	Shear Stress (kPa)	Normal Displacement (mm)	Normal Force (N)	Normal Stress (kPa)
0.000	27.254	8.74	0	311.79	100.02
-0.004	23.05	7.39	0	312.08	100.11
0.001	26.529	8.51	0	311.94	100.07
0.041	82.196	26.37	0.004	310.79	99.70
0.134	202.81	65.06	0.014	309.07	99.15
0.252	275.15	88.27	0.021	309.07	99.15
0.362	385.9	123.80	0.03	310.79	99.70
0.474	447.22	143.47	0.042	310.79	99.70
0.596	467.81	150.07	0.052	310.93	99.75
0.720	476.21	152.77	0.059	311.79	100.02
0.858	435.19	139.61	0.066	309.36	99.24
0.979	411.12	131.89	0.077	308.92	99.10
1.107	416.78	133.70	0.091	309.93	99.42
1.224	426.49	136.82	0.111	308.64	99.01
1.353	437.8	140.44	0.128	310.79	99.70
1.462	434.03	139.24	0.145	308.21	98.87
1.590	441.42	141.61	0.166	310.36	99.56
1.709	462.88	148.49	0.172	310.22	99.52

1.841	483.46	155.09	0.181	310.36	99.56
1.966	491	157.51	0.183	310.93	99.75
2.091	465.78	149.42	0.191	309.79	99.38
2.210	455.77	146.21	0.194	310.93	99.75
2.338	454.03	145.65	0.197	311.08	99.79
2.466	443.6	142.31	0.202	311.79	100.02
2.579	428.23	137.37	0.209	310.79	99.70
2.712	426.49	136.82	0.223	311.22	99.84
2.830	438.67	140.72	0.226	311.51	99.93
2.960	443.31	142.21	0.23	310.07	99.47
3.076	458.82	147.19	0.235	310.65	99.66
3.196	481	154.30	0.239	311.94	100.07
3.303	484.91	155.56	0.245	310.5	99.61
3.434	490.42	157.32	0.247	310.65	99.66
3.554	511.44	164.07	0.248	311.22	99.84
3.679	534.05	171.32	0.248	312.51	100.25
3.797	557.39	178.81	0.249	312.51	100.25
3.920	560.73	179.88	0.246	312.94	100.39
4.048	568.85	182.48	0.244	312.8	100.35
4.177	568.12	182.25	0.238	312.94	100.39
4.307	570.73	183.09	0.233	312.94	100.39
4.420	570.3	182.95	0.231	312.8	100.35
4.549	574.5	184.30	0.229	312.65	100.30
4.674	582.33	186.81	0.224	313.08	100.43
4.805	593.49	190.39	0.212	312.37	100.21
4.927	611.32	196.11	0.207	313.66	100.62
5.046	610.89	195.97	0.202	312.22	100.16
5.171	625.53	200.67	0.195	313.23	100.48
5.280	617.27	198.02	0.191	313.94	100.71
5.412	586.82	188.25	0.189	312.8	100.35
5.544	597.98	191.83	0.185	312.65	100.30
5.666	607.12	194.76	0.184	313.37	100.53
5.789	606.97	194.71	0.183	312.8	100.35
5.924	607.99	195.04	0.183	314.37	100.85
6.031	604.65	193.97	0.181	312.8	100.35
6.164	599.87	192.44	0.177	311.51	99.93
6.295	587.26	188.39	0.181	313.8	100.67
6.427	573.34	183.93	0.181	311.51	99.93
6.543	565.66	181.46	0.18	311.51	99.93
6.661	560.29	179.74	0.181	311.51	99.93
6.792	550.15	176.49	0.182	310.5	99.61
6.917	514.34	165.00	0.189	310.5	99.61
7.040	523.76	168.02	0.196	310.07	99.47
7.154	536.95	172.25	0.205	310.07	99.47

7.279	540.29	173.32	0.21	311.36	99.88
7.415	520.28	166.90	0.223	311.22	99.84
7.546	518.69	166.39	0.228	310.93	99.75
7.672	511.88	164.21	0.234	310.65	99.66
7.795	498.25	159.84	0.247	311.79	100.02
7.916	493.9	158.44	0.254	310.93	99.75
8.049	509.27	163.37	0.259	311.51	99.93
8.170	505.5	162.16	0.261	311.51	99.93
8.291	478.97	153.65	0.269	311.36	99.88
8.411	478.24	153.42	0.276	311.65	99.98
8.541	477.37	153.14	0.28	311.08	99.79
8.668	479.4	153.79	0.282	311.51	99.93
8.803	479.69	153.88	0.285	311.51	99.93
8.919	483.75	155.19	0.286	311.65	99.98
9.043	484.33	155.37	0.286	311.51	99.93
9.150	486.8	156.16	0.288	311.79	100.02
9.281	494.91	158.77	0.288	311.94	100.07
9.418	483.17	155.00	0.287	311.36	99.88
9.543	477.23	153.09	0.288	311.51	99.93
9.670	483.61	155.14	0.29	311.65	99.98
9.794	480.27	154.07	0.29	311.79	100.02
9.909	489.99	157.19	0.29	312.08	100.11
10.036	484.04	155.28	0.291	311.65	99.98
10.168	484.62	155.46	0.292	312.08	100.11
10.296	473.46	151.88	0.292	311.79	100.02
10.418	458.38	147.05	0.293	311.51	99.93
10.547	454.61	145.84	0.293	312.08	100.11
10.672	458.96	147.23	0.294	312.8	100.35
10.786	469.11	150.49	0.298	311.94	100.07
10.925	473.31	151.84	0.298	312.51	100.25
11.044	481.87	154.58	0.298	312.51	100.25
11.172	488.97	156.86	0.296	312.51	100.25
11.296	489.84	157.14	0.295	312.37	100.21
11.423	486.8	156.16	0.293	312.51	100.25
11.536	491.14	157.56	0.29	312.8	100.35
11.664	499.12	160.12	0.289	312.65	100.30
11.775	505.64	162.21	0.286	312.22	100.16
11.900	503.47	161.51	0.287	312.37	100.21
12.032	504.34	161.79	0.287	312.08	100.11
12.162	490.57	157.37	0.283	311.51	99.93
12.290	484.33	155.37	0.284	312.08	100.11
12.415	477.23	153.09	0.286	311.36	99.88
12.540	470.12	150.81	0.288	311.65	99.98
12.661	448.81	143.98	0.294	311.79	100.02

12.780	448.24	143.79	0.298	311.36	99.88
12.904	448.52	143.88	0.302	311.65	99.98
13.026	454.61	145.84	0.303	311.65	99.98
13.144	457.66	146.82	0.304	312.37	100.21
13.269	450.26	144.44	0.305	311.65	99.98
13.408	449.68	144.26	0.305	311.94	100.07
13.525	445.77	143.00	0.305	312.08	100.11
13.651	453.31	145.42	0.306	312.22	100.16
13.776	452.58	145.19	0.307	311.79	100.02
13.901	454.9	145.93	0.308	311.65	99.98
14.035	452	145.00	0.31	311.79	100.02
14.149	451.28	144.77	0.311	311.79	100.02
14.276	447.37	143.51	0.312	311.65	99.98
14.399	447.37	143.51	0.314	311.94	100.07
14.522	458.96	147.23	0.315	311.94	100.07
14.648	457.37	146.72	0.315	312.08	100.11
14.767	454.32	145.74	0.315	313.37	100.53
14.899	447.66	143.61	0.315	312.08	100.11
14.993	450.12	144.40	0.316	312.8	100.35

Infilled Joint 223 (300 kPa, t/a=1.0, MC3):

<i>Shear Displacement (mm)</i>	<i>Shear Force (N)</i>	<i>Shear Stress (kPa)</i>	<i>Normal Displacement (mm)</i>	<i>Normal Force (N)</i>	<i>Normal Stress (kPa)</i>
0.000	48.564	15.58	0	936.38	300.39
0.002	48.709	15.63	0	936.38	300.39
0.006	50.593	16.23	0	936.38	300.39
0.032	111.19	35.67	0.001	936.24	300.34
0.105	345.31	110.77	0.006	932.94	299.28
0.203	574.5	184.30	0.022	936.24	300.34
0.311	774.55	248.47	0.034	935.24	300.02
0.418	969.39	310.98	0.047	933.09	299.33
0.522	1153.3	369.97	0.054	934.09	299.65
0.638	1317.2	422.55	0.059	935.67	300.16
0.759	1471	471.89	0.059	937.24	300.66
0.883	1593	511.03	0.059	937.67	300.80
0.998	1682.2	539.64	0.056	937.24	300.66
1.130	1703.4	546.44	0.052	936.38	300.39
1.253	1667.4	534.90	0.048	937.82	300.85
1.380	1664.8	534.06	0.043	937.1	300.62
1.494	1680.2	539.00	0.037	938.54	301.08
1.600	1686.4	540.99	0.032	936.67	300.48
1.727	1676.7	537.88	0.026	937.24	300.66
1.874	1641.9	526.72	0.026	937.1	300.62
1.988	1606.8	515.46	0.026	937.39	300.71

2.109	1588.1	509.46	0.026	937.96	300.89
2.241	1580.1	506.89	0.026	936.81	300.52
2.361	1573.9	504.90	0.026	937.24	300.66
2.484	1567.2	502.75	0.026	937.82	300.85
2.604	1570	503.65	0.026	936.81	300.52
2.738	1563	501.40	0.019	936.81	300.52
2.860	1536.1	492.77	0.017	937.1	300.62
2.987	1485.8	476.64	0.016	934.81	299.88
3.108	1447.9	464.48	0.013	936.24	300.34
3.230	1412.1	453.00	0.013	936.1	300.30
3.346	1371.5	439.97	0.012	935.67	300.16
3.482	1294.8	415.37	0.013	934.95	299.93
3.608	1259.8	404.14	0.018	934.81	299.88
3.739	1213.7	389.35	0.022	935.81	300.20
3.861	1194.7	383.26	0.029	935.24	300.02
3.984	1181.5	379.02	0.037	936.24	300.34
4.110	1160.7	372.35	0.041	936.1	300.30
4.237	1161.5	372.60	0.045	935.81	300.20
4.367	1147.1	367.99	0.048	935.24	300.02
4.490	1143.9	366.96	0.052	936.24	300.34
4.615	1147	367.95	0.055	935.81	300.20
4.748	1141.9	366.32	0.058	936.1	300.30
4.872	1150	368.92	0.06	935.52	300.11
4.993	1146	367.63	0.063	936.1	300.30
5.115	1158.3	371.58	0.066	935.67	300.16
5.237	1164.5	373.57	0.068	935.67	300.16
5.356	1180.9	378.83	0.069	936.1	300.30
5.487	1167.1	374.40	0.072	936.1	300.30
5.616	1178.9	378.19	0.072	936.24	300.34
5.743	1184.8	380.08	0.074	936.1	300.30
5.862	1190.6	381.94	0.075	936.24	300.34
5.997	1194.4	383.16	0.074	936.38	300.39
6.116	1206.6	387.07	0.076	936.1	300.30
6.243	1216.6	390.28	0.077	936.24	300.34
6.366	1237.3	396.92	0.077	936.38	300.39
6.493	1242.9	398.72	0.077	936.38	300.39
6.608	1255.1	402.63	0.078	936.53	300.44
6.724	1256.6	403.11	0.08	936.38	300.39
6.859	1260	404.20	0.08	936.53	300.44
6.974	1260	404.20	0.081	936.1	300.30
7.100	1267.6	406.64	0.081	936.53	300.44
7.215	1272.4	408.18	0.081	936.67	300.48
7.340	1273.7	408.60	0.081	936.53	300.44
7.477	1275.7	409.24	0.081	936.67	300.48

7.605	1280.8	410.88	0.083	936.53	300.44
7.730	1275.7	409.24	0.084	936.38	300.39
7.849	1272.7	408.28	0.083	936.38	300.39
7.974	1267.3	406.54	0.084	936.1	300.30
8.110	1270.9	407.70	0.083	936.53	300.44
8.225	1268.7	406.99	0.084	936.38	300.39
8.347	1270.9	407.70	0.085	936.53	300.44
8.466	1274.1	408.73	0.084	936.53	300.44
8.596	1278.5	410.14	0.084	936.53	300.44
8.723	1276.6	409.53	0.085	936.38	300.39
8.856	1273.4	408.50	0.085	936.24	300.34
8.977	1277.3	409.75	0.086	936.24	300.34
9.098	1271.5	407.89	0.086	935.95	300.25
9.218	1264.7	405.71	0.087	936.38	300.39
9.340	1257.7	403.47	0.088	936.24	300.34
9.485	1261.5	404.68	0.089	936.24	300.34
9.607	1242.1	398.46	0.09	936.1	300.30
9.726	1251.6	401.51	0.091	936.1	300.30
9.851	1234.4	395.99	0.092	936.24	300.34
9.970	1224.7	392.88	0.094	936.24	300.34
10.095	1195.7	383.58	0.095	936.1	300.30
10.232	1193.9	383.00	0.096	936.24	300.34
10.352	1194.5	383.19	0.097	936.24	300.34
10.482	1184.7	380.05	0.098	936.1	300.30
10.609	1186.4	380.59	0.1	936.38	300.39
10.731	1166.5	374.21	0.101	936.38	300.39
10.857	1144.4	367.12	0.102	935.95	300.25
10.990	1141.6	366.22	0.104	936.1	300.30
11.110	1146.5	367.79	0.106	936.1	300.30
11.240	1127.4	361.67	0.106	936.24	300.34
11.371	1105.5	354.64	0.108	935.67	300.16
11.485	1090.6	349.86	0.11	936.1	300.30
11.603	1083.2	347.49	0.11	936.38	300.39
11.731	1079.7	346.36	0.112	936.1	300.30
11.872	1086.8	348.64	0.112	936.24	300.34
11.986	1085.8	348.32	0.114	935.95	300.25
12.101	1087.7	348.93	0.114	936.1	300.30
12.229	1086.7	348.61	0.115	936.1	300.30
12.358	1080.9	346.75	0.115	936.1	300.30
12.481	1082.8	347.36	0.118	936.38	300.39
12.597	1086.1	348.42	0.117	936.24	300.34
12.724	1084.5	347.90	0.121	936.24	300.34
12.847	1087.8	348.96	0.121	936.24	300.34
12.969	1087.1	348.74	0.122	936.24	300.34

13.095	1093.3	350.73	0.125	936.38	300.39
13.210	1094.2	351.02	0.126	936.38	300.39
13.338	1093.8	350.89	0.126	936.38	300.39
13.468	1094.3	351.05	0.13	936.38	300.39
13.584	1089.9	349.64	0.13	936.38	300.39
13.710	1099	352.55	0.131	936.38	300.39
13.834	1088.6	349.22	0.131	936.1	300.30
13.964	1092.5	350.47	0.133	936.24	300.34
14.083	1089.1	349.38	0.133	936.24	300.34
14.202	1085.8	348.32	0.134	935.95	300.25
14.329	1096.7	351.82	0.134	936.38	300.39
14.451	1094.1	350.98	0.135	936.24	300.34
14.577	1097.8	352.17	0.136	936.38	300.39
14.705	1095.7	351.50	0.135	936.53	300.44
14.825	1103.6	354.03	0.136	936.38	300.39
14.961	1102.6	353.71	0.137	936.67	300.48
14.980	1102.2	353.58	0.136	936.53	300.44

Infilled Joint 323 (500 kPa, t/a=1.0, MC3):

Shear Displacement (mm)	Shear Force (N)	Shear Stress (kPa)	Normal Displacement (mm)	Normal Force (N)	Normal Stress (kPa)
0.000	40.446	12.97	0	1560.8	500.70
0.003	43.635	14.00	0	1560.7	500.67
0.004	47.694	15.30	0	1560.8	500.70
0.023	166.57	53.43	0	1560.4	500.57
0.108	501.15	160.77	0.003	1558.8	500.06
0.209	801.66	257.17	0.007	1560.7	500.67
0.314	1014	325.29	0.012	1559.4	500.25
0.413	1270	407.41	0.017	1560.1	500.47
0.520	1532.6	491.65	0.023	1558.7	500.02
0.629	1780.2	571.08	0.03	1559.5	500.28
0.759	2015	646.40	0.039	1560.7	500.67
0.848	2200.1	705.78	0.039	1561.3	500.86

Infilled Joint 423 (700 kPa, t/a=1.0, MC3):

Shear Displacement (mm)	Shear Force (N)	Shear Stress (kPa)	Normal Displacement (mm)	Normal Force (N)	Normal Stress (kPa)
0.000	51.028	16.37	0	2185.3	701.04
0.003	50.883	16.32	0	2185.3	701.04
0.006	53.782	17.25	0.005	2185.3	701.04
0.007	58.711	18.83	0.005	2185.3	701.04
0.065	423.45	135.84	0.005	2184	700.62

0.146	777.02	249.26	0.01	2184.3	700.71
0.249	1155.7	370.74	0.017	2185	700.94
0.365	1356.3	435.10	0.028	2185.1	700.97
0.452	1661.2	532.91	0.038	2183.6	700.49
0.571	1879.3	602.87	0.047	2182.7	700.20
0.675	2093.2	671.49	0.057	2184.8	700.88
0.735	2201	706.07	0.063	2183.8	700.55

Infilled Joint 133 (100 kPa, t/a=1.5, MC3):

Shear Displacement (mm)	Shear Force (N)	Shear Stress (kPa)	Normal Displacement (mm)	Normal Force (N)	Normal Stress (kPa)
0.000	-0.72483	-0.23	0	311.79	100.02
0.013	15.801	5.07	0.001	311.94	100.07
0.018	20.44	6.56	0.001	311.94	100.07
0.034	42.91	13.77	0.001	311.36	99.88
0.092	113.07	36.27	0.009	307.2	98.55
0.205	181.64	58.27	0.031	309.93	99.42
0.320	217.01	69.62	0.044	309.36	99.24
0.446	200.78	64.41	0.048	311.94	100.07
0.573	226.29	72.59	0.048	311.65	99.98
0.676	269.78	86.54	0.061	307.92	98.78
0.821	310.08	99.47	0.082	308.21	98.87
0.928	341.11	109.43	0.099	310.22	99.52
1.059	369.81	118.63	0.112	307.35	98.60
1.177	397.06	127.38	0.123	310.93	99.75
1.296	420.98	135.05	0.138	308.49	98.96
1.412	445.19	142.82	0.152	309.93	99.42
1.546	466.94	149.79	0.158	311.36	99.88
1.672	482.88	154.91	0.167	310.5	99.61
1.779	491.87	157.79	0.172	310.22	99.52
1.906	492.45	157.98	0.178	311.65	99.98
2.027	498.68	159.97	0.182	310.22	99.52
2.156	506.95	162.63	0.186	310.65	99.66
2.275	517.38	165.97	0.189	311.79	100.02
2.403	528.26	169.46	0.194	311.08	99.79
2.533	532.17	170.72	0.203	311.79	100.02
2.645	529.85	169.97	0.205	311.51	99.93
2.776	527.82	169.32	0.209	310.93	99.75
2.889	528.98	169.69	0.209	311.36	99.88
3.024	527.53	169.23	0.214	311.79	100.02
3.135	528.4	169.51	0.215	311.51	99.93
3.254	531.16	170.39	0.217	311.36	99.88
3.380	535.65	171.83	0.22	311.65	99.98

3.500	539.56	173.09	0.222	311.51	99.93
3.616	540.87	173.51	0.224	311.94	100.07
3.751	541.59	173.74	0.225	311.65	99.98
3.884	542.9	174.16	0.227	311.36	99.88
3.982	547.39	175.60	0.235	311.94	100.07
4.106	551.45	176.90	0.238	311.79	100.02
4.243	549.71	176.34	0.243	311.36	99.88
4.364	554.93	178.02	0.245	311.94	100.07
4.499	560.44	179.79	0.246	311.65	99.98
4.619	559.42	179.46	0.247	311.79	100.02
4.742	560	179.65	0.249	311.65	99.98
4.860	569.43	182.67	0.251	311.79	100.02
4.988	577.54	185.27	0.252	311.51	99.93
5.120	582.04	186.72	0.253	311.36	99.88
5.242	588.56	188.81	0.256	311.79	100.02
5.363	590.59	189.46	0.259	311.79	100.02
5.484	595.96	191.18	0.26	311.36	99.88
5.614	599.29	192.25	0.263	311.65	99.98
5.731	597.98	191.83	0.264	311.94	100.07
5.859	590.59	189.46	0.268	311.51	99.93
5.990	595.23	190.95	0.27	311.36	99.88
6.118	602.33	193.23	0.275	311.65	99.98
6.233	604.51	193.92	0.277	311.65	99.98
6.366	603.64	193.65	0.28	311.51	99.93
6.483	603.2	193.50	0.282	311.79	100.02
6.611	597.12	191.55	0.285	311.65	99.98
6.730	601.61	192.99	0.288	311.79	100.02
6.857	602.04	193.13	0.29	311.65	99.98
6.971	609	195.36	0.292	312.08	100.11
7.108	609.29	195.46	0.293	311.79	100.02
7.232	611.9	196.30	0.295	311.51	99.93
7.361	613.64	196.85	0.296	311.51	99.93
7.478	614.95	197.27	0.298	311.51	99.93
7.611	611.18	196.06	0.301	311.51	99.93
7.728	613.06	196.67	0.304	311.79	100.02
7.851	612.77	196.57	0.308	311.22	99.84
7.977	609.87	195.64	0.313	311.08	99.79
8.106	610.16	195.74	0.314	311.36	99.88
8.218	607.7	194.95	0.315	311.94	100.07
8.343	611.61	196.20	0.316	311.79	100.02
8.463	607.41	194.85	0.317	311.79	100.02
8.602	608.42	195.18	0.317	311.51	99.93
8.709	611.03	196.02	0.317	311.51	99.93
8.848	613.93	196.95	0.318	311.79	100.02

8.969	616.98	197.92	0.319	311.65	99.98
9.092	619.29	198.67	0.32	311.65	99.98
9.213	618.14	198.30	0.321	311.79	100.02
9.352	616.54	197.78	0.321	311.65	99.98
9.470	615.96	197.60	0.322	311.65	99.98
9.596	613.06	196.67	0.323	311.36	99.88
9.717	613.79	196.90	0.324	311.65	99.98
9.848	615.09	197.32	0.325	311.65	99.98
9.965	615.53	197.46	0.325	311.65	99.98
10.085	615.38	197.41	0.327	311.65	99.98
10.211	618.43	198.39	0.327	311.65	99.98
10.335	616.11	197.65	0.328	311.65	99.98
10.459	617.12	197.97	0.329	311.79	100.02
10.586	618.28	198.34	0.33	311.36	99.88
10.713	622.63	199.74	0.332	311.51	99.93
10.837	625.82	200.76	0.334	311.51	99.93
10.966	627.12	201.18	0.337	311.36	99.88
11.090	630.6	202.29	0.339	311.94	100.07
11.213	630.75	202.34	0.34	311.79	100.02
11.347	632.05	202.76	0.343	311.79	100.02
11.459	631.18	202.48	0.343	311.65	99.98
11.572	632.78	202.99	0.343	311.65	99.98
11.698	636.69	204.25	0.345	311.79	100.02
11.840	636.84	204.30	0.347	311.65	99.98
11.960	633.79	203.32	0.35	311.65	99.98
12.073	635.68	203.92	0.351	311.65	99.98
12.203	630.75	202.34	0.355	311.51	99.93
12.334	629.01	201.78	0.359	311.79	100.02
12.463	630.31	202.20	0.361	311.51	99.93
12.574	632.92	203.04	0.363	311.79	100.02
12.711	634.23	203.46	0.365	311.79	100.02
12.830	636.4	204.15	0.366	311.36	99.88
12.953	636.55	204.20	0.368	311.51	99.93
13.076	634.81	203.64	0.369	311.79	100.02
13.199	633.94	203.37	0.371	311.94	100.07
13.326	640.03	205.32	0.371	311.94	100.07
13.453	638.43	204.81	0.373	311.65	99.98
13.576	640.46	205.46	0.374	311.65	99.98
13.702	642.92	206.25	0.375	311.79	100.02
13.825	643.07	206.29	0.377	311.79	100.02
13.956	645.24	206.99	0.379	311.94	100.07
14.072	645.68	207.13	0.382	311.79	100.02
14.194	644.08	206.62	0.382	311.65	99.98
14.323	644.52	206.76	0.383	311.65	99.98

14.450	646.11	207.27	0.384	311.79	100.02
14.573	643.65	206.48	0.384	311.79	100.02
14.693	639.45	205.13	0.385	311.94	100.07
14.816	634.23	203.46	0.385	311.79	100.02
14.948	636.69	204.25	0.385	311.79	100.02
14.961	637.27	204.43	0.385	311.79	100.02

Infilled Joint 233 (300 kPa, t/a=1.5, MC3):

Shear Displacement (mm)	Shear Force (N)	Shear Stress (kPa)	Normal Displacement (mm)	Normal Force (N)	Normal Stress (kPa)
0.000	17.976	5.77	0	936.38	300.39
0.007	25.659	8.23	0	936.38	300.39
0.013	29.863	9.58	0	936.38	300.39
0.020	33.487	10.74	0	936.38	300.39
0.094	184.25	59.11	0.005	934.52	299.79
0.183	355.46	114.03	0.015	935.09	299.97
0.306	499.7	160.30	0.015	933.8	299.56
0.417	589	188.95	0.026	935.81	300.20
0.528	674.53	216.39	0.035	934.09	299.65
0.647	720.05	230.99	0.042	933.52	299.47
0.772	732.8	235.08	0.05	936.38	300.39
0.902	809.78	259.77	0.053	933.95	299.61
1.017	902.27	289.44	0.057	936.24	300.34
1.141	990.55	317.76	0.061	935.24	300.02
1.257	1073.6	344.41	0.067	933.66	299.51
1.385	1150.3	369.01	0.078	935.81	300.20
1.496	1223.8	392.59	0.088	934.81	299.88
1.600	1296.6	415.94	0.102	935.81	300.20
1.725	1365.6	438.08	0.11	934.52	299.79
1.860	1427.6	457.97	0.117	934.95	299.93
1.979	1484.9	476.35	0.122	936.24	300.34
2.097	1522.9	488.54	0.131	935.67	300.16
2.220	1547.8	496.53	0.14	935.24	300.02
2.343	1564.5	501.89	0.145	935.38	300.07
2.465	1563.9	501.69	0.152	936.1	300.30
2.593	1561	500.76	0.161	935.67	300.16
2.715	1557.1	499.51	0.165	936.1	300.30
2.848	1560.7	500.67	0.168	936.24	300.34
2.962	1570.9	503.94	0.171	935.81	300.20
3.087	1583.8	508.08	0.173	935.52	300.11
3.210	1594.3	511.45	0.177	935.38	300.07
3.324	1606.4	515.33	0.18	936.38	300.39
3.451	1614.3	517.86	0.184	936.24	300.34
3.569	1619.6	519.56	0.187	936.24	300.34

3.683	1623.5	520.81	0.189	936.1	300.30
3.817	1622.7	520.56	0.192	935.95	300.25
3.939	1624.3	521.07	0.195	935.81	300.20
4.062	1626.5	521.77	0.197	935.52	300.11
4.193	1629.4	522.71	0.2	936.1	300.30
4.309	1628.4	522.38	0.202	936.38	300.39
4.439	1632.6	523.73	0.203	936.38	300.39
4.569	1633.6	524.05	0.205	936.24	300.34
4.688	1634.3	524.28	0.206	936.1	300.30
4.806	1635.8	524.76	0.209	935.95	300.25
4.927	1638.3	525.56	0.21	936.1	300.30
5.060	1638.3	525.56	0.211	936.1	300.30
5.175	1638.3	525.56	0.214	935.81	300.20
5.305	1638.6	525.66	0.216	935.95	300.25
5.427	1640.9	526.39	0.219	936.38	300.39
5.549	1642.5	526.91	0.221	936.1	300.30
5.667	1643.5	527.23	0.223	936.1	300.30
5.794	1644.3	527.48	0.224	935.81	300.20
5.928	1644.2	527.45	0.225	935.52	300.11
6.049	1644.9	527.68	0.226	935.81	300.20
6.178	1647	528.35	0.23	936.24	300.34
6.302	1648.6	528.86	0.231	936.38	300.39
6.432	1644.6	527.58	0.232	936.1	300.30
6.549	1645.4	527.84	0.235	935.95	300.25
6.673	1644.6	527.58	0.236	935.81	300.20
6.797	1647	528.35	0.237	935.67	300.16
6.926	1649.3	529.09	0.239	936.24	300.34
7.038	1649.1	529.02	0.241	936.1	300.30
7.174	1649.7	529.22	0.243	935.81	300.20
7.301	1650.6	529.51	0.245	935.67	300.16
7.417	1651.5	529.79	0.246	935.81	300.20
7.546	1651	529.63	0.248	936.1	300.30
7.671	1651.5	529.79	0.249	935.67	300.16
7.807	1650.9	529.60	0.251	935.38	300.07
7.931	1652.3	530.05	0.253	935.95	300.25
8.052	1652.2	530.02	0.253	936.24	300.34
8.179	1651.7	529.86	0.256	935.95	300.25
8.281	1653.8	530.53	0.258	935.81	300.20
8.408	1653.6	530.47	0.263	935.67	300.16
8.528	1655.2	530.98	0.266	935.95	300.25
8.657	1657	531.56	0.269	936.38	300.39
8.793	1657.1	531.59	0.273	935.81	300.20
8.917	1657.7	531.78	0.275	935.52	300.11
9.038	1658.8	532.14	0.278	936.24	300.34

9.152	1659.3	532.30	0.28	936.24	300.34
9.280	1657.4	531.69	0.282	935.81	300.20
9.424	1656.8	531.49	0.285	935.52	300.11
9.531	1657.7	531.78	0.287	936.24	300.34
9.666	1657.7	531.78	0.29	936.24	300.34
9.794	1656.8	531.49	0.293	936.1	300.30
9.918	1655.7	531.14	0.298	935.81	300.20
10.036	1656.1	531.27	0.304	935.67	300.16
10.153	1655.4	531.05	0.306	936.24	300.34
10.279	1655.4	531.05	0.308	936.1	300.30
10.422	1654.2	530.66	0.311	935.81	300.20
10.542	1655.5	531.08	0.315	936.24	300.34
10.672	1655.4	531.05	0.318	936.24	300.34
10.794	1656.4	531.37	0.323	936.24	300.34
10.919	1655.9	531.21	0.326	935.95	300.25
11.039	1655.5	531.08	0.329	935.95	300.25
11.178	1654.8	530.85	0.333	935.81	300.20
11.292	1653.5	530.44	0.338	935.67	300.16
11.420	1652.2	530.02	0.344	935.95	300.25
11.539	1651.9	529.92	0.347	936.38	300.39
11.658	1650.9	529.60	0.35	936.1	300.30
11.778	1651.5	529.79	0.353	935.95	300.25
11.905	1651.2	529.70	0.356	935.81	300.20
12.040	1652.2	530.02	0.361	936.24	300.34
12.164	1652	529.96	0.364	936.24	300.34
12.289	1651	529.63	0.367	936.1	300.30
12.411	1649.4	529.12	0.371	935.95	300.25
12.534	1648	528.67	0.382	935.81	300.20
12.664	1647.8	528.61	0.386	935.81	300.20
12.783	1647.4	528.48	0.388	935.95	300.25
12.903	1646.5	528.19	0.39	936.1	300.30
13.023	1646.8	528.29	0.392	935.95	300.25
13.149	1646.1	528.06	0.394	935.95	300.25
13.267	1646.7	528.25	0.398	936.38	300.39
13.388	1646.7	528.25	0.4	936.38	300.39
13.522	1646.4	528.16	0.403	936.24	300.34
13.638	1644.6	527.58	0.407	936.38	300.39
13.765	1644.6	527.58	0.414	936.1	300.30
13.894	1643.5	527.23	0.42	936.24	300.34
14.022	1640.7	526.33	0.425	936.1	300.30
14.142	1640.1	526.14	0.429	935.95	300.25
14.266	1640.1	526.14	0.431	935.95	300.25
14.393	1638.7	525.69	0.434	935.81	300.20
14.515	1639.9	526.07	0.435	935.81	300.20

14.642	1638.1	525.50	0.437	935.95	300.25
14.763	1638	525.46	0.44	935.95	300.25
14.884	1639.1	525.82	0.454	936.24	300.34
14.977	1638.7	525.69	0.454	936.24	300.34

Infilled Joint 333 (500 kPa, t/a=1.5, MC3):

Shear Displacement (mm)	Shear Force (N)	Shear Stress (kPa)	Normal Displacement (mm)	Normal Force (N)	Normal Stress (kPa)
0.000	-5.7986	-1.86	0	1560.7	500.67
0.025	30.733	9.86	0	1560.8	500.70
0.025	32.617	10.46	0	1560.8	500.70
0.049	69.439	22.28	0	1560.7	500.67
0.113	313.85	100.68	0.003	1559.1	500.15
0.186	602.04	193.13	0.016	1559.1	500.15
0.287	861.97	276.52	0.032	1556.7	499.38
0.378	1020.1	327.24	0.035	1559	500.12
0.508	1030.6	330.61	0.038	1560.8	500.70
0.583	1250	401.00	0.046	1557.1	499.51
0.686	1471.7	472.12	0.063	1560.1	500.47
0.805	1662.8	533.42	0.071	1558.1	499.83
0.915	1825.7	585.68	0.082	1560.8	500.70
1.036	1956.2	627.54	0.093	1559.7	500.35
1.147	2065.3	662.54	0.105	1560.5	500.60
1.283	2149.6	689.58	0.115	1559.7	500.35
1.345	2200.1	705.78	0.117	1560.8	500.70

Infilled Joint 433 (700 kPa, t/a=1.5, MC3):

Shear Displacement (mm)	Shear Force (N)	Shear Stress (kPa)	Normal Displacement (mm)	Normal Force (N)	Normal Stress (kPa)
0.000	8.408	2.70	0	2185.1	700.97
0.025	32.327	10.37	0.001	2185.1	700.97
0.027	34.212	10.98	0.001	2185.3	701.04
0.027	39.576	12.70	0	2185.3	701.04
0.073	206.87	66.36	0.002	2184.8	700.88
0.146	547.97	175.79	0.007	2183.4	700.43
0.245	920.53	295.30	0.021	2184.7	700.84
0.358	1265.6	406.00	0.034	2183.4	700.43
0.447	1556.4	499.29	0.041	2184.7	700.84
0.558	1854.3	594.85	0.048	2183	700.30
0.658	2129.6	683.17	0.058	2185	700.94
0.690	2201.6	706.26	0.06	2183.3	700.39